Pertanika Journal of

SCIENCE & TECHNOLOGY

JST

VOL. 18 (1) JAN. 2010

A scientific journal published by Universiti Putra Malaysia Press

Journal of Science & Technology

About the Journal

Pertanika is an international peer-reviewed journal devoted to the publication of original papers, and it serves as a forum for practical approaches to improving quality in issues pertaining to tropical agriculture and its related fields. *Pertanika* began publication in 1978 as the Journal of Tropical Agricultural Science. In 1992, a decision was made to streamline *Pertanika* into three journals to meet the need for specialised journals in areas of study aligned with the interdisciplinary strengths of the university. The revamped Journal of Science & Technology (JST) aims to develop as a pioneer journal focusing on research in science and engineering, and its related fields. Other *Pertanika* series include Journal of Tropical Agricultural Science (JTAS); and Journal of Social Sciences and Humanities (JSSH).

JST is published in **English** and it is open to authors around the world regardless of the nationality. It is currently published two times a year, i.e. in **January** and **July.**

Goal of *Pertanika*

Our goal is to bring the highest quality research to the widest possible audience.

Quality

We aim for excellence, sustained by a responsible and professional approach to journal publishing. Submissions are guaranteed to receive a decision within 12 weeks. The elapsed time from submission to publication for the articles averages 5-6 months.

Indexing of *Pertanika*

Pertanika is now over 30 years old; this accumulated knowledge has resulted in *Pertanika* journals being indexed in SCOPUS (Elsevier), EBSCO, AGRICOLA, and EconLit. etc. JST is indexed in EBSCO.

Future vision

We are continuously improving access to our journal archives, content, and research services. We have the drive to realise exciting new horizons that will benefit not only the academic community, but society itself.

We also have views on the future of our journals. The emergence of the online medium as the predominant vehicle for the 'consumption' and distribution of much academic research will be the ultimate instrument in the dissemination of research news to our scientists and readers.

Aims and scope

Pertanika Journal of Science and Technology aims to provide a forum for high quality research related to science and engineering research. Areas relevant to the scope of the journal include: *bioinformatics, bioscience, biotechnology and biomolecular sciences, chemistry, computer science, ecology, engineering, engineering design, environmental control and management, mathematics and statistics, medicine and health sciences, nanotechnology, physics, safety and emergency management,* and related fields of study.

Editorial Statement

Pertanika is the official journal of Universiti Putra Malaysia. The abbreviation for *Pertanika* Journal of Science & Technology is *Pertanika* J. Sci. Technol.

Editorial Board

Editorial Advisory Board

Pertanika Editorial Office

Research Management Centre (RMC),
1st Floor, IDEA Tower II, UPM-MTDC Technology Centre
Universiti Putra Malaysia, 43400 Serdang, Selangor, Malaysia
Tel: +603 8947 1622, 8947 1620
E-mail: ndeeps@admin.upm.edu.my

Publisher

The UPM Press
Universiti Putra Malaysia
43400 UPM, Serdang, Selangor, Malaysia
Tel: +603 8946 8855, 8946 8854 • Fax: +603 8941 6172
penerbit@putra.upm.edu.my
URL : http://penerbit.upm.edu.my

Pertanika Journal of Science & Technology
Vol. 18 (1) Jan. 2010

Contents

ISSN: 0128-7680
Pertanika J. Sci. & Technol. **18 (1)**: 1-6 (2010)

Short Communications

Ichthyotoxic Properties and Essential Oils of *Syzygium malaccense* (Myrtaceae)

Intan S. Ismail[1, 2 *], NorAkmar Ismail[2] and Nordin Lajis[1]
[1] Institute of Bioscience, Universiti Putra Malaysia,
[2] Department of Chemistry, Faculty of Science,
Universiti Putra Malaysia, 43400 UPM, Serdang, Selangor, Malaysia
[*]E-mail: intan@science.upm.edu.my

ABSTRACT

The preliminary ichthyotoxic test on all parts of *Syzygium malaccense* (Myrtaceae) revealed that the leaves fraction was the most ichthyotoxic against tilapia-fish (*Tilapia oreochromis*). Three compounds, namely ursolic acid (**1**), β-sitosterol (**2**) and sitost-4-en-3-one (**3**), were isolated and their structures were elucidated with the aid of spectroscopic data and comparison with previously reported investigations. However none of these compounds gave any significant ichthyotoxicity. The volatile constituents of the leaves and fruit were determined by Gas Chromatography-Mass Spectrometer (GC-MS), with 180 and 203 compounds being identified in the aroma concentrates, respectively.

Keywords: *Syzygium malaccense*, Myrtaceae, ichthyotoxicity, volatile constituents

INTRODUCTION

Syzygium malaccense (Myrtaceae), which is widely known as the Malay apple, is a medium-sized tree which is native to India and Malaysia. Now, the tree is cultivated throughout the tropics as far as east of Hawaii, as well as Central and South America (Whistler and Craig, 2006). The fruit are eaten raw or cooked as jam or made into juice. The whole plant has a variety of medicinal uses which range from dermatological, digestive, head and throat to endocrine remedy. In Malaysia, powder from the dried leaves is applied on cracked tongue, while a preparation of the roots is used to cure itching, given to alleviate swelling, to treat dysentery and serves as an emmenagogue and abortifacient (Brown, 1935). Some volatile constituents, such as 2-phenylethanol and its derivatives, were found to be the major compounds in the fruit (Pino *et al*., 2004). This plant has also been reported as a good xanthine oxidase (Guerrero *et al*., 1998) and an aldose reductase inhibitor (Guzman *et al.,* 2005). This paper deals with ichthyotoxic properties, the characterization of the isolated components from the hexane leaves extract, and volatile constituents of the leaves and fruits of *S. malaccense*.

MATERIALS AND METHODS

General Nuclear Magnetic Resonance (NMR) spectra were recorded on a Varian VXR-500 (500 MHz for ^{1}H and 125 MHz for ^{13}C) in $CDCl_3$. The chemical shifts are given in δ (ppm) values relative to that of the solvent [$CDCl_3$ (δ_H 7.26; δ_C 77.0)] on the tetramethylsilane scale. Infrared (IR) spectra were recorded on a Perkin-Elmer FTIR model 1725 spectrometer using KBr disc. The absorption bands were measured in cm^{-1}. The essential oils GC-MS data were determined

Received: 4 August 2008
Accepted: 10 September 2009
[*]Corresponding Author

using QP5050A Shimadzu GCMS with the AOC-20i Shimadzu Auto Injector (SGE 054148 non-polar column, 30 X 0.2 mm, an initial temperature of 250˚C with an interface temperature of 280˚C, column flow rate at 1.0 ml/min, dilution of sample in $CHCl_3$, mobile phase was hexane), and equipped with FID. An open column chromatography was performed with Merck Kieselgel 60 (70-230 mesh ASTM). Kieselgel $60F_{254}$ plates (0.2 mm thick, Merck) were used for TLC, and developed in the solvent system of a Hexane-Ethyl acetate (EtOAc) (9:1), (8:2) and/or b) Chloroform ($CHCl_3$)-Methanol (MeOH) (9:1), and spots were detected by either observation under UV (254 and 360 nm) and/or spraying with 10 % sulphuric acid in ethanol reagent.

Plant Material

Leaves, fruit, flower buds and barks of *S. malaccense* were collected from Kuala Selangor, in Selangor in November 2005 and identified by Mr. Shamsul Khamis, a botanist at the Institute of Bioscience.

Extraction and Isolation

The ground dried leaves (1 kg) were extracted with MeOH (3 l X 3), each time for 24 hours at the room temperature. The combined filtrates were concentrated to 900 mL, and extracted successively with hexane (3 X 500 ml) and EtOAc (3 X 500 ml). Part of the hexane soluble extract (2 g) was subjected to column chromatography on Silica gel 60 (i.d. 4 cm; length 30 cm) with $CHCl_3$-MeOH (5 to 90% MeOH), and 100% MeOH in the step-wise gradient mode. Compound **1** (7.3 mg) was afforded from the 5% MeOH fraction. Another portion (1g) of the hexane fraction was chromatographed on Silica gel 60 (i.d. 2 cm; length 30 cm) using hexane-EtOAc as a solvent, at increasing concentrations of EtOAc, i.e. from 10 to 90 %. Compounds **2** (9.1 mg) and **3** (8.4 mg) were isolated from 10 and 20% EtOAc, respectively.

Ursolic Acid (1)

White powder, mp: 282-285˚C (Lit. 283-285˚C; Gohari *et al.,* 2005) IR υ_{max} (cm^{-1}, KBr disc): 3401, 2926, 1688, 1455, 1359, 1030. ^{1}H NMR ($CDCl_3$, 500 MHz): δ_H 5.28 (1H, *t*, *J* = 17.5 Hz, H-12), 3.23 (1H, *dd*, *J* = 4.5/4.0 Hz, H-3), 2.20 (1H, *d*, *J* = 10.00 Hz, H-18), 2.01 (1H, *dd*, *J* = 4.0/3.0 Hz, Hb-22), 1.27 (3H, *s*, Me-23), 1.17 (1H, *m*, Ha-22), 1.15 (3H, *s*, Me-27), 1.09 (3H, *s*, Me-26), 1.00 (3H, *s*, Me-24), 0.92 (3H, *d*, *J* = 5.0 Hz, Me-29), 0.87 (3H, *d*, *J* = 6.5 Hz, Me-30), 0.77 (3H, *s*, Me-25). ^{13}C NMR ($CDCl_3$, 125 MHz): δ_C 39.1 (C-1), 27.5 (C-2), 79.3 (C-3), 38.7 (C-4), 55.5 (C-5), 18.5 (C-6), 33.2 (C-7), 39.7 (C-8), 47.8 (C-9), 36.9 (C-10), 17.3 (C-11), 126.1 (C-12), 138.2 (C-13), 42.2 (C-14), 29.9 (C-15), 24.4 (C-16), 46.7 (C-17), 52.9 (C-18), 39.3 (C-19), 39.3 (C-20), 30.8 (C-21), 36.9 (C-22), 28.2 (C-23), 15.8 (C-24), 15.7 (C-25), 17.2 (C-26), 23.2 (C-27), 182.2 (C-28), 21.4 (C-29), 21.4 (C-29), 23.5 (C-30).

β-sitosterol (2)

Colorless needles, mp: 139-140˚C (Lit. 140-14˚C; Jiang and Wang, 2006). IR υ_{max} (cm^{-1}, KBr disc): 3402, 2936, 2869, 1640, 1466, 1382, 1049. ^{1}H NMR ($CDCl_3$, 500 MHz): δ_H 5.35 (1H, *d*, *J* = 5.0 Hz, H-6), 3.53 (1H, *m*, H-3), 1.02 (3H, *s*, Me-19), 0.92 (3H, *d*, *J* = 6.8 Hz, Me-21), 0.84 (3H, *d*, *J* = 7.5 Hz, Me-27), 0.83 (3H, *d*, *J* = 7.0 Hz, Me-26), 0.82 (3H, *t*, Me-29), 0.69 (3H, *s*, Me-18). ^{13}C NMR ($CDCl_3$, 125 MHz): δ_C 37.5 (C-1), 31.9 (C-2), 72.0 (C-3), 42.5 (C-4), 141.0 (C-5), 122.0 (C-6), 32.2 (C-7), 32.2 (C-8), 50.4 (C-9), 36.7 (C-10), 21.3 (C-11), 40.0 (C-12), - (C-13), 57.0 (C-14), 24.5 (C-15), 28.5 (C-16), 56.3 (C-17), 12.1 (C-18), 19.6 (C-19), 36.4 (C-20), 19.0 (C-21), 34.2 (C-22), 26.3 (C-23), 46.1 (C-24), 29.4 (C-25), 20.1 (C-26), 19.3 (C-27), 23.3 (C-28), 12.2 (C-29).

Sitost-4-en-3-one (3)

Yellow powder, mp: 150-153 °C (Lit. 152-154°C; Mario *et al.,* 2001). IR υ_{max} (cm^{-1}, KBr disc): 2935, 2869, 1702, 1677, 1460, 1376. ^{1}H NMR ($CDCl_3$, 500 MHz): δ_H 5.73 (1H, *s*, H-4), 1.19 (3H, *s*, Me-19), 0.92 (3H, *d*, *J* = 6.5 Hz, Me-21), 0.85 (3H, *d*, *J* = 8.0 Hz, Me-26), 0.83 (3H, *d*, *J* = 9.0 Hz, Me-27), 0.81 (3H, *t*, Me-29), 0.72 (3H, *s*, Me-18). ^{13}C NMR ($CDCl_3$, 125 MHz): δ_C 36.4 (C-1), 32.3 (C-2), 199.9 (C-3), 172.0 (C-4), 124.0 (C-5), 39.9 (C-6), 33.2 (C-7), 34.1 (C-8), 54.1 (C-9), 35.9 (C-10), 21.3 (C-11), 38.8 (C-12), 42.6 (C-13), 56.3 (C-14), 24.4 (C-15), 28.4 (C-16), 56.1 (C-17), 12.2 (C-18), 19.3 (C-19), 35.9 (C-20), 17.6 (C-21), 34.2 (C-22), 26.3 (C-23), 46.1 (C-24), 29.4 (C-25), 20.1 (C-26), 18.9 (C-27), 23.3 (C-28), 12.2 (C-29).

Hydro-distillation

The fresh leaves (350 g) and fruit (53 g) were separately immersed in distilled water and refluxed under Dean Stark condition for 2 hours. The obtained volatile oils for the leaves and fruit were separated from the water layer and mixed with anhydrous sodium sulphate prior to filtering to get the respective/required oils.

Ichthyotoxic Assay

A test solution prepared by adding acetone (0.5 ml) to the weighed crude extract (4.0 mg) or pure compound (1.0 mg) was dissolved in aerated water (100 ml) to give a test solution of 40 ppm or 10 ppm, respectively (Kawazu *et al.,* 1968). In the control group, only acetone (0.5 ml) was added to the 100 ml aerated water. Five tilapia fish (*Tilapia oreochromis*: 2.5 – 3.5 cm) per test solution or control were added. The results were recorded after 24 h.

RESULTS AND DISCUSSION

As part of the present study on the ichthyotoxicity of the Malaysian medicinal plants using tilapia fish (*Tilapia oreochromis*), the researchers have isolated three known compounds from the hexane fraction of the leaves of *S. malaccense*. None of them showed toxicity to tilapia, even though two sub-fractions of the hexane fraction gave a very strong ichthyotoxicity. The ichthyotoxic test was observed in 24 hours.

In the 24 hours lethality, 40 ppm has been established as the least amount of drug which can lead to or cause death in a given fish species and sizes under controlled conditions. Based on the data derived from several studies conducted previously, 50% of death in fish in the first five hours indicated that the sample contained high ichthyotoxic constituents. There are different reporting methods used for ichthyotoxicity in the literature. One common designation in reporting the average concentration required to kill at least 50% of fish in a given period of time is defined as the median tolerance limit (TLm). However, some researchers simply reported a concentration that killed all the fish in a few minutes or hours, or reported a comparison of the piscicidal activity with that of a well-known fish poison, such as rotenone (Jonathan *et al.,* 2004).

A concentrated methanol (MeOH) extract from the dried leaves of *S. malaccense* was partitioned into hexane-, ethyl acetate- (EtOAc-) and water- (H_2O-) soluble portions. The hexane-soluble portion, which showed a significant ichthyotoxic activity (lethal dose 40 ppm after 2 hours), was subjected to bioassay-guided fractionation by column chromatography on Merck Silica gel 60 to yield two active fractions at 40 ppm, namely fractions 12 and 15 (Table 1). However, the amounts of these fractions were rather small (7.9 and 11.6 mg), based on their Thin-Layer Chromatography (TLC) profiles, and they contained too many compounds in each of the fractions. Thus, no further fractionation was pursued. Fractions with reasonable quantities were subjected

TABLE 1
Ichthyotoxicity test of sub-fractions at 40 ppm (in duplicate) from hexane soluble portion

Sample	Number of dead fish at specified time interval (hours)				Total number of dead fish in 24 hours
	1	3	6	18	
Standard	-	-	-	-	0
Fraction 1	-	-	1X	-	1X
2	-	2X	-	-	2X
3	-	1X	-	-	1X
4	-	2X	-	-	2X
5	-	-	-	-	1X
6	-	-	-	-	0
7	-	-	-	-	0
8	-	-	-	-	0
9	-	-	-	-	0
10	-	-	-	-	0
11	-	1X	-	-	1X
12	-	5X	-	-	5X
13	-	1X	-	-	1X
14	-	2X	-	-	2X
15	-	3X	2X	-	5X
16	-	1X	-	-	1X
17	-	-	-	-	0

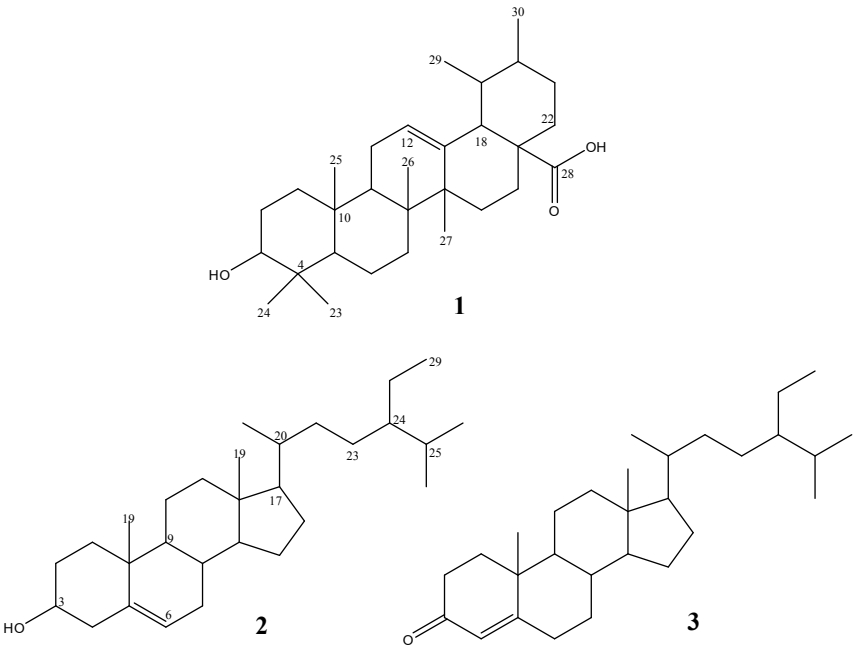

Fig. 1: Structures of 1 to 3

to another open-column chromatography to give compounds **1**, **2,** and **3**, which were identified as the ursolic acid (**1**), β-sitosterol (**2**), and sitost-4-en-3-one (**3**) respectively *(Fig. 1)*. The identity of these compounds were determined based on the spectral data and by the comparison of their physicochemical data with those in the reported literature (Gohari *et al*., 2005; Chien-Ya and Gow-Chin, 2001; Vincent *et al.,* 2001). However, the Ichthyotoxicity test on these compounds yielded no significant results.

The essential oil constituents of the leaves and fruit were also determined. In this study, the hydro-distillation-solvent extraction on the leaves and fruits of *S. malaccense* yielded 104.1 and 89.2 mg of essential oils, respectively. These concentrates were analyzed using the GC-MS, while their chemical compositions were quantified based on the GC-FID peak integration. The identification of the constituents was done by comparing them with the data available at the National Institute for Standard and Technology (NIST) and 1998 Mass Spectral Wiley library. The essential oil from the leaves contained 180 compounds, in which 15 (>1.0%) were major and identified as hexanoic acid (12.16%), methyl salicylate (8.27%), 3-hexen-1-ol (7.81%), 1-octen-3-ol (5.89%), *n*-hexadecanoic acid (5.07%), 2-hexenal (4.89%), 3-buten-2-one (3.68%), 1-hexanol (2.96%), phytol (2.95%), acetic acid (2.73%), 3-buten-2-one (2.58%), azulene (1.64%), 2-octen-1-ol (1.34%), alpha-cadinol (1.11%) and 3-hexen-1-ol (1.10%). Meanwhile, the minor compounds of the essential oil from the leaves are mostly aldehydes, ketones, sesquiterpenes, alcohols, esters and fatty acids. A wide range of different compound types were detected; however, no similarity with the components was reported from the Malay rose apple leaves (*S. malaccense*), in which (-)-*β*-caryophyllene, (+)-*α*-pinene, (-)-*β*-pinene, *p*-cymene and *α*-terpineol were found in more than 7% of the oil from Nigeria (Karioti *et al*., 2007).

Two hundred and three volatile constituents were identified from the essential oil of the fruit, with 11 major compounds such as *n*-hexadecanoic acid (18.59%), 9-octadecynoic acid (9.37%), (*Z,Z*)-9-12-octadecadien-1-ol (6.98%), (*E*)-3,7,11- trimethyl-1,6,10-dodecatrien-3-ol (6.28%), 1-octen-3-ol (2.33%), tetradecanoic acid (1.75%), phytol (1.56%), 2-ethylhexyl *p*-methoxycinnamate (1.43%), (*E*)-2-octen-1-ol (1.26%), 2-phenylethyl accetate (1.25%), and benzyl benzoate (1.00%). The minor compounds consist of a wide range of compound groups which include fatty acids, aldehydes, ketones, terpenes, alcohols, hydrocarbons, and esters. A study on the essential oil of Malay apple showed 2-phenylethyl acetate, 2-phenylethanol, 1-octen-3-ol and (*E*)-2-octen-1-ol to be the major components (Wong *et al.,* 1996). 1-octen-3-ol and (*E*)-2-octen-1-ol were also among the isolated constituents from the Cuban *S. malaccense* (Pino *et al*., 2004). Other major components were identified for the first time in the fruits.

One common major compound found in both volatile compositions of the leaves and fruit is phytol, which contributed 2.95 and 1.56% of the total oils, respectively.

CONCLUSIONS

The hexane soluble part of the leaves of *S. malaccense* was found to be most active towards tilapia fish. However, no chemical constituent was isolated from the active fractions due to their limited amounts. Three known compounds, namely ursolic acid, *β*-sitosterol and sitost-4-en-3-one, were obtained from the hexane fraction. Neverthless, none showed ichthyotoxicity. This study is the first report on these isolated compounds from *S. malaccense*. Further work with larger amount of plant is required for both isolation and characterization of the active component. Volatile compositions of the leaves and fruit were determined and different constituents were observed as compared to the previously reported investigations. These results suggested that the plants of the same species, which were collected in the different places or countries, gave large qualitative differences in the compositions of the fruit and leaves oil. The differences may be due to the different origins of the plants. Nonetheless, further systematic studies are still needed to prove this.

ACKNOWLEDGEMENTS

We would like to thank Research Management Centre of UPM for the grant (Geran Penyelidikan Pensyarah Lantikan Baru), and the NMR Laboratory of IBS, UPM. Our appreciation also goes to Mr. Zainal Abidin Kassim and the students, Ahmad Ridhwan Sahrom, Low Kok Wah, Ng Wee Siong, Lee Wei Har, and Mohd Izwan Mohd Lazim for the GC-MS analysis.

REFERENCES

Brown, F.B.H. (1935). Flora of Southeastern Polynesia. III. Dicotyledons. *Bishop Museum Bulletin, 130*, 210-202.

Chien-Ya, H. and Gow-Chin, Y. (2001). Extraction and identification of antioxidative components of Hsian-tsao (*Mesona procumbens* Hemsl.). *Lebensmittel-Wissenschaft und-Technologie*, *34*, 306-311.

Gohari, A.R., Hadjiakhoodi, Z., Esmaeil, S., Ebrahimi, S., Saeidnia, S. and Shaffiee, A. (2005). Cytotoxic terpenoids from *Satureja macrantha*. *DARU*, *13*, 177-181.

Guerrero, R.O. and Guzman, A.L. (1998). Inhibition of Xanthine oxidase by Puerto Rican plant extracts. *Puerto Rican Health Sciences Journal, 17*(4), 359-364.

Guzman, A. and Guerrero, R.O. (2005). Inhibition of aldose reductase by herbs extracts and natural subtances and their role in prevention of cataracts. *Revista Cubana Plantas Medicinales*, *10*, 3-4.

Jiang, A.L. and Wang, C.H. (2006). Antioxidant properties of natural components from *Salvia plebeia* on oxidative stability of ascidian oil. *Process Biochemistry*, *4*, 1111-1116.

Jonathan, G. C., Robert, A. B., Steven, G. W. and Noel, L. O. (2004). Naturally occurring fish poisons from plants. *Journal of Chemical Education*, *81*, 1457-1461.

Karioti, A., Skaltsa, H. and Gbolade, A.A. (2007). Analysis of the leaf oil of *Syzygium malaccense Merr. et* Perry from Nigeria. *Journal of Essential Oil Research, 19*(4), 313-315.

Kawazu, K., Ohigashi, H. and Mitsui, T. (1968). The piscicidal constituents of *Callophyllum innophyllum* LINN. *Tetrahedron Letters*, *19*, 2383-2385.

Mário, G. de C., Carlos, R. X. V., Raimundo, B. and William, F. da C. (2001). Acyl-lupeol Esters from *Parahancornia amapa* (Apocynaceae). *Journal of Brazzilian Chemical Society, 12*(4), 556-559.

Pino, J.A., Marbot, R., Rosado, A. and Vázquez, C. (2004). Volatile constituents of Malay rose apple [*Syzygium malaccense* (L.) Merr. & Perry]. *Flavour and Fragrance Journal, 19*, 32-35.

Vincent, C., Ange, B., Serge, R., Giovanni, M., Serafino, G., Jean-Marie, D. and Joseph, C. (2001). Composition and chemical variability of the triterpene fraction of dichloromethane extracts of cork. *Industrial Crops and Products*, *15*, 15–22.

Whistler, W.A and Craig, R.E. (2006). *Syzygium malaccense* (Malay apple), Myrtaceae (myrtle family). Species profiles for Pacific Island agroforestry. Retrieved on February, 2007 from www.traditionaltree.org.

Wong, K. C. and Lai, F. Y. (1996). Volatile constituents from the fruits of four *Syzygium* species grown in Malaysia. *Flavour and Fragrance Journal*, *11*, 61-66.

ISSN: 0128-7680
Pertanika J. Sci. & Technol. **18 (1)**: 7–12 (2010)

The Determination of Sediment Acceration Rate Using ^{210}Pb in Johore Coastal Water, Malaysia

Kamaruzzaman, B. Y.[1*], Noor Azhar M. S.[2] , Norhizam, H. A. G[2]. and Willison K. Y. S.[2]

[1]Institute of Oceanography and Maritime Studies, International Islamic University Malaysia, 25200 Kuantan, Pahang, Malaysia

[2]Institute of Oceanography, Universiti Malaysia Terengganu, 21030 Kuala Terengganu, Terengganu, Malaysia

[*]E-mail:kama@iiu.edu.my

ABSTRACT

Ocean sediments give information on the paleoclimatic evolution in the geological past which gives detailed information on both the age of the sediments and both paleoceanographic and paleoclimatic conditions during sedimentation. One possible way to date sediments is with ^{210}Pb method which can be used to date sediments up to 100 years. In this study, two core samples labelled as JB15 and JB17 were collected using pledging corer, analysed and measured for the activity of ^{209}Po and ^{210}Po using the alpha spectrometer. Applying the methods, average sedimentation rates for JB15 and JB17 were calculated as 0.38 cmyr^{-1} and 0.43 cmyr^{-1}, respectively. Assuming that the sedimentation rate values are accurate, this might imply that the sediments at the depth of 30 cm were deposited 70 years ago.

Keywords: Johore coastal water, ^{210}Pb, sedimentation rate

INTRODUCTION

The outfall of radionuclide in the marine environment has become a tool for tracing the history of the marine environment since 1960s. Several radionuclide such as ^{14}C, ^{230}Th and ^{137}Cs (Ritchie *et al*., 1990), ^{239}Pu, ^{240}Pu (Price, 1991), ^{230}Th (Kamaruzzaman and Willison, 2005) and ^{7}Be (Burch *et al*., 1988; Walling *et al*., 1999) were probably the most extensive elements which have been employed to trace the past of marine environment. Since these environments represent important commercial, residential and recreational importance, it is imperative to understand the processes operating in these coastal regions so as to determine the most suitable management practices in the surrounding areas. One such method used to obtain chronologies of deposition over the past 150 years is ^{210}Pb analysis. The ^{210}Pb method has successfully been applied to sediments from lagoons, estuaries and coastal environments (Jones and Chenhall, 2001; Kate, 2002; Krishnaswamy *et al.,* 1971) with sedimentation rates ranging from mm to cm per year. In more specific, the ^{210}Pb method is used as a dating method because ^{210}Pb is concentrated in a stratified manner and decays at a known rate (Wei and Murray, 1994).

In Malaysia, studies related to the characteristics of sediments and heavy metals of the coastal waters are well documented, but only little information is known about the accumulation rate of sediments. Furthermore, studies on accumulation rate using radinuclides from the Malaysian coastal areas have received little attention and therefore, only limited studies have been done regarding to their roles in the process of sedimentation. In view of potential importance of

[*]Corresponding Author

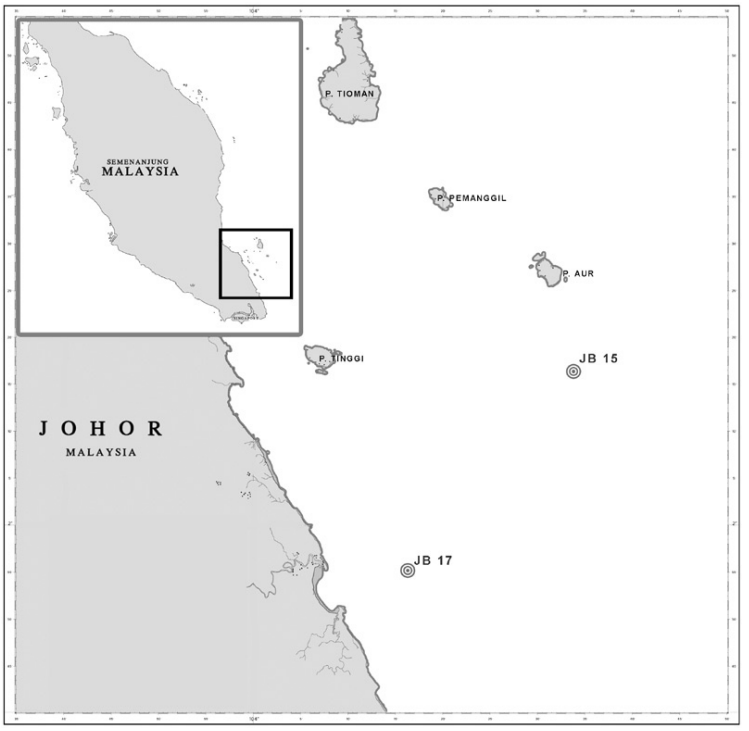

Fig. 1: Location of the core samples, JB15 (2° 16.250'N; 104° 33.850'E) and JB17 (1° 55.173'N; 104° 16.385'E) obtained in the study area

accumulation rate to various aspects of the environment, a research on the use of radionuclide (^{210}Pb) vertical profiles to determine the sedimentation rate was carried out.

MATERIALS AND METHODS

Sampling

The water circulation in Johore coastal water is strongly influenced by the East Asian monsoon system, where the circulation is predominantly cyclonic during the northeast monsoon (i.e. in the winter) and anti-cyclonic during the southeast monsoon in the summer (Wyrtki, 1961). The seasonal changes lead to significant variations in the mixed layer thickness, hydrographic properties and primary production (Gong *et al.,* 1992; Lui *et al*., 2002). Meteorologically, the Johore coastal water is influenced by the seasonal changes of monsoon which predominantly prevails from October to March each year. In this study, the sediment core sample was obtained from JB15, as shown in *Fig. 1*. Approximately 30 cm of the core sample was obtained and separated at 2 cm each. These samples were then dried in an oven and powdered before the chemical analysis was conducted.

Laboratory Analysis

^{210}Pb analysis was conducted based on the standard method (Carpenter *et al*., 1981). Briefly, 2g of the dried sample was placed in a beaker and digested with HNO_3 using a spike of 0.275ml of ^{209}Po. In order to maximize the detection of radioisotopes in the samples, both organic material and iron were removed with the treatment of H_2O_2 and HCL, respectively. The radioisotopes were concentrated into a solution by alternately heating it with acid $HClO_4$, HCl, and 6M of HCl on a hot plate at the temperature below 60°C for 24 hours. The sample solution was then centrifuged and plated onto a silver foil with the presence of ascorbic acid for 24 hours. Polonium-210 was also extracted using an auto deposition onto a silver plate and both the ^{210}Pb and ^{209}Po were analyzed using the alpha spectrometry counter known as the Canberra model.

Data Analysis

^{210}Pb was used to determine the sedimentation rates of the study areas (Krishnaswamy *et al*., 1971; Jones and Chenhall, 2001). The total ^{210}Pb activity was indirectly determined by the measurement of its alpha-emitting grand daughter nuclide, known as ^{210}Po (Kate, 2002). The measurement of ratio ^{210}Po and ^{209}Po activities will provide an adequate figure of supported ^{210}Pb as these two elements are assumed to be in equilibrium (Chung *et al*., 2004). Meanwhile, subtracting the supported ^{210}Pb from the total ^{210}Pb will determine the unsupported ^{210}Pb. The activity of ^{210}Pb is obtained using the formula proposed by Krishnaswamy *et al*. (1971), as follows:

Activity ^{210}Po (^{210}Pb) = A (dpm/g)

$$= \frac{\text{Actual } ^{209}\text{Po } (^{210}\text{Pb})}{\text{Actual } ^{209}\text{Po}} \text{ X } ^{209}\text{Po (24.74 dpm/g) X } \frac{\text{tracer weight } ^{209}\text{Pb (g)}}{\text{sample weight (g)}}$$

Where:
$A = A_o e^{-\lambda t}$ (*accumulative residual unsupported ^{210}Pb below the sediment age of t)*
$A_o = A / e^{-\lambda t}$ (*equal to the total unsupported Pb in the sediment column)*
$\lambda = \ln 2/t_{1/2} = 0.639$ (*decay constant of ^{210}Pb*)
$T_{1/2}$ = half-life (22.3 years)
t = depth (cm)/sedimentation rate in years

Inventory (I) of ^{210}Pb (unsupported) is expressed in dpm^{-2} and is calculated according to Carpenter (1981):

$$I = \Sigma A_i \rho_i h_i$$

Where:
A_i is the $^{210}Pb_{xs}$ (dpm g^{-1})
ρ_i represented the bulk density interval *i* (g cm^{-3})
h represented the thickness of the interval (cm)

Finally, the sedimentation rate is calculated using the following formula:

$A=A_o e^{-\lambda t}$
$A=A_o e^{-\lambda(x/S)}$
$\ln A=-(\lambda/S)x + \ln A_o$

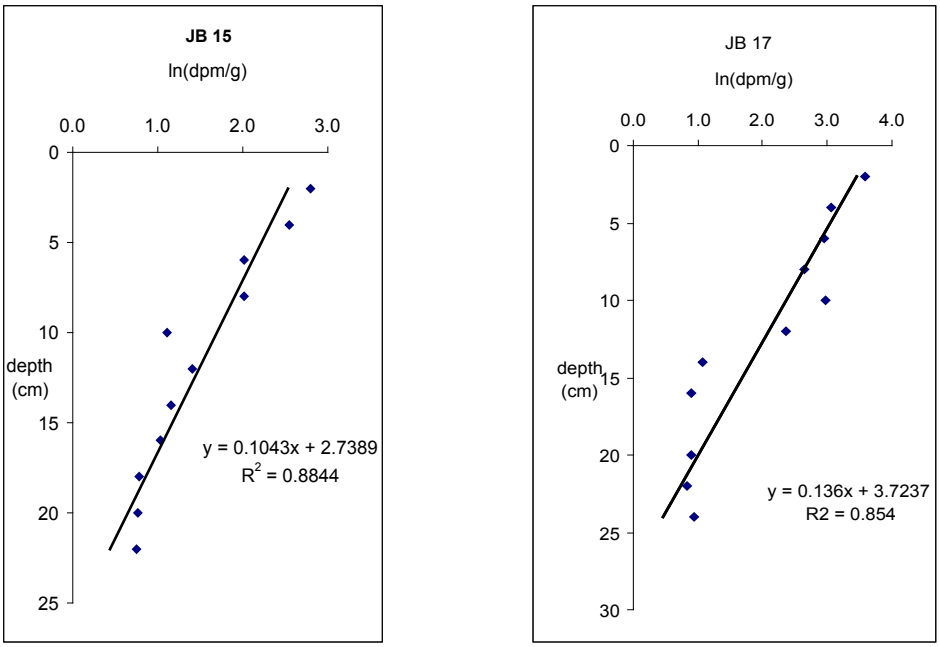

Fig. 2: The vertical distribution of ^{210}Pb in JB15 and JB17

Where:

A = Activity of excess ^{210}Pb in the sediment at any depth
A_o = Activity of excess ^{210}Pb in the freshly deposited sediment at depth=0 (the sediment-water interface)
S = Sedimentation rate in cm/year
λ = Radioactive decay constant (0.0311/year)
t = time in year

RESULTS AND DISCUSSION

Based on *Fig. 2*, the sedimentation rates in JB15 and JB17 were considered constant in the past 100 years, since the distribution of $^{210}Pb_{excess}$ was exponentially decreased according to depth (Tee *et al*., 2005). The bioturbation of the ^{210}Pb in both cores was shown as not significant as the R^2 value was higher than 0.80. However, JB17 which represented the activities of the ^{210}Pb was slightly uncertain compared to JB15, particularly at the depth of 10 cm to 16 cm.

The sedimentation rate of the study area was determined based on the assumption that the $^{210}Pb_{xs}$ was incorporated into the sediments at a constant rate (Chung *et al.,* 2004). Meanwhile, the "best curve" was identified based on the consideration of the graph vertical evenness of certain depth. As a result, the sedimentation rates of JB15 and JB17 of Johore coastal water was estimated as 0.38cmy^{-1} and 0.43cmy^{-1}, respectively. The sedimentation rate at JB17 was higher and this could be explained by the geographical position of the core, whereby their location is located near the estuary, or close to the mouth, providing it with 2 sediment sources known as fluvial and tidal. Greater water discharge from the river also brings much more suspended sediment to settle down to the sea bed. Assuming that the sedimentation rate values are accurate, this may imply that the sediments at the depth of 30 cm were deposited during the last 70 years.

The average sedimentation rate of this study was relatively higher compared to the study obtained in the northern South China Sea, which was 0.23 cm year^{-1} (Chung *et al*., 2004) but was much lower than the ones obtained for Terengganu estuary and Paka mangrove area which were 0.6cm yr^{-1} and 0.9cm yr^{-1}, respectively (Kamaruzzaman and Willison, 2005; Tan *et al*., 2004). The influence of the sedimentation rate in the South China Sea is mainly determined by the seasonal current movement, particularly the northeast monsoon and southeast monsoon. It is important to note that the sediment accumulation rate may be more significant during the northeast monsoon which increases the input of river in the coastal area.

ACKNOWLEDGEMENTS

This research was conducted with a joint funding from the Ministry of Science, Technology and Environmental, Malaysia, under the Intensified Research for Priority Areas (IRPA) project number 55016. The authors wish to express their gratitude to the Oceanography laboratory research teams for their invaluable assistance and hospitality throughout the sampling period.

REFERENCES

Burch, G.J., Barnes, C.J., Moore, J.D., Barling, R.D., Mackenzie, D.J. and Olley, J.M. (1988). Detection and prediction of sediment sources in catchments: The use of 7Be and 137Cs. In *Proceedings of theHydrology and Water Resources Symposium* (pp. 146–151). Aust. Nat'l Univ, Canberra.

Carpenter, R., Bennett. J.T. and Peterson, M.L. (1981). ^{210}Pb Activities in and fluxes to sediment of the Washington shelf and slope. *Geochimica et Cosmoschimica Acta, 45*, 1155-1172.

Cherry, R.D., Fowler, S.W., Beasley, T.M. and Heyraud, M. (1975). Polonium-210: Its vertical oceanic transport by zooplankton metabolic activity. *Marine Chemistry, 3,* 105-110.

Chung, Y., Chang, H.C. and Hung, G.W. (2004). Particulate flux and ^{210}Pb determined on the sediment trap and core samples from the northern South China Sea. *Continental Shelf, 24*, 673-691.

Goldberg, E.D. (1963). Geochronology with ^{210}Pb. Radioactive dating (pp.121-131). International Atomic Energy Agency, Vienna.

Gong, G.C., Liu, K.K., Liu, C.A. and Pai, S.C. (1992). The chemical hydrography of the South China Sea west of Luzon and a comparison with the west Philippine Sea. *Terrestrial, Atmospheric and Oceanic Science, 3*, 587– 602.

Jones, B.G. and Chenhall, B.E. (2001). Lagoonal and estuarine sedimentation during the past 200 years, In H. Heijins and K. Harle (Eds.), *Proceedings of the Archives of Human Impact of the last 200 years, Environment Workshop* (pp. 42 – 46). AINSE.

Kamaruzzaman, B.Y. and Willison, K.Y.S. (2005). The determination of estuarine sedimentation rates using artificial radionuclide profile. *Proceeding of the 4th Asia Pacific Symposium on Environmental Geochemistry*. January 6-9. Perth, Western Australia.

Kate, P. (2002). Use of Lead -210. Dating to Identify Recent Sedimentation in Estuaries: Case Study of Minnamurra River Estuary (pp. 342-345). School of Geoscience, University of Wollongong, NSW 2522.

Krishnaswamy, S., Lal, D., Martin, J.M. and Meybeck, M. (1971). Geochronology of lake sediments. *Earth and Planetary Science Letters II*, 407 – 414.

Lui, K.K., Chao, S.Y., Shaw, P.T., Gong, G.C., Chen, C.C. and Tang, T.Y. (2002). Monsoon forced chlorophyll distribution and primary production in the South China Sea: Observations and a numerical study. *Deep Sea Research I*, *49*, 1387-1412.

Price, K.R. (1991). The depth distribution of ^{90}Sr, ^{137}Cs, and ^{239}Pu, ^{240}Pu in soil profile samples. *RadiochimicaActa, 54*, 145–147.

Ritchie, J.C., Spraberry, J.A. and McHenry, J.R. (1974). Estimating soil erosion from the redistribution of fallout ^{137}Cs. *Soil Science Society of American Proceedings, 3*, 137–139.

Tan, C.S., Kamaruzzaman, B.Y. and Mohamed, C.A.R. (2004). Biogenic elements in the estuarine sediment: Case of Paka River, Terengganu. *Proceeding of the 3rd.Annual Seminar On Sustainability Science and Management*: *Role of Environmental Science and Technology in Sustainable Development of Resources*, Primula, May 4-5.

Tee, L.T. and Mohamed, C.A.R. (2005). Activities of 210Po and 210Pb in the water column at Kuala Selangor, Malaysia. *Journal of Environmental Radioactivity, 80*, 273-286.

Walling, D.E., He, Q. and Blake, W. (1999). Use of Be-7 and Cs-137 measurements to document short- and medium-term rates of water-induced soil erosion on agricultural land. *Water Resources Research, 35*(12), 3865–3874.

Wei, C.L. and Murray, J.W. (1994). The behavior of scavenged isotopes in marine anoxic environments: ^{210}Pb and ^{210}Po in the water column of the Black Sea. *Geochimica Cosmochimica Acta, 58*(7), 1795–1811.

Wyrtki, K. (1961). Physical oceanography of the Southeast Asian Water, *NAGA Reports*, *2,* pp.195. Scripp Institution of Oceanography, La Jolla, C.A.

ISSN: 0128-7680
Pertanika J. Sci. & Technol. **18 (1)**: 13 – 22 (2010)

Analysis of Stone Mastic Asphalt (SMA) Slab Dimensions for Evaluation of the Newly Developed Roller Compactor (Turamesin)

Jakarni, F.M.[1, 2*], Muniandy, R.[2], Hassim, S.[2] and Mahmud, A.R.[2]
[1]106 Ewart Road, Nottingham, NG7 6HH Nottinghamshire, United Kingdom
[2]Department of Civil Engineering, Faculty of Engineering,
Universiti Putra Malaysia, 43400 UPM, Serdang, Selangor, Malaysia
[*]E-mail: fauzan@eng.upm.edu.my

ABSTRACT

Stone Mastic Asphalt (SMA) is one type of asphalt mixture which is highly dependent on the method of compaction as compared to conventional Hot Mix Asphalt (HMA) mixture. A suitable laboratory compaction method which can closely simulate field compaction is evidently needed as future trend in asphalt pavement industry all over the world is gradually changing over to the SMA due to its excellent performance characteristics. This study was conducted to evaluate the SMA slab mixtures compacted using a newly developed Turamesin roller compactor, designed to cater for laboratory compaction in field simulation conditions. As the newly developed compaction device, there is a need for evaluating the compacted slab dimensions (which include length, width, and thickness), analyzing the consistency of the measured parameters to verify the homogeneity of the compacted slabs and determining the reliability of Turamesin. A total of 15 slabs from three different types of asphalt mixtures were compacted, measured, and analyzed for their consistencies in terms of length, width, and thickness. Based on study the conducted, the compacted slabs were found to have problems in terms of the improperly compacted section of about 30 mm length at both ends of the slabs and the differences in the thickness between left- and right-side of the slab which were due to unequal load distribution from the roller compactor. The results obtained from this study have led to the development of Turamesin as an improved laboratory compaction device.

Keywords: Asphalt mixtures, laboratory compaction, roller compactor, slab, stone mastic asphalt

ABBREVIATIONS

COV – Coefficient of Variation
HMA – Hot Mix Asphalt
n.d. – not dated
SMA – Stone Mastic Asphalt

INTRODUCTION

With a total land area of 329,758 km², Malaysia was linked by 73,402 km of roads in 2002 (Economic Planning Unit, 2004), with about 78% of the total road network comprise of paved roads, and the remaining are unpaved roads of natural soil or gravels (Hussain and Abd. Aziz, 2004). As compared to 1995, there was an increase of about 16.4% in the total road network system in 2003. Similarly, the number of vehicles between 1987 and 2002 grew from 3,674,484 to 12,021,939, with an average increasing rate of about 8% per year or three times more than in 1987 (Road Transport Department, 2003). Due to this massive traffic growth and higher axle loads,

[*]Corresponding Author

Fig. 1: Turamesin device

together with environmental and aging effects, there is a growing concern over rapid deterioration of the pavement. The consequences, initially in the forms of surface wear, rutting and cracking, if unattended to, would lead to more serious and irreparable damages, and consequently cause the pavement to lose serviceability life much earlier than expected (Wignall *et al*., 1991). Therefore, efficient techniques in designing and constructing roads are in demand so that the roads will perform better and last longer.

The application of Stone Mastic Asphalt (SMA) mixture is rapidly gaining acceptance due to its performance and excellent resistance to permanent deformation. In particular, an intriguing, alternative solution to overcome pavement problems (such as rutting and cracking) has become common with the use of conventional Hot Mix Asphalt (HMA) mixture. SMA is a gap graded asphalt surfacing material and it is stone-to-stone contact mixtures, whereby a high coarse aggregate content forms a skeletal matrix or interlocks to increase their stability. As a result, coarse stone-to-stone contact is prevalent in the SMA mixtures but it does not occur in conventional HMA. The HMA mixtures also have stone-to-stone contact, but most of this takes place within the fine aggregate particles which do not offer the same shear resistance as the SMA. This has resulted in loads for the SMA being carried by friction between the coarse aggregate particles instead of the asphalt binder and fine aggregates as in the conventional HMA mixtures (Brown and Manglorkar, 1993). Therefore, the SMA is highly dependent on the degree and method of compaction, which are related to the internal structure of the mixtures.

As the application of the SMA is rapidly gaining acceptance, there is a need for suitable laboratory compaction method that can closely simulate field compaction. The presently available laboratory compaction methods have intrinsic limitations due to the different modes in mechanical manipulation of the mixtures and different energy levels of compaction as compared to field compaction. Thus, they do not seem to be able to produce laboratory specimens that can truly represent the mixtures as it exists in the field, especially for the SMA mixtures (Button *et al*., 1992; Consuerga *et al*., 1992; Khan *et al*., 1998). Therefore, the researcher from Universiti Putra Malaysia (UPM), has come out with Turamesin, a newly developed laboratory compaction device, which was designed to provide a solution to the problem of producing laboratory specimens which are representative of materials laid and compacted in the field. *Figs. 1* and *2* show the Turamesin device which has the overall length and width of about 930 mm and 870 mm respectively, whereas the overall height is 474 mm, and the schematic drawing respectively.

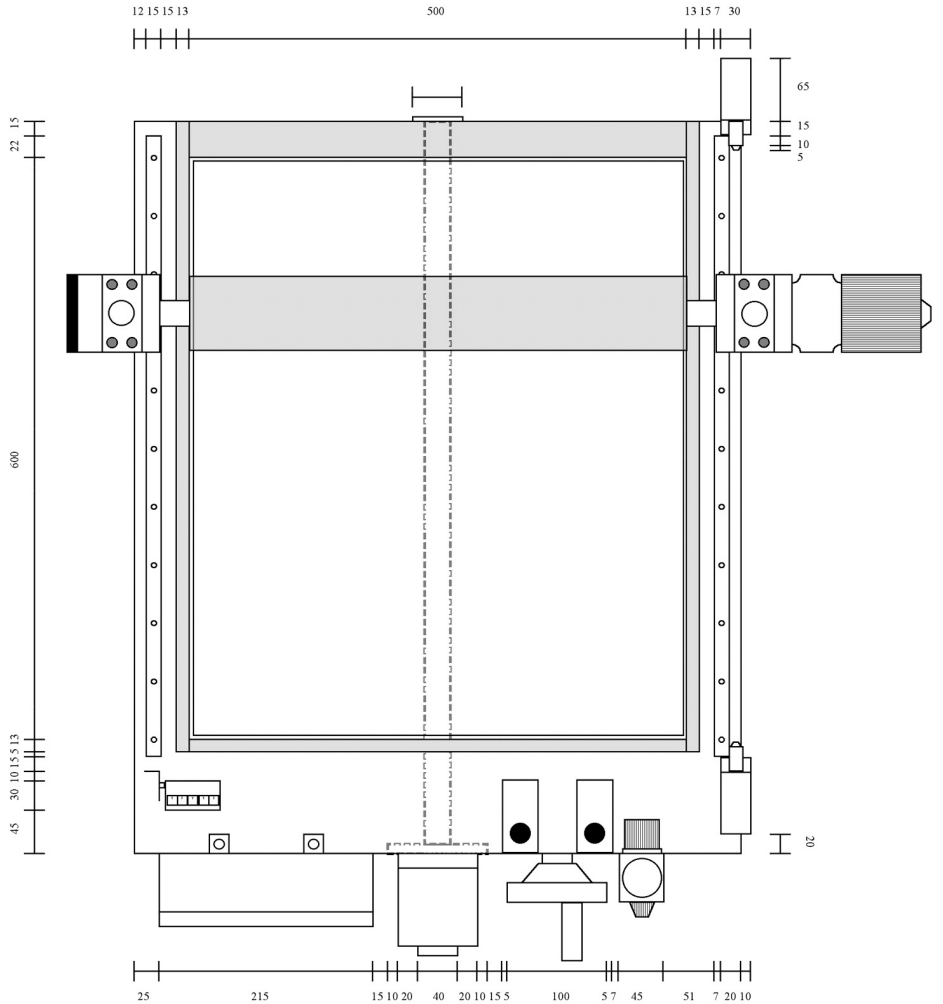

Fig. 2: Schematic drawing of Turamesin device

BACKGROUND

Turamesin is used to compact asphalt mix slab using a pneumatically powered steel wheel roller which is used just like the heavy duty steel wheel roller on-site. Different levels of pressure can be applied up to approximately 980 kPa (10.0 kgf/cm^2 or 142 psi) developed by a pneumatic system, and supplied through air compressor. Based on the preliminary studies conducted, Turamesin was developed based on 785 kPa (8.0 kgf/cm^2) of applied pressure and 75 numbers of passes that control the compaction efforts to yield the asphalt mix slab with the closest properties to in-service pavement of 4% air voids (Zaharudin and Muniandy, 2004; Jakarni and Muniandy, 2006). The thickness of the compacted slab can vary from 40 to 100 mm, depending on users' requirement. However, the compaction efforts of 785 kPa of applied pressure and 75 numbers of passes were developed based on the target thickness of the 70 mm slab.

As a newly developed compaction device, there is a need to evaluate the compacted slabs in terms of the slab dimensions and physical properties of the mixtures, so as to verify whether the slabs are uniformly compacted and to determine the ability and performance of Turamesin. This paper reports on the evaluation of the slab dimensions in terms of length, width, and thickness of the SMA mixtures compacted using Turamesin and the consistency analysis of the measured parameters of the slab dimension. This research was basically a sensitivity study to determine if significant differences in length, width, or thickness exist between the slabs and as a part of the verification for Turamesin. The results obtained from this study would lead to the development of Turamesin as an improved laboratory compaction device.

MATERIALS AND METHODS

Three types of asphalt binders (Grade 60/70, Grade PG76, and Grade 80/100) were utilized to consider a range of the SMA mixtures. The mineral aggregates used consisted of 14 mm nominal maximum aggregates size of granite and limestone as a mineral filler. Palletized cellulose fibres (VIATOP 80-20) were used as an additive and fibres were also added to the asphalt mixtures at a dosage rate of 0.3% by the total weight of the mixtures. Both the suitability of the aggregates and the asphalt binders taken into consideration in this study were determined by evaluating the characteristics of the material through various physical property tests. All the results obtained from the tests were conformed to the specification requirements.

Determination of the optimum asphalt content for each type of asphalt binders was done through the Marshall mix design analysis in accordance with ASTM D1559-89 Standard Test Method for Resistance to Plastic Flow of Bituminous Mixture using Marshall Apparatus and the optimum asphalt content values were found to be 5.60% for Grade 60/70, 6.04% for Grade PG76 and 6.05% for Grade 80/100, respectively. Then, five slabs were prepared for each type of asphalt binders which make up to a total of 15 slabs for the overall study. The slabs compacted in this study were designed to a target thickness of 70 mm. The target value of 4% for air voids was used in calculating the amount of materials required for each slab, based on the volume-density calculations. Each compacted slab was then measured for their length, width, and thickness. Vernier calliper of accuracy 0.20 mm was used to measure the thickness, whereas L-shaped ruler of accuracy 1.00 mm was to measure the length and width, respectively. The application of the L-shaped ruler of accuracy 1.00 mm is considered as sufficient due to the large values of length and width. Each recorded datum was then analyzed to determine the consistency of the measured parameters among the slabs. *Fig. 3* illustrates the sequence of the compaction procedures involved and the brief procedures are explained as follows.

i. Preheat Turamesin mould to a required compacting temperature. Apply grease on the surface of thin-steel plate, inner side of the mould area and collar, and roller compactor to prevent sticking.
ii. Place the thin-steel plate inside the mould.
iii. Transfer the asphalt mixtures from the mixing apparatus into the mould, and the temperature of the mixtures shall be within the compacting temperature range. Spread and level the mixtures uniformly throughout the mould using the level attached at the roller frame.
iv. Spade the surface of the mixtures rigorously with 25 freefall of tamping blows using a tamping plate. Repeat steps (iii) to (iv) when several batches of asphalt mixtures are required to be transferred from the mixing apparatus.
v. Set the required pressure for compaction by adjusting the pressure gauge and place a thermometer at one edge of the loosen asphalt mixtures to record the temperature during compaction.

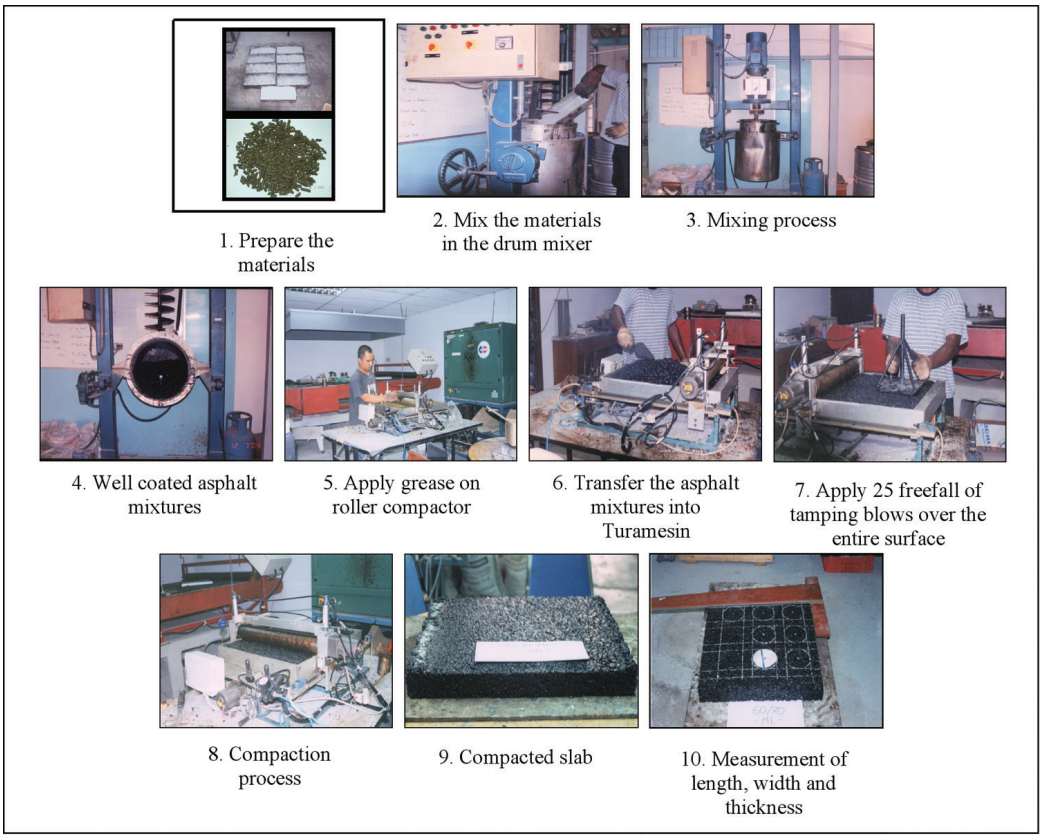

Fig. 3: Slab preparation and compaction procedures for Turamesin

vi. Release the roller compactor down so it will touch the surface of the mixtures and start compaction when the roller compactor frame is in position, i.e. where it touches the counter. Compaction is completed once the required number of passes is achieved.

vii. Turn the main switch off and allow the slab to cool to room temperature prior to removing it from the mould. Remove the side collars of the mould before sliding the slab off the mould and placing it on a clean, flat surface at the room temperature. Ensure that the thin-steel plate remains on the bottom of the slab while moving it to help support the slab and ensure minimum bending.

RESULTS

Table 1 shows the average, standard deviation, and coefficient of the variations of length and width measured at five different points of each slab. The average was calculated within each slab (using the length at each point), whereas the average, standard deviation, and coefficient of variations were calculated for each type of asphalt mixtures (using the average length of each slab). Based on the data presented in Table 1, it is noted that the variations of length and width between the slabs of the same type of asphalt mixtures was relatively low, as indicated by a small percentage of coefficient of variation. The average length and width of the slab were 589.84 mm and 500.36 mm for Grade 60/70, 590.12 mm and 499.48 mm for Grade PG76 and 589.96 mm and 500.16 mm, respectively.

TABLE 1
Length and width analysis

Asphalt mixtures	Slab	Length (mm)						Width (mm)					
		Pt.1	Pt.2	Pt.3	Pt.4	Pt.5	Average	Pt.1	Pt.2	Pt.3	Pt.4	Pt.5	Average
Grade 60/70	Slab 1	589	592	588	591	589	589.80	502	501	502	501	502	501.60
	Slab 2	591	592	592	593	590	591.60	501	502	500	501	502	501.20
	Slab 3	593	591	590	592	589	591.00	502	501	499	499	500	500.20
	Slab 4	589	590	590	589	586	588.80	498	500	499	499	500	499.20
	Slab 5	588	589	588	587	588	588.00	499	499	500	500	500	499.60
	Average						589.84						500.36
	[1]Std. Dev.						1.49						1.02
	[2]COV (%)						0.25						0.20
Grade PG76	Slab 1	591	588	590	589	588	589.20	499	500	498	500	499	499.20
	Slab 2	589	590	591	593	592	591.00	498	499	501	501	500	499.80
	Slab 3	591	590	588	589	589	589.40	499	498	499	499	500	499.00
	Slab 4	590	591	592	594	593	592.00	501	502	500	500	500	500.60
	Slab 5	588	590	589	589	589	589.00	499	499	498	499	499	498.80
	Average						590.12						499.48
	[1]Std. Dev.						1.32						0.73
	[2]COV (%)						0.22						0.15
Grade 80/100	Slab 1	588	586	589	587	589	587.80	499	500	498	501	502	500.00
	Slab 2	589	589	588	590	589	589.00	502	502	501	501	502	501.60
	Slab 3	590	589	589	590	591	589.80	500	499	498	499	500	499.20
	Slab 4	592	591	591	590	590	590.80	499	500	500	501	501	500.20
	Slab 5	590	594	592	592	594	592.40	501	499	500	499	500	499.80
	Average						589.96						500.16
	[1]Std. Dev.						1.75						0.89
	[2]COV (%)						0.30						0.18

Note: [1]Std. Dev - Standard Deviation
[2]COV - Coefficient of Variation

Table 2 shows the average thickness of the left-side and the right-side of the slabs respectively, measured at five different points for each slab, and also the difference in the thickness between the left- and right sides. It is also noted that the average thickness for the left-side and the right-side was 66.56 mm and 60.44 mm respectively for Grade 60/70, whereas these were 67.32 mm and 62.48 mm respectively for Grade PG76, and 65.72 mm and 60.48 mm respectively for Grade 80/100.

DISCUSSIONS

The general procedure for the analysis basically consists of performing a descriptive statistical analysis to determine the average, standard deviation, and coefficient of variation. The analysis is required to determine and analyze the consistency of length, width, and thickness of the slabs. This present work is basically a sensitivity study to determine if significant differences in length, width or thickness exist between the slabs. Similarly, based on length and width analysis, the significant differences between the slabs were also analyzed to determine whether the mould would potentially be affected by the compaction efforts of the roller compactor.

Coefficient of variation (COV) was used to evaluate and compare the variation between the data sets. Based on Volodin and Nom (n.d.), 25% or less is desirable for the cut-off value of coefficient of variation. Since there is no exact cut-off value, a pre-defined cut-off threshold value of 10% was used in this study to control the consistency level of the data sets. Based on the literature related to pavement areas, using the coefficient of variation as part of the data analysis, the selection of 10% as the cut-off value for the coefficient of variation seems to be reasonable (Kandhal, 1989; Wu and Hossain, 2003; Zhang, 2005).

Based on the data presented in Table 1, the variations terms of length and width between the slabs of the same type of asphalt mixtures were relatively low, as indicated by the small percentage of coefficient variation. From the analysis, the small coefficient of variation value, as compared to a predefined cut-off value of 10%, indicated that the length and width of the slabs were consistent with each other. However, the compacted slabs were found to have problems in terms of the improperly compacted section of about 30 mm length at both ends of the slabs (the encircled region) as shown in *Fig. 4*. These portions were not properly compacted due to end restriction of the mould and the roller compacter. However, unlike their length, the width of the slabs was completely covered from one side to another as the roller compactor makes its passes over the slab.

Slabs compacted in this study were designed to a target thickness of 70 mm. In the analysis, only the thickness along the length of the slabs was measured on both the left and right sides. The thickness along the width of the slabs was not included in the analysis since the end portions of the slabs along the width were not properly compacted. Based on the data given in Table 2, there was a significant difference in the thickness between the left-side and right-side although the variation of the thickness for each respective side of each asphalt mixture was relatively low, as indicated by the small percentage of coefficient of variation. Theoretically, there should be no difference in term of thickness as the slab was designed to a target thickness of 70 mm throughout the entire section.

Therefore, a hypothesis testing involving One-Sample t-Test procedure is required to determine whether there is any evidence of significant difference in the thickness between the left-side and right-side. The following hypotheses were then established.

i. The null hypothesis, H_o
   H_o: $\mu_{(Ln-Rn)} = 0$ (The average difference in the thickness between left-side and right-side is zero).
ii. The alternative hypothesis, H_1
   H_1: $\mu_{(Ln-Rn)} \neq 0$ (The average difference in the thickness between the left-side and right-side is not zero).

TABLE 2
Thickness analysis

Slab	Asphalt mixtures Grade 60/70			Asphalt mixtures Grade PG76			Asphalt mixtures Grade 80/100		
	Average Left-Side Thickness (mm)	Average Right-Side Thickness (mm)	Difference in Thickness between Left-Side and Right-Side (mm)	Average Left-Side Thickness (mm)	Average Right-Side Thickness (mm)	Difference in Thickness between Left-Side and Right-Side (mm)	Average Left-Side Thickness (mm)	Average Right-Side Thickness (mm)	Difference in Thickness between Left-Side and Right-Side (mm)
Slab 1	66.00	60.20	5.80	67.80	62.00	5.80	66.00	60.40	5.60
Slab 2	68.20	61.20	7.00	67.40	63.20	4.20	65.80	61.20	4.60
Slab 3	65.80	61.40	4.40	69.20	63.20	6.00	65.60	59.80	5.80
Slab 4	67.60	60.20	7.40	67.00	62.80	4.20	66.40	60.60	5.80
Slab 5	65.20	59.20	6.00	65.20	61.20	4.00	64.80	60.40	4.40
Average	66.56	60.44	6.12	67.32	62.48	4.84	65.72	60.48	5.24
[1]Std. Dev.	1.28	0.89	1.17	1.45	0.87	0.97	0.59	0.50	0.68
[2]COV (%)	1.92	1.47	19.14	2.15	1.39	20.12	0.90	0.83	13.06

Note: [1]Std. Dev - Standard Deviation
[2]COV - Coefficient of Variation

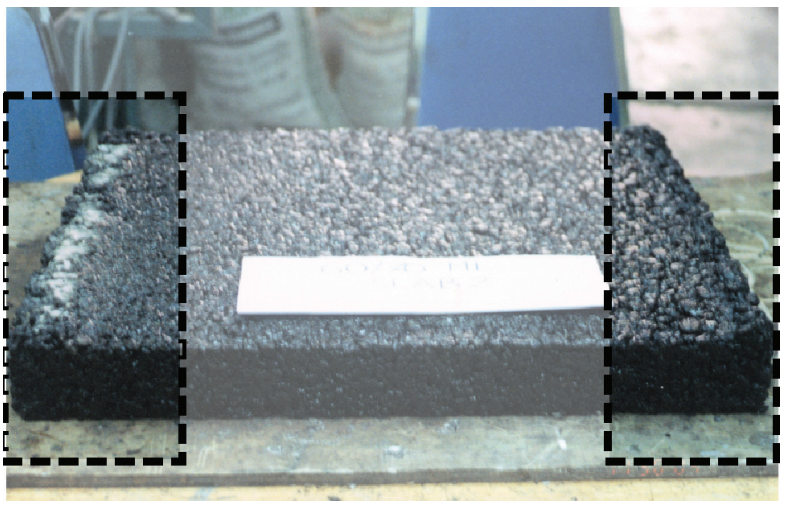

Fig. 4: Improperly compacted sections of slab

```
08-Aug-05 03:48:57 AM
Welcome to Minitab, press F1 for help.
One-Sample T: (Ln-Rn)
Test of mu = 0 vs mu not = 0

Variable          N      Mean     StDev   SE Mean
(Ln-Rn)          75     5.400     1.816     0.210

Variable              95.0% CI           T      P
(Ln-Rn)          (4.982,   5.818)    25.75  0.000
```

Fig. 5: MINITAB statistical analysis

Based on MINITAB statistical analysis, for a given sample size, n of 75 and level of significance, α of 0.05, the t-statistic, T was found to be 25.75 whereas the p-value was found to be 0.000 *(Fig. 5)*. The critical t-values were found to be ±1.9924, based on the (75-1) degrees of freedom and the area in the two tails of (0.025 + 0.025). Therefore, based on the value of t-statistic, T of 25.75, critical t-values of ±1.9924 and also p-value of 0.000, the null hypothesis, H_o is rejected at the level of significance, α of 0.05. The analysis shows that significant statistical difference exists in the thickness between the left-side and right-side. The average difference in term of thickness was 5.40 mm, as compared to the theoretical difference in the thickness of zero.

The difference in the thickness of the left-side and right-side was due to the unequal load distribution of the slab from the roller compactor during the compaction process. The motor, which is attached to one side of the roller compactor, has caused additional load and thus reduced the thickness on the respective side. Therefore, a proper adjustment should be made to balance the weight of the roller compactor so that an equally distributed load can be applied on the surface of the slab.

Moreover, the thickness of the slab was found to be less than the target thickness of 70 mm. This could possibly be attributed to many factors; nevertheless, it was most likely due to the whole process of sampling, mixing, transferring the asphalt mixtures as well as compacting which had caused some mixtures to be left behind. Although the thickness was found to be less than the target thickness of 70 mm, it had no significant effect on the slab properties. A tolerance of ±10 mm offset from the target thickness is allowed since the measurements of thickness were recorded manually. However, careful measurements should be taken prior to the compaction process so as to minimize the amounts of leftover mixtures.

CONCLUSIONS

Based on the statistical analysis conducted, the compacted slabs were found to have an average area of 590 mm of length by 500 mm of width and their thickness ranged from 60 mm to 68 mm. On the average, the variability of the measured parameters of length, width, and thickness for all the slabs were generally low. Therefore, it could be concluded that the mould of the Turamesin was rigid enough to withstand the compaction efforts from the roller compactor. However, the compacted slabs were found to have improperly compacted section of about 30 mm in length at both ends of the slabs and the difference in the thickness between left-side and right-side of the slab. Therefore, the roller compactor of Turamesin should be adjusted so that an equally distributed load could be applied over the slab during the compaction process. Motor, which is attached to one side of the roller compactor, should be removed or balanced on the other side to eliminate the problem in terms of the differences in thickness.

ACKNOWLEDGEMENT

The authors would like to thank the Department of Civil Engineering, Universiti Putra Malaysia for providing the required facilities and support to this project and to all the people who were directly and indirectly involved in the project for their help and co-operation given throughout this study.

REFERENCES

Brown, E.R. and Manglorkar, H. (1993). *Evaluation of laboratory properties of SMA mixtures* (Research Report-NCAT Report No. 93-5). Alabama: NCAT Auburn University.

Button, J.W., Little, D.W., Jagadam, V. and Pendleton, O.J. (1992). *Correlation of Selected Laboratory Compaction Methods with Field Compaction*. Texas A&M University, College Station: Texas Transportation Institute.

Consuerga, A., Little, D.N., Quintus, H.V. and Burati, J. (1992). Comparative evaluation of laboratory compaction devices based on their ability to produce mixtures with engineering properties similar to those produced in the field. *Transportation Research Record, 1228*, 80-87.

Economic Planning Unit. (2004). *Malaysian Quality of Life 2004.* Malaysia: Prime Minister's Department: Putrajaya.

Hussain, M.Z. and N. Abd. Aziz. (2004). Pavement recycling experience in Malaysia. *Ikram's International Seminar on Asphalt Pavement Technology II.* Putrajaya, Malaysia.

Jakarni, F.M. and Muniandy, R. (2006). *Properties of stone mastic asphalt slabs compacted using a newly developed roller compactor*. Thesis, Universiti Putra Malaysia.

Khan, Z.A., Wahab, H.I., Asi, I. and Ramadhan, R. (1998). Comparative study of asphalt concrete laboratory compaction methods to simulate field compaction. *Construction and Building Materials, 12*, 373-384.

Kandhal, P.S. (1989). *Testing and evaluation of large stone mixes using marshall mix design procedures* (Research Report-NCAT Report No. 89-4). Alabama: NCAT Auburn University.

Road Transport Department. (2003). *Statistics on Number of Vehicles in Malaysia (1987-2002)*. Malaysia: Road Transport Department of Malaysia.

Volodin, A. and Nom, P. (n.d.). Quandaries and Queries. In *Math Central.* Retrieved on September 28, 2005 from http://www.mathcentral.uregina.ca.

Wignall, A., Kendrick, P.S. and Ancill, R. (1991). *Roadwork-Theory and Practice* (3rd ed.). Oxford, UK: BH Newnes.

Wu, Z. and Hossain, M. (2003). *Pilot instrumentation of a superpave test section at the kansas accelerated testing laboratory* (Research Report-KSU Report No. 98-2). Manhattan: Kansas State University.

Zaharudin, M.F. and Muniandy, R. (2004). *Evaluation of turamesin for SMA slab compaction.* Thesis, Universiti Putra Malaysia.

Zhang, C. (2005). *Comparative Study of the physical and mechanistic properties of hma mixture: field vs. laboratory*, MSc Thesis, Louisiana State University.

ISSN: 0128-7680
Pertanika J. Sci. & Technol. **18 (1)**: 23 – 32 (2010)

Determination of Leaf Area Index for Oil Palm Plantation Using Hemispherical Photography Technique

M. A. Awal[1*], W. I. Wan Ishak[2] and S.M. Bockari-Gevao[2]
[1]Department of Farm Power and Machinery,
Bangladesh Agricultural University, Mymensingh-2202, Bangladesh
[2]Department of Biological and Agriculture Engineering,
Faculty of Engineering, 434000 UPM, Serdang, Selangor, Malaysia
[3]Department of Agril. Engg. Njala Univ. of Sierra Leone
[*]E-mail: awalbau@gmail.com

ABSTRACT

The present conventional (destructive) method used in determining LAI is laborious, difficult and time consuming. Thus, an image-based measurement using camera system with fish eye lens offers an alternative means for an accurate indirect measurement of LAI in oil palm. In this study, a methodology was developed to improve the leaf area index of the oil palm determination using hemispherical photography as an indirect method. A set of true LAI data, collected using the destructive method, were used as a reference to calibrate the LAI measurements obtained by the hemispherical photography. A good relationship (r = 0.85) was found between age of palm and hemispherical photographic LAI. However, the estimated LAI obtained by the hemispherical photographic method was underestimated as compared to the destructive method. Some means of calibration was necessary to determine the relationship between the actual LAI and the hemispherical photographic LAI. It was necessary to multiply the LAI value from 5 years to 16 years, by a clumping factor of 2.14 for 5 to 9 year old palms, 2.33 for 10 to 14-year old palms and 2.37 for above 15-year old palms to calculate the accurate LAI values. For palms which are less than 5 year old (i.e. 2 to 3 years in this study), the photography LAI value was equal to the calculated LAI value. This proposed that correction factors would solve this underestimation effect. In addition, two equations were also proposed to estimate the true LAI from the Photographic LAI for immature and mature oil palm plantation.

Keywords: Oil palm, digital camera, Leaf Area Index, measurement

INTRODUCTION

Leaf area index (LAI) of the oil palm plantation can be described as the ratio of the total leaflet area of the plantation to the total ground area of that plantation. Leaf Area Index (LAI) describes a fundamental property of the oil palm canopy and it is an important index which is related to the growth and metabolism of plant, as well as the accumulation of dry matter and yield (Awal, 2006). A variety of methods have been proposed for ground-based and remote estimation of LAI, and they have led lead to confusion and uncertainty in relation to the selection of methods, experimental design, and instrumentation (Hall, 2003). Destructive methods for the measurement of leaf area index in oil palm plantation are time consuming, difficult, can increase labour cost and are not suitable for tall palms. Several non-destructive methods, which utilize light attenuation through plant canopy to estimate the amount (and in some cases, the orientation of foliage) have been developed (Feldkirchner and Gower, 2001). For optical measurement of the LAI, an indirect method such as the LAI-2000 plant canopy analyzer (LI-COR, USA) is often preferred over

[*]Corresponding Author

conventional and laborious destructive methods. However, an increasing number of studies have indicated that the LAI-2000 tends to underestimate the LAI (Stenberg *et al.,* 1994; Nilson, 1999). Hemispherical canopy (fisheye) photography is a technique which has been successfully used under different canopy light regimes in the forest environments to measure the structure of canopy (LAI). This technique has been widely used in crops and forests for more than 40 years. Hill (1924) was the first to design the hemispherical (fisheye) lens to view the whole sky in order to study the formation of clouds. Meanwhile, Evans and Coombe (1959) studied woodland light environments to apply hemispherical photography, and they were probably the first researchers to use this technique for biological purposes. After that, a number of studies (Rich *et al.,* 1993; Easter and Spies, 1994; Breshears *et al*., 1997) have been carried out for the assessment of light environment under forest or plant canopy using hemispherical photography. Among other, Gardingen *et al.* (1999) and Macfarlane *et al.* (2000) successfully used hemispherical photography to estimate the leaf area index of clumped canopies in forest environments. In this study, a fish-eye lens which is incorporated with high pixel digital camera was proposed to be used for estimating LAI in oil palm plantation. Therefore, the main objective of this study was to examine the performance of the new hemispherical photography technique in estimating accurate LAI of oil palm plantation.

MATERIALS AND METHODS

Study Locations

A series of hemispherical canopy photographs were obtained to demonstrate the operation of the system under different amounts of canopy cover and clumping. The first set of images was collected on 15 April 2004 in immature and semi mature (3-year and 6-year) old palms at ENOVECY research plot, Malaysia Palm Oil Board (MPOB), located in Bangi, Kuala Lumpur, Malaysia, whereas the second set of images was collected from the MPOB field plot, located in Bangi Lama (Latitude 2^{o} $58^{/}$ $0.36^{//}$ N, Longitude 101^{o} $44^{/}$ $26^{//}$ E), at an average altitude of 66.5m from the sea level for both immature and mature palms (2, 9, 12 and 16-year old palms).

Experimental Design

Two types of experimental design were used for the two palm age groups, namely immature palm (age < 5-years) and mature palm (age > 5 years). Single palm photography (i.e. the photographs taken from every palm) was used for immature planting (Plate 3) as the fronds were too small and not overlapping or touching the neighbouring palms frond. As there was no coverage in between the palms, triangular photography method was therefore not applicable for immature plantation. The equilateral triangle photography method (i.e. photographs taken in between three palms) was used for mature planting (Plate 2). Immature oil palms were situated adjacent to the mature oil palm plantings. All the palms were located with the use of the oil palm planting field maps for the study area. A total of six age groups of palms (2, 3, 6, 7, 9, 12, and 16 years) were selected for the investigation. For every age group of oil palm plantation, four plots were selected for the experiment. The minimum plot size was 1.0 hectare. From every plot, 10 palms were selected for photography. An oil palm tree within the plot was randomly selected to minimize the variability of the LAI. Palms with uniform growth were selected to minimize the variation of the results in each plot. In the investigation of this study, planting materials DxP were used for all age groups of palms. *Figs. 1* and *2* illustrate the experimental design for immature and mature oil palm plantations, respectively.

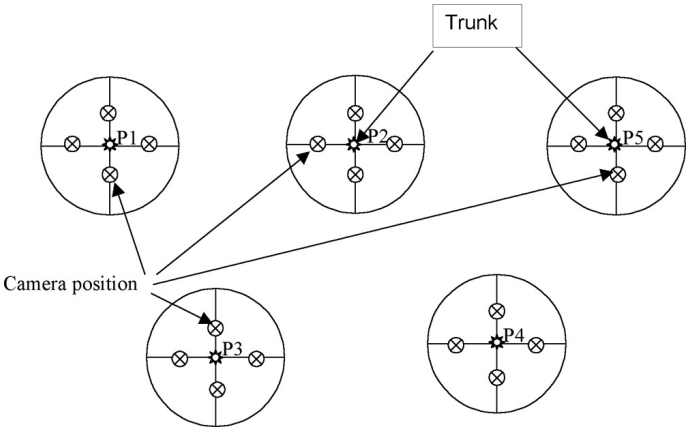

Fig. 1: Experimental design for immature oil palms

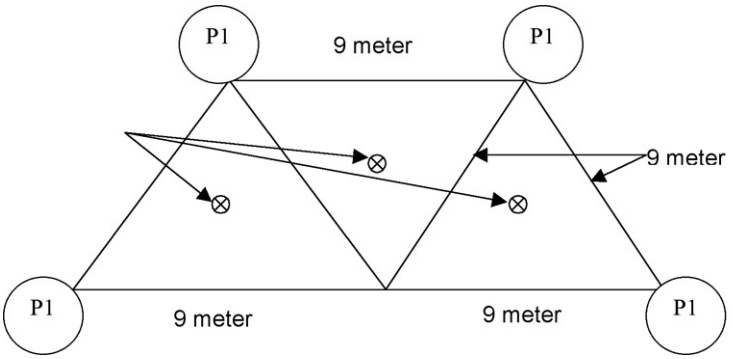

Fig. 2: Experimental design for mature oil palms

Image Acquisition and Analysis

A total of 240 good quality photos with high contrast images were chosen from the field to demonstrate the operation of the system under different amounts of canopy cover and clumping. Two sets of images were taken from two different sites. One set of images was collected in April 2004 at immature oil palm plantation (3-years) and mature oil palm plantation (6-years) at the MPOB research plot in Bangi. Meanwhile, another set of images was collected in May 2004 from the MPOB, UKM Research Station, in Bangi. Sampling locations were chosen to give a range of canopy cover and gap sizes. About 70 to 80 images were captured from each palm age group. Then, 40 best images were selected based on their quality and contrast. It is important to note that sufficient care was taken into consideration when selecting images to ensure that the selected images were free from any kinds of fault.

Images were recorded using a Nikon Coolpix 4500 mega pixel digital camera, (Fuji, Tokyo 100-8331, Japan) with a self-levelling mount and SLM2 type tripod, Delta-T Devices Ltd, UK (Plate 1). All images were taken with a high resolution of 2272 x 1704 pixels. In mature oil

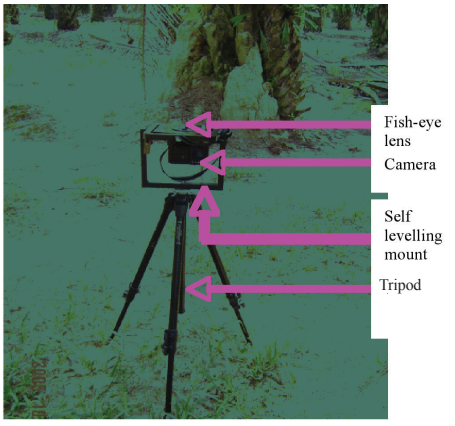

Plate 1

Plate 2

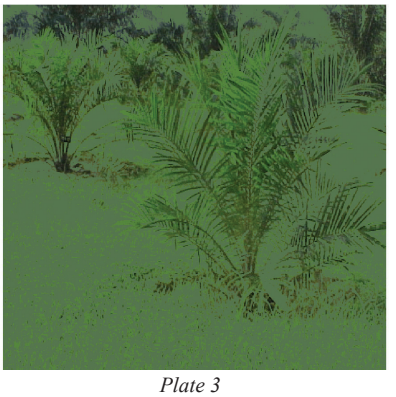

Plate 3

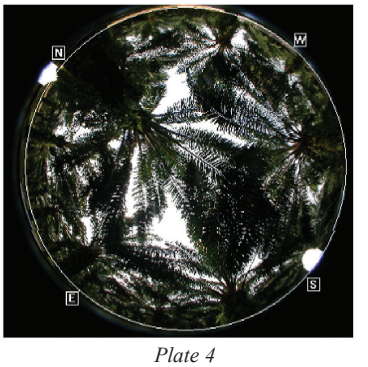

Plate 4

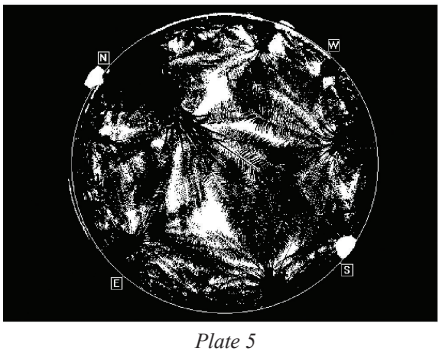

Plate 5

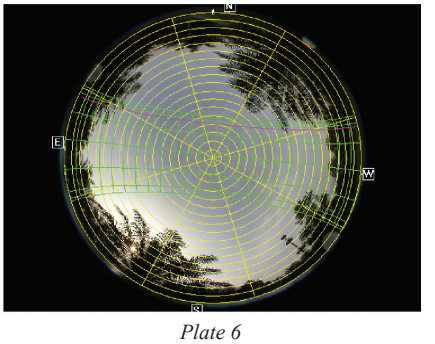

Plate 6

Plate 1: Hemispherical photographic system
Plate 2: Image taken by hemispherical photographics system in mature
Plate 3: Immature oil palm plantation oil palm plantation
Plate 4: Original RGB hemispherical photographics for mature palm
Plate 5: Gray scale (after image processing)
photograph for mature palm
Plate 6: Image processing photograph for mature palm

palm planting, images were taken in the middle position among three adjacent palms, as shown in *Fig. 2*. The camera was set on the tripod at 0.8 meter above the ground level. All images were taken immediately before all the foliage was harvested from the trees for destructive determining of the LAI. In immature oil palm planting, images were captured for each selected palm. Four photographs were taken from each palm oil tree. The self-levelling mount was detached from the tripod before the images were captured. A self-levelling mount with tripod was not used in the immature palm plantation because the lowest fronds of the immature oil palm were situated about 0.2 to 0.4 metre above the ground level. Therefore, the images were captured using the camera with a self-levelling mount which was placed at the ground level. The camera was oriented to magnetic north using integrated compass. Some images were recorded under conditions of diffuse skylight, normally after sunrise or immediately before sunset, and some images were taken in an overcast sky condition. These images were then analysed on a 60 MHz Pentium-IV computer (Dell Computer Corporation, Malaysia) configured with 256 MB RAM. Pictures were analyzed (conversion of the grey image into a binary of 1 bit image) according to a user-defined threshold and LAI calculation using image analysis software Hemi View, (Version 2.1, Delta –T Devices, UK). The LAI was derived from the gap fractions covering zenith angles of 0–90^{o}. The software was run using Microsoft Windows XP.

RESULTS AND DISCUSSION

Computation of Results

Hemi View software provides a toolbar for a wide range of results calculation. The results of the analysis are the output to a compatible worksheet in Excel 5.0, which can be further analysed within the Hemi View environment. The output obtained from the result of the image analysis are the proportion of visible sky in the sky map sectors, indirect side factor, direct site factors, direct radiation above and below canopy, diffuse radiation above and below canopy, leaf area index, mean leaf angle, etc. The procedures for the computation of results are important task, therefore they require more caution. A wide range of results computation procedures was utilized in this study. All the different oil palm age groups (namely 2, 3, 7, 9, 12, and 16 year) selected in this study were analyzed using the same procedure. Meanwhile, the statistical analysis was performed using the SPSS software, version 11.5. A simple descriptive statistics was also used to characterize the means and standard deviations in the datasets. For this purpose, at least 40 locations were selected from each of the four plots and one photograph was taken for each location. Each photograph was analyzed 4 to 8 times in order to minimize the spatial effects on the results *(Plates 4, 5, and 6)*.

Estimation of LAI by Hemispherical Photography

At least 240 photographs (representing 240 locations) were analyzed for the LAI calculation. Table 1 presents of the results gathered from the statistical analysis performed on the mean LAI. The range of LAI values for the 2 year old palms was 0.59 to 0.76, and this was 1.59 to 1.67 for the 12-year old palms. The maximum average LAI value observed for the 16-year old palms was 1.70, whereas the average LAI values for the 9, 7, and 3 year old palms were 1.59, 1.16 and 1.06, respectively. The largest variation (28%) of mean LAI was observed for the 2 year old palms, while the lowest variation (5%) of mean LAI was detected for the 12 year old palms. These results indicate that the variation of LAI at a particular site, even within a plot, is not dependent on the age of the palms. On the contrary, this variation is usually dependent mainly on the spatial variation of the canopy, physiological vigour of the palm and the management practices. The results also show that the LAI values were underestimated for the mature palm age group,

TABLE 1
Summary of average LAI measured by hemispherical photography

Palm age (Year)	Leaf area index (LAI)	95% Confidence interval	
		Lower	Upper
2	0.680±0.025	0.599	0.761
3	1.065±0.028	0.977	1.154
7	1.161±0.008	1.139	1.184
9	1.594±0.014	1.549	1.636
12	1.635±0.014	1.591	1.679
16	1.710±0.045	1.566	1.854

and this underestimation was closer to that found by Craig *et al*. (2000). As for the immature palm groups, however, the LAI values were found to be the closest to that of the destructive method.

The Relationship between Photographic LAI and Palm Age

Fig. 3 shows the relationship between hemispherical photographic LAI and the age of palm trees. A strong relationship ($R^2 = 0.73$) was found between the age of palm trees and hemispherical photographic LAI through a linear regression analysis. The results indicate a high degree of association (r = 0.85) between age of palm and photographic LAI with a standard error of estimation of 0.19. The standard error of estimate of coefficient was 0.01, whereas the standard error of estimate of constant was 0.21 for the linear analysis.

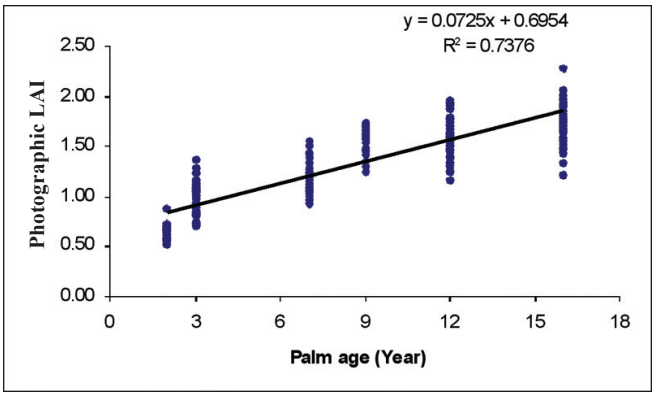

Fig. 3: Relationship between palm age and photographic LAI

A Comparison between Destructive LAI and Photographic LAI

Table 2 shows the LAI values for the different age groups of palms for both the destructive and photographic methods. For the 2 and 3 year old palms, the photographic LAI values were much closer to the true LAI (calculated by the destructive method). The observed photographic LAI values for the immature palms were less than 0.5% underestimated, as compared to the LAI values obtained by the destructive method. As for the mature palm groups (age ranging from six years

and above), the photographic LAI values were found to be underestimated when compared to the destructive method.

TABLE 2
LAI values obtained from the destructive method and the photographic method

Palm age (Year)	LAI	
	Destructive method	Photographic method
2	0.69	0.68
3	1.07	1.06
7	2.49	1.16
9	3.41	1.59
12	3.83	1.64
16	4.05	1.71

The Relationship between Photographic LAI and Destructive LAI

The relationship between the photographic LAI and the destructive LAI (obtained using the destructive method) can be established using a linear regression analysis. *Fig. 4* illustrates the relationship between the photographic LAI and destructive LAI for all age groups of palms (i.e. mature and immature). A strong linear relationship was found between the destructive LAI and the photographic LAI using the linear regression analysis. The results show that the data fitted strongly in the linear regression model. The linear regression analysis indicated a high degree of association between the destructive LAI and the photographic LAI with r = 0.93 and a low standard error of estimate of 0.43. Meanwhile, the standard error estimation of coefficient was 0.47. The following equation was proposed for estimating the true LAI from the photographic LAI:

$$LAI_t = 0.2555 * LAI_p + 0.6432 \quad (1)$$

Where, LAI_t is the true LAI and LAI_p is the photographic LAI obtained using the hemispherical photography. This model could be used to estimate the LAI for both mature and immature palms.

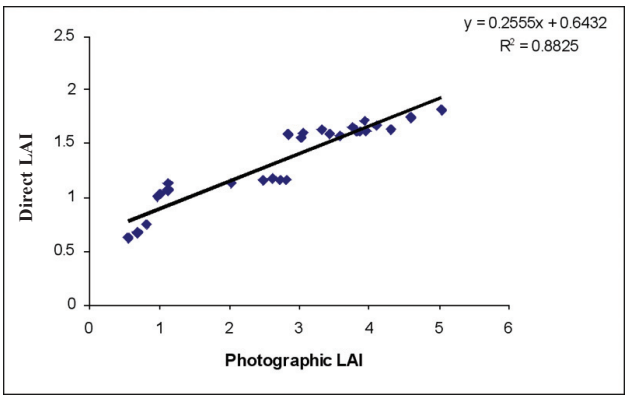

Fig. 4: The relationship between the photographic LAI and the destructive LAI for both mature and immature palms (2 to16 year old palms)

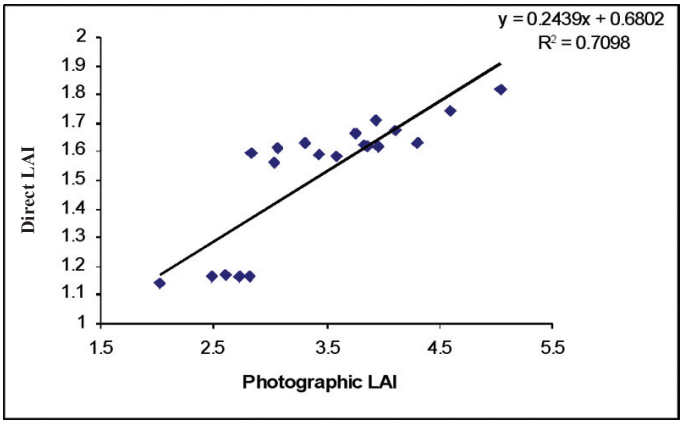

Fig. 5: The relationship between the photographic LAI, and the destructive LAI for mature palms

Fig. 5 shows the relationship between the photographic LAI and the destructive LAI for the mature palm groups (> 6 year old). A strong linear relationship was found between direct LAI and photographic LAI for the mature palms. The results show that the data fitted strongly in a linear regression model. The linear regression analysis indicates a high degree of association between the destructive sampling LAI and the photographic LAI, with r = 0.83 and a low standard error of estimate of 0.18. Meanwhile, the standard error estimation of coefficient was 0.43. Based on this observation, the following equation was proposed to be used in estimating the true LAI from the photographic LAI:

$$LAI_t = 0.2439 * LAI_p + 0.6802 \quad (2)$$

Where, LAI_t is the true LAI and LAI_p is the photographic LAI obtained by the hemispherical photography. The relationship between the photographic LAI and the destructive LAI was observed as linear with slope of 1:1, implying that the hemispherical photographic method could be useful for estimating the true LAI without calibration. Therefore, the model (Equation 2) is useful for estimating the true LAI for mature palms.

Determination of Correction Factor

As other photographic method of the LAI estimation, hemispherical photography generally gives an underestimation of the LAI values as compared to the destructive method. This underestimation was mainly observed for multiple canopy layers (clumping of the foliage) of oil palms. Thus, it was necessary to determine the correction factor for the true LAI estimation using the hemispherical photographic method. The application of a simple correction factor presumes a linear relationship between the true (destructively estimated) LAI and the indirect estimate of LAI provided by the hemispherical photography. Therefore, linearity between destructive and indirect LAI estimates could be useful, even without knowing the correction factor. Hence, observation on the changes of LAI is more important than knowing the absolute amount of leaf area presents at some specific age of the oil palms in monitoring their growth. The following approach was used to estimate of the correction factor:

$$LAI_t = LAI_p * C_f \quad (3)$$

$$C_f = \frac{LAI_t}{LAI_p} \quad (4)$$

Table 3 presents the numerical calculation of the correction factor for 2 to16 year old palms.

TABLE 3
Factor calculation of the photographic LAI measurement

Palm age (year)	Correction factor
2	1.007299
3	1.004695
7	2.146552
9	2.144654
12	2.335366
16	2.368421

CONCLUSION

LAI has often been used as a critical variable to simulate the growth and yield models, but it is difficult to measure destruction for oil palms. The present conventional method used in determining LAI is rather laborious, difficult and time consuming. Thus, an image-based measurement using a camera system with fish eye lens offers an alternative means for an accurate indirect measurement of LAI in oil palm. In this study, a new methodology was developed to improve the leaf area index of the oil palm determination using the hemispherical photography as an indirect method. A set of the true LAI data, which were collected using the destructive method, were used as a reference to calibrate the LAI measurements obtained by hemispherical photography.

The LAI values obtained by the hemispherical photographic method were underestimated as compared to the destructive method. However, the underestimation was systematic, indicating that some means of calibration were necessary to determine the relationship between the actual LAI and the hemispherical photographic LAI. The proposed correction factors are used to solve this underestimation effect. Once again, the two proposed equations could be used to estimate the true LAI from the photographic LAI. Finally, the hemispherical photographic method can be concluded as a useful tool which can confidently be used to estimate the LAI of oil palms. Moreover, it can also be used to estimate the leaf area index (LAI), apart from being reliable as compared to those which were obtained from other indirect methods.

ACKNOWLEDGMENTS

We acknowledged the co-operation of Dr. Johari from the Faculty of Engineering, UPM, Dr. Haniff, Senior Research Officer at the MPOB and MPOB, for giving us invaluable comments, logistic support, and providing us with the laboratory facilities as well as the permission to harvest the fronds. The authors would also like to thank the Ministry of Science, Technology and Innovation for the financial support granted to run this study.

REFERENCES

Awal, M.A. (2006). *Image-based measurement of leaf area index and radiation interception for modelling of oil palm*, PhD Thesis, Universiti Putra Malaysia.

Breshears, D.D., Rich, P.M., Barnes, F.J. and Campbell, K. (1997). Overstory-imposed heterogeneity in solar radiation and soil moisture in semiarid woodland. *Ecological Applications*, *7*, 1201-1215.

Craig M., Coote, M., Donald, A.W. and Mark, A.A. (2000). Photographic exposure affects indirect estimation of leaf area in Plantations of *Eucalyptus globulus* Labill. *Agricultural and Forest Meteorology*, *100*, 155–168.

Easter, M.J. and Spies, T.A. (1994). Using hemispherical photography for estimating photosynthetic photon flux density under canopies and in gaps in Douglas-fir forests of the Northwest Pacific. *Canadian Journal of Forest Research, 24,* 2050-2058.

Evans, G.C. and Coombe, D.E. (1959). Hemispherical and woodland canopy photography and the light climate. *Journal of Ecology*, *47*, 103–113.

Feldkirchner, D.C. and Gower, S.T. (2001). Using the li-cor LAI-2000 to estimate leaf area index and light transmittance in forest canopies. Methodology paper series of the *4th International Conference on ILTER in East Asia and Pacific Region* (pp.12-14). Ulaanbaatar-Hatgal, Mongolia.

Gardingen, P.R., van Jackson, G.E., Daumas, S.H., Russell, G. and Sharp, L. (1999). Leaf area index estimates obtained for clumped canopies using hemispherical photography. *Agricultural and Forest Meteorology*, *94*, 243-257.

Hall, R.J., Davidson, D.P. and Peddle, D.R. (2003). Ground and remote estimation of leaf area index in Rocky Mountain forest stands, Kananaskis, Alberta. *Canadian Journal of Remote Sensing*, *29*(3), 411–427.

Hill, R. (1924). A lens for whole sky photographs. *Quarterly Journal of the Royal Meteorological Soc*iety, *50*, 227-235.

Hemi View User Manual. Version 2.1, Delta-T Devices Ltd, 128 Low Road.

dMacfarlane, C., Coote, M., White, D.A. and Adams, M.A. (2000). Photographic exposure affects indirect estimation of leaf area in plantations of Eucalyptus globulus Labill. *Agricultural and Forest Meteorology*, *100*, 155–168.

Nilson, T. (1999). Inversion of gap frequency data in forest stands. *Agricultural and Forest Meteorology, 98–99*, 437–448.

Rich, P. M., Clark, D. B., Clark, D. A. and Oberbauer, S.F. (1993). Long-term study of solar radiation regimes in a tropical wet forest using quantum sensors and hemispherical photography. *Agricultural and Forest Meteorology*, *65*(1-2), 107-127.

Stenberg, P., Linder, S., Smolander, H. and Flower-Ellis, J. (1994). Performance of the LAI-2000 plant canopy analyzer in estimating leaf area index of some Scots pine stands. *Tree Physiology*, *14*, 981–995.

ISSN: 0128-7680
Pertanika J. Sci. & Technol. **18 (1)**: 33 – 41 (2010)

Neural Networks for Forecasting Daily Reservoir Inflows

Shahram Karimi-Googhari[1], Huang Yuk Feng[2], Abdul Halim B Ghazali[3] and Lee Teang Shui[4*]

[1]Department of Water Engineering, Shahid-Bahonar University of Kerman, Kerman, I.R. Iran

[2]National Hydraulic Research Institute of Malaysia, Ministry of Natural Resources and Environment, 43300 Seri Kembangan, Selangor, Malaysia

[3]Department of Civil Engineering, Faculty of Engineering,

[4]Department of Agricultural and Biological Engineering, Faculty of Engineering, Universiti Putra Malaysia, 43400 UPM, Serdang, Selangor, Malaysia

[*]E-mail: tslee@eng.upm.edu.my

ABSTRACT

Proper integrated management of a dam reservoir requires that all components of the water resource system be known. One of these components is the daily reservoir inflow which is the subject matter of this study, i.e. to establish predictions of what is coming in the next rainfall-runoff process over a catchment. The transformation of rainfall into runoff is an extremely complex, dynamic, and more of a non-linear process. The available six-year average daily rainfall data across the Sembrong dam catchment were computed using the well-known Theissen's polygon method. Daily reservoir inflow data were extracted by applying the water balance model to the Sembrong dam reservoir. Modelling of relationship between rainfall and reservoir inflow data was done using feed-forward back-propagation neural networks. The final selected model has one hidden layer with 11 neurons in the hidden layer. The selected model was applied for an independent data series testing. Results in relation to specific climatic and hydrologic properties of a small tropical catchment suggested that the model is suitable to be used in forecasting the next day's reservoir inflow. The efficiencies of the model Abtained indicated the validity of using the neural network for modelling reservoir inflow series.

Keywords: Reservoir inflow, neural network, forecasting, modelling

INTRODUCTION

Dam reservoirs plays a vital function at various times and for different purposes such as supplying water for irrigation, hydropower, mitigating disastrous environmental effects and impacts, as well as ensuring flood mitigation and as an insurance during periods of drought etc. In many instances, these dams have no established ydrometric data collection network. The absence of intense network (for the accuracy of data required for the establishment of a vast network facilities) is usually the norm in view of the high costs involved in setting them up. These conditions can result in a considerable uncertainty in the hydrologic information obtained. The non-linear relationship between input and output variables complicates the effort to forecast reservoir inflow events. Many of the techniques currently used in modelling hydrological time-series consider linear relationships among the variables. The two main technique groups are physically based conceptual models and time-series models. In the first group, the procedure is to mathematically simulate the sub-processes and physical mechanisms that prevail in the hydrological cycle. These models usually

[*]Corresponding Author

combined simplified forms of physical laws and are generally non-linear, time-invariant, and deterministic, with parameters which are representative of watershed characteristics (Hsu *et al*., 1995) but ignore the spatially distributed, time-varying, and stochastic properties evident in the rainfall–runoff process. The implementation and calibration of conceptual models can cause many difficulties which require intricate mathematical tools (Duan *et al*., 1992; Sorooshian and Gupta, 1995), significant amounts of calibration data (Yapo *et al*., 1996), and some degree of expertise and experience with the model (Hsu *et al*., 1995). With the time-series modelling approach in the second group, most of them fall within the framework of multivariate autoregressive moving average (ARMA) models (Raman and Sunilkumar, 1995). In runoff forecasting, the time-series models consider the stochastic structure of the time sequence of the runoff and precipitation values measured over time. They are more practical than the conceptual models in the sense that there is no need to understand the internal structure of the physical processes which are taking place in the system being modelled. The limitation of the univariate time-series methods is that the only information they incorporate is the value of the past flows. Many of the available techniques are deficient in that they are not considered as non-linear dynamics inherent in the transformation of rainfall to runoff.

New computing tools and black-box modelling techniques have been introduced to take into cognizance the above mentioned insufficiency. In the data driven modelling, the input variables connect to the output of a system with only limited knowledge about the physical behaviour of the system. Meanwhile, techniques used for data-driven modelling can be stated as machine learning (decision tree, Bayesian methods, neural networks, reinforcement learning), soft computing (fuzzy inference systems, neuro-fuzzy), data mining (which uses machine learning methods and statistics), non-linear dynamics, and chaos theory. These categories often overlap each other (Solomatine, 2002).

Many researches have applied Artificial Neural Networks (ANNs) to model different complex hydrological processes. Some ANN methods (Rumelhart *et al*., 1986) have been successfully employed to simulate the rainfall-runoff process. In addition, the ANN methods have good generalization efficiency and are commonly used in practical hydrologic projects (Zealand *et al*., 1999). Even when there are missing data values, the ANN methods can be applied to aid in the completion of missing hydrological records (Khalil *et al*., 2001). Some authors have compared Box–Jenkins with the ANN methods (Hsu *et al*., 1995; Abrahart and See, 1998) and confirmed, in most cases, the more accurate performance of the ANNs. Traditionally, it is just a matter of studying the cause-effect relationship with historical data. However, this simple statistics does not take into account other issues which take place in a time series.

This paper presents the results from a study on the application of the feed-forward back-propagation neural networks to forecast the next day's reservoir inflow. The modelling procedure is demonstrated for a dam reservoir in Malaysia, where stream inflows are not measured, catchment overland runoff inflow is virtually not measured and rainfall being measured in a three-station network strategically placed in the catchment.

METHODOLOGY - ANN MODELLING

There is this perpetual growing interest in the modelling of non-linear relationships. The artificial neural networks (ANNs) are essentially semi-parametric regression estimators and therefore suitable for this purpose. A significant advantage of the ANN approach in system modelling is that a well-defined physical relationship for systematically converting an input to an output is not required. What is needed for most networks is a collection of representative examples (input–output pairs) of the desired mapping. Then, the ANN adapts itself to reproduce the desired output

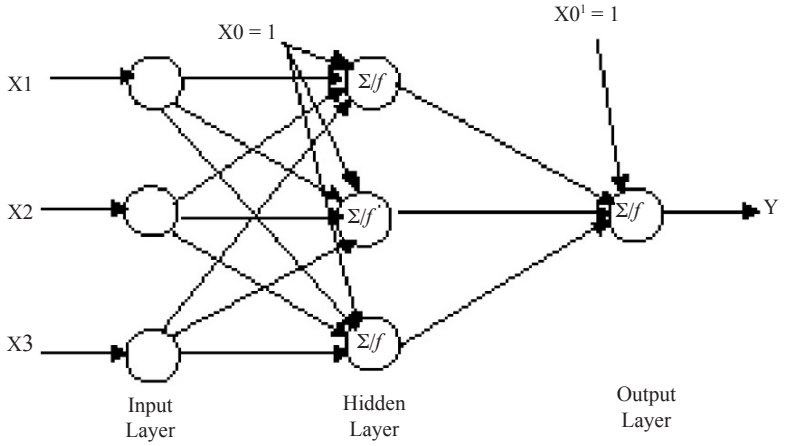

Fig. 1: Structure of a typical MLP

when presented with the training sample inputs. Meanwhile, network architecture determines the number of connection weights (free parameters) and the way information flows through the network. The determination of appropriate network architecture is not only one of the most important, but it is also one of the most difficult tasks in the model building process. The multi-layer perceptron (MLP) is the most popular network architecture in use today, due originally to Rumelhart *et al*. (1986), and it is discussed in most neural network text references. As shown in *Fig. 1*, a typical MLP has neurons which are arranged in a distinct layered topology with its three-layer relationship.

Network geometry determines the number of connection weights and how they are arranged. This is generally done by fixing a number of hidden layers and choosing the number of nodes in each of these. The ANNs with one hidden layer has been shown to be able to approximate any function. The number of nodes in the input layer is fixed by the number of model inputs, whereas the number of nodes in the output layer is equal to the number of the model outputs. In this study, there was only one output, i.e. the reservoir inflow. The selection of the final structure of the ANN model started with a minimum number of nodes in the hidden layer of two since the optimum number of hidden notes cannot be pre-determined, and the network is trained until a minimum mean square error is attained. Then, the number of nodes in a hidden layer is gradually increased until such increase does not significantly improve the performance of the neural network, and thus result in an optimal number of notes in the hidden layer.

The process of optimizing the connection weights is known as 'training' or 'learning.' Here, the Levenberg–Marquardt backpropagation training (LMBP) is used to train a feed-forward neural network. The transfer functions most commonly used are the sigmoidal type functions such as the logistic and hyperbolic tangent functions. In this study, hyperbolic and linear functions were considered for the hidden and output layers, respectively. The performances of the models developed in this study were evaluated using standard statistical performance evaluation based on error measures. More specifically, three different statistical performance indices have been employed, namely normal root mean squared error or NRMSE (which is preferred in many iterative prediction and optimization schemes), Pearson's correlation coefficient or R (which represents the relationship between two parameters giving a scatter plot by a linear relationship), and Nash–Sutcliff efficiency or CE (which includes both observed and predicted values of the same). These are defined as follows:

$$NRMSE = \frac{\left[(1/n)\sum_{t=1}^{n}(Q(t) - Q_o(t))^2\right]^{1/2}}{(1/n)\sum_{t=1}^{n} Q_o(t)} \quad (1)$$

$$R = \frac{\sum_{t=1}^{n}(Q_o(t) - \overline{Q_o})(Q(t) - \overline{Q})}{\sqrt{\sum_{t=1}^{n}(Q_o(t) - \overline{Q_o})^2 (Q(t) - \overline{Q})^2}} \quad (2)$$

$$CE = \frac{E_1 - E_2}{E_1} \quad (3)$$

where

$$E_1 = \sum_{t=1}^{n}(Q_o(t) - \overline{Q_o})^2 \quad (4)$$

$$E_2 = \sum_{t=1}^{n}(Q(t) - Q_o(t))^2 \quad (5)$$

Where $Q_0(t)$ is the observed inflow at time t, Q(t) is the estimated inflow at time t, n is the total number of inflow data points estimated from the developed ANN model, $\overline{Q_o}$ is the mean observed inflow, Q is the mean estimated inflow. E_i is the respective sum square of differences.

CASE STUDY

The Sembrong dam (*Fig. 2* and *Plate 1*), which is a dual purpose water supply cum flood mitigation dam was considered in this study. The catchment of dam lies to the east of the Kuala Lumpur-Singapore road and to the west of the Kuala Lumpur-Singapore railway in an area bounded by the latitude of $1^0$57'-$2^0$5' N and by the longitude of $103^0$8'-$101^0$17' E in the west part of Peninsular Malaysia, about 10km from Air Hitam town in the state of Johor and on the Air Hitam - Kluang road.

The data which were needed and available were sourced from the water supplies company and the Department of Irrigation and Drainage which is in charge of the reservoir operations whilst reservoir inflow data were extracted using water balance equation for the reservoir. The average rainfall across the catchment was calculated by constructing the well-known Theissen's polygon *(Fig. 3)*. The daily data, which were derived from a period of 6 years, i.e. from 1995-1998 and from 2002-2004 *(Fig. 4)*, were considered as the training-validation sets, whereas the other daily data taken for a period of 10 months, i.e. from March 2005 to the end of December 2005 *(Fig. 5)* were used as the testing set. Model inputs were selected by prior knowledge and research in the study area. Model inputs were reservoir inflow with four lags and average rainfall over the catchment with three lags and the output from the models was just the reservoir inflow for the next day. The evaluation procedure of the number of lags for the reservoir inflow and rainfall is not shown here since it is well-known. After the input (Q(t), Q(t-1), Q(t-2), Q(t-3), Q(t-4), R(t), R(t-1), R(t-2), R(t-3), where Q(t-i) and R(t-i) represent the reservoir inflow and rainfall at the *i*th lag number respectively) and output (Q(t+1) in output layer represented the reservoir inflow at

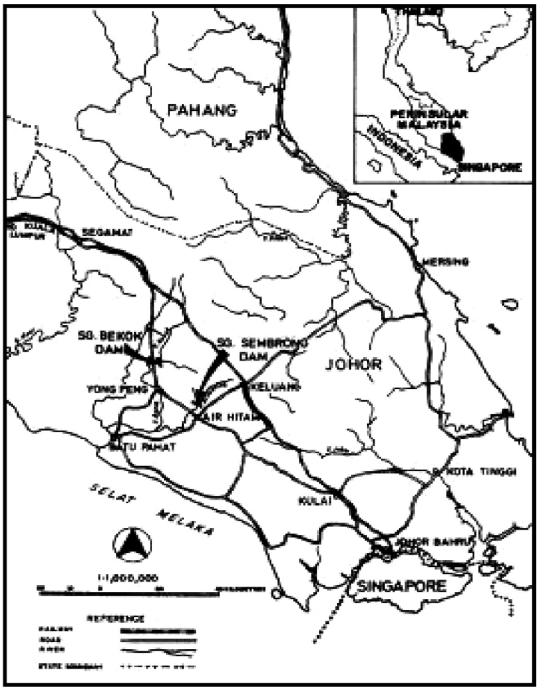

Fig. 2: Location map of the Sembrong Dam in Johor, Malaysia

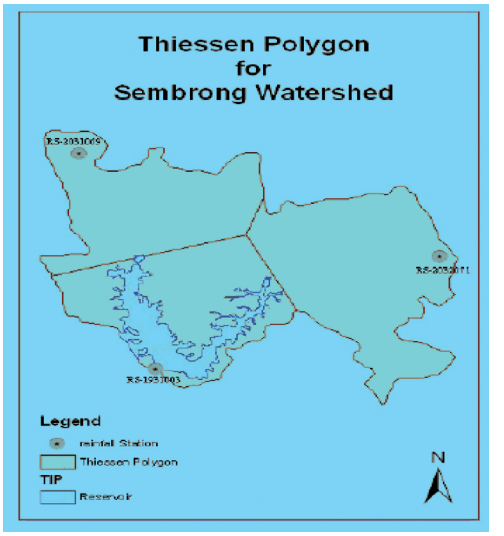

Fig. 3: Theissen's polygon showing the locations of the three rainfall stations

Plate 1: An aerial view of the Sembrong Dam and reservoir and the river downstream of the dam (Courtesy of Department of Irrigation and Drainage, Kuala Lumpur)

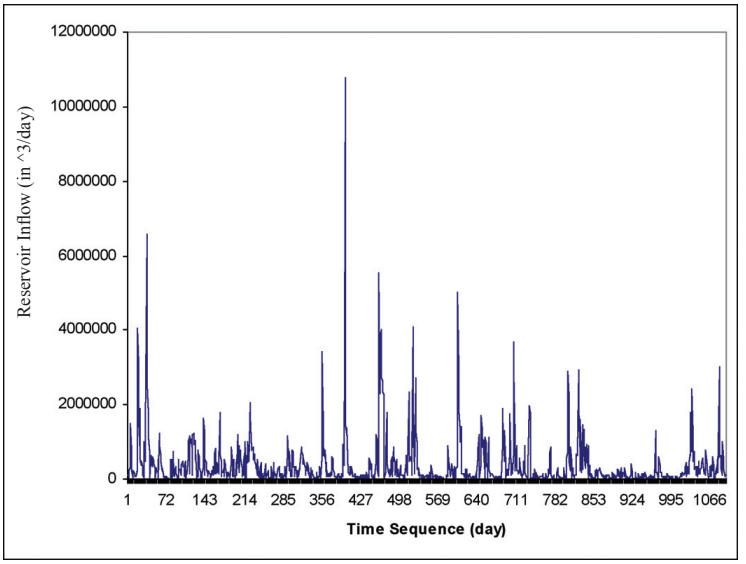

Fig. 4: Daily reservoir inflow data for training and validation during 1995 to1998 and 2002 to 2004

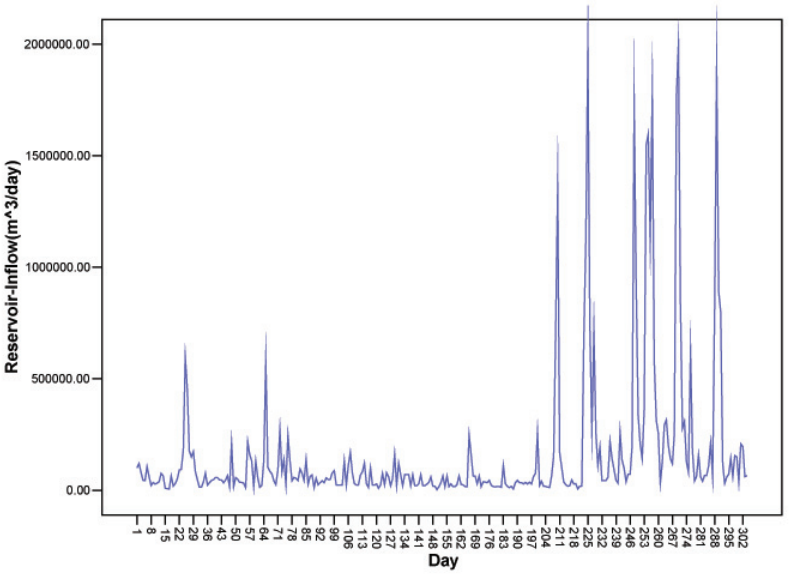

Fig. 5: Daily reservoir inflow data for testing (March – December, 2005)

time t+1) variables were selected, the ANN architecture 9-N-1 was explored for the capturing of the complex, dynamic, and non-linear, rainfall-discharge process. The architecture of the models is a 9-N-1 format in which N represent the number of neuron in hidden layer.

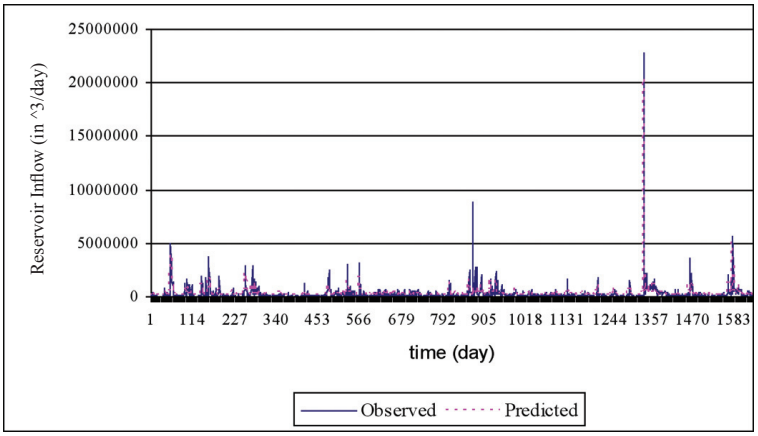

Fig. 6: Observed and predicted of selected AAN model in the training

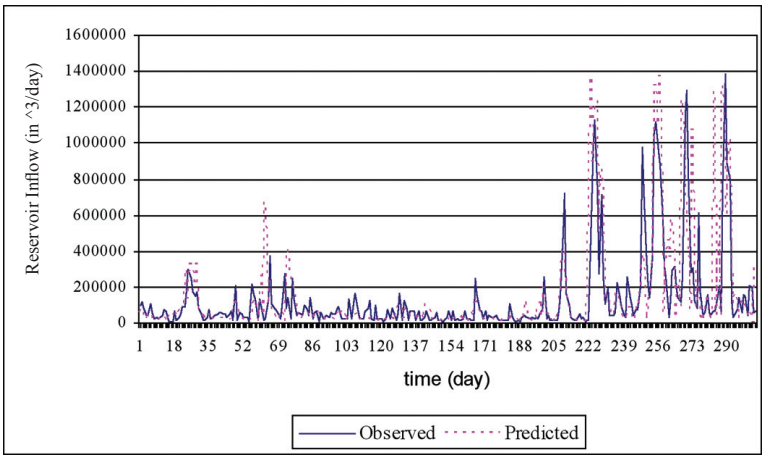

Fig. 7: Observed inflows and selected ANN model predicted inflows during the testing phase

RESULTS AND DISCUSSIONS

Different ANN models were trained with different number of neurons in hidden layer. Each model compromised of nine inputs, one hidden layer and one output. The performance criterion for each model during the training process is presented in Table 1. These results have been obtained using raw reservoir inflow and rainfall data (non-transformed, but scaled). On comparing the results, it was revealed that adding neurons (until 11neurons) to hidden layer increases the R and CE values and decrease NRMSE, which is desirable. Based on table 1, there is no point to add more neurons to the hidden layer thereafter (after 11 neurons) in view of the decreasing performance criteria with increasing neuron numbers. The best architecture obtained was selected with respect to maximum values of R and CE and minimum NRMSE value and this was from the model 9-11-1. This model was further employed to simulate the independent testing data and the results are also presented in Table 1. In the testing stage, although the selected model was found to result in improved NRMSE criterion but however, it simultaneously showed decreased R and CE values.

TABLE 1
Performance criteria of the ANN models with different architecture during the training and testing phases

During training			
Architecture	Pearson's correlation coefficient (R)	Nash-Sutcliff efficiency coefficient (CE)	Normal root mean square error (NRMSE)
9-2-1	0.758	0.566	173.483
9-3-1	0.841	0.688	147.001
9-4-1	0.830	0.686	147.505
9-5-1	0.822	0.666	152.091
9-6-1	0.823	0.675	150.104
9-7-1	0.831	0.689	146.773
9-8-1	0.838	0.690	146.613
9-9-1	0.812	0.643	157.367
9-10-1	0.844	0.710	141.679
9-11-1	**0.862**	**0.738**	**134.648**
9-12-1	0.829	0.675	150.139
9-13-1	0.840	0.700	144.207
9-14-1	0.821	0.618	162.612
9-15-1	0.847	0.716	140.304
During Testing			

Fig. 6 shows the simulation results of the 9-11-1 model for the training data section. The model has some over prediction in base-flows but nevertheless, it was not able to capture the high peaks. Simulation results for testing period *(Fig. 7)* shows good generalization for base-flows and some over-prediction in peak flows.

CONCLUSIONS

In this study, the potential of a feed-forward multi layer perceptron for forecasting the daily reservoir inflow was investigated for the Sembrong dam catchment in Malaysia. An appropriate architecture of ANN model was found by trial and error. The model was examined for an independent data set. Results showed good generalization for base-flows and medium peaks but over-estimation in high peaks (which tends to err on the conservative side). With respect to specific climatic and hydrologic properties of small tropical catchment, the results of study show the validity of using neural network for modelling reservoir inflow series.

REFERENCES

Abrahart, R.J. and See, L. (1998). Neural networks vs. ARMA modelling: Constructing benchmark case studies of river flow prediction. Retrieved from http://divcom.otago.ac.nz/sirc/GeoComp/GeoComp98/05/gc_05.htm.

Duan, Q., Sorooshian, S. and Gupta, V.K. (19920. Effective and efficient global optimization for conceptual rainfall–runoff models. *Water Resources Research, 28* (4), 1015–1031.

Hsu, K., Gupta, H.V. and Sorooshian, S. (1995). Artificial neural network modeling of the rainfall–runoff process. *Water Resources Research, 31*(10), 2517–2530.

Khalil, M., Panu, U.S. and Lennox, W.C. (2001). Groups and neural networks based stream flow data infilling procedures. *Journal of Hydrology*, *241*, 153–176.

Raman, H. and Sunilkumar, N. (1995). Multivariate modelling of water resources time series using artificial neural networks. *Journal of Hydrology Science*, *40*(2), 145–163.

Rumelhart, D.E., Hinton, G.E. and Williams, R.J. (1986). Learning internal representations by error propagation. In D.E. Rumelhart and J.L. McClelland (Eds.), *Parallel distributed processing: Explorations in the microstructure of cognition* (vol. 1) (pp. 318–362). Cambridge, MA : MIT Press.

Solomatine, D.P. (2002). Applications of data-driven modelling and machine learning in control of water resources. In M. Mohammadian, R.A. Sarker and X. Yao (Eds.), *Computational intelligence in control* (pp. 197 – 217). Idea Group Publishing.

Sorooshian, S. and Gupta, V.K. (1995). Model calibration. In V.J. Singh (Ed.), *Computer models in watershed hydrology* (pp. 23 – 68). USA: Water Resources Publications, Co.

Yapo, P., Gupta, V.K. and Sorooshian, S. (1996). Calibration of conceptual rainfall–runoff models: Sensitivity to calibration data. *Journal of Hydrology*, *181*, 23–48.

Zealand, C.M., Burn, D.H. and Simonovic, S.P. (1999). Short-term streamflow forecasting using artificial neural networks. *Journal of Hydrology, 214*, 32–48.

ISSN: 0128-7680
Pertanika J. Sci. & Technol. **18 (1)**: 43 – 59 (2010)

Modelling the Effects of Sediment on the Seismic Behaviour of Kinta Roller Compacted Concrete Dam

Huda A.M.[1], M.S. Jaafar[1], J. Noorzaei[1*], Waleed A. Thanoon[2] and T. A. Mohammed[1]
[1]Department of Civil Engineering, Universiti Putra Malaysia,
43400 UPM, Serdang, Selangor, Malaysia
[2]Faculty of Engineering, University of Nizwa, Oman
[*]E-mail:jamal@eng.upm.edu.my

ABSTRACT

An attempt was made in this investigation to trace the dynamic response of roller compacted concrete dam, which is subjected to horizontal ground motion by considering the interactions between flexible foundations, reservoir water, and bottom reservoir sediments. Two-dimensional finite-infinite element was used for the non-linear elasto-plastic dynamic analysis. In this analysis, special emphasis was given to the non-linear behaviour of discontinuities along RCC dam-bedding rock foundation which was modelled by thin layer interface. Analysis was first carried out under static loading (self-weight and hydrostatic pressure), and this this was followed by seismic analysis, with hydrodynamic pressure effect in a dam-reservoir system. Based on the numerical dynamic results, it is concluded that the bottom reservoir sediment has significant effect on the seismic response of the RCC gravity dam. Moreover, there is a redistribution of the stresses at thin layer interface with significant stresses reduction, which is resulted from the release of energy through different modes of deformation in this region.

Keywords: Seismic analysis, roller compacted concrete dam, coupled finite-infinite elements, sediment, thin layer interface

ABBREVIATIONS

2D	Two dimension
B	Strain-displacement matrix
c	Cohesion
$\overline{C_e}$	Local elastic matrix of thin layer interface
C_e	Global elastic matrix of thin layer interface
C_{ep}	Elasto-plastic matrix of thin layer interface
CVC	Conventional concrete
D_e	Elastic matrix of the material
D_{ep}	Elasto-plastic matrix of the material
E	Young's modulus
f	Yield function
FE	Finite element method
FFT	Fast Fourier Transform technique
f_t	Tensile strength
f_c	Compressive strength
hs	Height of sediment

[*]Corresponding Author

K Stiffness matrix of the system
k_{nn} Normal stiffness of thin layer interface
k_{ss} Shear stiffness of thin layer interface
PGA Peak ground acceleration
RCC Roller compacted concrete dam
t Thickness of thin layer interface
T Transformation matrix of thin layer interface
v Poisson ratio
α , β Coefficient of Newmark method
ϕ Friction angle
ρ Mass density of material
σ_n Normal stress
τ Shear stress

INTRODUCTION

Reservoir sedimentation reduces storage capacity. This loss is considerable and reservoir sedimentation is one of the primary problems to be dealt with in the 21st century. The problem arises from geological sources, agricultural cultivation, destruction of forest, and other natural causes and hazards. Considerable efforts have also been devoted in the recent years to investigate the seismic response on the concrete dams. To obtain realistic results, the reservoir sedimentation must be taken in the analysis of the dam-reservoir-foundation interaction.

Dam-reservoir-foundation-sediment interaction has been investigated by many researchers. Among other, Fenves and Chopra (1984: 1985) presented a model which includes reservoir bottom absorption for the seismic analysis of gravity dam by the means of an absorbing boundary condition. The study concluded that the sediment could significantly reduce the hydrodynamic pressure effect on the seismic response of the dam. Meanwhile, Lotfi *et al*. (1987) modelled the sediments as linearly viscoelastic, which was included as hyper-elements in a finite element analysis. The water-sediment-foundation interaction was taken into account rigorously. A model based on the boundary-element method was presented by Medina *et al*. (1990). In their analysis, the sediment was considered as a viscoelastic material which could only transmit compressional waves. The effect of the two-phase poroelastic sediments on the seismic response of gravity dams was investigated by Bougacha and Tassoulas (1991). The sediment was considered as a uniform horizontal layer and included as a hyper-element in their finite element model.

An investigation into the effect of reservoir bottom sediment on the seismic response of concrete gravity dams was carried out by Zhao *et al*. (1995) using coupled finite-infinite elements and Fast Fourier Transform (FFT) technique. They suggested that (1) the finite and infinite element coupled method is more suitable for the seismic analysis of a concrete gravity dam, and (2) the reservoir bottom sediment has a significant effect on the seismic response of concrete gravity dam. More recently, Dominguez *et al*. (1997) presented a boundary-element approach for the dynamic analysis of concrete gravity dam. The dam was subjected to ground motions and it interacted with water, foundation, and bottom sediment.

Based on the review of some published papers, none of them has addressed the effects of sediment and its dynamic non-linear interaction with roller compacted concrete (RCC) dam in time history analysis, particularly when the RCC dam-reservoir-foundation-sediment interaction is considered with the coupled finite and infinite elements.

Attempting to fill the apparent gap, an RCC dam-reservoir-foundation-sediment interaction which is subjected to earthquake ground acceleration is modelled using finite-infinite elements. Elasto-plastic non-linear dynamic analysis was carried out in time domain using modified two dimensional finite element program to represent the unbounded domain in the foundation and interfacial behaviour along discontinuities. For more realistic analysis, the non-linear behaviour along discontinuities between RCC dam-bedding foundations was investigated for safety evaluation. Therefore, Kinta dam in Malaysia was selected to be used in this investigation.

MATERIALS AND METHODS

Finite Element Computer Code

An existing two-dimensional finite element code by Noorzaei *et al*. (1995) was modified for the purpose of this study. The modification was made by:

(i) Adding infinite elements and thin layer interface elements in the element library.

(ii) Strengthening the library of the yield with evolved elasto-plastic constitutive models of thin layer interface element to simulate failure mechanism of the discontinuity based on the modified Mohr-Coulomb criterion *(Fig. 1)*.

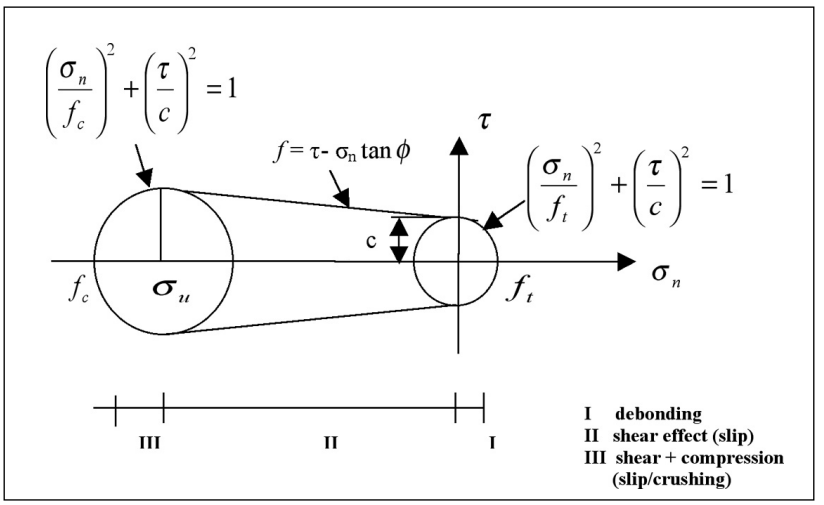

Fig. 1: Modified Mohr-Coulomb criterion (Linsbauer, 1999)

Details of the formulations and modification had been presented by Thanoon *et al*. (2006), and the generalized flowchart of this computer program is illustrated in *Fig. 2*. The program consists of the main sub-routines that execute the program processes and reads the various control parameters such as material properties, element type, element node connectivity number, nodal coordinates, and boundary conditions. Meanwhile, earthquake records and numbers of iterations for seismic analysis are executed in the main sub-routines. The software is of multi-element features, which is achieved by identifying each element of a particular code number. Based on their pre-assigned element code number, the number of nodes per element, order of integration, shape function, and

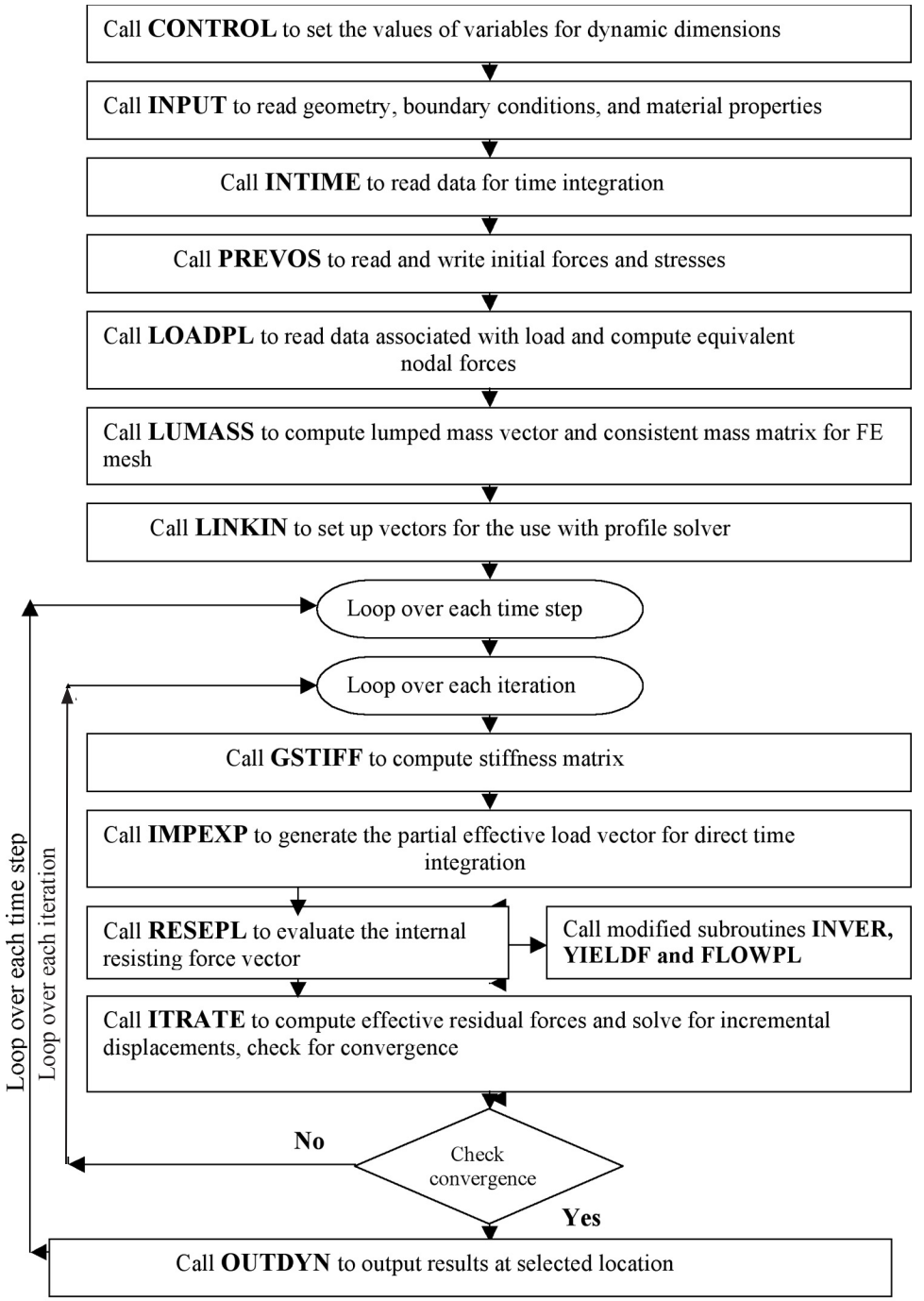

Fig. 2: General flow chart of 2D FE program

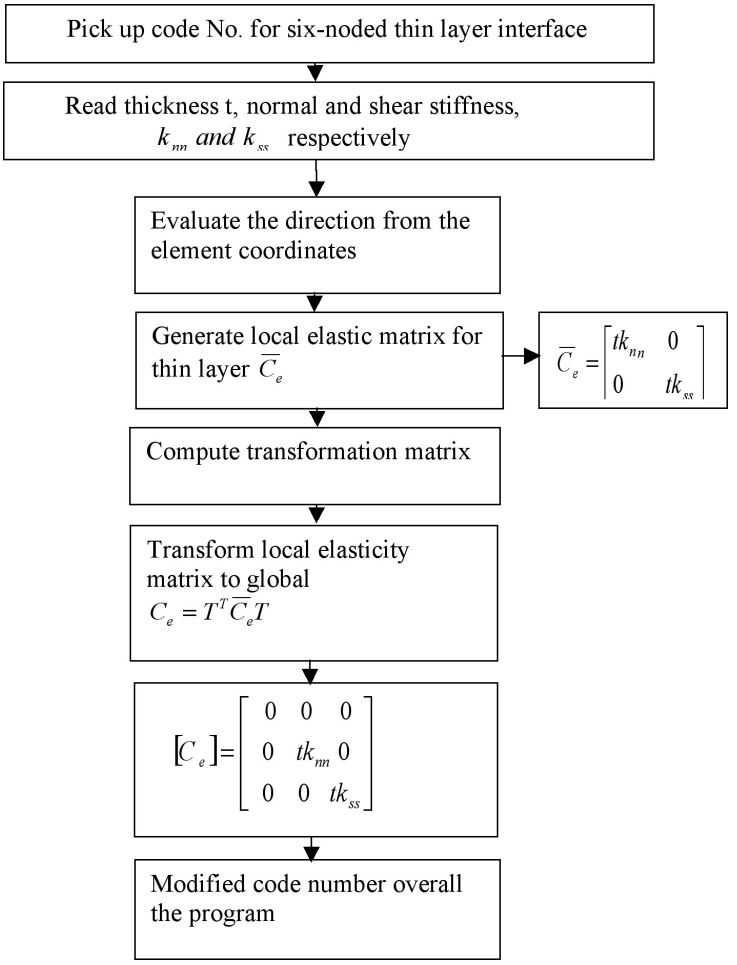

Fig. 3: Flowchart of the implementation of thin layer interface element

their derivations were picked up automatically.

The sub-routine MODPS was developed to account for the calculation of elasticity matrix for the thin layer interface element. The flowchart of the developed sub-routine is shown in *Fig. 3*. The implementation was carried out in such a way that the constitutive relations were codified and made compatible with the original program over all the sub-routines that are related to the use of elasticity matrix.

Based on the theory of plasticity, the finite element program was modified for modelling the different modes of deformation of the thin layer interface element. Sub-routines which were developed are INVAR, YIELDF, FLOWPL, GSTIFF, and RESEPL and they represent the elasto-plastic constitutive laws for debonding, slipping, and crushing behaviour of the thin layer interface. The stiffness matrix for each element was calculated in the GSTIFF sub-routine to account for any plastic deformation of the material and consequently the elasto-plastic matrix must be employed. The flowchart of the developed sub-routine GSTIFF is shown in *Fig. 4*.

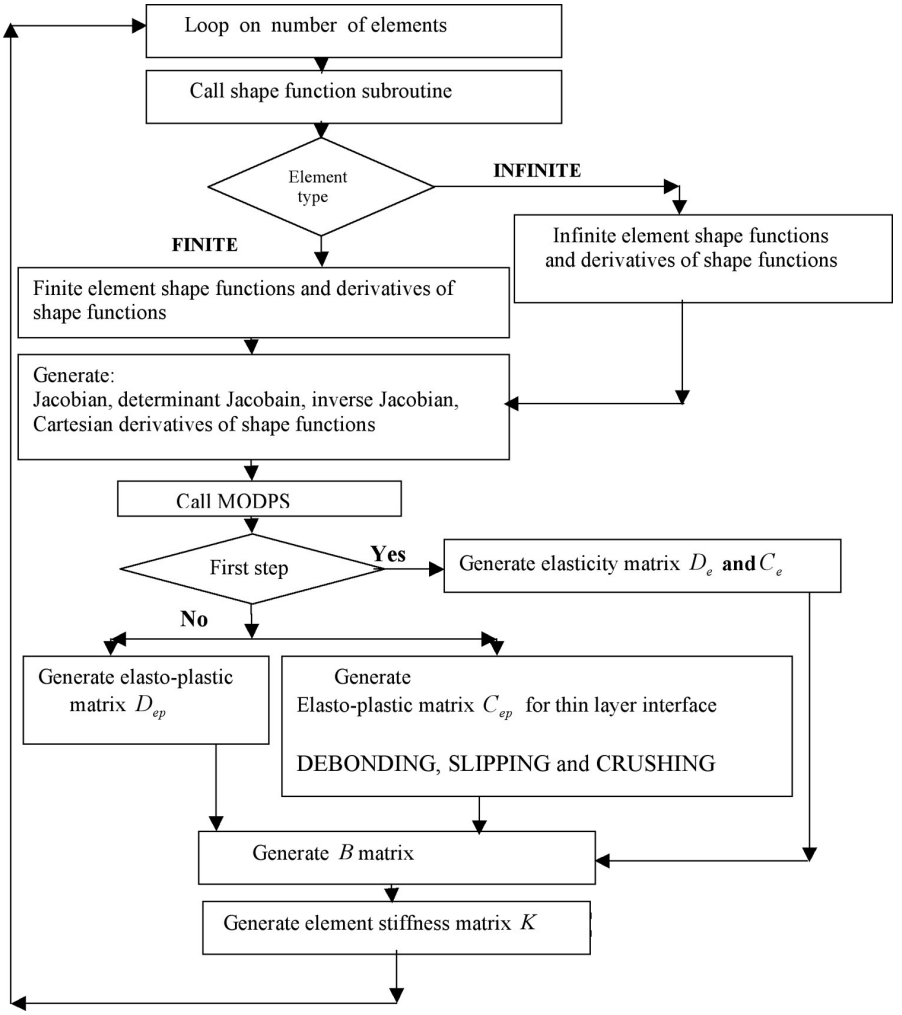

Fig. 4: Flowchart of the developed sub-routine GSTIFF

RCC Kinta Dam - Case Study

The Kinta Dam is a roller compacted concrete (RCC) gravity dam and is the first RCC dam in Malaysia. In the present study, the Kinta dam is selected to assess the response of an RCC dam under seismic excitation. The structural geometry of dam-foundation-sediment is illustrated in *Fig. 5*. Meanwhile, the finite-infinite and thin layer mesh of the dam-foundation-sediment is shown in *Fig. 6.* The following elements are used for discretization purposes:

(a) Eight noded isoparametric finite elements to represent RCC dam-sediment-bedding foundation for the near field (Zienkiewicz *et al*., 1972).
(b) Five noded infinite elements to represent the far field media of the foundation bedding system (Noorzaei, 1991).
(c) The interfacial behaviour between the RCC dam body-foundation bedding media is idealized using six noded thin layer interface elements (Sharma *et al*., 1992).

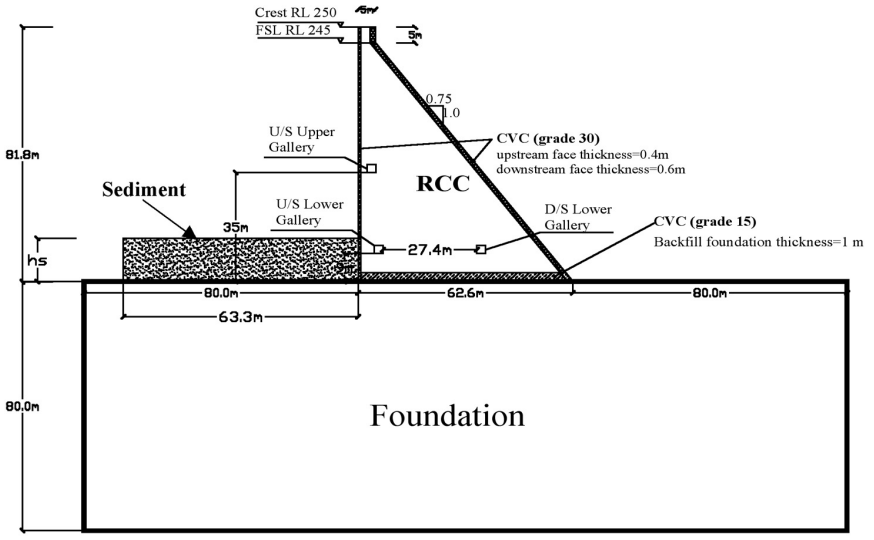

Fig. 5: Structural geometry of the RCC dam-sediment-foundation system at the deepest section

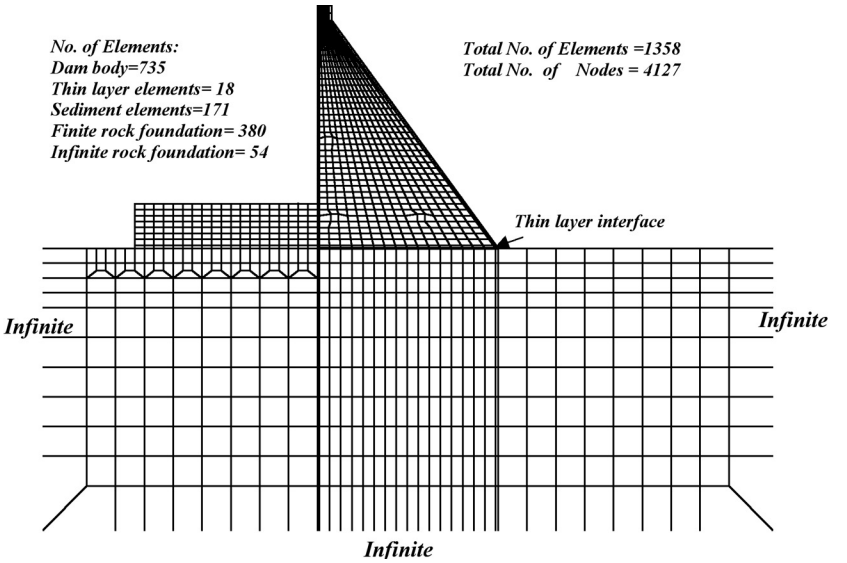

Fig. 6: Coupled finite-infinite idealization of Kinta RCC dam-foundation-sediment system

The dynamic material properties of the RCC dam-foundation-sediment system and selected grade of conventional concrete (CVC) are shown in Table 1. The dynamic properties were obtained by considering the static properties from the technical report by GHD 2002. Since specific information on the sediment behind the RCC dam is not available, the sediment properties are utilized on the basis of the available properties in the literature, similar to those used by Zhao (1995). The properties of the thin layer interface are shown in Table 2.

TABLE 1
Dynamic material properties of Kinta RCC dam-foundation-sediment system

Material parameters	RCC	CVC G30	CVC G15	Foundation	Sediment
Young's modulus E (N/m^2)	0.23E+11	0.32E+11	0.23E+11	0.30E+11	0.252E+9
Poisson ratio v	0.2	0.2	0.2	0.2	0.3
Mass density ρ (kg/m^3)	2386	2352	2325	2650	2000
Compressive strength f_c (MPa)	20	40	20	18	-
Tensile strength f_t (MPa)	2.5	5.0	2.5	2.25	-

TABLE 2
Properties of the thin-layer interface

Material parameters	Thin layer
Mass density ρ (kg/m^3)	2325
Normal stiffness k_{nn} (N/m^3)	0.47E+12
Shear stiffness k_{ss} (N/m^3)	0.19E+12

TABLE 3
Mohr-Coulomb yield surface parameters

Material	f_c (MPa)	f_t (MPa)	c (MPa)	ϕ
Concrete (RCC and CVC G15)	20	2.5	3.535	51.06
Concrete facing (CVC G30)	40	5.0	7.06	51.06
Foundation	18	2.25	3.182	51.06
Sediment	-	-	0.098	29
Thin layer interface	18	1.0	0.7	30

The Mohr-Coulomb yield criterion was adopted for the RCC dam-foundation-sediment system. The modified Mohr-Coulomb criteria were used to simulate the different modes of deformations which could occur at the thin layer interface. Table 3 shows the parameters c and ϕ which are related to material tensile and compressive strength, and required to define yield the surface for the Mohr-Coulomb criterion.

Prior to the seismic excitation, the static stresses due to the gravity weight and hydrostatic load for full reservoir were calculated and stored separately. The hydrodynamic effect of the impounded reservoir water due to seismic loading was calculated by Westergaard added mass method (U.S., 2003) on the upstream face of the RCC dam. The horizontal ground motion, which was used for

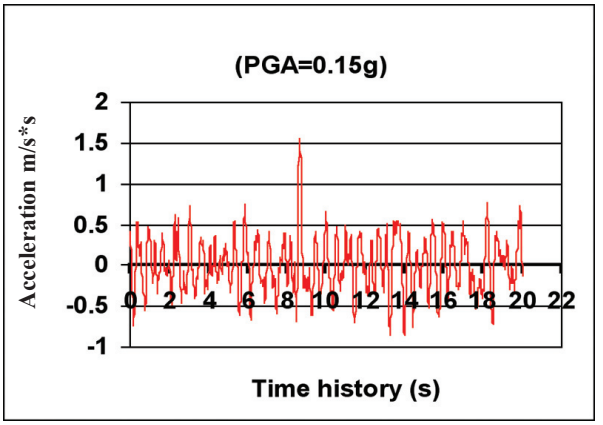

Fig. 7: Horizontal earthquake records excitation

the seismic analysis, was a Malaysian earthquake record, with a peak ground acceleration (PGA) of 0.15g, as shown in *Fig. 7*.

Dynamic Analysis

The non-linear dynamic analysis of the RCC dam-reservoir-foundation-sediment was carried out with a structural damping ratio of 5%. The integration of the dynamic equation of motion was done in the time domain using the Newmark method with $\alpha = 0.25$ and $\beta = 0.5$ and a time step of 0.02 sec. Massless foundation was considered in the analysis. Meanwhile, the time history response of the dam was carried out under plane stress condition. Therefore, the responses of the RCC dam, under seismic excitation with respect to the acceleration, displacement and stress, are presented and discussed.

RESULTS AND DISCUSSION

The absolute peak envelopes values of acceleration, displacement and stresses generally occur at different time steps during earthquake excitation; they serve to identify the critical values (U.S. army, 2003). In the next step, the time history of the nodal points or Gaussian points are plotted to evaluate the seismic response of the RCC dam.

The horizontal acceleration, with and without sediment effect along the height, is shown in *Fig. 8*. The top part of the dam experiences higher acceleration at the crest of about 1.02g and 1.1g for the two cases with and without sediment, respectively. The effect of sediment has lowered the magnitude of peak acceleration along the height, where the greatest influence is at the lower part of the dam. The lower part of the dam indicates about 30% reduction in the peak acceleration value.

The variation of peak absolute horizontal acceleration along section A-A at the foundation is shown in *Fig. 9*. The maximum value is about 0.30g and 0.41g for the two cases with and without sediment effect, respectively. As observed from these plots, the seismic response is affected by the sediment, where the peak acceleration is reduced at the foundation. This reduction is due to the absorption of the bottom reservoir sediment to the ground motion acceleration.

The envelopes of contour lines of the peak absolute displacement in the RCC dam body for both cases, i.e. with and without sediment effects, are shown in *Fig. 10*. As observed from these plots, the maximum value is located at the crest of the dam. The crest displacement is about 2.0 to

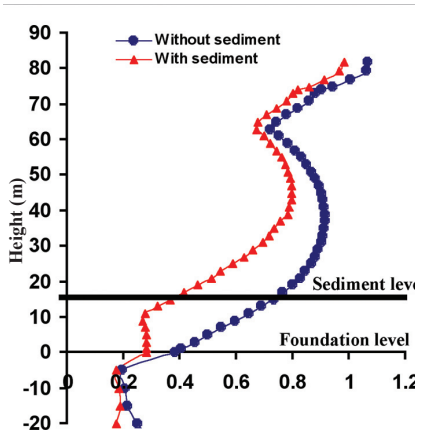

Fig. 8: Variation of the peak absolute horizontal acceleration along the height

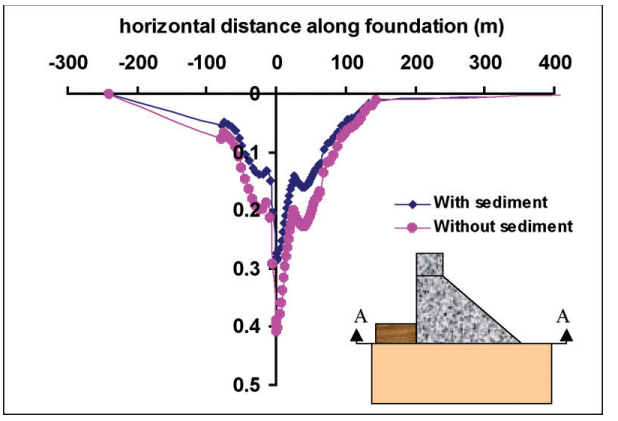

Fig. 9: Variation of the peak absolute horizontal acceleration along section A-A

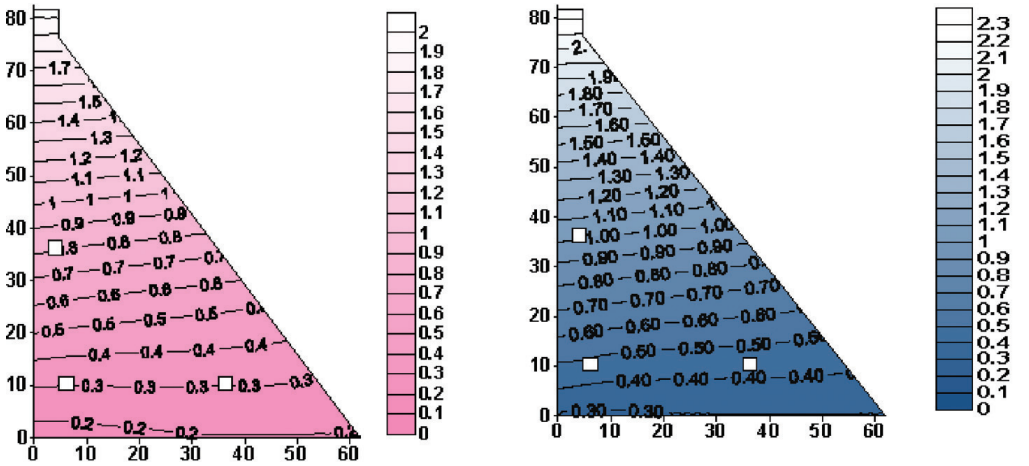

(a) With sediment *(b) Without sediment*

Fig. 10: Envelopes of the peak absolute horizontal displacement in the RCC dam

2.36 cm, indicating the reduction in peak displacement of about 15%. Since the highest value of horizontal displacement occurred at the crest, the horizontal displacement time history responses for both cases are plotted as in *Fig. 11*.

In this study, the level of stresses in the RCC dam body, the envelopes of contour lines in the peak tension and the compression stresses in dam body *(Figs. 12-13)* were respectively assessed for both cases. In general, these plots demonstrate that the maximum value of the tensile stress is observed at the base of the dam heel on the upstream face. The sediment reduces the seismic response of the hydrodynamic pressure, especially at the dam heel on the upstream face where the sediments are present.

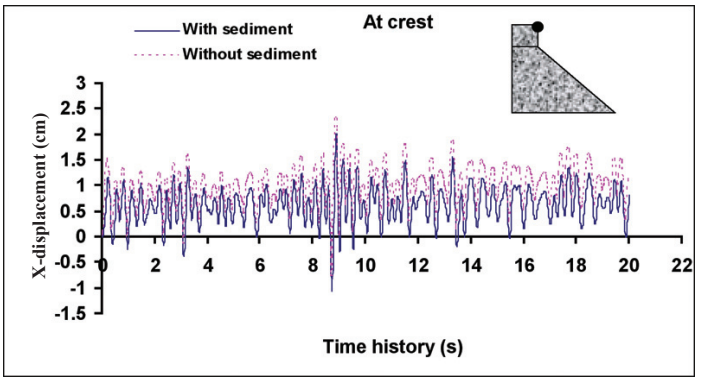

Fig. 11: Time history graphs of the horizontal displacement at crest

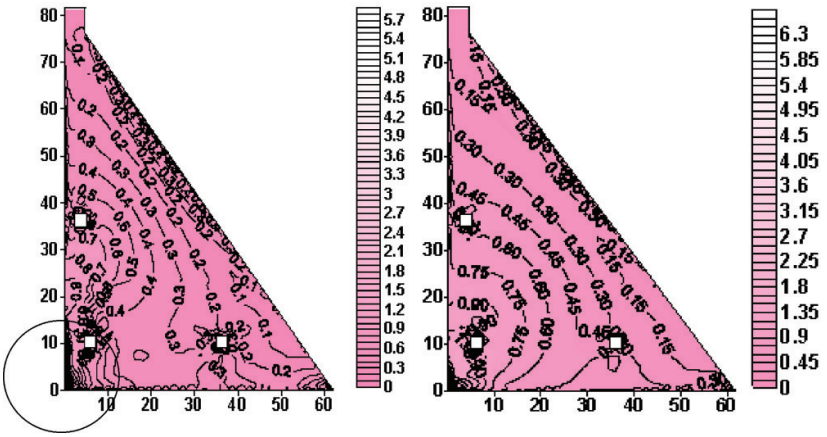

(a) With sediment *(b) Without sediment*

Fig. 12: Envelopes of the contour lines of peak maximum principal stress in the RCC dam

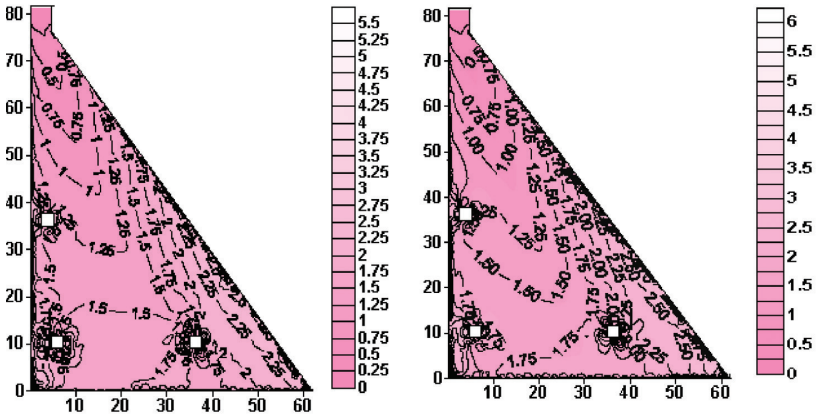

(a) With sediment *(b) Without sediment*

Fig. 13: Envelopes of the contour lines of peak minimum principal stresses in the RCC dam

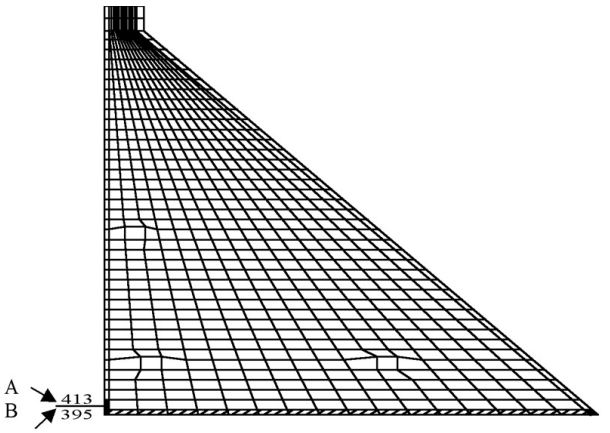

Fig. 14: Selected elements on the finite element mesh

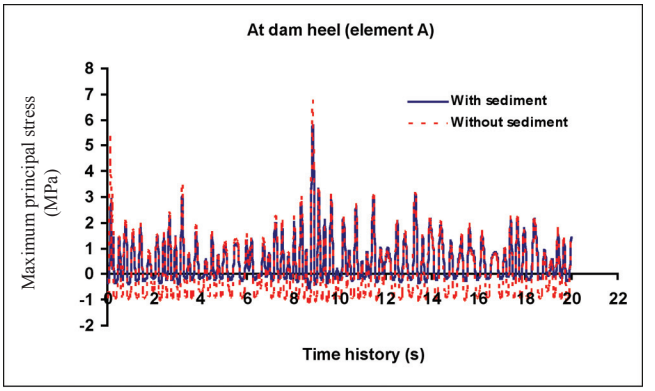

(a) Maximum

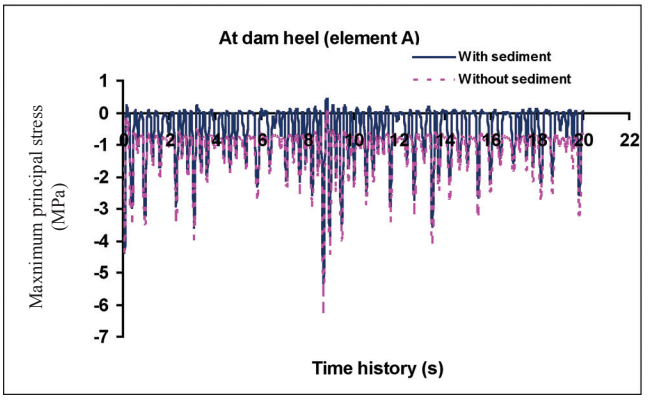

(b) Minimum

Fig. 15: Time history responses of the maximum and minimum principal stresses at the heel of the RCC dam, with and without sediment effect

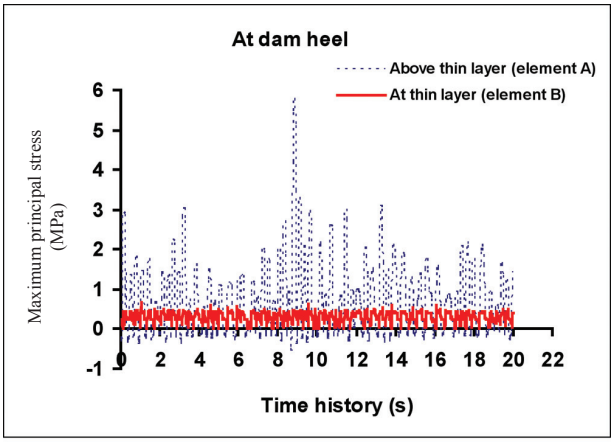

(a) Maximum

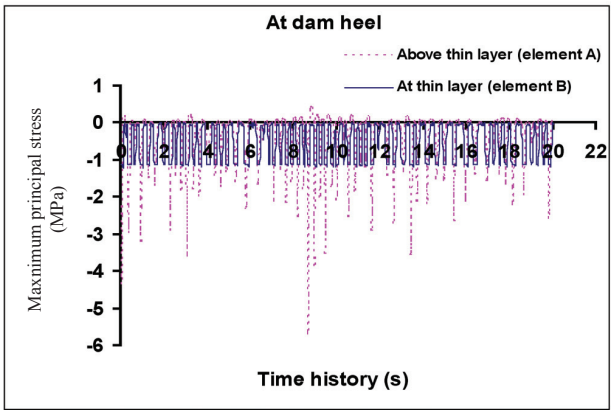

(b) Minimum

Fig. 16: *Time history response of the principal stresses, above and within the thin layer interface with the effect of sediment*

Based on this analysis, these elements were then selected together with the other elements at the thin layer interface element to plot the time history response graphs so as to trace the dam response at the dam heel. The location of those elements is marked on the mesh, as shown in *Fig. 14*. The responses of the maximum and minimum principal stresses occurred in these elements are presented in *Figs. 15-16*. The maximum peak tensile stress (σ_1) is represented in element 413, i.e. at the base of the dam at the upstream faces. This value reaches approximately 5.7 and 6.7 MPa for the two cases, indicating a reduction in the value of the peak tensile stress by about 15% due to the sediment effect. The analysis leads to a maximum peak compressive stresses of (σ_3) -5.6 and -6.2 MPa for the two cases. Similar to the tensile stress, the presence of the sediment has also reduced the compressive stress. The reduction in the compressive stress is about 10%. The seismic response in terms of stresses above and within the thin layer interface can be observed in the graph of the time history response with sediment effect *(Fig. 16)*. The stresses within the thin layer reflect the response when the modified Mohr-Coulomb failure criterion governs the

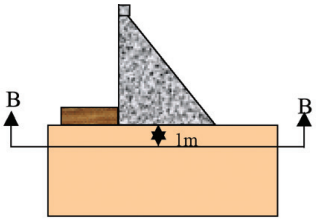

(a) Tensile

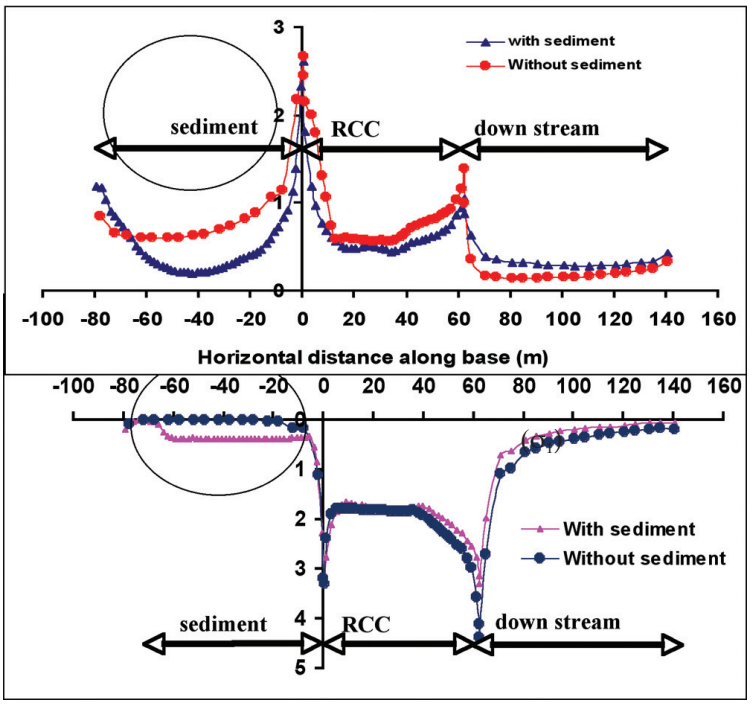

(b) Compressive

Fig. 17: Variation of the peak tensile and compressive principal stresses along section B-B on the dam foundation

behaviour of the thin layer between the RCC dam-bedding foundations. Meanwhile, the peak values of the tensile stress (σ_1) is 5.7 MPa and the compressive stress (σ_3) is 5.6 MPa, which are located at the dam heel. The distribution of the stresses in the thin layer interface during the plasticity is also shown in *Fig. 16*. The peak tensile and compressive principal stresses range between 0.7 to -1.2 MPa, respectively. A comparison of the seismic response above and within thin layer demonstrates that there is a redistribution of the stresses at the thin layer leading to stress reduction. This is due to the release of stresses during debonding and slipping deformations.

The predicted stresses at the rock foundation, with and without sediment effects, are summarized in *Fig. 17*. These plots are made at section B-B which is located 1 m below the foundation elevation. For the whole foundation response, the peak tensile value was located below

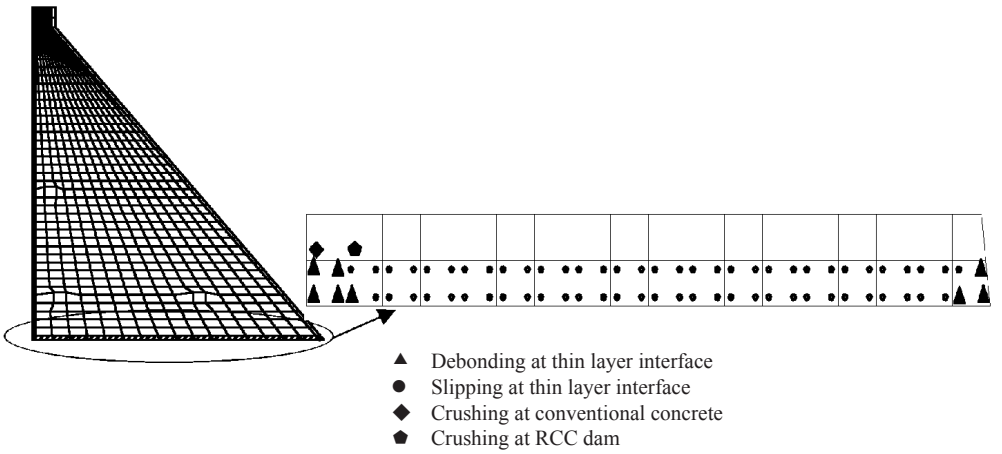

Fig. 18: Spread of plasticity at the base of the dam at 20.0 sec. of earthquake excitation

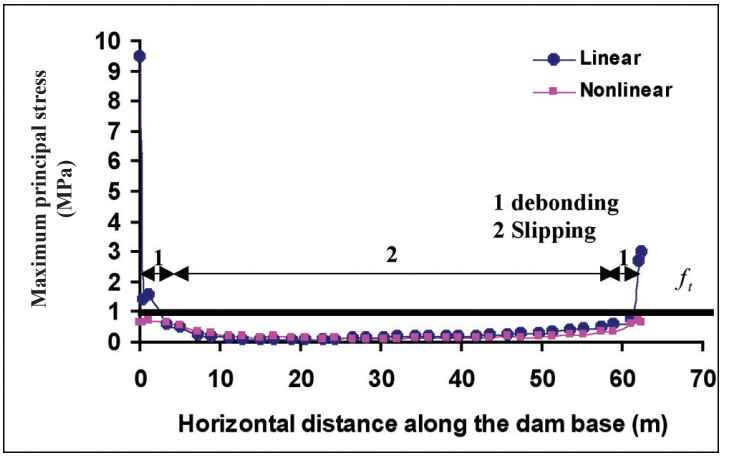

Fig. 19: Debonding and slipping deformation at the thin layer interface elements

the heel of the dam and the peak compressive value was located below the toe of the dam. The seismic response of the tensile and compressive stress is clearly affected by the presence of the sediment.

Fig. 18 summarizes the results gathered from the distribution of the plastic deformation at the lower part of the dam and at the end of the earthquake excitation (t=20 sec). The results of the non-linear elasto-plastic analysis carried out at the lower part of the dam show that the plasticity deformation occurred at about 74 Gauss points after 20 sec of seismic excitation. The locations of these points are presented in the CVC and RCC dam and in the thin layer interface at the base of the dam. The printed index refers to debonding and slipping deformation at the thin layer interface elements, as shown in *Fig. 19*.

Based on the results, the overall trend of the seismic response is found to be higher for the RCC dam without the reservoir bottom sediment as compared to the dam with the reservoir bottom

sediment. This finding indicates that the reservoir bottom sediment has a certain effect on the dynamic analysis of the RCC dam-reservoir-sediment-foundation interaction. The results for the effect of the bottom reservoir sediment are generally in agreement with those obtained by Zhao (1995).

CONCLUSIONS

An investigation into the effect of reservoir bottom sediment on the seismic response of the RCC dam was carried out using the coupled finite-infinite elements. For this purpose, the non-linear elasto-plastic time history analysis was also applied to the dam-reservoir-sediment-foundation interaction, with special emphasis given to the non-linear behaviour of discontinuous along the dam-bedding foundation. A thin layer element was utilized to simulate the actual behaviour between the RCC dam and bedding foundation.

Therefore, the following conclusions can be made based on the findings of the present study:

1. Since the far field of the system was modelled using the infinite elements, the infinite extension of the foundation could be simulated more appropriately. Thus, the finite-infinite coupled method is more suitable for the seismic analysis of the RCC-sediment-foundation interaction.
2. The implementation of the failure mechanism of the thin layer interface element was carried out based on modified Mohr-Coulomb failure criterion. The major advantage of such formulation is that it permits computerized programming of the yield function which allows deformation modes such as debonding, slipping, and crushing.
3. The overall trend of the response of the RCC dam-bedding system is observed to have been affected by the bottom sediment. Thus, the reservoir bottom sediment has significant effect on the seismic response of the RCC dam-reservoir-sediment-foundation interaction.
4. The failure mode of the thin layer interface element is debonding and slipping mode of deformation. The results demonstrate that the deformation model is able to predict the non-linear behaviour of discontinuity.

REFERENCES

Bougacha, S. and Tassoulas, J.L. (1991b). Seismic analysis of gravity dam. II: Effects of sediments. *Journal of Engineering Mechanics*, *ASCE, 117*(8), 1839-1850.

Bougacha, S. and Tassoulas, J.L. (1991a). Seismic analysis of gravity dam. I: Modelling of sediments. *Journal of Engineering Mechanics, ASCE*, *117*(8), 1826-1837.

Dominguez, J., Gallego, R. and Japon, B.R. (1997). Effects of porous sediments on seismic response of concrete gravity dams. *Journal of Engineering Mechanics*, *ASCE*, *123*(4), 302-311.

Fenves, G. and Chopra, A.K. (1985). Effects of reservoir bottom absorption and dam-water-foundation rock interaction on frequency response functions for concrete gravity dams. *Journal of Earthquake Engineering and Structural Dynamics*, *13*(1), 13-31.

Fenves, G. and Chopra, A.K. (1984). Earthquake analysis of concrete gravity dams including reservoir bottom absorption and dam-water-foundation rock interaction. *Journal of Earthquake Engineering and Structural Dynamics*, *12*, 663-680.

Linsbauer, H.N. and Bhattacharjee, S. (1999). Dam safety assessment due to uplift pressure action in a dam-foundation interface crack. *Fifth Benchmark Workshop on Numerical Analysis of Dams*, Denver, Colorado USA.

Lotfi, V., Roesset, J. M. and Tassoulas, J.L. (1987). A technique for the analysis of the response of dams to earthquake. *Journal of Earthquake Engineering and Structural Dynamics, 15*, 463-490.

Medina, F., Dominguez, J. and Tassoulas, L.J. (1990). Response of dams to earthquake including effects of sediments. *Journal of Structural Engineering*, *ASCE*, *116*(11), 3108-3121.

Noorzaei J., Viladkar, M.N. and Godbole, P.N. (1995). Influence of strain hardening on soil-structure interaction of framed structures. *Computers & Structures*, *55*(5), 789-795.

Noorzaei, J. (1991). *Non-linear soil structure interaction in framed structure*. Ph.D thesis, Department of Civil Engineering, University of Roorkee, India.

Sharma, K.G. and Desai, C.S. (1992). Analysis and implementation of thin-layer element for interface and joints. *Journal of Engineering Mechanics*, *118*, 2442- 2462.

SUNGAI Kinta dam RCC. (2002). Study of restrictions on RCC temperature, Stage 2 development of Ipoh water supply. *Technical report GHD, Sdn. Bhd*, Malaysia.

Thanoon, H.A., Jaafar, M.S., Thanoon, W.A., Mohamed, T.A. and Noorzaei, J. (2006). Dedonding, slipping and crushing effects on seismic response of RCC dam. In *8th International Conference on Computational Structures Technology*, Las Palmas de Gran Canaria, Spain.

United States Army Corps of Engineers. (2003). Time-history dynamic analysis of concrete hydraulic structures. *EM 1110-2-6051*.

Zhao, C., Xu, T. P. and Valliappan, S. (1995). Seismic response of concrete gravity dams including water-dam-sediment-foundation interaction. *Computers & Structures*, *54*(4), 705-715.

Zienkiewicz, O.C. and Nayak, G.C. (1972). Elasto-plastic stress analysis, a generalization for various constitutive relations including strain softening. *International Journal of Numerical Methods in Engineering*, *5*(1), 113-135.

ISSN: 0128-7680
Pertanika J. Sci. & Technol. **18 (1)**: 61 – 76 (2010)

Modelling and Simulation of Vibration and Input Tracking Control of a Single-Link Flexible Manipulator

Mohd Ashraf Ahmad[1*] and Zaharuddin Mohamed[2]
[1]Faculty of Electrical and Electronics Engineering,
Universiti Malaysia Pahang, 25000 Kuantan, Pahang, Malaysia
[2]Faculty of Electrical Engineering, Universiti Teknologi Malaysia,
81310 Skudai, Johor, Malaysia
[*]E-mail: mashraf@ump.edu.my

ABSTRACT

This paper presents investigations into the development of control schemes for end-point vibration suppression and input tracking of a flexible manipulator. A constrained planar single-link flexible manipulator is considered and the dynamic model of the system is derived using the assumed mode method. To study the effectiveness of the controllers, a Linear Quadratic Regulator (LQR) was initially developed for control of rigid body motion. This is then extended to incorporate a non-collocated PID controller and a feedforward controller based on input shaping techniques to control vibration (flexible motion) of the system. For feedforward controller, positive and modified specified negative amplitude (SNA) input shapers are proposed and designed based on the properties of the system. Results from the simulation of the manipulator responses with the controllers are presented in time and frequency domains. The performances of the control schemes are assessed in terms of level of vibration reduction, input tracking capability and time response specifications. Finally, a comparative assessment of the control techniques is presented and discussed.

Keywords: Flexible manipulator, vibration control, input shaping, LQR control, PID control

ABBREVIATIONS

AMM	-	Assumed Mode Method
IIR	-	Infinite Impulse Response
LQR	-	Linear Quadratic Regulator
LTI	-	Linear Time Invariant
NZVDD	-	Negative Zero-Vibration-Derivative-Derivative
PD	-	Proportional Derivative
PID	-	Proportional Integral Derivative
PSD	-	Power Spectral Density
PZVDD	-	Positive Zero-Vibration-Derivative-Derivative
SNA	-	Specified Negative Amplitude
UM	-	Unity-Magnitude
ZV	-	Zero-Vibration
ZVD	-	Zero-Vibration-Derivative
ZVDD	-	Zero-Vibration-Derivative-Derivative

Received: 3 March 2008
Accepted: 14 April 2009
[*]Corresponding Author

INTRODUCTION

Flexible manipulators exhibit many advantages over their rigid counterparts; among other, they require less material, are lighter in weight, have higher manipulation speed, lower power consumption, require smaller actuators, are more manoeuvrable and transportable and much safer to operate due to reduced inertia, as well as have less overall cost and higher payload to robot weight ratio. However, the control of flexible manipulators to maintain accurate positioning is challenging. Due to the flexible nature and distributed characteristics of the system, the dynamics are highly non-linear and complex. Problems arise due to precise positioning requirements, system flexibility leading to vibration, the difficulty in obtaining an accurate model of the system and the non-minimum phase characteristics of the system (Azad, 1995).

The control strategies for flexible manipulator systems can be classified as feedforward (open-loop) and feedback (closed-loop) control. In particular, the feedforward control techniques were mainly developed for vibration suppression which involved developing the control input through the consideration of the physical and vibrational properties of the system, so that the system vibrations could be reduced at the response modes. This method does not require any additional sensors or actuators and it also does not account for the changes in the system once the input is developed. A number of techniques have been proposed as the feedforward control schemes to control the vibration in the flexible structures. These include utilisation of Fourier expansion (Aspinwall, 1980), development of computed torque (Bayo, 1988), utilisation of single and multiple-switch bang-bang control functions (Onsay and Akay, 1991) and construction of input functions from the ramped sinusoids or versine functions (Meckl and Seering, 1990). Moreover, command shaping techniques have also been investigated in reducing the system vibration in flexible manipulators. These include filtering techniques based on low-pass, band-stop, and notch filters (Singhose *et al*., 1995; Tokhi and Poerwanto, 1996a) and input shaping (Singer and Seering, 1990; Mohamed and Tokhi, 2002). Previous experimental studies on a single-link flexible manipulator have shown that input shaping gives higher level of vibration reduction and robustness than filtering techniques. However, the major drawbacks of the feedforward control schemes are their limitations in coping with the parameter changes and the disturbances to the system (Khorrami *et al*., 1994). Moreover, the technique requires relatively precise knowledge of the dynamics of the system.

Investigations have also shown that with the input shaping technique, a system response with delay is obtained. To reduce the delay and thus increase the speed of the response, negative amplitude input shapers have been introduced and investigated in vibration control. The shaper duration can be shortened by allowing the shaper to contain negative impulses, while satisfying the same robustness constraint. A significant number of negative shapers for vibration control have also been proposed. These include negative unity-magnitude (UM) shaper, specified-negative-amplitude (SNA) shaper, negative zero-vibration (ZV) shaper, negative zero-vibration-derivative (ZVD) shaper and negative zero-vibration-derivative-derivative (ZVDD) shaper (Singhose *et al*., 1994; Singhose and Mills, 1999; Mohamed *et al*., 2006). Some comparisons made to compare the positive and negative input shapers for vibration control of a single-link flexible manipulator have also been reported (Mohamed *et al*., 2006).

In general, control of flexible manipulators can be made easier by locating every sensor exactly at the location of the actuator, as collocation of the sensors and actuators guarantees stable servo control. In the case of flexible manipulator systems, the end-point position is controlled by obtaining the parameters at the hub and the end-point of the manipulator, as well as using the measurements as a basis for applying control torque at the hub. Thus, the feedback control can be divided into collocated and non-collocated control. By applying the control torque based on the non-collocated sensors, the problems of non-minimum phase and achieving stability are of concern. Several

approaches which utilise closed-loop control strategies have been reported for control of flexible manipulators. These include linear state feedback control (Cannon and Schmitz, 1984; Hasting and Book, 1987), adaptive control (Feliu *et al*., 1990; Yang *et al*., 1992), robust control techniques based on H-infinity (Moser, 1993), and variable structure control (Moallem *et al*., 1998) as well as intelligent control based on the neural networks (Gutierrez *et al*., 1998) and fuzzy logic control schemes (Moudgal *et al*., 1994).

An important aspect of the flexible manipulator control which has received little attention is the interaction between the rigid and flexible dynamics of the links. An acceptable system performance with reduced vibration which accounts for system changes can be achieved by developing a hybrid control scheme that caters for rigid body motion and vibration of the system independently. This can be realised by utilising control strategies consisting of either non-collocated with collocated feedback controllers or feedforward with feedback controllers. In both cases, the former can be used for vibration suppression and the latter for input tracking of a flexible manipulator. A combination of the control techniques would practically position the end-point of the flexible manipulator from one point to another with reduced vibration. Both the feedforward and feedback control structures have been utilised in controlling flexible manipulator systems. A hybrid of the collocated and non-collocated controller has previously been proposed to control a flexible manipulator (Tokhi and Azad, 1996b). The controller design utilises end-point acceleration feedback through a proportional-integral-derivative (PID) control scheme and a proportional-derivative (PD) configuration to control rigid body motion. Experimental investigations have shown that the control structure gives a satisfactory system response with a significant vibration reduction as compared to the response with a collocated controller. A PD feedback control, with a feedforward control to regulate the position of a flexible manipulator, has also been proposed (Shchuka and Goldenberg, 1989). Results from the simulation showed that although the pole-zero cancellation property of the feedforward control could speed the response of the system up, it would increase overshoot and oscillation. A control law partitioning scheme which uses end-point sensing device has been reported (Rattan *et al*., 1990). The scheme uses the end-point position signal in an outer loop controller to control the flexible modes, whereas the inner loop controls the rigid body motion which is independent of the flexible dynamics of the manipulator. The performance of the scheme has been demonstrated in both simulation and experimental trials which have incorporated the first two flexible modes. A combined feedforward and feedback method, in which the end-point position is sensed by an accelerometer and fed back to the motor controller operating as a velocity servo, has been proposed to control a flexible manipulator system (Wells and Schueller, 1990). This particular method uses a single mass-spring-damper system to represent the manipulator and thus the technique is not suitable for a high speed operation.

This paper presents investigations into the development of techniques for the end-point vibration suppression and input tracking of a flexible manipulator. A constrained planar single-link flexible manipulator is considered. The control strategies based on the feedforward with LQR controllers and with combined non-collocated and LQR controllers have also been investigated. A simulation environment was developed within the Simulink® and Matlab® to evaluate the performance of the control schemes. In this work, the dynamic model of the flexible manipulator was derived using the assumed mode method (AMM). Some previous simulation and experimental studies have shown that the AMM method gives an acceptable dynamic characterisation of the actual system (Martins *et al*., 2003). Moreover, two modes of vibration are sufficient to describe the dynamic behaviour of the manipulator reasonably well. Therefore, an LQR controller which utilises full-state feedback was initially developed to control rigid body motion and thus demonstrate the effectiveness of the proposed control schemes. This was then extended to incorporate non-collocated and feedforward controllers for vibration suppression of the manipulator.

The end-point displacement feedback through a PID control configuration was developed for the non-collocated control, whereas in the feedforward scheme, the positive and modified SNA input shapers are utilised as these have been shown to be effective in reducing system vibration. The results from the simulation of the response of the manipulator to the controllers are presented in time and frequency domains. The performances of the control schemes are assessed in terms of their level of vibration reduction, input tracking capability and time response specifications. Finally, a comparative assessment of the control techniques is also presented and discussed.

THE FLEXIBLE MANIPULATOR SYSTEM

Fig. 1 shows the single-link flexible manipulator system considered in this work, where X_oOY_o and XOY represent the stationary and moving coordinates frames, respectively, and τ represents the applied torque at the hub. E, I, ρ, L, A and I_h represent the Young modulus, area moment of inertia, mass density per unit volume, length, cross-sectional area and hub inertia of the manipulator, respectively. In this work, the motion of the manipulator is confined to X_oOY_o plane. Transverse shear and rotary inertia effects are neglected, since the manipulator is long and slender. Thus, the Bernoulli-Euler beam theory is allowed to be used to model the elastic behaviour of the manipulator. The manipulator is assumed to be stiff in vertical bending and torsion, allowing it to vibrate dominantly in the horizontal direction and thus, the gravity effects are neglected. Moreover, the manipulator is considered to have a constant cross-section and uniform material properties throughout. In this study, an aluminium type flexible manipulator, with dimensions of $900 \times 19.008 \times 3.2004$ mm^3, $E = 71 \times 10^9$ N/m^2, $I = 5.1924 \times 10^{11}$ m^4, $\rho = 2710$ kg/m^3 and $I_h = 5.8598 \times 10^{-4}$ kgm^2, was considered. These parameters constitute a single-link flexible manipulator experimental-rig which was developed to test and verify the control algorithms (Tokhi *et al*., 2001).

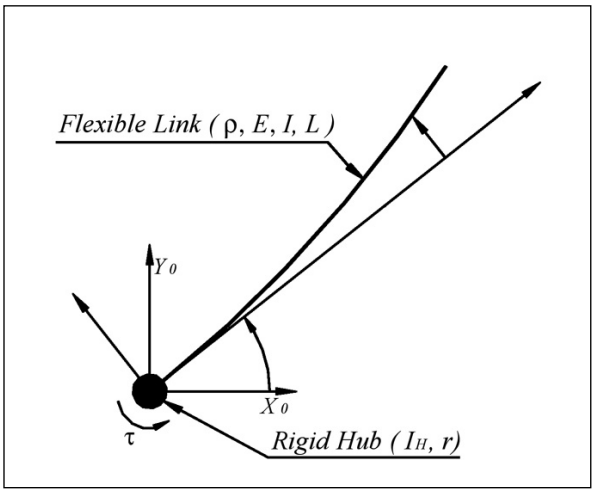

Fig. 1: Description of the flexible manipulator system

MODELLING OF THE FLEXIBLE MANIPULATOR

This section provides a brief description on the modelling of the flexible manipulator system, which serves as a basis of a simulation environment for the development and assessment of the control schemes. The AMM with two modal displacements is considered in characterising the dynamic behaviour of the manipulator incorporating structural damping and hub inertia. Further details of the description and derivation of the dynamic model of the system can be found in Subudhi and Morris (2002). The dynamic model has also been validated through experimental exercises where a close agreement between both theoretical and experimental results has been achieved in Martins *et al*. (2003).

Considering revolute joints and motion of the manipulator on a two-dimensional plane, the kinetic energy of the system can thus be formulated as:

$$T = \frac{1}{2}(I_H + I_b)\dot{\theta}^2 + \frac{1}{2}\rho \int_0^L (\dot{v}^2 + 2\dot{v}x\dot{\theta})\,dx \tag{1}$$

Where, I_b is the beam rotation inertia about the origin O as if it were rigid. The potential energy of the beam could be formulated as:

$$U = \frac{1}{2}\int_0^L EI\left(\frac{\partial^2 v}{\partial x^2}\right)^2 dx \tag{2}$$

This expression states the internal energy which is due to the elastic deformation of the link as it bends. The potential energy due to gravity is not accounted for since only the motion in the plane perpendicular to the gravitational field is considered.

Next, the energy expressions in Equations (1) and (2) are used to formulate the Lagrangianto $L = T - U$ obtain a closed-form dynamic model of the manipulator. Assembling the mass and stiffness matrices and utilising the Euler-Lagrange equation of motion, the dynamic equation of motion of the flexible manipulator system can be obtained as:

$$M\ddot{Q}(t) + D\dot{Q}(t) + KQ(t) = F(t) \tag{3}$$

Where, *M, D* and *K* are global mass, damping and stiffness matrices of the manipulator, respectively. The damping matrix is obtained by assuming the manipulator which exhibits the characteristic of Rayleigh damping. *F(t)* is a vector of the external forces and *Q(t)* is a modal displacement vector which is given as:

$$Q(t) = \begin{bmatrix}\theta & q_1 & q_2 & \ldots & q_n\end{bmatrix}^T = \begin{bmatrix}\theta & q^T\end{bmatrix}^T \tag{4}$$

$$F(t) = \begin{bmatrix}\tau & 0 & 0 & \ldots & 0\end{bmatrix}^T \tag{5}$$

Here, q_n is the modal amplitude of the i th clamped-free mode considered in the assumed modes method procedure and n represents the total number of the assumed modes. The model of the uncontrolled system could be represented in a state-space form as:

$$\begin{aligned}\dot{x} &= Ax + Bu \\ y &= Cx\end{aligned} \tag{6}$$

with the vector $x = \begin{bmatrix}\theta & \dot{\theta} & q_1 & q_2 & \dot{q}_1 & \dot{q}_2\end{bmatrix}^T$ and the matrices **A** and **B** are given by:

$$\mathrm{A} = \begin{bmatrix} 0_{3\times3} & I_{3\times3} \\ -M^{-1}K & -M^{-1}D \end{bmatrix}, \quad \mathrm{B} = \begin{bmatrix} 0_{3\times1} \\ M^{-1} \end{bmatrix}$$
$$\mathrm{C} = \begin{bmatrix} I_{1\times3} & 0_{1\times3} \end{bmatrix}, \qquad \mathrm{D} = \begin{bmatrix} 0 \end{bmatrix} \tag{7}$$

CONTROL SCHEMES

In this section, control schemes for rigid body motion control and vibration suppression of a flexible manipulator are proposed. Initially, an LQR controller was designed. Then, a non-collocated PID control and feedforward control based on input shaping were incorporated in the closed-loop system to control vibration of the system.

LQR Controller

A more common approach in the control of the manipulator systems involves the utilizatio of LQR design (Ogata, 1997). Such an approach was adopted at this stage of the investigation. Therefore, a linear state-space model of the flexible manipulator was obtained by linearising the equations of the system motion to design the LQR controller. For a LTI system:

$$\dot{x} = Ax + Bu, \tag{8}$$

The technique involves choosing a control law $u = \psi(x)$ which stabilizes the origin (i.e. regulates x to zero), while minimizing the quadratic cost function:

$$J = \int_0^\infty x(t)^T Qx(t) + u(t)^T Ru(t)\,dt \tag{9}$$

Where, $Q = Q^T$ and $R = R^T > 0$. The term "linear-quadratic" refers to the linear system dynamics and the quadratic cost function.

The matrices Q and R are called the state and control penalty matrices, respectively. If the components of Q are chosen largely relative to those of R, the deviations of x from zero will then be penalized heavily and relatively to the deviations of u from zero. On the other hand, if the components of R re largely relative to those of Q, the control effort will then be more costly and the state will not converge to zero as quickly.

A famous and somewhat surprising result due to Kalman is that the control law which minimizes J always takes the form $u = \psi(x) = -Kx$. The optimal regulator for a LTI system, with respect to the quadratic cost function above, is always a linear control law. With this observation in mind, the closed-loop system takes the following form:

$$\dot{x} = (A - BK)x \tag{10}$$

and the cost function J takes the form:

$$J = \int_0^\infty x(t)^T Qx(t) + (-Kx(t))^T R(-Kx(t))\,dt \tag{11}$$

$$J = \int_0^\infty x(t)^T (Q + K^T RK)x(t)\,dt$$

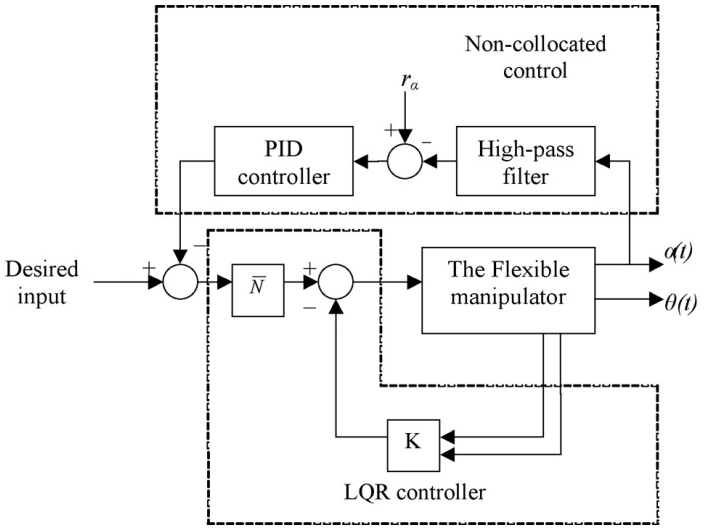

Fig. 2: The LQR and non-collocated PID control structure

Assuming that the closed-loop system is internally stable, which is a fundamental requirement for any feedback controller, the following theorem allows the computation value of the cost function for a given control gain matrix *K*.

LQR with Non-collocated Control

A combination of full-state feedback and non-collocated control scheme to control rigid body motion and vibration suppression of the system is presented in this section. As more reliable output measurement is obtained, the use of a non-collocated control system can be applied to improve the overall performance, where the end-point of the manipulator is controlled by measuring its position. The control structure comprises two feedback loops: (1) the full-state feedback as input to optimize the control gain matrix for rigid body motion control, and (2) the end-point residual (elastic deformation) as input to a separate non-collocated control law for vibration control. These two loops are then summed together to give a torque input to the system. A block diagram of the control scheme is shown in *Fig. 2*, in which α represents the end-point residual. Meanwhile, r_α represents the end-point residual reference input, which is set to zero as the control objective is to have zero vibration during movement of the manipulator.

For rigid body motion control, the LQR control strategy developed in the previous section was adopted, whereas the end-point residual feedback through a PID control scheme was utilised for the vibration control loop. For the two control loops to work well, they have to be decoupled from one another. This can be achieved using a high-pass filter in the non-collocated control loop.

LQR with Feedforward Control

A control structure used to control rigid body motion and vibration suppression of the flexible manipulator based on the LQR and feedforward control is proposed in this section. For feedforward controller, the positive and modified specified negative amplitude (SNA) input shapers were proposed and designed based on the properties of the system. In this study, the feedforward control scheme was developed using a ZVDD input shaping technique for both positive and negative shapers.

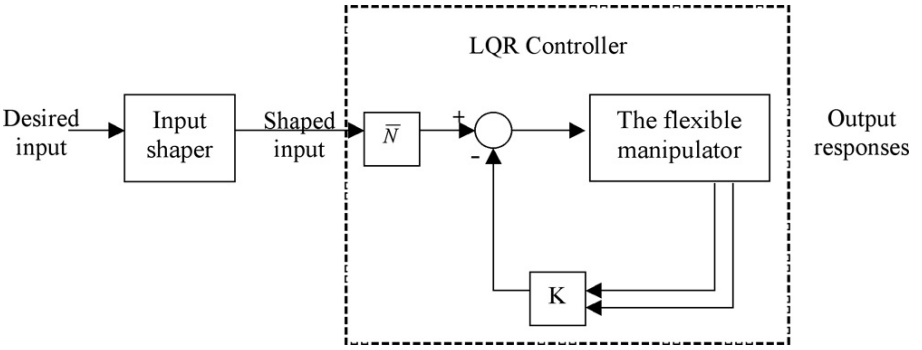

Fig. 3: The LQR and input shaping control structure

An experimental study previously conducted with a flexible manipulator showed that significant vibration reduction and robustness was achieved using a ZVDD technique (Mohamed and Tokhi, 2002). *Fig. 3* depicts a block diagram of the LQR with input shaping control technique.

The input shaping method involves convolving a desired command with a sequence of impulses known as input shaper. The objectives of the design were to determine the amplitude and time location of the impulses based on the natural frequencies and damping ratios of the system. The positive input shapers have been used in most input shaping schemes. The requirement of positive amplitude for the impulses is to avoid the problem of large amplitude impulses. In this case, each individual impulse must be less than one to satisfy the unity magnitude constraint. In addition, the robustness of the input shaper to errors in natural frequencies of the system can be increased by solving the derivatives of the system vibration equation. This yields a positive ZVDD shaper with parameter as:

$$t_1 = 0,\ t_2 = \frac{\pi}{\omega_d},\ t_3 = \frac{2\pi}{\omega_d},\ t_4 = \frac{3\pi}{\omega_d}, \tag{12}$$

$$A1 = \frac{1}{1 + 3H + 3H^2 + H^3},\ A2 = \frac{3H}{1 + 3H + 3H^2 + H^3}$$

$$A_3 = \frac{3H^2}{1 + 3H + 3H^2 + H^3},\ A_4 = \frac{H^3}{1 + 3H + 3H^2 + H^3}$$

where

$$H = e^{-\zeta\pi/\sqrt{1-\zeta^2}} \quad , \qquad \omega_d = \omega_n\sqrt{1-\zeta^2}$$

ω_n and ζ represent the natural frequency and damping ratio, respectively. As for the impulses, t_j and A_j are the time location and amplitude of the impulse j, respectively.

Input shaping techniques based on the positive input shaper has been proven to be able to reduce vibration of a system. The duration of the shaper is increased to achieve higher robustness, and thus, increase the delay incurred in the system response. The shaper duration can be shortened by allowing the shaper to contain negative impulses, while satisfying the same robustness constraint. Therefore, to include negative impulses in a shaper requires the impulse amplitudes to switch between 1 and -1 as:

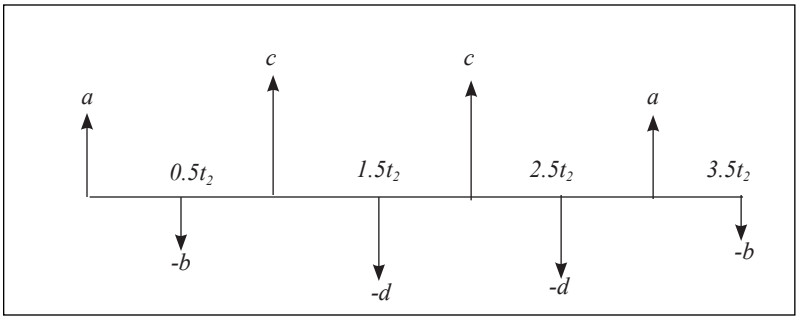

Fig. 4: Modified SNA-ZVDD shaper

$$A_i = (-1)^{i+1}; \quad i = 1, \ldots \ldots, n \tag{13}$$

The constraint in Equation (13) yields useful shapers as they can be used with a wide variety of inputs. In this work, the previous SNA input shaper (Mohamed *et al*., 2006) was modified by locating the negative amplitudes at the centre between each positive impulse sequences with the even number of the total impulses. This made the shaper duration as one-fourth of the vibration period of an undamped system as shown in *Fig. 4*. The modified SNA ZVDD shaper was proposed and applied in this work to enhance the robustness capability of the controller while increasing the speed of the system response. By considering the form of the modified SNA-ZVDD shaper (shown in *Fig. 4*), the amplitude summation constraints equation can be obtained as:

$$2a + 2c - 2b - 2d = 1 \tag{14}$$

The values of *a*, *b, c,* and *d* can be set to any values which satisfy the constraint in Equation (14). However, the suggested values of *a*, *b, c,* and *d* are less than |1| so as to avoid the increase of the actuator effort.

IMPLEMENTATION AND RESULTS

In this section, the proposed control schemes are implemented and tested within the simulation environment of the flexible manipulator, and the corresponding results are presented. The manipulator is required to follow a trajectory within the range of ± 0.8 radian as shown in *Fig. 5*. System responses namely the end-point trajectory, displacement, and end-point acceleration are also observed. To investigate the vibration of the system in the frequency domain, power spectral density (PSD) of the end-point acceleration response is obtained. The performances of the control schemes are assessed in terms of their vibration suppression, input tracking, and time response specifications. Finally, a comparative assessment of the performance of the control schemes is presented and discussed.

LQR Controller

In this investigation, the tracking performance of the LQR applied to the flexible manipulator was investigated by setting the value of vector K and $\overline{N}$ to determine the feedback control law and eliminate steady state error capability, respectively. For the single-link flexible manipulator (described by the state-space model given by Equation 6) and with M, K, and D matrices calculated earlier, the LQR gain matrix for

$$Q = \begin{bmatrix} I_{3\times3} & 0_{3\times3} \\ 0_{3\times3} & 0_{3\times3} \end{bmatrix} \text{ and } R = 1$$

was calculated using the Matlab® and was therefore found to be:

$$K = [3.1623 \;\; 4.1006 \;\; 42.7052 \;\; 0.4956 \;\; 0.6449 \;\; 6.7017]$$

$$\bar{N} = [3.1623]$$

Fig. 6 shows the responses of the flexible manipulator to the reference input trajectory in the time-domain and frequency domain (PSD). These results were considered as the system response under rigid body motion control and were used to evaluate the performance of the non-collocated PID and feedforward control. The steady-state end-point trajectory of +0.8 radian for the flexible manipulator was achieved within the rise and settling times, and overshoot of 0.421 s, 1.233 s, and 6.06%, respectively. The manipulator was found to reach the required position from +0.8 rad to -0.8 rad within 2 s, with little overshoot. However, a noticeable amount of vibration was detected during the movement of the manipulator. From the displacement response, the vibration of the system was noted to settle within 1 s with a maximum residual of ±0.15 m. This is similar for the end-point acceleration response, whereby the vibration of the system was indicated to settle within 0.5 s with a maximum acceleration of ±600 m/s^2. Moreover, from the PSD of the end-point acceleration response the vibrations at the end-point are dominated by the first two vibration modes, which were obtained as 16 and 56 Hz.

QR with Non-collocated and Feedforward Control

In the full-state feedback and the non-collocated control scheme of LQR-PID, the PID controller parameters were tuned with the Ziegler-Nichols method using a closed-loop technique, where the proportional gain K_p was initially tuned and the integral gain K_i and derivative gain K_d were then calculated (Warwick, 1989). Accordingly, the PID parameters K_p, K_i, and K_d were deduced as 0.7, 5 and 0.03, respectively. A third-order infinite impulse response (IIR) Butterworth high-pass filter was utilised to decouple the end-point measurement from the rigid body motion of the manipulator. In this investigation, a high-pass filter with the cut-off frequency of 5 Hz was designed.

In the case of the LQR and feedforward control scheme, the combination of the LQR with positive ZVDD shaper (LQR-PZVDD) and the modified SNA ZVDD shaper (LQR-NZVDD) were respectively designed, based on the dynamic behaviour of the closed-loop system, which was obtained using only the LQR control. As demonstrated in the previous section, the natural frequencies of the manipulator were 16 Hz and 56 Hz. Previous experimental results showed that the damping ratio of the flexible manipulator ranged from 0.024 to 0.1 (Azad, 1994). In this work, however, the damping ratios were deduced as 0.086 and 0.096 for the first two modes, respectively. The magnitudes and time locations of the impulses for positive shaper were obtained by solving Equation (12) for the first two modes. However, the amplitudes of the modified SNA ZVDD shaper were deduced as [0.3 -0.1 0.5 -0.2 0.5 -0.2 0.3 -0.1], and the time locations of the impulses were chosen at the half of the time locations of positive ZVDD shaper, as shown in *Fig. 4*. As for the digital implementation of the input shaper, the locations of the impulses were selected at the nearest sampling time. The developed input shaper was then used to pre-process the input reference shown in *Fig. 5*.

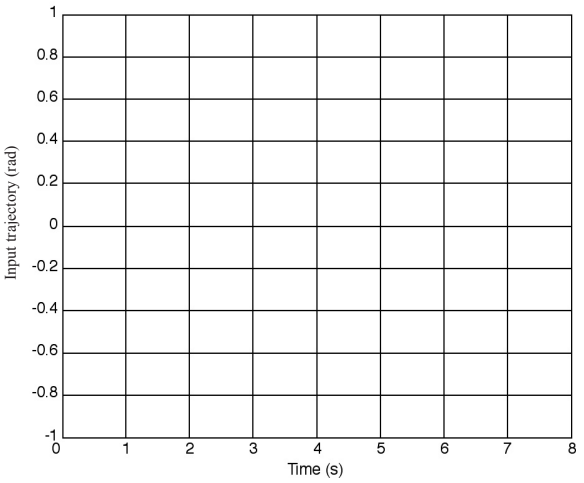

Fig. 5: The reference input trajectory

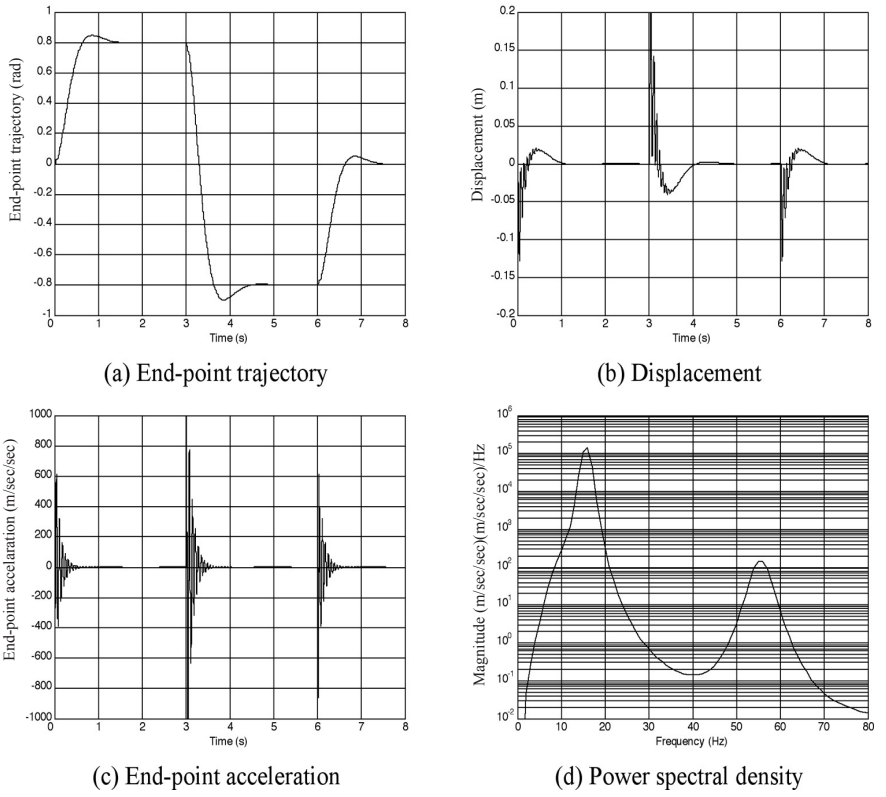

Fig. 6: Response of the manipulator with the LQR control

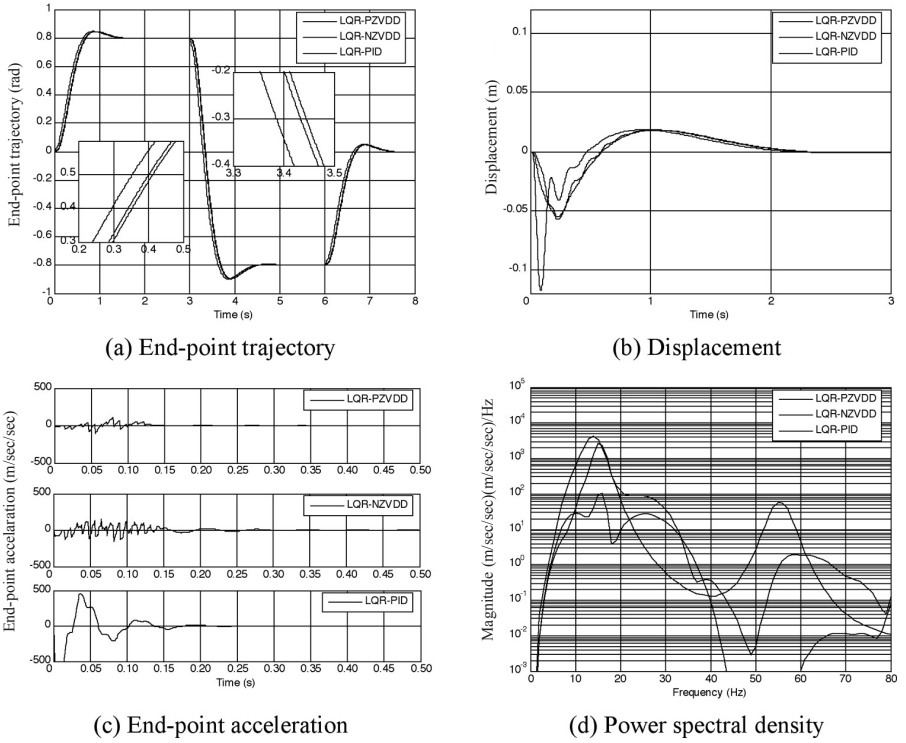

(a) End-point trajectory (b) Displacement

(c) End-point acceleration (d) Power spectral density

Fig. 7: Response of the manipulator with the LQR-PZVDD, LQR-NZVDD and LQR-PID control

TABLE 1
Level of vibration reduction of the end-point acceleration and specifications of end-point trajectory response for hybrid control schemes

Controller	Attenuation (dB) of vibration end-point acceleration		Specifications of end-point trajectory response		
	Mode 1	Mode 2	Rise time (s)	Settling time (s)	Overshoot (%)
LQR – PID	37.14	8.04	0.418	1.232	6.06
LQR - PZVDD	62.59	146.73	0.423	1.291	6.00
LQR - NZVDD	35.04	40.14	0.424	1.280	5.99

The corresponding responses of the manipulator are shown in *Fig. 7*. The proposed control schemes were found to be capable of reducing the system vibration while maintaining the input tracking performance of the manipulator. Similar end-point trajectory, displacement, and end-point acceleration responses were also observed as compared to the LQR controller. Table 1 summarises the levels of vibration reduction of the system responses at the first two modes as compared to the LQR control. In overall, the highest levels of vibration reduction for the first two modes

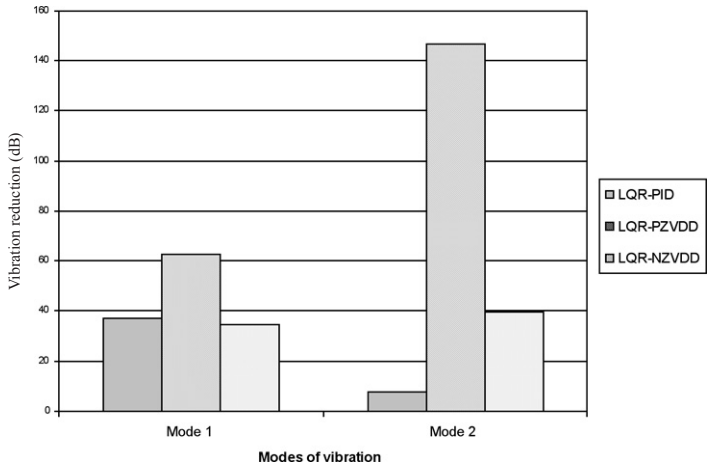

Fig. 8: Level of vibration reduction with the LQR-PID, LQR-PZVDD and LQR-NZVDD control at the end-point of the manipulator

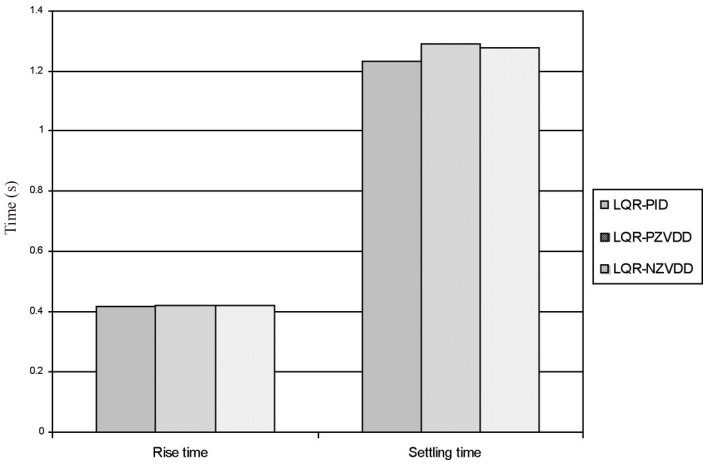

Fig. 9: Rise and settling times of the end-point trajectory with the LQR-PID, LQR-PZVDD and LQR-NZVDD control

were obtained using the LQR-PZVDD, and this was followed by the LQR-NZVDD and LQR-PID. However, the fastest system response was obtained using the LQR-PID, followed by the LQR NZVDD and LQR-PZVDD. Meanwhile, the impulses sequence in input shaper was found to increase the delay in the system response with the use of the feedforward controller. Table 1 depicts the corresponding rise time, setting time and overshoot of the end-point trajectory response using the LQR-PZVDD, LQR-NZVDD and LQR-PID. Moreover, the minimum phase behaviour of the manipulator was found to be unaffected, as demonstrated in the end-point trajectory response with the LQR-PID control. A significant amount of vibration reduction was demonstrated at the end-point of the manipulator with both control schemes. The maximum displacement at the end-point is ±0.1 m while with the LQR-PZVDD and LQR-NZVDD control is ±0.05 m when the LQR-PID control is used. A similar pattern was shown for the end-point acceleration result with the

maximum accelerations of ±100 m/s^2, ±200 m/s^2 and ±500 m/s^2 for LQR-PZVDD, LQR-NZVDD and LQR-PID, respectively. Hence, the magnitude of oscillation was found to be significantly reduced using the LQR with the feedforward control as compared to the case of the LQR with the non-collocated PID control. Overall, the performance of the control schemes at the input tracking capability is maintained as the LQR control.

The results from the simulation show that the performance of LQR-PZVDD control scheme is better than LQR-NZVDD and LQR-PID schemes in suppressing the vibration of the flexible manipulator. This is further evidenced in *Fig. 8*, whereby the level of vibration reduction at the resonance modes of the LQR with the non-collocated and feedforward control is respectively shown as compared to the LQR controller. Higher vibration reduction is achieved with the use of LQR-PZVDD at the first two modes of vibration. Almost two-fold and more than four-fold improvements were observed in the vibration reduction in the first and second resonance modes, respectively using the LQR-PZVDD as compared to using LQR-NZVDD and LQR-PID. Moreover, the implementation of the LQR with feedforward control is easier than the application of the LQR with the non-collocated PID control as a large amount of design effort is required to determine the best PID parameters. It is important to note that a properly tuned PID could produce better results. Nevertheless, slightly slower response was obtained using the LQR with the feedforward control as compared to the LQR with the non-collocated control, as demonstrated in the end-point trajectory response. *Fig. 9* summarizes the comparisons of the specifications of the end-point trajectory responses for the rise and settling times. Thus, the work developed and reported in this paper forms the basis for designing and developing the hybrid control schemes for input tracking and vibration suppression of multi-link flexible manipulator systems which can be extended to and adopted in other practical applications.

CONCLUSION

The development of techniques for end-point vibration suppression and input tracking of a flexible manipulator has been presented. The control schemes have been developed based on the LQR with non-collocated PID control and the LQR with feedforward control based on positive and modified SNA input shaper techniques. The proposed control schemes have been implemented and tested within a simulation environment of a single-link flexible manipulator. The performances of the control schemes have been evaluated in terms of the end-point vibration suppression and input tracking capability at the resonance modes of the manipulator. Meanwhile, acceptable performance at the end-point vibration suppression and input tracking control has been achieved using the proposed control strategies. A comparative assessment of the control schemes has shown that the LQR control, with input shaping (feedforward), performs better than the LQR with non-collocated PID control in terms of vibration reduction at the end-point of the manipulator. However, the speed of the response is slightly improved at the expenses of decreasing the level of vibration reduction using the LQR with non-collocated PID control. Therefore, the proposed controllers can be concluded as being capable of reducing the system vibration, while maintaining the input tracking performance of the manipulator.

REFERENCES

Aspinwall, D.M. (1980). Acceleration profiles for minimising residual response. *Transactions of ASME: Journal of Dynamic Systems, Measurement and Control*, *102*(1), 3-6.

Azad, A.K.M. (1994). *Analysis and design of control mechanism for flexible manipulator systems*. PhD. Thesis, Department of Automatic Control and Systems Engineering, University of Sheffield, UK.

Bayo, E. (1988). Computed torque for the position control of open-loop flexible robots. *Proceedings of IEEE International Conference on Robotics and Automation* (pp.316-321). Philadelphia.

Cannon, R.H. and Schmitz, E. (1984). Initial experiment on the end-point control of a flexible one-link robot. *International Journal of Robotics Research*, *3*(3), 62-75.

Feliu, V., Rattan, K.S. and Brown, H.B. (1990) Adaptive control of a single-link flexible manipulator. *IEEE Control Systems Magazine*, *10*(2), 29 –33.

Gutierrez, L.B., Lewis, P.L. and Lowe, J.A. (1998). Implementation of a neural network tracking controller for a single flexible link: Comparison with PD and PID controllers. *IEEE Transactions on Industrial Electronics*, *45*(3), 307-318.

Hasting, G.G. and Book, W.J. (1987). A linear dynamic model for flexible robot manipulators. *IEEE Control Systems Magazine*, *7*, 61-64.

Khorrami, F., Jain, S. and Tzes, A. (1994). Experiments on rigid body-based controllers with input preshaping for a two-link flexible manipulator. *IEEE Transactions on Robotics and Automation*, *10*(1), 55-65.

Martins, J.M., Mohamed, Z., Tokhi, M.O., Sá da Costa, J. and Botto, M.A. (2003). Approaches for dynamic modelling of flexible manipulator systems. *IEE Proceedings-Control Theory and Application*, *150*(4), 401-411.

Meckl, P.H. and Seering, W.P. (1990). Experimental evaluation of shaped inputs to reduce vibration of a Cartesian robot. *Transactions of ASME: Journal of Dynamic Systems, Measurement and Control*, *112*(6), 159-165.

Moallem, M., Khorasani, K. and Patel, R.V. (1998). Inversion-based sliding control of a flexible-link manipulator. *International Journal of Control*, *71*(3), 477-490.

Mohamed, Z. and Tokhi, M.O. (2002). Vibration control of a single-link flexible manipulator using command shaping techniques. *Proceedings IMechE-I: Journal of Systems and Control Engineering*, *216*, 191-210.

Mohamed, Z., Chee, A.K., Mohd Hashim, A.W.I., Tokhi, M.O., Amin, S.H.M. and Mamat, R. (2006). Techniques for vibration control of a flexible manipulator. *Robotica*, *24*, 499-511.

Moser, A.N. (1993). Designing controllers for flexible structures with H-infinity/μ-synthesis. *IEEE Control Systems Magazine*, *13*(2), 79-89.

Moudgal, V.G., Passino, K.M. and Yurkovich, S. (1994). Rule-based control for a flexible-link robot. *IEEE Transactions on Control Systems Technology*, *2*(4), 392-405.

Ogata, K. (1997). *Modern Control Engineering*. Upper Saddle River, NJ: Prentice-Hall International.

Onsay, T. and Akay, A. (1991). Vibration reduction of a flexible arm by time optimal open-loop control. *Journal of Sound and Vibration*, *147*(2), 283-300.

Rattan, K.S., Feliu, V. and Brown, H.B. (1990). Tip position control of flexible arms. *Proceedings of the IEEE Conference on Decision and Control* (pp.1803-1808). Honolulu.

Shchuka, A. and Goldenberg, A.A. (1989). Tip control of a single-link flexible arm using feedforward technique. *Mechanical Machine Theory*, *24*, 439-455.

Singer, N.C. and Seering, W.P. (1990). Preshaping command inputs to reduce system vibration. *Transactions of ASME: Journal of Dynamic Systems, Measurement and Control*, *112*(1), 76-82.

Singhose, W., Singer, N.C. and Seering, W.P. (1994). Design and implementation of time-optimal negative input shapers. *Proceedings of International Mechanical Engineering Congress and Exposition* (pp. 151-157). Chicago.

Singhose, W.E., Singer, N.C. and Seering, W.P. (1995). Comparison of command shaping methods for reducing residual vibration. *Proceedings of European Control Conference* (pp. 1126-1131). Rome.

Singhose, W. and Mills, B.W. (1999). Command generation using specified-negative-amplitude input shapers. *Proceedings of the American Control Conference* (pp. 61-65). San Diego, California.

Subudhi, B. and Morris, A.S. (2002). Dynamic modelling, simulation and control of a manipulator with flexible links and joints. *Robotics and Autonomous Systems*, *41*, 257-270.

Tokhi, M.O. and Poerwanto, H. (1996a). Control of vibration of flexible manipulators using filtered command inputs. *Proceedings of International Congress on Sound and Vibration* (pp. 1019-1026). St. Petersburg.

Tokhi, M.O. and Azad, A.K.M. (1996b). Control of flexible manipulator systems. *Proceedings IMechE-I: Journal of Systems and Control Engineering*, *210*, 113-130.

Tokhi, M.O., Mohamed, Z. and Shaheed, M.H. (2001). Dynamic characterisation of a flexible manipulator system. *Robotica*, *19*(5), 571-580.

Wells, R.L. and Schueller, J.K. (1990). Feedforward and feedback control of a flexible manipulator. *IEEE Control System Magazine*, *10*, 9-15.

Warwick, K. (1989). *Control Systems: An Introduction*. London: Prentice Hall.

Yang, T.-C., Yang, J.C.S. and Kudva, P. (1992). Load-adaptive control of a single-link flexible manipulator systems. *IEEE Transactions on Systems, Man and Cybernetics*, *22*(1), 85-91.

ISSN: 0128-7680
Pertanika J. Sci. & Technol. **18 (1)**: 77– 81 (2010)

Anthraquinones from *Cratoxylum aborescens* (Guttiferae)

G.C.L. Ee*, V.Y.M. Jong, M.A. Sukari, T.K. Lee and A. Tan
Department of Chemistry, Faculty of Science, Universiti Putra Malaysia,
43400 UPM, Serdang, Selangor, Malaysia
**E-mail: gwen@fsas.upm.edu.my*

ABSTRACT

Our continuing interest in anthraquinones from the Guttiferae family has led us to look at the genus *Cratoxylum*. A detailed chemical study on *Cratoxylum aborescens* resulted in the isolation of three anthraquinones, namely 1,8-dihydroxy-3-methoxy-6-methylanthraquinone (**1**), vismiaquinone (**2**) and vismione (**3**). These compounds were identified using 1D and 2D NMR spectroscopy. This is the first report on the chemistry of *Cratoxylum aborescens*.

Keywords: *Cratoxylum aborescens*, Guttiferae, anthraquinones

INTRODUCTION

Cratoxylum belongs to the Guttiferae family, but it is sometimes categorized under the family of Hypericaceae. It is a small genus which consists of a total of six species. The wood of *Cratoxylum* is used for construction of houses and farm huts. Meanwhile, poles from moderately big trees are used as beams, joists, rafters, and posts in farm hut construction (Pearce *et al*., 1987). The stem bark of the species is known to be used in traditional medicine (Bennet *et al*., 1993). The bark, roots, and leaves are reported to be used in folk medicine to treat fevers, cough, diarrhoea, itches, ulcers, and abdominal complaints (Lien *et al.*, 1998). There are not many reports on the chemistry of the *Cratoxylum* species. However, some phytochemical studies on this genus have revealed the plant to be rich in flavonoids, xanthones, and triterpenoids (Iinuma *et al*., 1996; Bennett *et al*., 1993; Sia *et al*., 1995; Nguyen *et al*., 1998; Bennett and Lee, 1989). This paper describes the isolation and identification of three anthraquinones from *Cratoxylum aborescens.*

MATERIALS AND METHOD

Plant Material

The stem bark of *Cratoxylum aborescens* was collected from Sri Aman Sarawak, Malaysia. The plant materials were identified by Ms. Runi Sylvester from the Herbarium of Sarawak Forestry Department, Kuching, Sarawak, Malaysia.

General

Infrared spectra were measured in KBr/NaCl pellet on a Perkin-Elmer FTIR Spectrum BX spectrometer. EIMS were recorded on a Shimadzu GCMS-QP5050A spectrometer. NMR spectra were obtained using a Unity INOVA 500MHz NMR/ JEOL 400MHz FT NMR spectrometer with tetramethylsilane (TMS) as its internal standard. Ultra violet spectra were recorded in $CHCl_3$ on a Shimadzu UV-160A, UV-Visible Recording Spectrophotometer.

Received: 9 April 2008
Accepted: 17 March 2009
*Corresponding Author

Extraction and Isolation

The air-dried and powdered stem bark of *Cratoxylum aborescens* (2.5 kg) was successively extracted with hexane, chloroform, and methanol at room temperature. The extracts were evaporated to dryness under reduced pressure to yield 15.8 g, 39.5 g, and 30.6 g of hexane chloroform and methanol extracts, respectively. Each of the crude extracts was subjected to a series of column chromatography over silica gel columns, using a stepwise gradient system (hexane/chloroform, chloroform/ethyl acetate, and ethyl acetate/methanol). The column chromatography of the hexane extract gave vismiaquinone (**2**) (6 mg) and vismione (**3**) (5 mg) (3). Meanwhile, the methanol extract gave 10 mg of 1,8-dihydroxy-3-methoxy-6-methylanthraquinone (**1**).

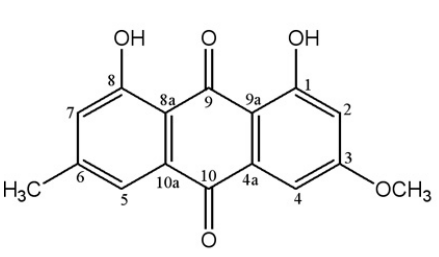

(1)

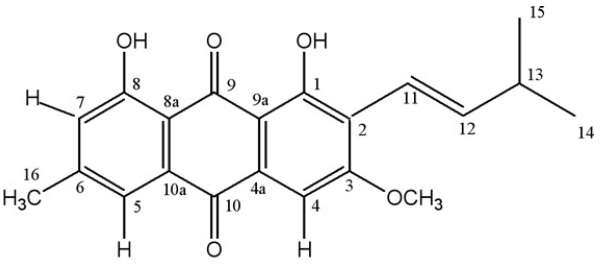

(2)

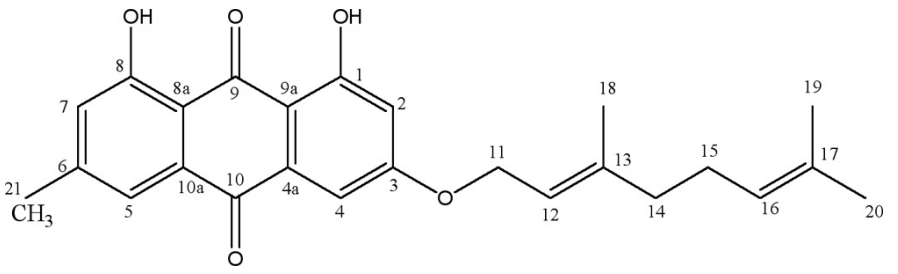

(3)

Vismiaquinone (**2**) - orange crystals, m.p. 200-202ºC (Lit. 202-204ºC, Lourdes *et al.,* 1981). UV (EtOH) λ_{max} nm: 276.0, 445. IR ν_{max}: 3448, 2924, 2854, 1626, 1476. EI-MS m/z: 352, 337, 309, 297, 283, 267, 237, 211, 189, 168, 161, 152, 138, 115, 89, 63 and 41. ^{1}H NMR (400 MHz, $CDCl_3$): δ 12.96 (s, 1H, 1-OH), δ 12.11 (s, 1H, 8-OH), δ 7.62 (s, 1H, H-5), δ 7.42 (s, 1H, H-4), δ 7.07 (s, 1H, H-7), δ 6.92 (dd, *J* = 16.5, 7.3Hz, 1H, H-12), δ 6.65 (d, *J* = 16.5Hz, 1H, H-11), δ 4.05 (s, 3H, 3-OMe), δ 2.52 (m, 1H, H-13), δ 2.45 (s, 3H, H-16), δ 1.14 (s, 3H , H-14), δ 1.14 (s, 3H , H-15). ^{13}C NMR (100 MHz, $CDCl_3$): δ 191.5 (C-9), δ 182.0 (C-10), δ 163.0 (C-3), δ 162.5 (C-8), δ 162.1 (C-1), δ 148.4 (C-6), δ 146.8 (C-11), δ133.2 (C-10a), δ 132.1 (C-4a), δ 124.4 (C-7), δ 121.1 (C-5), δ 120.0 (C-2), δ 115.8 (C-12), δ 113.8 (C-8a), δ 110.6 (C-9a), δ 103.4 (C-4), δ 56.3 (3-OMe), δ 33.4 (C-15), δ 29.7 (C-13), δ 22.5 (C-14), δ 22.2 (C-16).

1,8-dihydroxy-3-methoxy-6-methylanthraquinone (**1**) - orange powder, m.p. 207-209ºC. (Lit. 210ºC, Kitanaka *et al*., 1985). UV (EtOH) λ_{max} nm: 273.6, 445.0. IR ν_{max}: 3442, 1628, 1478, 1370. EI-MS m/z: 284, 255, 241, 241, 227, 213, 198, 185, 167, 151, 128, 106, 89, 77, 69, 51, 41. ^{1}H

NMR (400 MHz, $CDCl_3$): δ 12.31 (s, 1H, OH-1), δ 12.11 (s, 1H, 8-OH), δ 7.62 (s, 1H, H-5), δ 7.36 (d, *J* = 2.7Hz, H-4), δ 7.08 (s, 1H, H-7), δ 6.68 (d, *J* = 2.7Hz, 1H, H-2), δ 3.94 (s, 3H, 3-OMe), δ 2.45 (s, 3H, 6-CH_3). ^{13}C NMR (100 MHz, $CDCl_3$): δ 190.8 (C-9), δ 182.0 (C-10), δ 166.5 (C-3), δ 165.1 (C-1), δ 162.5 (C-8), δ 148.4 (C-6), δ135.2 (C-10a), δ 133.2 (C-4a), δ 124.5 (C-7), δ 121.3 (C-5), δ 113.6 (C-8a), δ 110.2 (C-9a), δ 108.2 (C-4), δ 106.7 (C-2), δ 56.1(3-OMe), δ 22.1 (6-CH_3).

RESULTS AND DISCUSSION

Vismione (**3**) was obtained from the n-hexane extract as yellow crystals with a melting point of 141-143ºC (Lit. 141-143 ºC, Mohamed *et al.,* 1993). The mass spectrum showed the presence of a molecular ion peak at m/z 406, corresponding to the molecular formula, $C_{25}H_{26}O_5$. The existence of hydroxyl groups was confirmed by the strong IR absorption observed at 3438 cm^{-1} in the IR spectrum. The absorption observed at 2928 cm^{-1} was due to the carbon hydrogen stretching for the methyl group. The absorption at 1626 cm^{-1} was due to the carbonyl groups. The UV spectrum gave maximum absorptions at 267.5 and 456.0 nm.

The ^{1}H NMR spectrum revealed signals for aromatic protons at δ 6.67 (1H, d, *J*= 2.8 Hz) and δ 7.36 (1H, d, *J*= 2.8 Hz) for H-2 and H-4, and also two singlets at δ 7.61 for H-5 and δ 7.07 for H-7. An olefinic methyl proton signal, at δ 1.78 (3H, s) for H-18 and the geminal-dimethyl protons, at δ 1.61 (3H, s) for H-19 and δ 1.67 (3H, s) for H-20, in addition to the methyl proton signals at δ 2.45 (3H, s) for H-21 were also observed. The ^{1}H NMR spectrum also exhibited two sets of methylene proton signals at δ 2.11 (2H, m) and δ 2.13 (2H, m) and these were attributed to H-14 and H-15. Beside that, another methylene proton signal also appeared at δ 4.67 (2H, d, *J*= 6.4Hz) for H-11. Two vinyl methine proton signals appeared at δ 5.47 (1H, t, *J* = 6.4Hz) for H-12 and δ 5.09 (1H, t, *J* = 6.9Hz) for H-16. The signal of the methylene proton (δ 4.67) of the chain, which appeared in the relatively low field region, indicated that the geranyl group is oxygenated. The ^{1}H NMR spectrum also showed the presence of two hydroxyl groups at δ 12.29 (OH, s) and δ 12.13 (OH, s). There are 25 carbon signals from the ^{13}C NMR spectrum. Two typical conjugated carbonyl groups were observed at δ 190.7 for C-9 and δ 182.1 for C-10. The resonances at δ 165.1 (C-1) and δ 162.5 (C-8) were due to the oxygenated aromatic carbons.

In the ^{1}H-^{1}H COSY spectrum, the olefinic proton at δ 4.67 for H-11 was correlated to the proton at δ 5.47 for H-12. Six methine, three methylene, four methyl, and twelve tertiary carbon signals were observed from the DEPT spectrum, supporting the structure of vismione.

From the HMBC spectrum, ^3J correlations were observed between H-21 (δ 2.45) and C-5 (δ 121.2), as well as between H-21 (δ 2.45) and C-7 (δ 124.4). HMBC also gave ^2J correlations between the peak at H-21 (δ 2.45) and C-6 (δ 148.4).

The HMBC spectrum correlated all the protonated carbons to their respective protons. The chelated hydroxyl group (1-OH) was correlated to three aromatic carbons, namely C-1 (δ 165.1), C-2 (δ 107.5), and C-9a (δ 110.1). Another chelated hydroxyl group (8-OH) was also correlated to the three aromatic carbons, which are C-7 (δ 124.4), C-8 (δ 162.5), and C-8a (δ 113.7). Hence, compound 3 was assigned vismione, previously isolated from *Psorospermum febrifugum* (Mohamed *et al.,* 1993). The ^{1}H, ^{13}C NMR assignments and the HMBC correlations are shown in Table 1.

TABLE 1
^{1}H NMR (400 MHz, CDCl3), ^{13}C NMR (100 MHz, CDCl3)
& HMBC assignments of Vismione (3)

Position	δ_H	δ_C	HMBC
1	-	165.1	-
2	6.67 (1H, d, *J* = 2.8 Hz)	107.5	165.1(C-1), 110.1 (C9a).
3	-	165.9	-
4	7.36 (1H, d, *J* = 2.8 Hz)	108.8	107.5 (C-2), 182.1 (C-10), 110.1 (C-9a).
4a	-	133.2	-
5	7.61(1H,s)	121.2	124.4 (C-7), 182.1 (C-10), 113.7 (C-8a), 22.1 (C-21).
6	-	148.4	-
7	7.07 (1H, s)	124.4	121.2 (C-5), 113.7 (C-8a), 22.1 (C-21).
8	-	162.5	-
8a	-	113.7	-
9	-	190.7	-
9a	-	110.1	
10	-	182.1	-
10a	-	132.0	-
11	4.67 (2H, d, *J* = 6.4 Hz)	65.8	165.9 (C-3), 117.9 (C-12), 142.9 (C-13).
12	5.47 (1H, t, *J* = 6.4Hz)	117.9	39.5 (C-14), 16.8 (C-18).
13	-	142.9	-
14	2.11 (2H,m)	39.5	117.9 (C-12), 26.2 (C-15).
15	2.13 (2H,m)	26.2	142.9 (C-13), 39.5 (C-14).
16	5.09 (1H, t, *J* = 6.9Hz)	123.6	-
17	-	132.0	-
18	1.78 (3H, s)	16.8	117.9 (C-12), 142.9 (C-13), 39.5 (C-14).
19	1.61 (3H, s)	17.7	123.6 (C-16), 132.0 (C-17), 25.7 (C-20).
20	1.67 (3H, s)	25.7	123.6 (C-16), 132.0 (C-17), 17.7 (C-19).
21	2.45 (3H, s)	22.1	121.2 (C-5), 148.4 (C-6), 124.4 (C-7).
1-OH	12.29 (OH, s)	-	165.1 (C-1), 107.5 (C-2), 110.1 (C-9a).
8-OH	12.13 (OH, s)	-	124.4 (C-7), 162.5 (C-8), 113.7 (C-8a).

1,8-dihydroxy-3-methoxy-6-methylanthraquinone (**1**) was obtained as orange powder, with a melting point of 207-209ºC (Lit. 210ºC, Kitanaka *et al.,* 1985). The spectral data for this compound are in agreement with published data (Kitanaka *et al.,*1985).

On the other hand, vismiaquinone (**2**) was obtained as orange crystals which melt at 200-202ºC (Lit. 202-204ºC, Lourdes *et al.,* 1981). The structure of this compound was deduced by comparing its spectral data with the ones available in the literature (Lourdes *et al.,* 1981).

ACKNOWLEDGEMENTS

We thank the Malaysian IRPA grant for the financial support, Dr Jegak Uli for collecting the plant samples and Mr Johadi Iskander for recording the NMR spectra.

REFERENCES

Bennet, G.J. and Lee, H.H. (1989). Xanthones from Guttiferae. *Phytochemistry*, *28*(4), 967-998.

Bennet, G.J., Harrison, L.J., Sia, G-L. and Sim, K-Y. (1993). Triterpenoids, tocotrienols and xanthones from the bark of *Cratoxylum cochinchinese*. *Phytochemistry*, *32*(5), 1245-1251.

Iinuma, M., Tosa, H., Ito,T., Tanaka, T. and Madulid, D.A. (1996). Two xanthones from roots of *Cratoxylum formosanum*. *Phytochemistry*, *43*(4), 1195-1198.

Kitanaka, S., Kitamura, F. and Tachio, M. (1985). Studies on the constituents of purgative crude drugs. XVII. Studies on the constituents of the seeds of *Cassia obtusifolia* Linn.The structures of two new anthraquinone glycosides. *Chemical and Pharmaceutical Bulletin, 33*(3), 1274-1276.

Lien, H.D.N. and Harrison, L.J. (1998). Triterpenoid and xanthone constituents of *Cratoxylum cochinchinese. Phytochemistry*, *50*, 471-476.

Lourdes, M.D., Goncalves and Mors, W.B. (1981). Vismiaquinone Isopenthnyl Substituted Anthraquinone from *Vismia Reichartiana*. *Phytochemistry, 20*, 1947-1950.

Mohamed A-S., Suwanborirux Abdul-Azim, K., Habib, M., Chang, C.J. and Cassady, J.M. (1993). Xanthones and Vismiones from *Psorospermum Febrifugum*. *Phytochemistry, 34*, 1413-1420.

Nguyen, L.H.D. and Harrison, L.J. (1998). Triterpenoid and xanthones constituents of *Cratoxylum cochinchinese*. *Phytochemistry*, *50*, 471-476.

Pearce, K.G., Amen, V.L. and Jok, S. (1987). An ethnobotanical study of an iban community of the Pantu sub-district, Sri Aman, Division 2, Sarawak. *The Sarawak Museum Journal, XXXVII*(58), 193-270.

Sia, G.L., Bennett, G.J., Harrison, L.J. and Sim, K.Y. (1995). Minor xanthones from the bark of *Cratoxylum cochinchinese*. *Phytochemistry, 38*(6), 1521-1528.

ISSN: 0128-7680
Pertanika J. Sci. & Technol. **18 (1)**: 83 – 93 (2010)

Modelling of Single and Binary Adsorptions of Heavy Metals Onto Activated Carbon - Equilibrium Studies

Luqman Chuah Abdullah[1*], Muhammad[1], Saidatul Shima J.[1] and Thomas S. Y. Choong[2]
[1]Department of Chemical and Environmental Engineering,
[2]Department of Agricultural Engineering and Biology,
Faculty of Engineering, Universiti Putra Malaysia,
43400 UPM, Serdang, Selangor, Malaysia
[*]E-mail: chuah@eng.upm.edu.my

ABSTRACT

A series of batch laboratory studies were conducted to investigate the suitability of activated carbon SA2 for the removal of cadmium ions and zinc ions from their aqueous solutions. The single component equilibrium data were analyzed using the Langmuir and Freundlich isotherms. Overall, the Langmuir isotherm showed a better fitting for all adsorptions under investigation in terms of correlation coefficient and error analysis (SSE only 18.2 for Cd^{2+} and 47.95 for Zn^{2+}). As the binary adsorption is competitive, extended Langmuir models could not predict the binary component isotherm well. The modified extended Langmuir models were used to fit the binary system equilibrium data. The binary isotherm data could be described reasonably well by the modified extended Langmuir model, as indicated in the error analysis.

Keywords: Activated carbon, adsorption, binary isotherm, cadmium, zinc

NOMENCLATURES

a_F = Freundlich constant (L/mg)
a_L = Langmuir constant for energy of the sorbent (L/mg)
C_e = residue metal ions concentration remaining after adsorption (mg/L)
C_o = initial dye concentration (mg.L)
K_F = Freundlich constant for adsorption capacities (L/mg)
K_L = Langmuir constant (L/mg)
$1/n$ = Freundlich exponent (surface heterogeneity)
m = Amount of activated carbon used for metal ions adsorption during equilibrium (g)
N = Number of points in data set
q_e = Amount of metal ions adsorbed by activated carbon at equilibrium (mg/g)
q_m = Monolayer capacity of the Langmuir isotherm (mg/g)
V = Initial volume of metal ions used (L)
η_i = Langmuir correction coefficients of component i

Received: 7 July 2008
Accepted: 1 December 2009
[*]Corresponding Author

TABLE 1
Environmental Quality Act 1974, Environmental Quality (Sewage and Industrial Effluents) Regulations, 1979, Malaysia: Selected parameter limits of effluent of Standards A and B (Department of Environment, DOE, Malaysia)

Parameters	Unit	Standard	
		A*	B
Mercury (Hg)	mg/L	0.005	0.05
Cadmium (Cd)	mg/L	0.01	0.02
Arsenic (As)	mg/L	0.05	0.10
Lead (Pb)	mg/L	0.10	0.50
Chromium (Cr), Trivalent	mg/L	0.20	1.0
Copper (Cu)	mg/L	0.20	1.0
Nickel (Ni)	mg/L	0.20	1.0
Zinc (Zn)	mg/L	1.0	1.0
Iron (Fe)	mg/L	1.0	5.0

* This standard applies to the industrial and development projects which are located within catchment areas (areas upstream of surface or above sub-surface water supply intakes, for the purpose of human consumption including drinking).

INTRODUCTION

Heavy metals have been known as having very toxic elements and their discharge into receiving water can cause detrimental effects on human health and the environment. Heavy metal contamination exists in aqueous waste streams of many industries such as metal plating, mining, and agricultural fields. Zinc and cadmium are among the harmful heavy metal wastes produced by these industries, and they pose a risk of contaminated groundwater and other water resources. The removal of cadmium and zinc from water has become a great concern because of their uses in many industries.

Effluents from metallurgical and chemical industries, ceramics, electrogalvanization, and textile industries are potential sources of water pollution by Cd^{2+} ions (Hizal and Apak, 2006). Cd^{2+} ions cause serious cases of acute toxicity and diseases such as lung cancer and kidney failure. In Japan, a bone disease named 'itai-itai' emerged in the mid-fifties especially in children (Hizal and Apak, 2006) as a result of the consumption of cadmium-contaminated rice as food, because the rice plant was watered with effluents from Cd–Ni battery factories.

Elevated levels of zinc may come from a variety of sources such as effluents from manufacturing of batteries, pharmaceuticals, and agricultural chemicals. Other sources of metallic zinc traces in drinking water are water treatment processes and pickup of metallic ions during storage distribution. These toxic metals can cause accumulative poisoning, cancer, brain damage, etc. when they are found above the tolerant levels (Berman, 1980). According to some surveys from the public health services of different countries, significant numbers of people have been exposed to the hazards of excess metals in the municipal water supplies (Chuah *et al.*, 2005; WHO, 1971).

Table 1 shows the Environmental Quality Act 1974, Environmental Quality (Sewage and Industrial Effluents) Regulations, 1979 in Malaysia with selected parameter limits of effluent of heavy metals (Corapcioglu and Huang, 1987; Chuah *et al*., 2005). Treatment processes for metals contaminated waste streams include chemical precipitation, membrane, filtration, ion exchange, carbon adsorption, and coprecipitation/adsorption (Bailey *et al.*, 1999). Theses processes usually need expensive facility and high maintenance cost. Therefore, there is a need for more economical

TABLE 2
Current treatment technologies for heavy metals and dyes removal involving physical and/or chemical process

Physical and/or chemical methods	Advantages	Disadvantages
Oxidation	Rapid process for dye removal	High energy costs and formation of by-products
Ion exchange	Good removal of a wide range of heavy metals and dyes	Absorbent requires regeneration or disposal
Membrane filtration technologies	Good removes of heavy metals and dye	Concentrated sludge production, expensive
Coagulation/flocculation	Economically feasible	High sludge production and formation of large particles
Electrochemical treatment	Rapid process and effective for certain metal ions	High energy costs and formation of by-products
Ozonation	Applied in gaseous state: alteration of volume	Short half life
Photochemical	No sludge production	Formation of by-products
Irradiation	Effective at lab scale	Required a lot of dissolved O_2
Electrokinetic coagulation	Economically feasible	High sludge production
Fentons reagents	Effective decolourisation of both soluble and insoluble dyes	Sludge generation
Biological treatment	Feasible in removing some metals and dyes	Technology yet to be established and commercialized

alternative technologies or sorbents for the treatment of metals contaminated waste streams. Some examples are summarised in Table 2.

Activated carbons have been used as adsorbents with promising results. The potential and capability of activated carbon for the removal of heavy metals from water have been very well documented in the literature. Many studies have reported removal of toxic Cd^{2+} and Zn^{2+} from aqueous solutions using biomass (Bailey *et al.*, 1999) or inorganic materials such as calcite (Yavuz *et al.*, 2007).

Unlike organic pollutants which are mostly susceptible to biological degradation, heavy metals will not degrade. Thus, the treatment of aqueous wastes containing soluble heavy metals requires concentration of the metals into a smaller volume, followed by a recovery or a secure disposal. The removal of heavy metals using activated carbons and other adsorbents still remains a topic of most recent investigations (Marzal *et al*., 1996; Martin *et al*., 2004).

Several studies have been carried out and reported on cadmium and zinc as a binary system using various sorbents (Liu *et al.*, 2006; Hajialigol *et al.*, 2006; Horsfall *et al.*, 2006). However, only a few researchers have reported on the binary system modelling which deals with the competitive adsorption of cadmium and zinc ions onto activated carbon. For instance, Srivastava *et al.* (2006) studied individual and competitive adsorption of Cd^{2+} and Zn^{2+} metal ions from aqueous solution onto bagasse fly ash (BFA). Equilibrium isotherms for the binary adsorption of Cd^{2+} and Zn^{2+} ions on BFA were analyzed using non-modified Langmuir, modified Langmuir, extended-Langmuir, Sheindorf-Rebuhn-Sheintuch (SRS), non-modified R-P, and modified R-P adsorption models. The researchers found that the SRS model could fit most of the adsorption equilibrium data of Cd^{2+} and Zn^{2+} ions well onto BFA with low SSE values. Meanwhile, Fagundes-Klen (2007) studied the equilibrium data of the binary system of Cd^{2+} and Zn^{2+} ions by the biomass of *Sargassum filipendula* species using six adsorption isotherms models of the Langmuir type. Based on the regression analysis, the neural network could adjust to the equilibrium data of the binary system much as compared to the conventional sorption isotherm models. Mohsen *et al*. (2009) reported the work on the adsorption of two reactive dyes, Reactive Black 5 and Reactive Red E onto palm kernel shell-activated carbon (PKSAC). Their experimental data showed that competitive adsorption for active sites on the carbon surface resulted in a reduction of the overall uptake capacity of the reactive dyes, whereas the equilibrium was successfully described by the Modified Extended Freundlich model for the binary system.

In this study, the equilibrium experiments were performed to evaluate the effectiveness of the Norit coal based activated carbon for both single and binary adsorptions. Single component adsorption equilibrium was modelled using two isotherms, namely the Langmuir and Freundlich. Meanwhile, the binary component adsorption equilibrium was modelled using the extended Langmuir (EL) and modified extended Langmuir (MEL) models. The applications of these mathematical models provide a quantitative measure of their evaluation and optimize their operational conditions.

MATERIALS AND METHODS

Materials

In this study, analytical grade Cd $(NO_3)_2.4H_2O$ and Zn $(NO_3)_2.6H_2O$ and Norit activated carbon grade SA2 used in the experiments were supplied by Fisher Scientific, Malaysia. These activated carbons are commonly used in treating drinking water and are relatively cheaper than the others. Stock solutions of metal ions were prepared using deionised water. All solutions were adjusted to pH 7.0 using diluted NaOH and HNO_3.

Procedures

Batch sorption studies were performed at different concentrations of 5, 10, 15, 20, 25, 30, 35, 40, 45, and 50 mg/L to obtain the equilibrium isotherms. The metals chosen for the investigation in the single component studies were Cd^{2+} and Zn^{2+}. As for the isotherm studies, a series of 1000 ml conical flasks were employed. Each conical flask was filled with 500 ml of metal ion solution of varying concentrations and adjusted to pH 7.0. For the binary isotherms studies, a 1:1 ratio of cadmium-zinc solution was prepared. The conical flask with heavy metal ions solution was then shaken using an orbital incubator shaker, which was operated at 150 rpm and $30\pm1^{o}C$. When the desired temperature was reached, a pre-determined amount of norit activated carbon was added into each conical flask and mechanical shaking agitated the solutions. Equilibrium was reached after six hours (from contact time studies). To ensure equilibrium was attained, 96 hours of shaker

time were used for all the equilibrium experiments for both the single and binary systems. After this period, the solution was filtered using the Whatman filter paper (Grade 2, diameter 110mm) and analyzed for the concentration of the metal ions remaining in the solution using atomic absorption spectrophotometer (Hitachi Model Z-8100, Japan.) at the maximum wavelength (λ_{max}) of 228.8 nm for cadmium and 213.9 nm for zinc, respectively (Jumasiah *et al*., 2005).

The adsorption isotherms for the binary-component systems were obtained at pH 7.0. Meanwhile, a 1:1 ratio was used to determine the effect of other metal ions on the adsorption of Cd^{2+} and Zn^{2+} onto activated carbon. The metal ions concentration at equilibrium, q_e (mg/g), can be calculated from:

$$q_e = \frac{V(C_o - C_e)}{m} \tag{1}$$

where C_0 (mg/L) is the initial metal ions concentration in the liquid phase, C_e (mg/L) is the metal ions concentration in the liquid phase at equilibrium, V (L) is the total volume of metal ions solution, and m (g) is mass of adsorbent.

RESULTS AND DISCUSSION

Effect of Initial pH

The pH of the solution affects the surface charge of the adsorbents, as well as the degree of ionization and speciation of different pollutants. A change in pH affects the adsorptive process through dissociation of functional groups on the adsorbent surface active sites. The adsorption of various anionic and cationic species on such adsorbents has been explained on the basis of the competitive adsorption of H^+ and ions with the adsorbates (Allen, 2004). It is a common observation that the surface adsorbs anions favourably at lower pH due to the presence of H^+ ions, whereas, the surface is active for the adsorption of cations at higher pH due to the deposition of ions. The effect of initial pH on the adsorption equilibrium was studied by varying the initial pH of the solution, with a fixed initial concentration of 10 mg/L.

Fig. 1 indicates the effect of pH on the removal of Cd^{2+} and Zn^{2+} onto activated carbon from aqueous solutions. In strong acidic condition, the adsorption capacity was found to be very low. Overall, the maximum uptake percentage of cadmium and zinc removal was observed at pH 7.0.

Single Component Isotherms

Non-linear optimisation techniques have been applied to determine the isotherm parameters. The isotherm parameters were determined by minimising error function using Microsoft Excel Solver. The error function used in this work is the sum of the square of the errors (SSE), as defined in equation [2] (Chen *et al.*, 2001):

$$SSE = \sum_{i=1}^{N} (q_{e,cal} - q_{e,\exp})_i^2 \tag{2}$$

where the subscripts '*exp*' and '*cal*' indicate the experimental and calculated values and N is the number of measurement.

The equilibrium established between the adsorbed component on the adsorbent and unadsorbed component in solution can be represented by the adsorption isotherms. The most widely used isotherm equation for modelling equilibrium is the Langmuir equation which is valid for monolayer sorption onto a surface with a finite number of identical sites which are homogeneously distributed over the sorbent surface, as given in equation [3].

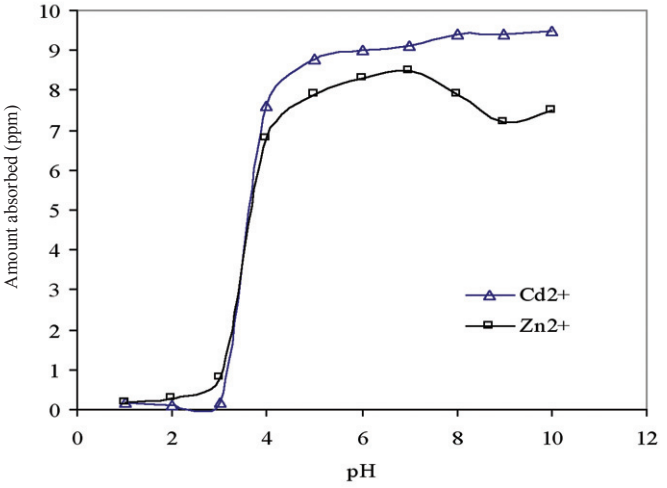

Fig. 1: Effect of the initial pH on adsorption of cadmium and zinc onto norit activated carbon at initial concentrations of 10 mg/L and a constant temperature of 30°C

$$q_e = \frac{K_L C_e}{1 + a_L C_e} \tag{3}$$

where K_L indicates the solute adsorptivity, a_L is related to the energy of adsorption and C_e is the residue metal ions concentration remaining after adsorption (mg/L). The Langmuir isotherm is characterized by a "plateau". The monolayer capacity of the Langmuir isotherm, q_m is given as:

$$q_m = \frac{K_L}{a_L} \tag{4}$$

where a_L is Langmuir constant for energy of the sorbent (L/mg), K_L is Langmuir constant (L/mg) and q_m is the monolayer capacity of the Langmuir isotherm (mg/g). The Langmuir and Freundlich models were used to describe the adsorption systems of Cd^{2+} and Zn^{2+} onto the norit activated carbon. The SSE and isotherm parameters for Cd^{2+} and Zn^{2+} adsorption are presented in Table 3. The determination of the isotherm parameters for cadmium and zinc by the non-linear regression appears to give acceptable fits to the experimental data, as shown in *Fig. 2*.

The monolayer of adsorption capacity (q_m) of the Cd^{2+} and Zn^{2+} systems on the activated carbon were 46.88 mg/g and 45.41 mg/g, respectively. This finding showed that the activated carbons used in this study had a slightly higher adsorption capacity on Cd^{2+} and Zn^{2+}.

The Freundlich isotherm describes the equilibrium on a heterogeneous surface where, the energy of adsorption is not equivalent for all the adsorption sites, and thus allowing multi-layer adsorption. The Freundlich equation is given as follows (Schay, 1982):

$$q_e = a_F C_e^{\frac{1}{n_f}} \tag{5}$$

where a_F is the Freundlich constant and n is the Freundlich exponent. The larger the value of the adsorption capacity, a_F, the higher the adsorption capacity is. The more heterogeneous the surface, the closer $\frac{1}{n_f}$ is to zero. The results presented in Table 3 show that the heterogeneity factor, from the Freundlich model $\frac{1}{n_f}$, are 0.36 for cadmium and 0.51 for Zn^{2+}, respectively.

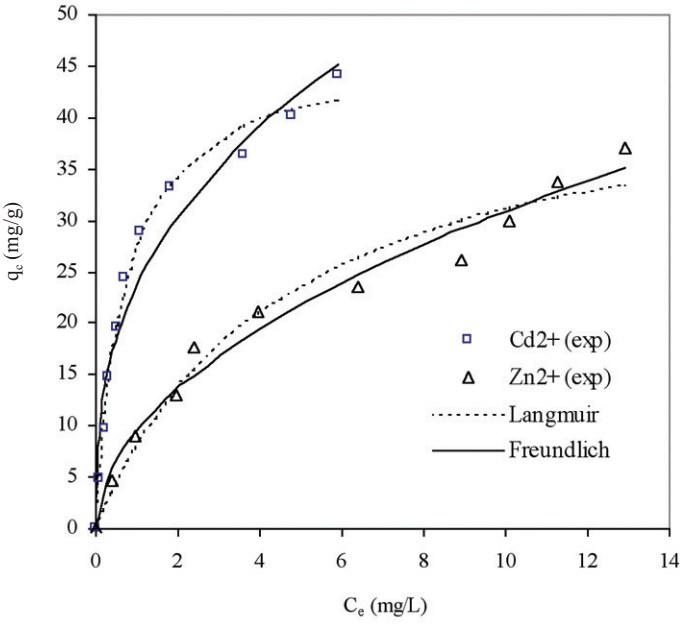

Fig. 2: Single component Langmuir and Freundlich isotherms and experimental data derived by nonlinear regression

The non-linear correlation obtained from *Fig. 2* shows that the experimental data also obeyed the Freundlich isotherm model, but they are not as good as the Langmuir isotherm especially for Cd^{2+}.

Binary Component Isotherms

One of the difficulties in describing the adsorption of heavy metals from wastestreams is that wastewaters contain more than one type of heavy metals. When several components are present, interference and competition phenomena for adsorption sites occur and may lead to a complex mathematical formulation of the equilibrium.

The modelling of binary adsorption equilibrium is still a challenging task. Several isotherms have been proposed to describe the equilibrium of such system. These isotherms could broadly be divided into (a) predictive models (where only individual isotherm parameters are used), and (b) correlative models (where individual isotherm parameters and correction factors are used).

The single-component adsorption Langmuir isotherm can be extended to describe the adsorption for multi-sorbate solution, as follows (Chen *et al*., 2001):

$$q_{e,i} = \frac{K_{L,i}^{0} C_{e,i}}{1 + \sum_{j=1}^{N} a_{L,i}^{0} C_{e,i}} \qquad (6)$$

where i is the number of components, $C_{e,i}$ is the equilibrium concentration of the component i in the multi-component solution (mg/L), $q_{e,i}$ is the equilibrium uptake of the component i (mg/g), and $K_{L,i}^{0}$ and $a_{L,i}^{0}$ are the single component Langmuir parameters for the component i.

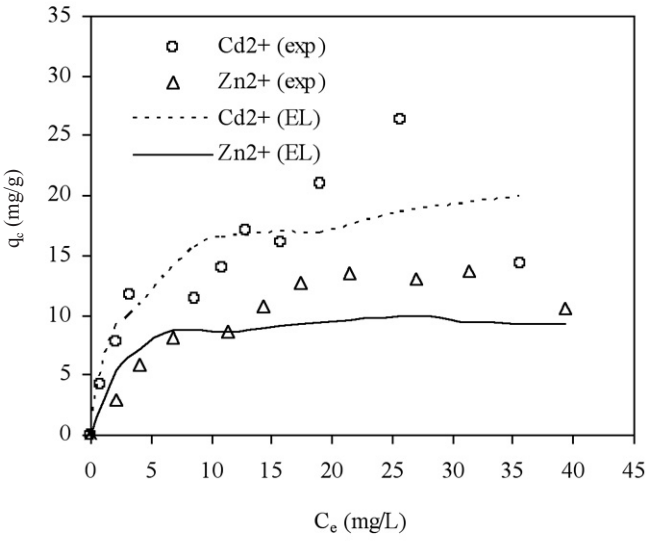

Fig. 3: Application of extended Langmuir isotherm model for simultaneous sorption of Cd^{2+} and Zn^{2+} onto norit activated carbon

The extended Langmuir (a predictive model) model assumes a homogeneous surface with respect to the energy of adsorption, no interaction between adsorbed species, and that all sites are equally available to all adsorbed species. The single-component parameter sets for the two heavy metals (as obtained in sub-section 3.2) were substituted into equation (6) to enable prediction of the binary component isotherms using the extended Langmuir (EL) isotherm. A comparison of the EL isotherm predictions and the experimentally measured values is presented in *Fig. 3*. Meanwhile, the SSE values for the EL isotherm for both heavy metals are given in Table 4. From the SSE values, the quality of fit using the EL isotherm for zinc was rather good, but the quality of fits for Cd^{2+} was very poor. The failure of the EL model suggested that the binary adsorption might be competitive.

For competitive adsorption, Schay (1982) introduced the modified extended Langmuir (MEL) by incorporating interaction parameters (Pagnanelli *et al*., 2001):

$$q_{e,i} = \frac{K^0_{L,i}\left(C_{e,i}/\eta_{L,i}\right)}{1 + \sum_{j=1}^{N} a^0_{L,j}\left(C_{e,j}/\eta_{L,j}\right)} \tag{7}$$

where is the Langmuir correction coefficients of the component *i* extracted from the competitive adsorption data.

The MEL models for the adsorption of cadmium and zinc onto activated carbon are plotted in *Fig. 4*. The model parameters of the MEL model, which were estimated from the binary adsorption data and their respective SSE, are given in Table 4. Based on the information presented in *Fig. 4*, the isotherm parameters for cadmium and zinc which were obtained using the non-linear regression method appeared to have given acceptable fits to the experimental data. Cd^{2+} and Zn^{2+} will compete with each other in the binary adsorption system, and more Zn^{2+} is being adsorbed in this system as compared to Cd^{2+}. The maximum uptakes for Cd^{2+} and Zn^{2+} in the binary system are 43.096 and 19.214 mg/g, respectively.

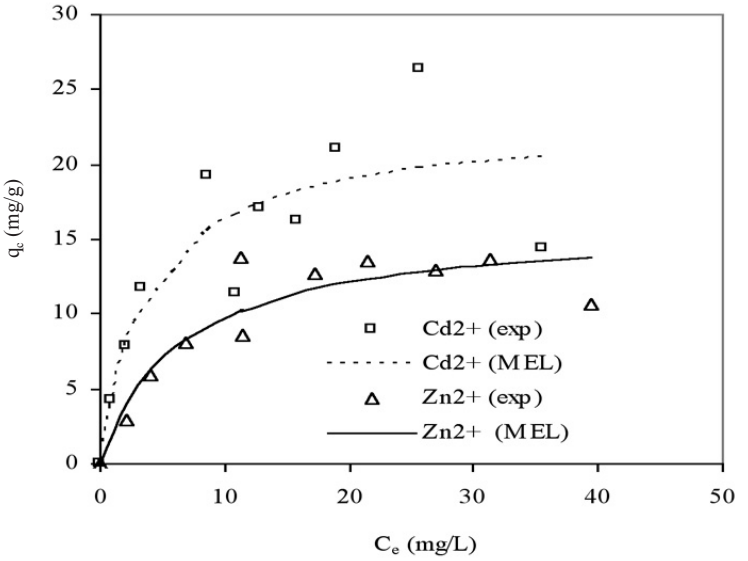

Fig. 4: Application of modified extended Langmuir for simultaneous sorption of Cd^{2+} and Zn^{2+} onto norit activated carbon

TABLE 3
Langmuir and Freundlich isotherm parameters for single component adsorption of cadmium (II) and zinc (II) onto norit activated carbon

Models	Cadmium (II)	Zinc (II)
Langmuir		
q_m (mg g^{-1})	46.88	45.41
K_L (L mg^{-1})	64.62	9.78
a_L (L mg^{-1})	1.38	0.22
SSE	18.26	47.95
Freundlich		
a_F (mg g^{-1})	23.79	9.65
$1/n_F$ (L mg^{-1})	0.36	0.51
SSE	96.31	28.83

TABLE 4
Comparison of the SSE for each component evaluated from the modified extended Langmuir (MEL) and extended Langmuir (EL) models for simultaneous sorption of Cd^{2+} and Zn^{2+}

Component	Modified Extended Langmuir					Extended Langmuir		
	η_{L1}	η_{L2}	K_L^0	a_L^0	SSE	K_L^0	a_L^0	SSE
Cd^{2+}	9.179	1.546	64.621	1.378	171.856	9.866	0.229	137.384
Zn^{2+}	13.413	4.521	9.779	0.2154	34.371	4.138	0.2154	66.650

CONCLUSIONS

Single component equilibrium data for both cadmium and zinc were studied and the adsorption data were found to be fitted best using the Langmuir model. The combined effects of the two metals onto Norit activated carbon are competitive. A predictive model, namely the Extended Langmuir model, described the adsorption equilibrium of zinc in a binary mixture rather well. However, it did not accurately predict the adsorption equilibrium of cadmium in a binary mixture. A correlative model, namely the modified extended Langmuir model, was found to be able to describe the binary components adsorption equilibrium well using single component parameters and additional correction factors. The maximum uptakes of Cd^{2+} and Zn^{2+} in binary system are 43.096 and 19.214 mg/g, respectively.

REFERENCES

Allen, S. J., McKay, G. and Porter, J. F. (2004). Adsorption isotherm models for basic dye adsorption by peat in single and binary component systems. *Journal of Colloid and Interface Science*, *280*, 322-333.

Bailey, S. E., Olin T. J., Bricka, R. M. and Adrian, D. D. (1999). A review of potentially low-cost sorbents for heavy metals. *Water Res., 33*, 2469-2479.

Berman, E. (1980). *Toxic Metals and Their Analysis*. London: Heyden Press.

Burrell, D.C. (1974). *Atomic Spectrometric Analysis of Heavy Metal Pollutants in Water*. Michigan: Ann Arbor Science Publishers Inc.

Chen, B., Hui, C. W. and McKay, G. (2001). Film-pore diffusion modelling for the sorption of metal ions from aqueous effluents onto peat. *Water Res.*, *35*, 3345-3356.

Chuah, T.G., Jumasiah, A., Azni, I., Katayon, S. and Thomas Choong, S.Y. (2005). Rice husk as a potentially low-cost biosorbent for heavy metal and dye removal: An overview. *Desalination*, *175*, 305-316.

Corapcioglu, M. O. and Huang, C. P. (1987). The adsorption of heavy metals onto hydrous activated carbon. *Water Res., 21*, 1031-1044.

Fagundes-Klen, M.R., Ferri, P., Martins, T.D., Tavares, C.R.G. and Silva, E.A. (2007). Equilibrium study of the binary mixture of cadmium–zinc ions biosorption by the *Sargassum filipendula* species using adsorption isotherms models and neural network. *Biochemical Engineering Journal*, *34*, 136-146.

Hajialigol, S., Taher, M.A. and Malekpour, A. (2006). A new method for the selective removal of cadmium and zinc ions from aqueous solution by modified clinoptilolite. *Adsorption Science & Technology*, *24*, 487-496.

Hizal, J. and Apak, R. (2006). Modeling of cadmium (II) adsorption on kaolinite-based clays in the absence and presence of humic acid. *Appl. Clay Sci., 32*, 232-244.

Horsfall Jr. M., Abia, A.A. and Spiff, A.I. (2006). Kinetic studies on the adsorption of Cd^{2+}, Cu^{2+} and Zn^{2+} ions from aqueous solutions by cassava (Manihot sculenta Cranz) tuber bark waste. *Bioresource Technology*, *97*, 283-291.

Jumasiah, A., Chuah, T. G., Gimbon, J., Choong, T.S.Y. and Azni, I. (2005). Adsorption of basic dye onto palm kernel shell activated carbon: Sorption equilibrium and kinetics studies. *Desalination, 186*, 57-67.

Liu, Y.G., Fan, T., Zeng, G.M., Li, X., Tong, Q., Ye, F., Zhou, M., Xu, W.H. and Huang, Y.E. (2006). Removal of cadmium and zinc ions from aqueous solution by living Aspergillus niger. *Transactions of Nonferrous Metals Society of China*, *16*, 681-686.

Martins, R.J.E., Pardob, R. and Boaventura, R.A.R. (2004) Cadmium (II) and zinc (II) adsorption by the aquatic moss Fontinalis antipyretica: Effect of temperature, pH and water hardness. *Water Res., 38*, 693-699.

Marzal, P., Seco., A., Gabaldon, C. and Ferrer, J. (1996). Cadmium and zinc adsorption onto activated carbon: Influence of temperature pH and metal/carbon ratio. *J. Chem. Tech. Biotechnol., 66*, 279-285.

Moshen, N., Luqman Chuah, A. and Thomas Choong, S. Y. (2009). Equilibrium and kinetic study on reactive dyes adsorption by palm kernel shell-based activated carbon in single and binary system. *J. Envn. Eng.*, *135*(1), 1393-1398..

Pagnanelli, F., Trifoni, M., Beolchini, F., Esposito, A. and Veglio, F. (2001). Equilibrium biosorption studies in single and multi-metal systems. *Process Biochemistry*, *37*, 115-124.

Schay, G. (1982). On the definition of interfacial excesses in a system consisting of an insoluble solid adsorbent and a binary liquid mixture. *Colloid and Polymer Science*, *26*, 888-891.

Srivastava, V.C., Mall, I.D. and Mishra, I.M. (2006). Modelling individual and competitive adsorption of cadmium (II) and zinc (II) metal ions from aqueous solution onto bagasse fly ash. *Separation Science and Technology*, *41*, 2685-2710.

WHO. (1971). *World Health Organization International Standards for Drinking Water*. Geneva: WHO.

Yavuz, Ö., Guzel, R., Aydin, F., Tegin, I. and Ziyadanogullari, R. (2007). Removal of cadmium and lead from aqueous solution by calcite. *Polish Journal of Environmental Studies*, *16*, 467-471.

ISSN: 0128-7680
Pertanika J. Sci. & Technol. **18 (1)**: 95 – 103 (2010)

Crop Establishment Technologies for Lowland Rice Cultivation in Bangladesh: Hand Seeding vs. Machine Seeding

Md. Syedul Islam[1] and Desa Ahmad[2*]
[1]Bangladesh Rice Research Institute, Gazipur 1701, Bangladesh
[2]Department of Biological and Agricultural Engineering, Faculty of Engineering, Universiti Putra Malaysia, 43400 UPM, Serdang, Selangor, Malaysia
[*]E-mail: desa@eng.upm.edu.my

ABSTRACT

Experiments were conducted to determine the field and economic performances of machines and techniques for crop establishment in lowland paddy in Bangladesh. In machine seeded field, the crops were grown in rows to allow the operation of rotary type weeder for weed control. In hand broadcasted field, crops were not arranged in rows and weed control operation was therefore done through traditional means. Results obtained showed that the effect of rice seeding techniques, using pre-germinated rice seed of BR-1 variety on the effective field capacity, was highly significant. The work rate of hand broadcasting was found to be one to one and a half times faster than that of seeding by manually driven drum type row seeder. Field efficiency of hand broadcasting was about 90 percent, and this was found to be significantly higher than those of machine seeding which ranged from 70-80 percent at both seed rates, since no time was lost in turning. BRRI modified drum type row seeder, with a seeding rate of 60 kg/ha, was shown to be better for an optimum crop yield. Based on partial budget analysis, a farmer can save about US$53.34 per hectare in a year using the BRRI modified drum type row seeder, followed by a rotary weeder as compared to hand seeding, followed by hand weeding.

Keywords: Drum seeder, effective field capacity, partial budget analysis, break even analysis

INTRODUCTION

Rice has been accepted as a staple food for more than half of the world's population and it is generally grown under wetland condition. It may be grown in direct seeded or in transplanted condition. The high yielding rice varieties have been growing in transplanted condition since their introduction, with a belief that transplanted rice usually produces 10-15% more yield than direct seeded rice (Ramiah and Hanumontha, 1936; Bautista, 1938; Ghose *et al.,* 1960; IRRI, 1971). Some recent studies reveal that there is no yield difference between direct seeding and transplanting practices of rice production when weed control and other intercultural operations are done properly. This finding is applicable for both high yielding and traditional varieties.

Due to the rapid industrialization in the region, such as that experienced by countries like Thailand and Malaysia, the labour cost has not only increased substantially but farm labourers have become scarce as well. Therefore, direct seeding is practiced extensively and most farmers in the areas are expected to eventually switch to direct seeding so as to reduce the cost of cultivation in some of the irrigated areas (De Datta and Nantasamsaran, 1991).

In central Luzon, Philippines, where rice has been traditionally grown in transplanted condition, the adoption of broadcast seeding rapidly increased, i.e. from less than 2 percent in 1979 to 16 percent in 1982 (Moody and Cordova, 1985). Erguisa *et al.* (1990) reported that farmers who were

Received: 31 July 2008
Accepted: 26 November 2009
[*]Corresponding Author

practicing a combination of transplanting and wet seeding in 1980 had entirely shifted to broadcast seeding by 1986. During the 1987 off season in Malaysia, 99 percent of the planted areas in the Muda irrigation scheme were direct seeded (Ho *et al.,* 1990).

In the case of hand seeding, the seeds are usually broadcast at random. As a result, the crops stand in the field without any specific rows. Therefore, the operation of rotary type rice weeder is not possible and the farmers are compelled to use indigenous hand tools for weed control operation. It is important to note that weed control, using indigenous hand tools, is a highly labour intensive farming operation. Islam and Haq (1985) found that weed control with the use of traditional hand tools required 300 man-hr/ha of labours, but this was only 25 man-hr/ha when the rotary type weeding machine was used. Other means of controlling weeds in the random planted rice field is by the application of chemicals, but this is rather discouraged as it has adverse effects on the environment. Therefore, a row type paddy seeder is necessary. The International Rice Research Institute (IRRI) had developed a manually operated drum type row seeder for lowland paddy, and this was later modified by the Bangladesh Rice Research Institute (BRRI).

The objectives of the study were: (a) to identify the advantages and limitations of the existing rice seeding techniques, (b) to determine their field performances, and (c) to determine the comparative economics of machine and hand seeding of paddy.

MATERIALS AND METHODS

Experiments were conducted at the Bangladesh Rice Research Institute (BRRI) farm in silty clay loam soil to evaluate the performances of the BRRI designed drum type row seeder, using two different seeding rates and the results were compared with those of the hand broadcasting method. The treatments were as follows:

T_1 = Seeding by drum type row seeder at the rate of 60 kg/ha
T_2 = Seeding by drum type row seeder at the rate of 80 kg/ha
T_3 = Hand broadcasting at the rate of 100 kg/ha

BRRI Designed the Drum Type Row Seeder

The BRRI drum type row seeder was designed based on the IRRI design prototype, which is a manually operated machine suitable for sowing pre-germinated paddy seeds in rows, as shown in *Fig. 1.* It consists of four metallic drums, one metallic axle, a main frame, a cage wheel, two skids, and a handle. It is made of mild steel pipe, mild steel rod, and galvanized iron sheet. The drums have holes through which seeds are dropped when the machine is pulled backward on the prepared field. It has 8 rows with a spacing of 20 cm between two consecutive rows.

The IRRI designed machine has no mechanism to collect seeds while turning at headlands. As a result, some seeds are lost in every turn, and this consequently reduces the crop yield. A seed collector assembly made from galvanized iron sheet and rod was therefore incorporated to overcome the unwanted seed dropping at the headlands. Every drum is provided with a tray with the size of 36cm long and 30 cm wide. The trays are engaged at the headlands and disengaged during seeding operation. The presence of seed collector during turning was found to be able to save 5-7 kg of the seeds per hectare as compared to the IRRI seeder. The modified prototype of the drum type row seeder, termed as the BRRI modified drum seeder, is shown in *Fig. 2.* The operating principle is similar to that of the IRRI designed seeder, with the advantage of having a seed collecting assembly to collect seeds while turning at the headlands.

Fig. 1: IRRI designed drum type row seeder

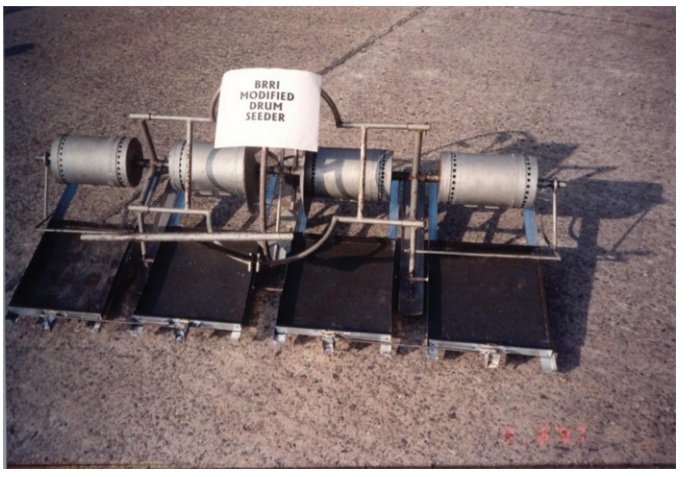

Fig. 2: BRRI modified drum seeder

Design of the Experiment

The experiments were conducted under a Randomized Complete Block (RCB) design and the treatments were replicated thrice in each block.

Experimental Procedure

Before field test, the drum seeder was tested in the laboratory to ensure the workability of all the functional components. The seeder was tested for two seeding rates, namely 60 and 80 kg/ha, and a comparison was made with the conventional hand broadcasting method. The experimental plots were selected as per treatments and layout plan. The plot was well puddled with a sufficient number of ploughing and levelled by laddering. The seeds were soaked in clean water three days prior to the final land preparation. After 24 hours of soaking, the water was drained out and the seeds were put in a gunny bag for sprouting. The duration of sprouting was 48 hours. The degree of sprouting

was observed very carefully so that the seeds could easily be passed through the seeder holes. After loading the sprouted seeds in the drums, the seeder was pulled backward and the seeds were dispensed by the action of gravity. After seeding, about a week of bird watching was necessary, depending on the cropping pattern of the surrounding field. The effective field capacities and field efficiencies were calculated from the collected data. Data on plant population, plant spacing, plant height, and root length were recorded. The crops were managed with irrigation, drainage, weeding, fertilizer, and insecticide application. The data on the yield parameters such as tiller/m^2, panicle/m^2, filled grain/panicle, and percentage of filled grains were recorded. Finally, they were harvested, threshed, cleaned and dried and the yields were expressed in tonnes per hectare at 14% moisture content dry basis. The data recorded from the experiment were subjected to analysis of variance and Duncan's Multiple Range Test (DMRT) using the IRRISTAT package.

The partial budget analysis between hand and machine seeding was also carried out. The seed rates for hand and machine seeding were 100 kg/ha and 60 kg/ha, respectively. In the analysis, the costs for two operations (seeding and weeding) were considered. In the hand broadcast field, weeding was carried out by indigenous hand tools as the crops did not have specific rows. In the machine seeded field, on the other hand, weeding was done using the rotary type rice weeder as crops were arranged in specific rows. The parameters, such as fixed and variable costs for seeder and weeder, were taken into account. An additional benefit from the drum seeder renting was considered, however, the crop yields for hand and machine seeding were considered as identical. A break-even analysis was conducted to find out the minimum acreage at which the machine seeding was profitable over hand seeding.

RESULTS AND DISCUSSION

Advantages and Limitations of the Existing Rice Seeding Techniques

From the analysis of variance, it was evident that the effect of rice seeding techniques using pre-germinated rice seed of BR-1 variety on the effective field capacity was highly significant. In the drum type row seeder operations, 75-78% of the time was actually required for seeding, 10-12% for turning, and 10-13% in loading. The addition of seed collectors increased the overall weight of the machine by 3 kg and its pulling force by 20%, but these were still within the capability of an average size labour. Similarly, the seeder also has a problem of lateral stability as it moves on one steel wheel and requires an experienced worker to keep it straight while pulling it backwards. In the case of hand broadcasting, about 88% of the time was engaged in actual broadcasting, while 12% was lost in loading the seed pot.

Field Performance

The effective field capacities of the BRRI drum seeder, with the seeding rates of 60 kg/ha and 80 kg/ha, were 0.15 ha/hr and 0.12 ha/hr, respectively, and there were statistically not significant. On the contrary, the field capacity of hand broadcasting at the rate of 100 kg/ha was 0.22 ha/hr, and this was found to be significantly higher than the drum seeder seeding at both rates (Table 1). The field efficiencies of the drum seeder, at the rates of 60 kg/ha and 80 kg/ha, were 73.91 and 77.77 percents, respectively, whereas that of hand broadcasting, at the rate of 100 kg/ha was 87.30 percent. The results revealed that the field efficiency of the hand broadcasting was significantly higher than those of the machine seeding at both seed rates because no time was lost in turning in the case of hand seeding.

TABLE 1
Field performance of the drum seeder compared to hand broadcasting method

Operations	Different methods of seeding		
	BRRI drum seeder (60 kg/ha)	BRRI drum seeder (80 kg/ha)	Hand broadcasting (100 kg/ha)
Effective field capacity (ha/hr)	0.153 b	0.117 b	0.223 a
Theoretical field capacity (ha/hr)	0.207 ab	0.150 b	0.257 a
Field efficiency (%)	73.91 b	77.777 ab	87.307 a
Plant population 18 days after seeding (no/m^2)	238.3 c	358.3 b	502.5 a
Average plant spacing (cm)	5.86 a	5.73 b	8.30 a
Average plant height (cm)	23.27 a	22.60 a	23.72 a
Average root length (cm)	4.41 a	5.53 a	5.20 a

In a row, means followed by a common letter are not significantly different at 5% level by DMRT.

Test conditions:

Soil type	:	Silty clay loam	Parameters	:	LSD (5%)
Plot size	:	4 m x 20 m	Theoretical FC	:	0.07149
Variety	:	BR1	Effective FC	:	0.3998
Seeder speed	:	16.95 m/min	Field efficiency	:	10.37
Walking speed	:	40 m/min	Plant population	:	63.83
			Average plant spacing (cm)	:	1.72
			Average plant height (cm)	:	2.03
			Average root length (cm)	:	1.6

The average plant population, taken at 18 days after seeding in the drum seeder plot at the seeding rates of 60 kg/ha and 80 kg/ha, was 238.33 and 358.33 Nos/m^2, respectively, whereas that of the hand broadcasting at the rate of 100 kg/ha was 500 Nos/m^2, and this was found to be significantly different at 5% level (Table 1). In the drum seeder plot, the distance between rows was 20 cm, however the distance between hill to hill along the rows varied with the seeding rates. In the drum seeder, the seeding at the rates of 60 kg/ha and 80 kg/ha for the hill to hill distances were 5.86 cm and 5.73 cm, and they were not statistically different, as compared to the higher seeding rate, where the seedling per hill was found to be higher as well. The average plant spacing in the hand broadcasting field was 8.30 cm, and this was higher than the hill to hill distance of the machine seeded field.

The average root lengths in the drum seeder plots were 4.41 cm and 5.53 cm for the seeding rates of 60 kg/ha and 80 kg/ha respectively, whilst that of the hand broadcasting plot the root length was 5.20 cm with a seeding rate of 100 kg/ha and was found to be not statistically different.

Meanwhile, the results revealed that at 18 days of seedling, the methods of seeding did not have any effect on the root development. The rice yield in the drum seeder fields at the seeding rates of 60 kg/ha and 80 kg/ha were 3.13 ton/ha and 2.84 ton/ha, respectively. On the other hand, the yield

at the hand broadcasting field at the seeding rate of 100 kg/ha was 2.73 ton/ha (Table 2). The results indicated that there was no significant yield difference among the three seeding practices.

TABLE 2
Yield parameters in the fields for different seeding methods

Parameter	BRRI drum seeder (60 kg/ha)	BRRI drum seeder (80 kg/ha)	Hand broadcasting (100 kg/ha)
Tiller/m^2	562.3 c	623.7 b	694.3 a
Panicle/m^2	435.7 b	483.7 a	503.3 a
No. filled grain/panicle	64.47 a	59.14 a	61.33 a
Filled grain (%)	70.46 a	68.55 ab	64.24 b
Grain yield (ton/ha)	3.13 a	2.84 a	2.73 a

In a row, means followed by a common letter are not significantly different at 5% level by DMRT.

Parameters	LSD (5%)
Tiller/m^2	65.58
Panicle/m^2	39.52
Filled grain/panicle	8.06
Filled grain (%)	5.76
Grain yield	0.639

Economic Performances

In the conventional hand broadcasting, the seeds were randomly scattered so there were no specific rows, and that the operation of rotary type weeder was not possible for weed control. Meanwhile, the weed control operations for the machine seeded and hand seeded fields were different. In the partial budget analysis, the costs of two operations (i.e. seeding and weeding) were therefore taken into account. The partial budget analysis revealed that a farmer could earn a net benefit of US$53.34 per hectare using the drum type seeder and the rotary type weeder as compared to hand broadcasting method followed by hand weeding (Table 3).

Table 4 shows the labour wage rate and the prices of goods. The price of the rotary weeder is much lower and for this reason, every farmer will be able to afford it. Therefore, renting of weeder is assumed to be impossible. Based on the wage rate and the prices of goods, as presented in Table 4, the break-even analysis showed that the farmer could own a drum type seeder and a rotary type weeder if he had only 0.3 hectare of land, as shown in *Fig.3*.

TABLE 3
Partial budget analysis of seeding and weeding costs between machine and hand system

Added return	(US$/ ha)	Added cost	(US$/ ha)
(A) EXTRA REVENUE:		(B) EXTRA COSTS	
1. Benefit from drum seeder renting	1.53	1. Cost of drum seeder (FC + VC)	16.14
		2. Cost of rotary weeder (FC + VC)	12.24
(C) SAVINGS IN COSTS:		(D) LOSS IN REVENUE:	
1. Labour saved from hand seeding labour	0.64		
2. Cost saved from seed in hand seeding	22.73		
3. Cost saved from hand weeding	56.82		
Total	81.72	Total	28.38

Net benefit from machine seeding over hand seeding (US$/ha)

= Added return - Added cost
= (A + C) - (B + D)
= 81.72 -28.38
= 53.34

TABLE 4
Labour wage rate and prices of goods

Price of seed paddy	:	US$0.23/kg
Price of non-seed paddy	:	US$0.16/kg
Labour wage for machine operation	:	US$1.36/day
Helpers' wage	:	US$1.14/day
Rotary weeder price	:	US$6.82/piece
Drum seeder price	:	US$68.18/piece
Farmer's yearly work load for drum seeder	:	3 ha
Drum seeder yearly renting service	:	27 ha
Drum seeder renting charge	:	US$1.70/ha

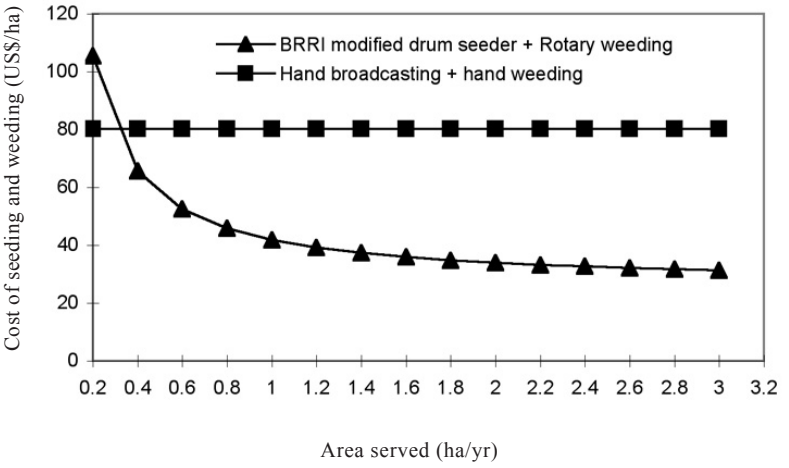

Fig. 3: A comparison between cost of seeding and weeding between machine and hand systems

CONCLUSIONS

Based on the results from the above experiments, it can therefore be concluded that:

1. The effect of rice seeding techniques using pre-germinated rice seed of BR-1 variety on the effective field capacity was highly significant.
2. The field efficiency of hand broadcasting was significantly higher than those of machine seeding at both seed rates since no time was lost in turning.
3. The BRRI modified drum type row seeder with a seeding rate of 60 kg/ha was better for an optimum crop yield.
4. A shift from manual to mechanised seeding and weeding operations with drum type seeder and rotary type weeder in lowland rice culture would benefit the farmers of Bangladesh at about US$53.34 per hectare.

REFERENCES

Bautista, B.R. (1938). Palagad rice culture in the Philippines. *Phillippine Journal of Agriculture 2,* 381-391.

De Datta, S.K. and P. Nantasamsaran (1991). Status and prospects of direct seeded rice in tropical Asia. Direct seeded flooded rice in the Tropics. Selected papers from the *IRRI Conference*. International Rice Research Institute, P.O. Box. 933, Manila, Philippines.

Erguiza, A., Duff, B. and Khan, C. (1990). Choice of rice crop establishment techniques: Transplanting Vs wet seeding, IRRI Research paper series. 139. 10p.

Ghose, R.L.M., Chatge, M.B. and Subrahmanyan, V. (1960). Rice in India. *Indian Conference of Agricultural Research*, New Delhi. 470.

Ho, N.K., Zuki, I.M. and Othman, A.B. (1990). The implementation of strategic extension campaign on the integrated weed management in the Muda area, Malaysia. Paper presented at the *Third International Conference on Crop Protection in the Tropics* (pp. 20-23).Gentings Highlands, Malaysia.

IRRI. (1971). Annual Report. International Rice Research Institute (IRRI), Los Banos, Philippines.

IRRISTAT SOFTWARE.www.irri.org/science/software/irristat.asp.

Islam, M.S. and Haq, K.A. (1991). Development of a Low-cost Weeder for Lowland Paddy. *Agricultural Mechanisation in Asia, Africa and Latin America*, *22*(1), 45-48.

Moody, K. and Cordova, V.G. (1985). Wet-seeded rice. Women in Rice Farming. International Rice Research Institute. P.O. Box. 933, Manila, Philippines.

Ramiah, K. and Hanumantha, K. (1936) Broadcasting vs transplanting. *Tropical Agriculture, 26*(5), 310-313.

ISSN: 0128-7680
Pertanika J. Sci. & Technol. **18 (1)**: 105 – 110 (2010)

Development of Automatic Feeding Machine for Aquaculture Industry

S. J. Yeoh, F. S. Taip*, J. Endan, R.A. Talib and M.K. Siti Mazlina
Department of Process and Food Engineering, Faculty of Engineering, Universiti Putra Malaysia, 43400 UPM, Serdang, Selangor, Malaysia
**E-mail: saleena@eng.upm.edu.my*

ABSTRACT

Aquaculture is a growing industry with a great potential towards the contribution of the country's total fish requirement. Serious efforts have been done to develop and improve the production of fish by rearing high value fish in tanks or ponds. Under the Third National Agricultural Policy (1998-2010), the target is to annually produce 1.93 million tonnes of fish worth approximately RM8.3 billion by the year 2010. Consequently, the development of an automatic fish feeding machine can be very beneficial to the growth of the aquaculture industry. This device was developed to overcome labour problems in the industry and introduce a semi-automatic process in the aquaculture industry. It has the ability to dispense dried fish food in various forms such as pellets, sticks, tablets or granules into fish tanks or ponds in a controlled manner for a stipulated time. The automatic fish feeder is controlled by a digital timer and it is capable of feeding the fish in accordance with a pre-determined time schedule without the presence of an operator, and at a feeding rate of 250g/min. The feeder can be adjusted to the desired height and conveniently moved around to be positioned adjacent to the pond or tank. Meanwhile, its hopper can be covered and easily dissembled to change the size of the hopper to accommodate different capacities of feed. This automatic fish feeder can be implemented in aquaculture system to convenience to fish culturists.

Keywords: Automatic fish feeder, aquaculture

INTRODUCTION

Asia dominates the aquaculture production, contributing around 91% of the world's total by volume and 82% by value. Asian countries, such as Thailand, have been the top ten aquaculture producers in the world. The region has the highest variety of cultured species. Asia has also been the highest seafood-consuming region of the world, accounting for two-third of the world's food fish supply, the increase of which mainly came from aquaculture in recent years (Liao, 2001).

The fisheries sector in Malaysia has provided direct employment to 89,453 fishermen and 21,507 fish culturists. The consumption of fish in Malaysia is expected to increase by 14% by 2010 and currently, the country is producing 89% of the fish supply for its own consumption. With the marine harvest almost stagnating, the industry is dependent on the aquaculture to cater for the growing demand. Currently, the aquaculture industry contributes to about 13.2% of the total fish produced. Malaysia has the potential to become a major player in the aquaculture industry in Asia Pacific, if more companies enter the sector (Subasinghe, 2007; Alongi *et al*., 2003).

The importance of aquaculture in the overall fish supply is growing. In the future, aquaculture production is expected to overtake capture production of food supply. The growth in aquaculture for high value species has an important impact on international fish trade. In recent years, tilapia and catfish have also entered international trade successfully. The unit values of tilapia and catfish were surprisingly strong and have shown an increasing trend (Helga, 2006).

Received: 21 July 2008
Accepted: 10 July 2009
*Corresponding Author

TABLE 1
Feeding frequency for various sizes of tilapia at 28°C (National Research Council, Washington, 1993)

Size of fish (grams)	Times fed dairy
0-1	8
1-5	6
5-20	4
20-100	3-4
>100	3

Tilapia is the second most important cultured food fish in the world after carp. Tilapias are also among the easiest and most profitable fish to farm. This is due to their omnivorous diet, mode of reproduction, strong resistance to diseases and rapid growth (Rafeal, 2007). They grow best when fed 2-3 times per day although adequate growth can be obtained with a single daily feeding (Williams, 2000). Catfish has also become an important and popular food traded globally, with a great potential to feed the world and contribute significantly to the economies of the developing countries (Subasinghe, 2007).

Feeding fish is labour-intensive and also expensive. Feeding frequency is dependent on labour availability, farm size, as well as fish species and sizes. Large catfish farms with several ponds can usually be fed only once per day because of time and labour limitations, while this may be done twice per day at smaller farms. Generally, growth and feed conversion increases with feeding frequency. In the intensive fish culture systems, fish may be fed as many as five times a day in order to maximize growth at optimum temperatures. Table 1 shows the feeding frequency for Tilapia of different sizes.

The feeding rate also varies depending upon the size and temperature of temperature. The feeding rate can be set on the basis of a percentage of the total body weight of fish being fed and adjusted for the size and total number of fish, and water temperature (Beem and Gebhart, 2000).

Feeding rates also vary with fish size and water temperature. Appropriate amount is measured as a percent of the average body weight. As the weight of fish increases, the percentage for body weight fed decreases. Fish are fed at 2–3 hour interval, and they eat more feed than their stomachs can hold. The extra feed eaten passes over the stomach and is considered wasted. The result is an increased cost of production and lower profits. Fish fed at 4–5 hour interval eat nearly the same amount of feed needed to refill their stomachs. This suggests that the optimal interval between feedings is around 4–5 hours, depending on the energy and composition of the diet (Riche and Garling, 2003).

Cultivating fish in tanks and ponds is quite common in Malaysia. One way of ensuring a continuous availability and success of rearing fish in tanks is through the implementation of the new technology. The objective of this study is to provide a fish feeding machine with a simplified means of regulating a specific amount of fish pellets during each dispensing operation. Automatic and demand feeders save time, labour and money, but at the expense of the vigilance that comes with hand feeding (Craig and Helfrich, 2002).

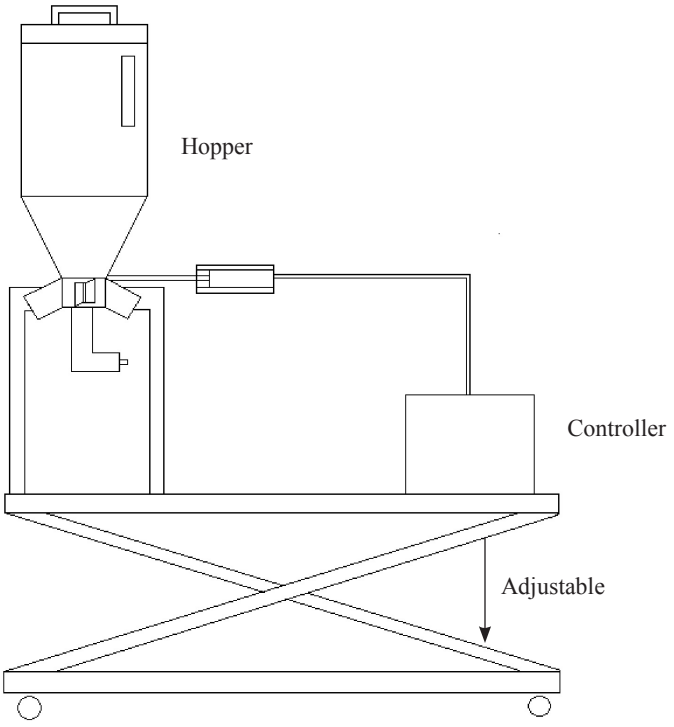

Fig. 1: Automatic fish feeder

There are several automatic feeders which have been developed to fulfil certain objectives and requirements (Chang *et al*., 2005; Velazquez and Martinez, 2005). This automatic fish feeder was developed to fulfil certain objectives and requirements with added advantages such as a detachable hopper to accommodate various sizes of hopper according to user's requirement. It was also designed to have adjustable height, speed, and opening angle to accommodate different sizes of fish tanks and ponds, as well as provide a mobile fish feeder with pneumatic system for safety reasons. These features make it suitable to be specifically used for culturing tilapia and catfish.

METHODOLOGY

In designing the feeder, several criteria need to be determined; these include the characteristics of the fish, types and sizes of fish feed, and functions of the feeder. For this purpose, data and information have been collected to gain a baseline for the design. Factors or problems influencing the process have also been considered to ensure the efficiency of the machine. The device should be simple, compact, and efficient in operation. Complete drawings were then prepared using the Autodesk Inventor 2008 software. This was followed by the fabrication of the fish feeder. Upon completion of the fabrication, the machine had to undergo several tests to evaluate its performance.

Design of the Machine

Fig. 1 illustrates the automatic fish feeder machine. The dimensions of this machine are 0.8m (length) x 0.5m (width) x 1.6m (height). In general, the machine consists of a few components such as hopper, lift, compressor, propeller, dosing valve, and process control panel.

The design of the hopper will affect the rate and type of particle flows in the hopper. The properties taken into consideration when designing the hopper include the effective angle of internal friction, the material flow function, and the angle of the wall friction between the particles and the wall particles. Mass flow of solids in the hopper, which was chosen as the motion of dry fish food, is uniformed and in a steady state whenever any of it is drawn from the outlet. This part is the most critical part of the design, where detailed calculations were made to determine the size, angle, and the opening of the orifice. The hopper was designed based on the average bulk density for the different sizes of feed pellets. Using the Jenike Shear Tester, semi-included angle and minimum outlet dimension could therefore be obtained.

The scissor lift can be adjusted to the desired height with the minimum height of 30 cm and the maximum height of 90 cm. The height is easily adjusted to accommodate the different tank heights. The wheels of the scissor lift can be locked for stationary position. The air operated pellet propeller system is operating within 0-5 bar. The maximum rotation speed is 1000 rpm, and this can be adjusted at solenoid operated ball valve. The propeller consists of 6 vanes which are thin, rigid with flat surfaces that are readily mounted along an axis.

The operating pressure for this valve is 4 bars. The stroke for this valve is 5 cm and it is made from stainless steel to prevent food contamination. This dosing valve is reliable and easy to clean. The thickness of this valve is only 0.2 cm, and this is to avoid any damage to the pellets. This dosing valve is operated using air supply from an air compressor connected to the pneumatic cylinder. The operation of the feeder is controlled by a control panel which is connected to the pneumatic cylinder and solenoid operated ball valve. The process control panel includes a cycle timer, dispensing timer, main buttons, as well as auto start and manual start buttons. The cycle and dispensing timer can be set either in seconds, minute or hour. Moreover, it can be adjusted according to the desired interval between the feedings and the required amounts of the food.

PERFORMANCE EVALUATION

A trial run on the automatic fish feeder was conducted to determine the distance of the fish pellets being dispensed. Two types of pellets were used. The density for the large pellet used is 0.344 g/cm^3, whereas the density for the smaller pellet is 0.386 g/cm^3.

Ten kg of small and large pellets were used in testing the feeder. For the same purpose, different speeds of the propeller, height positions of the hopper and angles of the opening were also used. The speed of the propeller was adjusted at 1000 rpm, 900 rpm and 800 rpm. The height position of the hopper was set at 80 cm, 100 cm, 120 cm and 140 cm, while the angle of the opening was 0°, 30° and 60°. The minimum and maximum distances of the pellets dispense were recorded.

Figs. 2 and *3* show the distance of the small and large pellets, dispensed at different height positions and different angle opening of the hopper at 1000 rpm. The results obtained from different operating speeds (800 and 900 rpm) corroborate the findings and they are therefore not shown here. From the graphs, it can be observed that when the hopper is fixed at a higher position, the pellets will be dispensed much further. Meanwhile, the opening angle of the hopper was found to have a minimal effect on the distance of pellets being dispensed.

The dispensing widths versus height of hopper for small and large pellets at 1000 rpm are shown in *Figs. 4* and *5*, respectively. When the position of the hopper is raised, the width of the small and large pellets being dispensed will also increase. Moreover, the opening angles of the hopper have some effects on the distribution of the pellets. As the opening angle is increased from 0° to 30°, the dispensing width also increases at an average of only 20%, but the increment is more significant when the opening is at 60°, where the pellets are dispensed up to 80% further.

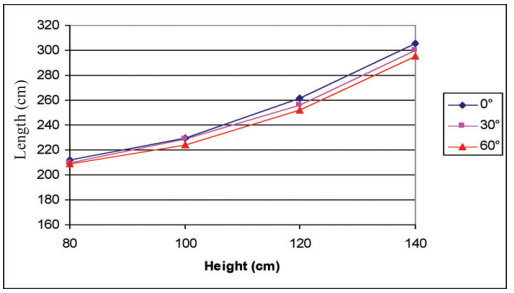

Fig. 2: Dispensing length versus height of the hopper for small pellets at 1000 rpm

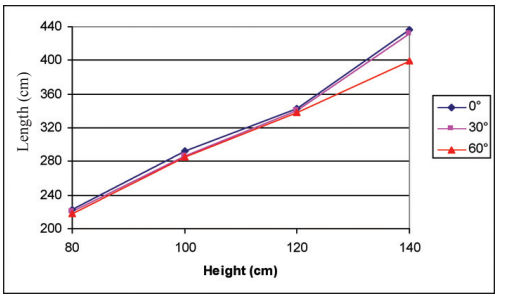

Fig. 3: Dispensing length versus height of the hopper for large pellets at 1000 rpm

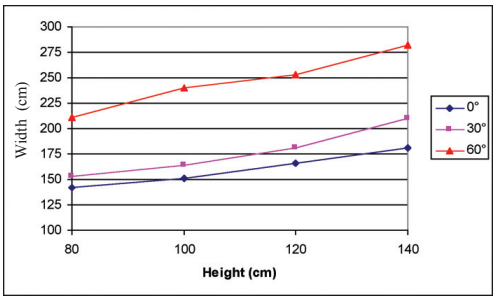

Fig. 4: Dispensing widths versus height of the hopper for small pellets at 1000 rpm

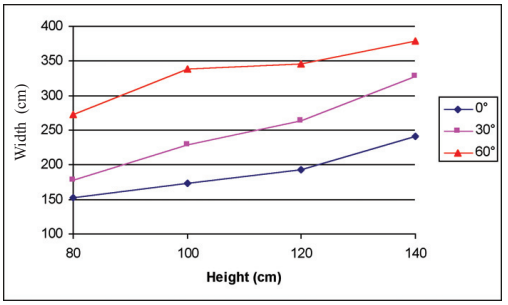

Fig. 5: Dispensing widths versus height of the hopper for large pellets at 1000 rpm

Several tests were also conducted to determine the total amount of fish pellets being dispensed at different intervals. For this purpose, different amounts of fish pellets (10 kg, 5 kg, and 2 kg) were separately put in the hopper. The dispensing rate for the small pellets is around 300 g/s and this is 200 g/s for the large pellets. Thus, the dispensing rate can be assumed constant at all times. An analysis of the moisture content in the hopper was also conducted. The automatic fish feeder was exposed to the sun and rain. In fact, the moisture content of the pellets was tested every day for two weeks. The test revealed that the moisture content of the pellets had remained constant, indicating that the feeder is moisture resistant.

CONCLUSION

An automatic fish feeding machine for aquaculture industry in Malaysia was developed in this study. It is a simple and yet reliable, feasible, and quite efficient feeding machine. The automatic fish feeder was constructed using stainless steel grade 304 to avoid contamination. It is controlled by a digital timer which allows the owner to adjust the cycle time and dispensing time as and when required. More importantly, the timing can be programmed to ensure that the feeding schedule is consistent. The feeding mechanism is easily and widely adjustable. Among other, the height of the feeder is adjustable to accommodate different heights of tanks used in the industry. Furthermore, the hopper size can be changed to accommodate different capacity of feed. Moreover, the opening angle can also be adjusted to suit the different sizes of tanks or ponds. The feeder is air operated

and it is connected to the controller using air pipe. This way, the control panel can be allocated in a safe place near the power supply and the feeder can be located at any place near the tank.

ACKNOWLEDGEMENT

The authors would like to acknowledge Universiti Putra Malaysia (UPM) for the financial support given.

REFERENCES

Alongi, D.M., Chong, V.C., Dixon, P., Sasekumar, A. and Tirendi, F. (2003). The influence of fish cage aquaculture on pelagic carbon flow and water chemistry in tidally dominated mangrove estuaries of Peninsular Malaysia, Malaysia. *Marine Environmental Research*, *55*, 313-333.

Beam, M. and Gebhart, G. (2000). *Aquaculture*. Langston University, Agricultural Research and Extension Programs.

Chang, C.M., Fang, W., Jao, R.C., Shyu, C.Z. and Liao, I.C. (2005). Development of an intelligent feeding controller for indoor intensive culturing of Eel. *Aquacultural Engineering*, *32*, 343-353.

Craig, S. and Helfrich, L. A. (2002). *Understanding Fish Nutrition, Feeds and Feeding*. U.S. Virginia Tech.

Helga, J. (2006). Aquaculture production impact on markets and international trade, Kuala Lumpur. *Infofish International*, 60-64.

Liao, I.C. (2001). *Trends and perspectives in Asian aquaculture*, China, Report of the APO Seminar.

Rafeal, D.G. (2007). Tilapia production in Southeast Asia. *Infofish International*, 8-13. Kuala Lumpur.

Riche, M. and Garling, D. (2003). *Feeding Tilapia in Intensive Recirculating Systems*, North Central Regional Aquaculture Center, UK.

Subasinghe, S. (2007). Vannamei, tilapia, catfish…what next? *Infofish International*, *3*. Kuala Lumpur,

Velazquez, M. and Martinez, F.J. (2005). Design and testing of a faeces-collecting device for fish digestibility studies using demand or automatic feeding. *Aquacultural Engineering*, *33*, 126-134.

Williams, K. (2000). *Tilapia culture in cages and open ponds*. PhD. Thesis, U.S., Langston University.

ISSN: 0128-7680
Pertanika J. Sci. & Technol. **18 (1)**: 111 – 120 (2010)

Development and Validation of a Mathematical Model for Ventilation Rate in Crop Protection Structures

Faisal Mohammed Seif Al-Shamiry[1] and Desa Ahmad[2*]
[1]Agricultural Engineering Department
Sana'a University, P.O. Box 13383
Sana'a, Yemen
[2]Department of Biological and Agricultural Engineering,
Faculty of Engineering, Universiti Putra Malaysia,
43400 UPM, Serdang, Selangor, Malaysia
[*]E-mail: desa@eng.upm.edu.my

ABSTRACT

Natural ventilation is defined as the number of air exchanges per hour per unit floor area necessary to reduce high indoor air temperature and humidity. In addition, it maintains the concentration of carbon dioxide. Natural ventilation is preferred in mechanical system as the ventilation opening is built into the greenhouse, with lower construction cost and no energy and maintenance inputs are required. A mathematical model to quantify natural ventilation rates was developed and verified in large-scale greenhouse structures. For this purpose, four Naturally Ventilated Tropical Greenhouse Structures were designed and constructed at the Malaysian Agricultural Research and Development Institute (MARDI). These were single, double, triple, and quadruple span structures with floor areas of 500 m^2, 1000 m^2, 1500 m^2 and 2000 m^2, respectively. This paper presents the validation of a mathematical model which was developed to quantify natural ventilation rates which are very crucial to reduce high in-house temperature built up in the tropics. Regression equations of natural ventilation against wind speed were found to be $\Phi_w = 0.0632V$, $\Phi_w = 0.0395V$, $\Phi_w = 0.0316V$ and $\Phi_w = 0.0276V$ for the single, double, triple and quadruple spans, respectively. Meanwhile, coefficients of determination showed strong relationships between ventilation rate and wind speed, with $R^2 = 0.9999$ for all structures. Larger floor area was found to have higher in-house temperature than smaller ones. Ventilation rate inside the single-span structure was found to be higher compared to the multi-span structures, which increased linearly with the increasing wind speed at the eaves of structure.

Keywords: Natural ventilation, wind effect, multi-span, greenhouse structure

NOMENCLATURE

A_g	the floor area of the greenhouse	(m^2)
A_n	area of the nth opening	(m^2)
ΣA_{TO}	total areas of vent openings	(m^2)
C	ventilation coefficient	(m^2/m^2)
C_{pe}	external pressure coefficient	(dimensionless)
C_{pi}	internal pressure coefficient	(dimensionless)
C_d	discharge coefficient	(dimensionless)

Received: 9 June 2008
Accepted: 7 December 2009
[*]Corresponding Author

j	number of opening (1, 2,…)	
n	total number of openings	
V	outside wind speed at eaves level	(m/s)
V_n	air velocity moving through the nth opening	(m/s)
Φ_w	ventilation rate by wind effect	(m^3/m^2s)

INTRODUCTION

A greenhouse is defined as a construction used to protect plants from undesirable climatic variation and it provides an in-house environment conducive to plant production (Bin Gadhi and Haidrah, 1999). This technique is necessary to replace the high risk of open field production against damaging elements such as high rainfall, extreme solar radiation, weed competition, as well as damages caused by diseases and insects. The main function of the greenhouse is to increase the yield and quality of vegetable, fruit, flower and herb productions. Moreover, the production can be made continuous throughout the year. In Malaysia, crop production in the greenhouses plays an important role to supply sufficient food to substitute the high import bill of processed and unprocessed horticultural products. Currently, the import bill for food is more than RM 13 billion annually (Rezuwan, 2002).

The design of the greenhouses in the tropics is significantly different from that in regions with cooler climates. In particular, the greenhouses in the tropics require heat dissipation as opposed to heat conservation in temperate regions. This is usually followed by ventilation to remove the excess heat which builds up during hot sunny days. The ventilation rate is the number of air exchanges between inside and outside the greenhouse through the openings per unit time and floor area. Ventilation systems, in general, are operated as either natural ventilation or forced ventilation (Baptista *et al.,* 1999). Natural ventilation is usually induced by the stack (buoyancy) or wind effects or a combination of both, while forced ventilation is driven by electrical fans or other mechanical means. Natural ventilation is preferred because it uses less energy, requires lower maintenance and is quieter in operation than the forced ventilation method (Rezuwan, 1999).

Air exchange occurs when there is a pressure difference across the ventilator opening. Pressure differences induced by the wind force are acted at the eave level (wind effect) or temperature difference between the inside and outside of the greenhouse (stack or chimney effect). In general, both wind and stack effects occur together. Ventilation is necessary to provide air exchange and good climatic control in the greenhouse. It limits the temperature rise on hot days, controls excessive humidity caused by transpiration and prevents excessive depletion of the concentration of carbon dioxide. Therefore, an understanding of air exchange rate is necessary because it directly affects both the development and production of crops (Rezuwan, 1999; Rezuwan, 2005). When the average maximum outside temperature is less than 27°C, ventilation can prevent excessive internal temperatures during the day. However, if the average maximum outside temperature exceeds 28°C, artificial cooling may then be necessary. It is important to note that the maximum greenhouse temperature should not exceed 30-35°C for prolonged periods (Bailey, 2004).

Generally, open field farming gives low production, poor quality, and crops are totally destroyed at times. For example, losses by insects and diseases have been reported to range from 50-100% when infestation levels are high (Hawa *et al*., 1992). Moreover, heavy rainfalls throughout the year cause damages to crops, difficult working conditions, make them susceptibility to diseases and fertilizer loss by surface runoff. Furthermore, extreme solar radiation can be detrimental to crops. In addition, hot and humid weather does not seem to be conducive for the growth and production of sub-tropical and temperate crops. As these conditions are more pronounced in

enclosed greenhouses, the requirement for good ventilation is increased. To address these problems, naturally ventilated tropical crop protection structures have been developed by the Malaysian Agricultural Research and Development Institute (MARDI). The structures were introduced to replace the imported naturally ventilated polytunnel or glasshouse, which are less suitable for use in the tropics. The imported structures were designed to conserve heat in cold temperate weather, while the requirement in the tropics is for a heat dissipation type of greenhouse (Rezuwan, 1999; Rezuwan, 2005; Rezuwan *et al.,* 2001). This naturally ventilated greenhouse relies primarily on the air blowing into a windward side opening and out the open roof vents. Work on ventilation rate have been carried out by several researchers (e.g. Bailey *et al*., 2003; Montero *et al*., 1997; Munoz *et al*., 1999; Sase and Christianson, 1990; Teitel and Tanny, 1999; Von Zabeltitz, 1999) and only a few of these studies have considered ventilation rate and microclimate of the greenhouses under humid tropics. Models estimating the ventilation rate in some specific greenhouse structures have been studied by Baptista *et al*. (2001) and Munoz *et al*. (1999), but the structures used only had small ventilation openings. For the humid tropics, naturally ventilated greenhouses normally have larger ventilation openings. This paper presents the development and validation of a mathematical model to quantify natural ventilation rates by the wind effect, which is very crucial to reduce high in-house temperature built up in the tropics.

MATERIALS AND METHODS

Greenhouses Structure

Naturally ventilated tropical greenhouse structures were designed and constructed at the Malaysian Agricultural Research and Development Institute (MARDI). The single-span structure was made 50 m long x 10 m wide x 4.0 m high with straight side walls and tunnel roof shape with a jack-roof. Moreover, the double, triple, and quadruple spans were also constructed in the prefabricated and modular form. *Plates 1* and *2* are typical types of the single and quadruple span structures, respectively. All the structures were made of galvanized steel frame, transparent polyethylene film roofing, and polyethylene insect-screen side cladding with 32 mesh netting. The dimensions of the greenhouse structures are listed in Table 1.

Plate 1: Single-span greenhouse structure

Plate 2: Quadruple-span greenhouse structure

TABLE 1
Dimensions of naturally ventilated tropical greenhouse structures

Structure	Length (m)	Width (m)	Height (m)	Floor area (m^2)	Volume (m^3)
Single span	50	10	4.0	500	2300
Double span	50	20	4.0	1000	4600
Triple span	50	30	4.0	1500	6900
Quadruple span	50	40	4.0	2000	9200

Data Collection

The micro climate parameters were measured continuously for more than six months using an Integrated Data Acquisition and Monitoring System. In addition, thermometers were used to support and check the measurements. The system consists of computer software, circuit integration, data logger, electronic actuators, and sensors. The sensors were used for the temperature, wind speed, and wind pressure. Each location had three sensors. The locations of the sensors are shown in *Fig. 1*. All the sensors were calibrated before the measurement in order to minimize error or unreliable data by verifying using hand-held thermometers for the temperature, and standing fan for wind speed. A total of 30 readings were recorded for each structure.

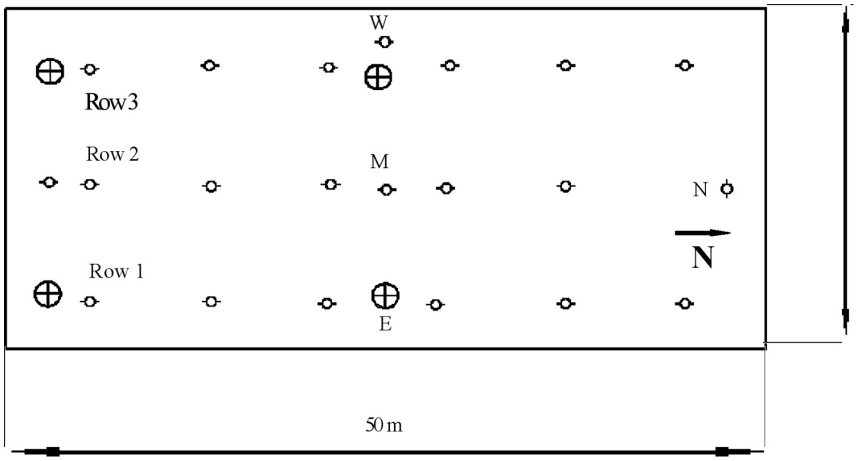

Fig. 1: Layout of the system in the experimental greenhouse (⊕ Misting Fan, ⊙ -location of sensors, N – North, S – South, W – West, E – East, M - Middle)

MODEL DEVELOPMENT

Ventilation by Wind Effect

The theory on the prediction of ventilation rate was first developed by Bruce (1982), and it was experimentally verified by Foster and Down (1987) using the half-scale models. Wind around a building creates a pressure field at the openings and hence produces air flow through them. These

pressures may be positive when the air flows into the building or negative (suction) when the air flows out. As the wind speeds measured were higher than 1m/s and reaching as high as 4.26m/s at 12.00 noon, the buoyancy effect (i.e. the temperature difference between inside and outside the greenhouse generating the density difference of air) is considered small and the ventilation rate can therefore be considered as only a function of the wind. Bruce (1975) described the ventilation due to wind as:

$$\Phi_w = \sum_{j=1}^{n} A_j \frac{\left| C_{pei} - C_{pi} \right|}{C_{pej} - C_{pi}} \tag{1}$$

Where, C_{pe} is external pressure coefficient, C_{pi} is internal pressure coefficient, and j is opening (1,2,…). The ventilation rate can be calculated using the formula adopted by Rezuwan *et al.* (2001), as follows:

$$\Phi_w = \frac{1}{2A_g} \sum_{i=1}^{n} A_n V_n \tag{2}$$

Where, Φ_w is the ventilation rate by wind effect (m^3/m^2s), A_n is the area of the nth opening, V_n is the air velocity moving through the nth opening and A_g is the floor area.

$$V_n = C_d \frac{\left| C_{pej} - C_{pi} \right|^{\frac{3}{2}}}{C_{pej} - C_{pi}} \tag{3}$$

For the greenhouse structures in this study, the ventilation rate can be calculated using the following equation:

$$\Phi_w = \frac{1}{2A_g} \sum (A_1 V_1 + ... + A_n V_n) \tag{4}$$

which can be reduced to:

$$\Phi_w = \frac{1}{2A_g} C_d \frac{\left| C_{pe} - C_{pi} \right|^{\frac{3}{2}}}{C_{pe} - C_{pi}} \sum (A_1 + ... + A_n) . V \tag{5}$$

Finally, the ventilation rate due to wind can be calculated using the following formula:

$$\Phi_w = C_d \frac{\sum_{i=1}^{n} A_{TO}}{2A_g} V \frac{\left| C_{pe} - C_{pi} \right|^{\frac{3}{2}}}{C_{pe} - C_{pi}} \tag{6}$$

Where, C_d is the discharge coefficient, V is the speed of the outside wind and ΣA_{TO} are the total areas of the vent openings.

RESULTS AND DISCUSSION

Temperature

The highest average values of the inside temperature were 41.00ºC, 41.25ºC, 41.50ºC, and 41.75ºC at 14:00 pm, with the standard errors of 0.49ºC, 0.39ºC, 0.43ºC, and 0.34ºC for single, double, triple and quadruple-span, respectively, while the highest value of the outside temperature was 34.20ºC, with a standard error of 0.49ºC as shown in *Fig. 2*. The differences between the inside and outside temperatures were between 6.80ºC, 7.05ºC, 7.30ºC, and 7.55ºC for the single, double, triple and quadruple spans, respectively. These results showed that the temperature increased from early morning until afternoon, and then declined towards late evening. The increasing and declining trends are in line with the solar radiation intensity and the outside air temperature throughout the day. The average in-house temperature was found to be higher than that of the outside of the structures. This is because any enclosed structure restricts air movement and the cooling effect is more dependent on natural ventilation rate. Meanwhile, small floor area has lower in-house temperature compared to larger floor area due to fast air movement and air exchanges (Hemming *et al.,* 2006).

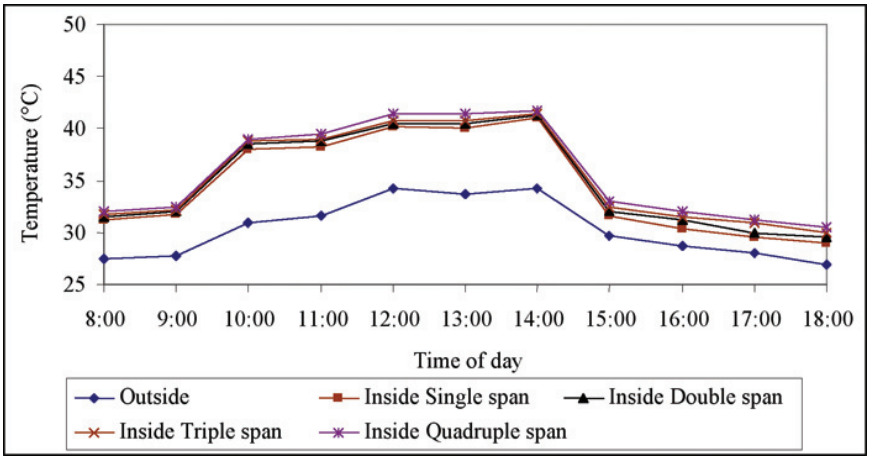

Fig. 2: Effects of single, double, triple and quadruple floor areas on in-house average air temperature

Wind Speed

Wind speed is influenced by many factors such as surrounding vegetative growth, ground formation and local climate. *Fig. 3* shows the comparison between single, double, triple, and quadruple-span structures in terms of wind speed. The highest average wind speed was recorded at 14:00 pm, i.e. 1.39 m/s for the outside and 0.4 m/s for the inside single span structure of 500 m^2 floor area. At 12:00 noon, this was 4.257 m/s for the outside, 0 m/s, 0 m/s, 0.15 m/s, and 0.25 m/s respectively for the inside single, double, triple, and quadruple-structure. There was a significant difference in terms of wind speeds between the outside and inside of the structure. This was due to the effects of wind speed and direction and pressure outside the greenhouse. Moreover, the main contributing factor could be the effect of pressure drop when the wind flowed across the insect screen wall. Smaller screen size tends to reduce the wind speed and hence reduces its pressure. For this study, only 32 mesh netting was used.

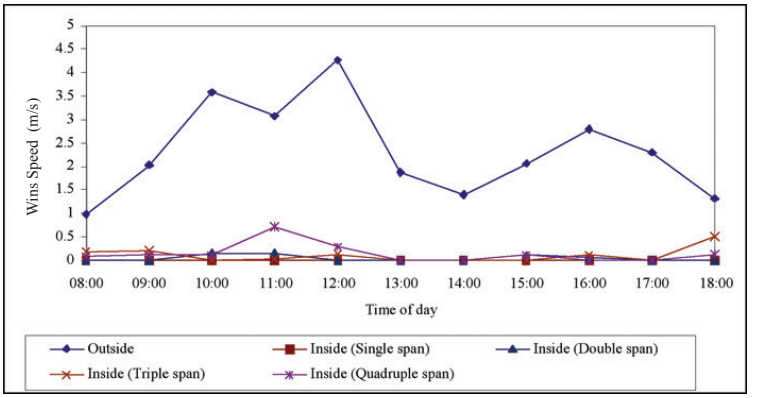

Fig. 3: Comparison between single, double, triple and quadruple-span structures in terms of wind speed

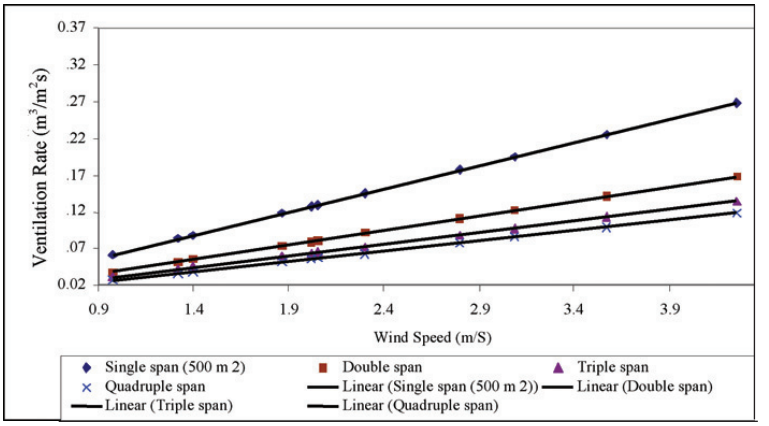

Fig. 4: Effect of wind speed on ventilation rate for various floor areas

Ventilation Rate

Ventilation rates by the wind effects were calculated using equation (6) for the single and multi-span structures. The discharge coefficient, the outside pressure coefficient, and the inside pressure coefficient were based on the recommended values of 0.411, 0.46, and 0.05, respectively (Rezuwan, 1999). *Fig. 4* shows the relationships between ventilation rate and wind speed in the single, double, triple, and quadruple-span structures. The results indicated that the ventilation rate increased with increasing wind speed at the eaves height of the structure. In addition, the ventilation rate in the single span structure was found to be greater than in the other structures, since the small floor area allowed the wind to flow in and out much faster than the larger area. The regression equations of the single, double, triple and quadruple-span structures are summarized in Table 2. These results are in a good agreement with the previous studies by Rezuwan (1999), De Jong (1990) and Bot (1983). Moreover, the adjusted coefficients of determinations (R^2) showed a strong relationship between the ventilation rate and wind speed. All the coefficients of determination are 0.9999. Based on the data presented in Table 2, a general regression equation can therefore be formulated as:

$$\Phi_w = CV \tag{7}$$

where Φ_W is the ventilation rate by wind effect (m^3/m^2s), V is the outside wind speed at eaves level (m/s) and C is the ventilation coefficient, which is a function of screen size, coefficient of discharge, wind direction, floor area and opening area, as shown in equation (6), where C can be written as:

$$C = C_d \frac{\sum_{i=1}^{n} A_{TO}}{2A_g} \cdot \frac{\left| C_{pe} - C_{pi} \right|^{\frac{3}{2}}}{C_{pe} - C_{pi}} \tag{8}$$

TABLE 2
Regression equations showing effects of wind speed on the ventilation rate for various floor areas

Structure	Regression equation	Adjusted R^2	No. of observation
Single-span ($500m^2$)	$\Phi_w = 0.0632$ V	0.9999	30
Double-span ($1000m^2$)	$\Phi_w = 0.0395$ V	0.9999	30
Triple-span ($1500m^2$)	$\Phi_w = 0.0316$ V	0.9999	30
Quadruple-span ($2000m^2$)	$\Phi_w = 0.0276$ V	0.9999	30

CONCLUSIONS

The developed mathematical model of ventilation rate, which takes into consideration the effects of wind, has helped in the design and quantification of the ventilation rates for the single, double, triple, and quadruple-span versions of the naturally ventilated greenhouses for the tropics. Understanding of wind effect is very important because of the high in-house air temperatures during the no wind condition. This gives heat stress which is detrimental to the growth of crops or plants. When there is wind, the stress is reduced as ventilation is dominated by the wind, together with the pressures of the differences in temperature. The ventilation rate caused by the wind effect increases linearly as the wind speed becomes greater. In addition, the ventilation rate in the single-span became higher than in the multi-span structure. This was due to the small floor area which allows the wind to flow in and out much faster than the larger area.

ACKNOWLEDGMENTS

This project was funded by MOSTI under IRPA Project No.09-02-04-0873 EA001. The authors wish to thank Dr Rezuwan Kamaruddin and also those at the Malaysian Agricultural Research and Development Institute (MARDI) who were directly or indirectly involved in this work.

REFERENCES

Bailey, B. J., Montero, B. I., Perez Parra, J., Robertson, A. P., Baeza, E. and Kamaruddin, R. (2003). Airflow resistance of greenhouse ventilators with and without insect screens. *Biosystems Engineering 86*(2), 217-229.

Bailey, B. J. (2004). Natural and Mechanical Greenhouse Climate Control. *Acta Horticulturae*, *710*.

Baptista, F. J., Bailey, B. J., Randall, J. M. and Meneses, J. F. (1999) Greenhouse ventilation rate: Theory and measurement with tracer gas techniques. *Journal of Agriculture Engineering Research*, *72*, 363-374.

Baptista, F.J., Bailey, B.J. and Meneses, F.J. (2001). Natural ventilation of greenhouses: Comparison of measured and predicted ventilation rates. *Agribuilding, 3-6,* 136-151, September 2001- Campinas, SP, Brazil.

Bin Gadhi, S. and Haidrah, M. (1999). Thermal analysis best orientation for optimum solar radiation and heat load for summer and winter greenhouse in Yemen. *Journal of Science and Technology, Special Issue, 4*, 1-8.

Bot, G.P.A. (1983). *Greenhouse climate: From physical process to a dynamic model.* Ph.D. Thesis, Agricultural University, Wageningen.

Bruce, J.M. (1975). Natural ventilation of cattle buildings by thermal buoyancy. *Farm Building Progress, 42*, 17- 20.

Bruce, J.M. (1982). Ventilation of a model livestock building by thermal buoyancy. *Trans. ASAE, 25*(6), 1724-1726.

DeJong, T. (1990). *Natural ventilation of large multi-span greenhouses*. Ph.D. thesis, Agricultural University, Wageningen.

Foster, M. P. and Down, M. J. (1987). Ventilation of livestock buildings by natural convection. *Journal of Agricultural Engineering Research, 37*, 1-13.

Hawa, J., Embi, Y. and Rezuwan, K. (1992). Vegetable cultivation under simple rain shelters in Malaysia. Food and Fertilizer Technology Center, Taipei City, Republic of China on Taiwan. *Extension Bulletin,* N0. 350.

Hemming, S., Waaijenberg, D., Campen, J. B., Impron and Gerard, P.A.B. (2006). Development of a Greenhouse System for Tropical Lowland in Indonesia. *Acta Horticulture* (ISHI), 710.

Montero, J.I., Muñoz, P. and Antón, A. (1997). Discharge coefficient of greenhouse windows with insect-proof screen. *Acta Hort*. (ISHS), *443*, 71-78.

Munoz, P., Montero, J.I., Anton, A. and Giuffrida, F. (1999). Effect of insect-proof screens and roof openings on greenhouse ventilation. *Journal of Agricultural Engineering Research*, *73*, 171-178.

Rezuwan, K. (1999*). A naturally ventilated crop protection structure for tropical conditions*. Ph.D. Thesis, Cranfield University.

Rezuwan, K., Bailey, B.J. and Montero, J.I. (2001). Design and development of naturally ventilated greenhouse structure for temperate vegetable production in the Tropics. *Acta Horticulturae, 578*, 97-103.

Rezuwan, K. (2002). Design and fevelopment of tropical greenhouse structures. *Proceedings of 2nd World Engineering Congress* (pp. 22-25). Sarawak, Malaysia.

Rezuwan, K. (2005). Design and development of naturally ventilated tropical crop protection structures and hydroponics systems. *Proceedings of the International Conference & Exhibition on Soiless Culture (ICESC 2005),* Fort Canning Gallery, Singapore, 5-8 September 2005.

Sase, S. and Christianson, L. L. (1990). Screening greenhouse – some engineering considerations. NABEC Paper No. 90 – 201. Presented at *NABEC Conference*, University Park, PA. USA. pp. 13.

Teitel, M. and Tanny, J. (1999). Natural ventilation of greenhouses: experiments and model. *Agricultural and Forest Meteorology*, *96*, 56-70.

Von Zabeltitz, C. (1999). *Greenhouse Structures*. *Ecosystems of the World's 20 Greenhouses*. Amsterdam: Elsevier Publication.

ISSN: 0128-7680
Pertanika J. Sci. & Technol. **18 (1)**: 121– 138 (2010)

Microwave Dielectric Characterization of Hevea Rubber Latex at 2.6, 10 and 18 GHz

Jumiah Hassan*, Kaida Khalid and W. Mohd. Daud W. Yusoff
Department of Physics, Faculty of Science,
Universiti Putra Malaysia, 43400 UPM, Serdang, Selangor, Malaysia
**E-mail: jumiah@fsas.upm.edu.my*

ABSTRACT

Dielectric properties of natural rubber *Hevea brasiliensis* latex were measured at frequencies 0.2 to 20 GHz, at temperatures of 2, 15, 25, 35, and 50°C and around 30-98% moisture content. Measurements were done using open-ended coaxial line sensor and automated network analyzer. As expected, results showed that dielectric constant increased with increasing moisture. From 0.2 to 2.6 GHz, the losses were governed by conductive losses but for frequencies greater than 2.6 GHz, these were mainly due to dipolar losses. The former is due to conducting phases in hevea latex, while the latter is mainly governed by the orientation of water molecules. The results were analyzed at 2.6, 10, and 18 GHz, respectively. These were then compared with the values predicted by the dielectric mixture equations recommended by Weiner, Bruggeman and Kraszewski. All the measured values were found to be within the Weiner's boundaries and close to the upper limit of Weiner's model. It is also close to the predicted values of Bruggeman's model with $a/b = 0.1$. All the models including Kraszewski are suitable for predicting the dielectric properties of hevea latex for frequencies 2.6 to 18 GHz, moisture content 30 to 98% and temperatures 2 to 50°C.

Keywords: Complex permittivity, dielectric loss factor, dipoles

INTRODUCTION

The dielectric properties of a material refer to the complex relative permittivity $\varepsilon^* = \varepsilon' - j\varepsilon''$, where ε' is the real relative permittivity, which is also known as the dielectric constant, whereas the imaginary part ε'' is the dielectric loss factor. The dielectric constant is a measure of the ability of the material to be polarised or energy stored, while the loss factor is a measure of the ability of the material to heat or energy loss by absorbing energy.

The samples are freshly tapped hevea latex, latex concentrate, diluted fresh hevea latex, diluted latex concentrate with moisture content (MC) varying from 40%-98% (wet basis) and deionised water. Hevea latex consists of 55%-80% water, 15%-45% rubber hydrocarbon and approximately 2%-4% non-rubber constituents (Chin, 1979). Excluding water, the most abundant non-rubber constituents are proteins, lipids, quebrachitol (methyl inositol), and inorganic salt of about 0.5%. These include potassium, phosphate ions and traces of copper, iron, sodium, calcium and magnesium (Chen, 1979). About 2%-3% conducting phases arise from these non-rubber constituents. This composition varies widely according to season, weather, soil condition, clone, tapping system, etc. The latex concentrate used was preserved with 0.025% tetramethyl-thiuram disulphide/zinc oxide and 0.2%-0.3% ammonia and supplied by the Rubber Research Institute of Malaysia (RRIM). Freshly tapped hevea latex was obtained from the Research Park of Universiti Putra Malaysia (UPM).

Received: 3 June 2008
Accepted: 8 December 2009
*Corresponding Author

Dielectric properties of hevea rubber latex at various moisture contents and temperature have been reported at microwave frequencies. Besides the water content, previous studies have shown that for the frequency range of 2 GHz to 20 GHz, the dielectric properties also depend on the geometrical shape of the water molecule which is ellipsoidal (Khalid and Yusoff, 1992; Khalid *et al*., 1994; Hassan *et al*., 1997). Below 2 GHz, the dielectric properties of latex are mainly due to the migration of dissolved ions which originate from the conducting phases in the latex (Gorton and Pendle, 1985).

In this study, hevea rubber latex is treated as a biphase liquid, where the rubber particles and the non-rubber constituents are considered as a single solid phase or solid content of hevea latex while the other is water. This biphase mixture of water and solid components is assumed to be isotropic and randomly distributed in space.

BIPHASE MIXTURE MODEL

The dielectric properties of mixtures containing two or more dielectrics are common. It is assumed that one component of the mixture forms a matrix, in which the other or several others sparsely in the form of particles, where in general their shape is taken to be ellipsoidal (Suresh *et al*., 1967). The complex permittivity of water and rubber can be written as:

$$\varepsilon^* = \varepsilon^*_w \delta_w f_w + \varepsilon^*_r \delta_r f_r \tag{1}$$

and

$$\delta_w f_w + \delta_r f_r = 1 \tag{2}$$

where $\varepsilon^*_r, \varepsilon^*_w$ are the complex relative permittivity of latex particles or solid continuum and complex relative permittivity of water molecules, respectively. Likewise, δ_w and δ_r are the volume fractions of moisture and latex particles respectively and f is the field ratio. From equations (1) and (2), the general forms for the effective complex dielectric constant in terms of the average field for the water and solid continuum can be expressed as:

$$\varepsilon^* = \varepsilon^*_r + (\varepsilon^*_w - \varepsilon^*_r)\delta_w f_w \tag{3}$$

and

$$(\varepsilon^* - \varepsilon^*_w)\delta_w f_w + (\varepsilon^* - \varepsilon^*_r)\delta_r f_r = 0 \tag{4}$$

The volume fraction δ_w is related to the moisture content by the following expression (Krazewski, 1974);

$$\delta_w = M_w \Big/ \left[M_w + \frac{\gamma_r}{\gamma_w}(1 - M_w) \right] \tag{5}$$

where M_w is the wet basis moisture content, γ_r and γ_w are the relative of the solid continuum and water, respectively.

From equations (3) and (4), the complex permittivity of the mixture can be written as:

$$\varepsilon^* = \varepsilon^*_r + \frac{(\varepsilon^*_w - \varepsilon^*_r)}{3}\delta_w \sum_l \frac{\varepsilon^*_r}{\varepsilon^*_r + (\varepsilon^*_w - \varepsilon^*_r)A_l} \tag{6}$$

where A_l is known as the depolarisation factor dependent on the axial ratios of the ellipsoid. Equation (6) was extended (Boned and Peyrelasse, 1983) for high concentrations of inclusion or high moisture content following Bruggeman's method (Bruggeman, 1935; Chaloupka *et al*., 1980). In this method, the low concentration is gradually increased by the addition of volume fraction $d\delta = \frac{d\delta_w}{1-\delta_w}$ of the moisture content which gives an increment to the complex dielectric constant $d\varepsilon$ as:

$$d\varepsilon^* = \frac{d\delta_w}{(1-\delta_w)} \frac{\varepsilon^*_w - \varepsilon^*}{3} \varepsilon^* \sum_l \frac{1}{\varepsilon^* + (\varepsilon^*_w - \varepsilon^*)A_l} \tag{7}$$

In this process, the permittivity of the medium around a particle slowly changes from ε^*_r to the final complex permittivity of the mixture ε^*. For the case of a spheroid $b = c$, A_l depends only on the ratio a/b and $A_a + A_b + A_c = 1$. By integrating equation (7) from 0 to δ and from ε^*_r to ε^*, the following equations can be obtained for a spheroid with $a \neq b = c$,

$$(1-\delta_w) = \left(\frac{\varepsilon^*_r}{\varepsilon^*}\right)^{3d} \left(\frac{\varepsilon^*_w - \varepsilon^*}{\varepsilon^*_w - \varepsilon^*_r}\right) \left[\frac{\varepsilon^*_r(1-3A) + \varepsilon^*_w(2-3A)}{\varepsilon^*(1-3A) + \varepsilon^*_w(2-3A)}\right]^K \tag{8}$$

where, $A = A_b = A_c$, $d = \frac{1}{\sum_l A_l^{-1}} = \frac{A(1-2A)}{(2-3A)}$ and $K = \frac{2(3A-1)^2}{(2-3A)(1-3A)}$

The complex permittivity of the mixture $\varepsilon^* = \varepsilon' - j\varepsilon''$ could be obtained from equation (8) using the numerical root seeking method (Khalid, 1994).

Another analysis was developed by Weiner where the upper and lower limits of the complex permittivity can be calculated from:

$$\frac{\varepsilon^* - 1}{\varepsilon^* + n} = \delta_w \frac{\varepsilon^*_w - 1}{\varepsilon^*_w + n} + \delta_r \frac{\varepsilon^*_r - 1}{\varepsilon^*_r + n} \tag{9}$$

The mixing condition *n* provides a means of deducing the orientation assumed by the water molecules and could be used to obtain information about the degree of binding of the water molecules in the latex solution (Hassan *et al*., 2003). According to Weiner's theory, the complex relative permittivity reaches a maximum limit, ε^*_{max} or Weiner's upper bound when n = ∞. This corresponds to the case where the water molecules, in the form of ellipsoids with their major axis, are parallel to the direction of the applied field. In this manner of configuration, the water molecules are said to be loosely bound and are therefore free to move or orientate. The minimum limit, ε^*_{min} or Weiner's lower bound, is obtained when $n = 0$. This is when the major axis of the ellipsoids is perpendicular to the applied field and is tightly bound. From equation (9), the following could be obtained:

$$\varepsilon^*_{\max} = \delta_w \varepsilon^*_w + \delta_r \varepsilon^*_r \tag{10a}$$

$$\frac{1}{\varepsilon^*_{\min}} = \frac{\delta_w}{\varepsilon^*_w} + \frac{\delta_r}{\varepsilon^*_r} \tag{10b}$$

The dielectric relative permittivity of the mixture is always bound by $\varepsilon^*_{\max}$ in the upper range and $\varepsilon^*_{\min}$ in the lower range. With *n* increasing, more water molecules are aligned parallel

to the applied field, whereas with decreasing *n*, more water molecules are aligned perpendicular to the field.

Kraszewski *et al.* (1976) developed a simple model for a quick analysis from the relation of the propagation constant, where the complex relative permittivity of the mixture may be written as:

$$\varepsilon^{*1/2} = \delta_w \varepsilon^{*1/2}_w + \delta_r \varepsilon^{*1/2}_r \quad (11)$$

MATERIALS AND METHODS

Measurement of the complex relative permittivity of latex was done using 4 mm open-ended coaxial line probes (HP 85070B), coupled with automated network analyser (HP 8720B) and computer, at the frequencies of 0.2 to 20 GHz. The sensor translates changes in the permittivity of a test sample into changes in the input reflection coefficient. The system software calculates the dielectric parameters from the phase and the amplitude of the reflected signal at the interface between the open-ended coaxial line and the sample to be analyzed. With proper calibrations (Kraszewski *et al*., 1982), the accuracy of the measurement is about ± 5% for ε' and ± 3% for ε''.

A series of solutions were prepared from the latex concentrate and freshly tapped latex. These solutions were diluted with deionised water with a difference in the moisture content of about 2 to 3%. Latex concentrate registered the minimum moisture of about 38%, whilst deionised water had the maximum of 100%. Latex concentrate was supplied by the Rubber Research Institute of Malaysia and freshly tapped latex (RRIM 600 clone) was obtained from the university's research park.

The measurements were made at the temperatures of 2 to 50°C using ice bath and water bath to cool and warm the samples, respectively (Hassan *et al*., 1997). The actual moisture content (wet basis) was obtained by oven drying three 1.5 to 2.5 grams of the samples at 70°C and the average results were recorded.

RESULTS AND DISCUSSION

The experimental values of the dielectric properties of hevea rubber latex, at 2, 15, 25, 35, and 50°C, with the values predicted from the mixture equations are summarised in *Figs. 1* to *3*. Curves show the dielectric constant, ε' and the dielectric loss factor, ε'' at the frequencies of 2.6, 10 and 18 GHz, respectively. The dielectric constant and loss factor increased with increasing moisture at all frequencies, except that the loss factor is almost independent of the moisture at 2.6 GHz. This is because the total losses are dominated by conductive losses at 2.6 GHz, and by dipolar losses above 2.6 GHz. Complex permittivity of the biphase mixture model was for identical ellipsoidal particles which were randomly distributed in space. The dielectric properties of liquid do not only depend on the content of water, but they are also strongly dependent upon the geometrical shape of the water molecules (Chaloupka *et al*., 1980). The values predicted from the mixture models include Weiner's (upper and lower bound), Kraszewski and Bruggemann, with *a/b* = 0.01, 0.1 10 and 100 (Bruggeman, 1935; Boned and Peyrelasse, 1983). Both the fitted experimental data and predicted values are tabulated in Tables 1-3. From the figures shown, all the measured values lie within the Weiner's boundaries, and they are also well below and close to the upper limit of the Weiner's model. This means that the water molecules are loosely bound and they can be easily polarised.

The measured values were very close to the predicted values of Bruggeman's model with *a/b* = 0.1 (prolate spheroid) for all temperatures and frequencies, except at 50°C for 2.6, 10 and 18 GHz and 35°C for 10 GHz, where *a/b* = 10 (oblate spheroid). A better fit of Bruggeman's model to the data is given if water molecules are treated as oblate rather than prolate spheroids at 50°C.

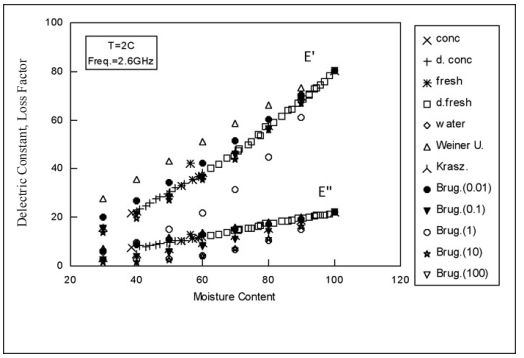

Fig. 1 (a)

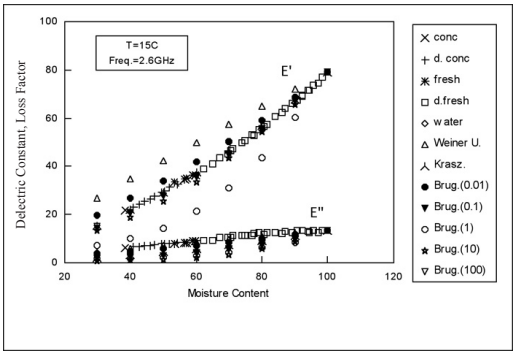

Fig. 1 (b)

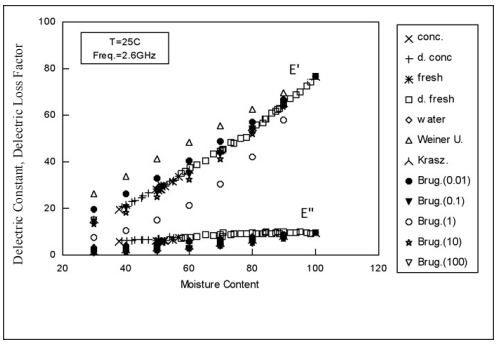

Fig. 1 (c)

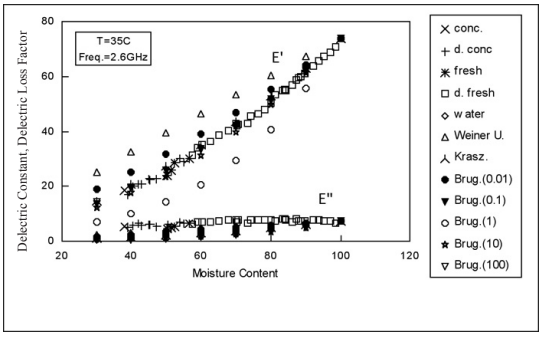

Fig. (d)

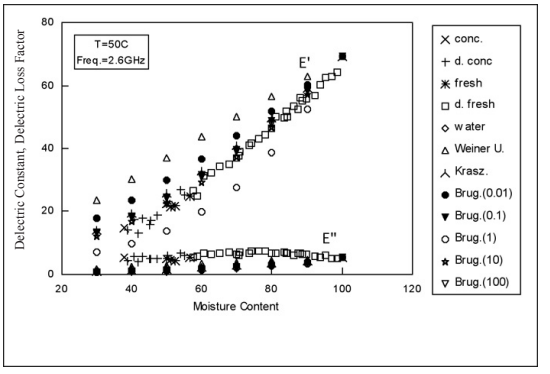

Fig. 1 (e)

Fig. 1(a-e): Experimental dielectric data for Hevea latex solution with the theoretical data calculated from the mixture equations, Weiner's upper, Bruggeman (a/b = 0.01, 0.1, 1, 10, 100) and Kraszewski at 2.6 GHz and 2, 15, 25, 35 and 50°C, respectively

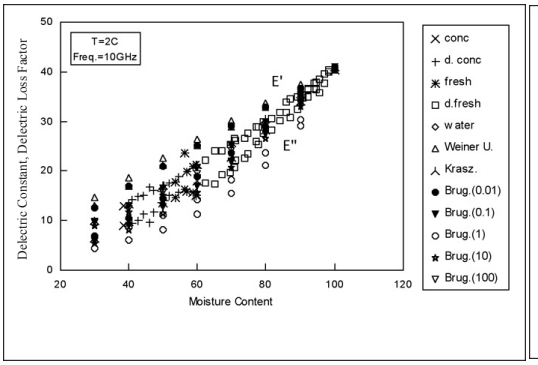

Fig. 2 (a)

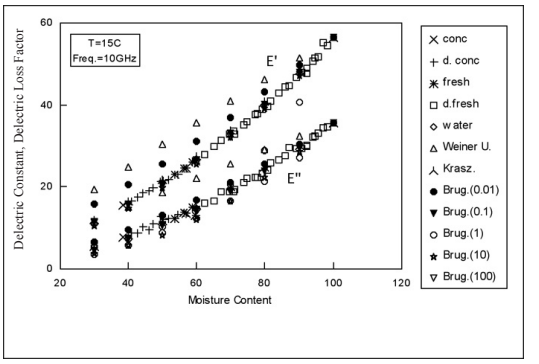

Fig. 2 (b)

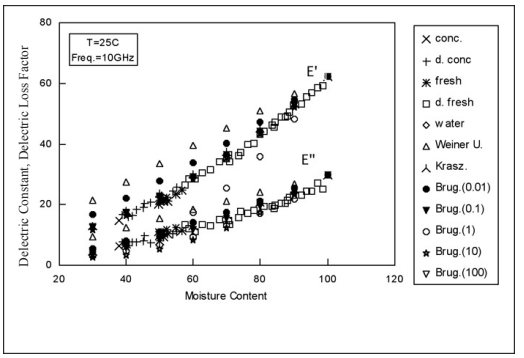

Fig. 2 (c)

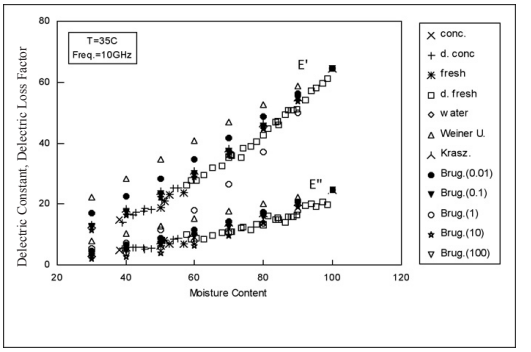

Fig. 2 (d)

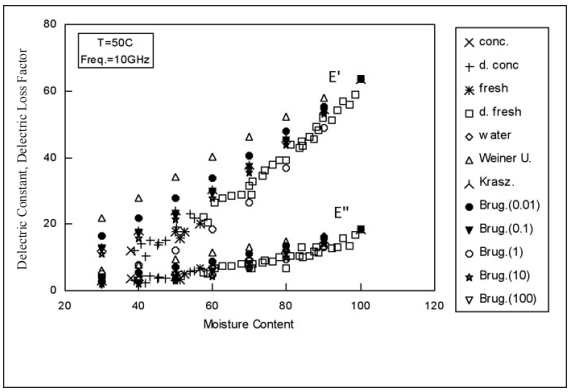

Fig. 2 (e)

Fig. 2(a-e): Experimental dielectric data for Hevea latex solution with the theoretical data calculated from the mixture equations, Weiner's upper, Bruggeman (a/b = 0.01, 0.1, 1, 10, 100) and Kraszewski at 10 GHz and 2, 15, 25, 35 and 50°C, respectively

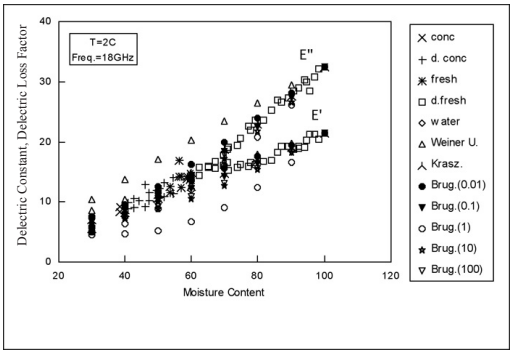

Fig. 3 (a)

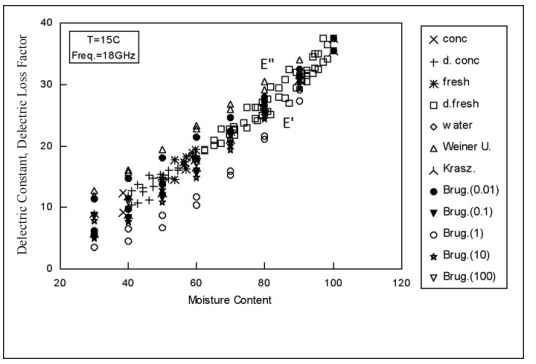

Fig. 3 (b)

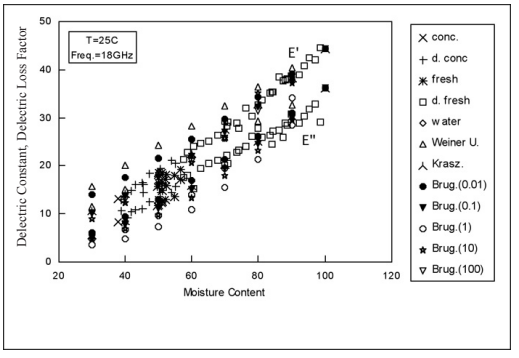

Fig. 3 (c)

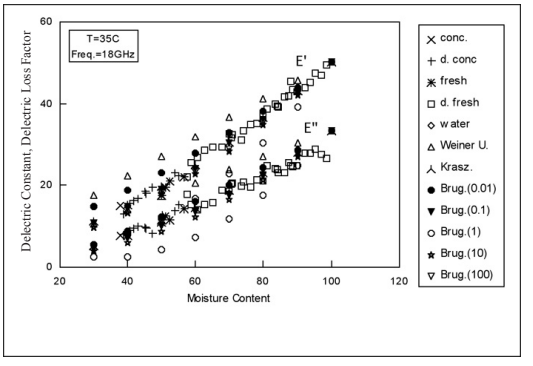

Fig. 3 (d)

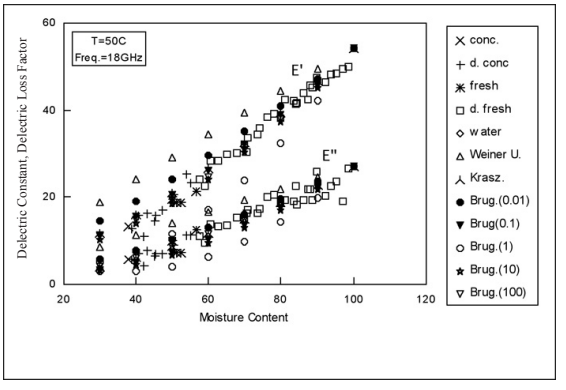

Fig. 3(e)

Fig. 3(a-e): Experimental dielectric data for Hevea latex solution with the theoretical data calculated from the mixture equations, Weiner's upper, Bruggeman (a/b = 0.01, 0.1, 1, 10, 100) and Kraszewski at 18 GHz and 2, 15, 25, 35 and 50°C, respectively

TABLE 1(a)
Complex permittivities of Hevea rubber latex at 2°C with the values estimated using the calculation from the mixed models ($\gamma w / \gamma r$ = 1.08) at 2.6 GHz

Moisture Content, % (Wet basis)	Fitted Experimental data		Calculation by mixed equations with ε_w= 80.61-j22.31 and ε_r=2.83-j0.09															
			Bruggeman										Kraszewski		Weiner's			
			a/b = 0.01		*a/b* = 0.1		*a/b* = 1		*a/b* = 10		*a/b* = 100				Upper bound		Lower bound	
	ε'	ε''	ε'	ε''	ε'	ε''	ε'	ε''	ε'	ε''	ε'	ε''	ε'	ε''	ε'	ε''	ε'	ε''
30	17.6	5.4	20.0	6.3	15.0	2.3	5.9	2.5	13.9	1.5	15.6	2.4	16.0	3.3	27.4	7.1	4.1	0.1
40	23.3	7.6	26.8	8.5.	21.3	3.9	9.6	2.6	19.7	1.5	21.8	3.6	22.5	5.1	35.4	9.4	4.7	0.2
50	30.0	9.8	34.2	10.8	28.3	5.8	15.2	2.9	27.0	2.3	28.2	5.4	30.0	7.2	43.2	11.6	5.7	0.2
60	37.9	12.1	42.3	13.0	36.5	8.2	21.9	4.3	35.4	4.2	36.5	7.8	38.4	9.6	50.9	13.8	7.0	0.3
70	46.8	14.5	51.3	15.1	45.9	11.0	31.4	6.7	44.1	7.2	45.7	10.7	47.7	12.4	58.5	16.0	9.2	0.5
80	56.9	17.0	60.1	17.3	56.8	14.2	44.6	10.3	56.0	11.2	56.1	14.1	57.9	15.4	66.0	18.1	13.2	0.8
90	68.0	19.5	70.2	19.4	68.4	17.8	61.3	14.9	67.0	16.2	67.2	18.2	68.9	18.7	73.4	20.2	22.9	2.1

TABLE 1(b)
Complex permittivities of Hevea rubber latex at 15°C with the values estimated using the calculation from the mixed models ($\gamma w / \gamma r$= 1.07) at 2.6 GHz

Moisture Content, % (Wet basis)	Fitted Experimental data		Calculation by mixed equations with ε_w = 79.29-j13.42 and ε_r = 2.81-j0.2															
			Bruggeman										Kraszewski		Weiner's			
			a/b = 0.01		*a/b* = 0.1		*a/b* = 1		*a/b* = 10		*a/b* = 100				Upper bound		Lower bound	
	ε'	ε''	ε'	ε''	ε'	ε''	ε'	ε''	ε'	ε''	ε'	ε''	ε'	ε''	ε'	ε''	ε'	ε''
30	17.1	4.3	19.9	3.7	14.4	1.9	7.2	1.6	13.4	1.0	15.2	1.5	15.6	2.2	26.9	4.4	4.0	0.3
40	22.8	6.1	26.8	4.6.	20.7	2.3	10.7	1.6	18.8	1.1	20.9	1.9	22.0	3.3	34.7	5.7	4.7	0.3
50	29.5	7.8	34.1	5.7	27.7	3.1	14.4	2.1	25.6	1.2	27.6	2.7	29.3	4.5	42.3	7.0	5.6	0.4
60	37.3	9.3	42.0	7.0	35.8	4.2	21.4	3.0	33.6	2.0	35.6	3.9	37.6	6.0	49.9	8.3	6.9	0.5
70	46.1	10.7	50.2	8.4	45.0	5.8	31.1	4.4	43.4	3.5	44.7	5.4	46.8	7.6	57.4	9.6	9.0	0.7
80	56.0	11.8	59.2	9.9	55.5	7.8	43.4	6.2	54.6	5.8	55.0	7.3	56.8	9.4	64.8	10.9	12.9	1.1
90	66.9	12.8	68.9	11.6	67.1	10.3	60.2	8.5	65.8	8.8	67.4	9.5	67.6	11.3	72.1	12.2	22.3	2.1

TABLE 1(c)

Complex permittivities of Hevea rubber latex at 25°C with the values estimated using the calculation from the mixed models ($\gamma w / \gamma r$ = 1.07) at 2.6 GHz

Moisture Content, % (Wet basis)	Fitted Experimental data		Calculation by mixed equations with ε_w = 76.75-9.71 and ε_r=2.9-j0.08															
			Bruggeman										Kraszewski		Weiner's			
			a/b = 0.01		*a/b* =0.1		*a/b* = 1		*a/b* = 10		*a/b* = 100				Upper bound		Lower bound	
	ε'	ε''	ε'	ε''	ε'	ε''	ε'	ε''	ε'	ε''	ε'	ε''	ε'	ε''	ε'	ε''	ε'	ε''
30	15.2	4.6	19.6	2.7	14.2	1.0	7.3	1.4	13.2	1.1	14.9	0.9	15.4	1.5	26.1	3.1	4.2	0.1
40	21.3	5.7	26.1	3.7	20.2	1.3	10.4	1.6	18.5	1.5	20.4	1.1	21.6	2.3	33.6	4.1	4.8	0.1
50	28.3	6.8	33.1	4.6	27.1	1.9	15.0	2.1	24.9	2.1	26.9	1.6	28.6	3.2	41.1	5.1	5.8	0.2
60	36.1	7.7	40.6	5.6	35.0	2.8	21.4	2.9	32.4	3.0	34.6	2.5	36.6	4.2	58.4	6.0	7.1	0.2
70	44.8	8.5	48.6	6.6	43.9	3.9	30.4	4.1	41.4	4.1	43.4	3.6	45.5	5.4	55.6	7.0	9.3	0.3
80	54.3	9.1	57.3	7.6	53.9	5.4	42.3	5.7	51.9	5.5	53.3	5.1	55.1	6.7	62.8	7.9	13.2	0.5
90	64.6	9.6	66.7	8.7	65.0	7.1	57.8	7.6	63.7	7.1	64.6	6.9	65.6	8.2	69.8	8.8	22.6	1.2

TABLE 1(d)

Complex permittivities of Hevea rubber latex at 35°C with the values estimated using the calculation from the mixed models ($\gamma w / \gamma r$ = 1.07) at 2.6 GHz

Moisture Content, % (Wet basis)	Fitted Experimental data		Calculation by mixed equations with ε_w = 73.86-j7.35 and ε_r =2.79-j0.06															
			Bruggeman										Kraszewski		Weiner's			
			a/b = 0.01		*a/b* =0.1		*a/b* = 1		*a/b* = 10		*a/b* = 100				Upper bound		Lower bound	
	ε'	ε''	ε'	ε''	ε'	ε''	ε'	ε''	ε'	ε''	ε'	ε''	ε'	ε''	ε'	ε''	ε'	ε''
30	13.4	4.4	18.8	1.7	13.6	1.0	6.9	1.0	12.5	1.2	14.3	0.6	14.8	1.1	25.1	2.4	4.2	0.1
40	19.2	5.4	25.2	2.5.	19.4	1.0	10.0	1.0	17.8	1.3	19.6	0.6	20.7	1.7	32.4	3.1	4.8	0.1
50	25.9	6.2	31.9	3.3	26.1	1.3	14.4	1.3	23.8	1.5	25.9	0.9	27.6	2.4	39.5	3.8	5.8	0.2
60	33.4	6.9	39.1	4.2	33.7	1.8	20.7	1.9	31.4	2.0	33.2	1.5	35.2	3.2	46.6	4.6	7.1	0.2
70	41.9	7.3	46.9	5.0	42.2	2.6	29.4	2.9	39.8	2.7	41.7	2.4	43.8	4.1	53.5	5.3	9.3	0.3
80	51.2	7.5	55.2	5.8	51.9	2.7	40.7	4.2	50.0	3.7	51.2	3.6	53.0	5.1	60.4	6.0	13.2	0.5
90	61.5	7.6	64.2	6.6	62.5	5.1	55.6	5.8	61.3	5.0	62.0	5.0	63.1	6.2	67.2	6.7	22.6	1.2

TABLE 1 (c)

Complex permittivities of Hevea rubber latex at 50°C with the values estimated using the calculation from the mixed models (γ_w / γ_r = 1.06) at 2.6 Ghz.

Moisture Content, % (Wet basis)	Fitted Experimental data		Calculation by mixed equations with ε_w= 69.3-j5.23 and ε_r=2.73-j0.07															
			Bruggeman										Kraszewski		Weiner's			
			a/b = 0.01		*a/b* = 0.1		*a/b* = 1		*a/b* = 10		*a/b* = 100				Upper bound		Lower bound	
	ε'	ε''	ε'	ε''	ε'	ε''	ε'	ε''	ε'	ε''	ε'	ε''	ε'	ε''	ε'	ε''	ε'	ε''
30	8.4	6.3	17.7	0.8	12.9	0.5	6.8	0.7	12.0	1.1	13.4	0.5	14.0	0.8	23.5	1.7	3.9	0.1
40	14.6	10.3	23.6	1.0.	18.3	0.5	9.7	0.8	16.6	1.5	18.4	0.5	19.5	1.3	30.3	2.2	4.5	0.1
50	21.5	14.5	29.9	1.4	24.5	0.6	13.8	1.0	22.4	1.9	24.3	0.8	25.9	1.7	37.0	2.7	5.4	0.1
60	29.1	19.2	36.7	1.9	31.6	0.9	19.7	1.4	29.2	2.3	31.0	1.2	33.0	2.3	43.6	3.2	6.7	0.2
70	37.5	24.2	44.1	2.5	39.6	1.5	27.6	1.9	37.4	2.8	39.0	1.8	41.0	2.9	50.1	3.7	8.6	0.3
80	46.6	29.6	51.8	3.2	48.7	2.3	38.7	2.5	46.7	3.4	47.8	2.5	49.7	3.6	56.6	4.2	12.3	0.4
90	56.5	35.3	60.3	4.1	58.6	3.3	52.6	3.3	57.3	3.9	58.3	3.4	59.2	4.4	63.0	4.7	20.9	0.8

TABLE 2(a)

Complex permittivities of Hevea rubber latex at 2°C with the values estimated using the calculation from the mixed models ($\gamma_w / \gamma_r = 1.08$) at 10 GHz

Moisture Content, % (Wet basis)	Fitted Experimental data		Calculation by mixed equations with ε_w= 41.0-j40.4 and ε_r =2.6-j0.29															
			Bruggeman										Kraszewski		Weiner's			
			a/b = 0.01		*a/b* =0.1		*a/b* = 1		*a/b* = 10		*a/b* = 100				Upper bound		Lower bound	
	ε'	ε''	ε'	ε''	ε'	ε''	ε'	ε''	ε'	ε''	ε'	ε''	ε'	ε''	ε'	ε''	ε'	ε''
30	10.5	7.6	12.6	6.9	9.8	5.9	6.6	4.3	9.0	5.5	9.6	5.9	10.1	6.5	14.7	13.0	3.7	0.5
40	13.7	9.7	16.9	10.5.	13.0	9.0	8.6	6.0	11.8	8.1	12.3	9.0	13.4	9.7	18.7	17.1	4.3	0.6
50	17.2	12.7	21.0	14.5	16.6	12.7	11.0	8.2	15.1	11.5	15.7	12.7	17.2	13.6	22.5	21.1	5.2	0.7
60	21.1	16.6	25.1	18.8	20.7	17.0	14.2	11.3	19.1	15.7	19.6	17.0	21.3	18.0	26.3	25.1	6.4	1.0
70	25.5	21.3	29.0	23.6	25.1	21.9	18.3	15.5	23.6	20.7	24.1	21.9	25.7	22.8	30.1	29.0	8.3	1.5
80	30.3	26.9	32.9	28.8	30.0	27.5	23.6	21.2	28.7	26.5	29.1	27.3	30.5	28.2	33.8	32.8	11.7	2.6
90	35.4	33.4	36.7	34.3	35.2	33.6	30.4	29.1	34.4	33.1	34.8	33.4	35.6	34.1	37.4	36.6	19.4	6.2

TABLE 2(b)

Complex permittivities of Hevea rubber latex at 15°C with the values estimated using the calculation from mixed models (γ_w / γ_r= 1.07) at 10 GHz

Moisture Content, % (Wet basis)	Fitted Experimental data		Calculation by mixed equations with ε_w= 56.55-j35.78 and ε_r =2.45-j0.3															
			Bruggeman										Kraszewski		Weiner's			
			a/b = 0.01		*a/b* =0.1		*a/b* = 1		*a/b* = 10		*a/b* = 100				Upper bound		Lower bound	
	ε'	ε''	ε'	ε''	ε'	ε''	ε'	ε''	ε'	ε''	ε'	ε''	ε'	ε''	ε'	ε''	ε'	ε''
30	12.7	6.4	15.8	6.5	11.4	4.5	5.2	3.4	10.6	3.9	11.6	4.9	12.0	5.5	19.5	11.5	3.5	0.5
40	16.5	8.6	20.6	9.6.	15.8	7.2	7.4	5.7	14.8	5.7	15.5	7.6	16.5	8.4	25.0	15.1	4.1	0.5
50	21.1	11.5	25.7	13.1	20.9	10.4	10.4	8.7	19.8	8.4	20.3	10.8	21.7	11.8	30.4	18.6	4.9	0.7
60	26.5	15.0	31.1	16.9	26.7	14.3	14.6	12.3	25.6	12.1	25.8	14.7	27.6	15.7	35.8	22.2	6.0	0.9
70	32.7	19.2	36.9	21.1	33.1	18.8	20.5	16.6	32.1	16.7	32.3	19.0	34.0	20.0	41.1	25.6	7.9	1.3
80	39.7	24.1	43.1	25.6	40.2	23.9	28.9	21.5	39.3	22.2	39.5	24.0	41.0	24.8	46.3	29.1	11.2	2.0
90	47.5	29.6	49.7	30.4	48.0	29.6	40.7	27.0	47.3	28.7	47.6	29.5	48.5	30.1	51.5	32.4	19.2	4.6

TABLE 2(c)
Complex permittivities of Hevea rubber latex at 25°C with the values estimated using the calculation from the mixed models ($\gamma_w/\gamma_r = 1.07$) at 10 GHz

Moisture Content, % (Wet basis)	Fitted Experimental data		Calculation by mixed equations with ε_w = 76.75-9.71 and ε_r =2.9-j0.08															
			Bruggeman										Kraszewski		Weiner's			
			a/b = 0.01		*a/b* =0.1		*a/b* = 1		*a/b* = 10		*a/b* = 100				Upper bound		Lower bound	
	ε'	ε''	ε'	ε''	ε'	ε''	ε'	ε''	ε'	ε''	ε'	ε''	ε'	ε''	ε'	ε''	ε'	ε''
30	11.9	6.2	16.9	5.3	12.5	3.4	5.4	3.1	11.7	2.6	12.6	3.9	13.1	4.6	21.4	9.5	3.8	0.3
40	16.3	7.6	22.1	7.9	17.3	5.7	7.2	4.5	16.5	3.5	17.0	6.0	18.1	6.9	27.5	12.5	4.5	0.4
50	21.6	9.6	27.8	10.8	22.9	8.4	11.2	6.7	22.1	5.4	22.4	8.6	23.9	9.7	33.5	15.5	5.3	0.5
60	27.8	12.1	33.9	14.0	29.2	11.7	17.3	9.4	28.4	8.3	28.6	11.7	30.3	13.0	39.4	18.4	6.6	0.7
70	34.9	15.2	40.3	17.5	36.3	15.4	25.5	12.9	35.6	12.3	35.7	15.3	37.4	16.6	45.3	21.3	8.6	0.9
80	42.9	18.7	47.2	21.2	44.2	19.7	35.7	17.0	43.5	17.4	43.7	19.4	45.1	20.6	51.0	24.1	12.2	1.6
90	51.8	22.7	54.5	25.3	52.9	24.4	48.1	21.8	52.2	23.4	52.6	24.1	53.4	25.0	56.7	26.9	20.7	3.7

TABLE 2(d)
Complex permittivities of Hevea rubber latex at 35°C with the values estimated using the calculation from the mixed models ($\gamma_w/\gamma_r = 1.07$) at 10 GHz

Moisture Content, % (Wet basis)	Fitted Experimental data		Calculation by mixed equations with ε_w = 64.5-j24.6 and ε_r =2.63-j0.27															
			Bruggeman										Kraszewski		Weiner's			
			a/b = 0.01		*a/b* =0.1		*a/b* = 1		*a/b* = 10		*a/b* = 100				Upper bound		Lower bound	
	ε'	ε''	ε'	ε''	ε'	ε''	ε'	ε''	ε'	ε''	ε'	ε''	ε'	ε''	ε'	ε''	ε'	ε''
30	11.2	5.1	17.0	4.7	12.6	2.8	5.4	2.8	11.7	2.1	12.8	3.2	13.3	3.9	22.1	7.9	3.8	0.4
40	15.5	5.6	22.5	6.7	17.6	4.5	7.4	4.0	16.6	2.6	17.4	4.9	18.5	5.9	28.4	10.4	4.4	0.5
50	20.9	6.8	28.4	8.9	23.4	6.7	11.6	5.6	22.3	4.0	22.9	7.1	24.4	8.2	34.6	12.8	5.2	0.6
60	27.3	8.5	34.8	11.5	30.0	9.3	17.9	7.8	28.9	6.4	29.4	9.6	31.1	10.9	40.7	15.3	6.5	0.8
70	34.7	10.9	41.6	14.3	37.4	12.5	26.4	10.6	36.4	9.7	36.8	12.6	38.5	13.8	46.8	17.6	8.4	1.1
80	43.2	13.9	48.8	17.4	45.6	16.0	37.0	13.8	44.7	14.0	45.1	16.0	46.5	17.1	52.8	20.0	11.9	1.7
90	52.6	17.5	56.4	20.8	54.6	20.1	49.8	17.6	53.9	19.1	54.4	19.8	55.2	20.7	58.7	22.3	20.4	3.6

TABLE 2(e)

Complex permittivities of Hevea rubber latex at 50°C with the values estimated using the calculation from the mixed models ($\gamma_w / \gamma_r = 1.06$) at 10 GHz

Moisture Content, % (Wet basis)	Fitted Experimental data		Calculation by mixed equations with ε_w= 63.79-j18.27 and ε_r =2.61-j0.2															
			Bruggeman										Kraszewski		Weiner's			
			a/b = 0.01		*a/b* = 0.1		*a/b* = 1		*a/b* = 10		*a/b* = 100				Upper bound		Lower bound	
	ε'	ε''	ε'	ε''	ε'	ε''	ε'	ε''	ε'	ε''	ε'	ε''	ε'	ε''	ε'	ε''	ε'	ε''
30	8.1	3.4	16.4	4.0	12.4	1.6	5.2	2.8	11.1	2.0	12.6	1.8	13.0	2.9	21.7	5.8	3.7	0.3
40	12.2	3.7	21.8	5.3.	17.4	2.4	7.6	2.9	15.8	2.0	17.2	3.0	18.1	4.3	27.9	7.7	4.3	0.4
50	17.5	4.5	27.7	6.9	23.2	3.7	12.0	3.5	21.4	2.8	22.6	4.6	24.0	6.0	34.1	9.5	5.2	0.4
60	24.0	5.8	34.0	8.8	29.8	5.6	18.3	4.7	28.0	4.4	29.0	6.5	30.6	8.0	40.2	11.3	6.4	0.6
70	31.6	7.7	40.7	11.0	37.1	8.0	26.6	6.7	35.4	6.8	36.3	8.8	37.9	10.2	46.2	13.1	8.3	0.8
80	40.4	10.0	47.8	13.4	45.2	11.0	36.8	9.5	43.8	10.0	44.5	11.5	45.9	12.7	52.1	14.8	11.7	1.2
90	50.3	12.8	55.4	16.1	54.0	14.5	49.0	13.0	53.2	13.9	53.7	14.5	54.5	15.4	58.0	16.6	20.0	2.6

TABLE 3(a)

Complex permittivities of Hevea rubber latex at 2°C with the values estimated using the calculation from the mixed models ($\gamma_w / \gamma_r = 1.08$) at 18 GHz

Moisture Content, % (Wet basis)	Fitted Experimental data		Calculation by mixed equations with ε_w = 21.51-j32.59 and ε_r =2.47-j0.18															
			Bruggeman										Kraszewski		Weiner's			
			a/b = 0.01		*a/b* = 0.1		*a/b* = 1		*a/b* = 10		*a/b* = 100				Upper bound		Lower bound	
	ε'	ε''	ε'	ε''	ε'	ε''	ε'	ε''	ε'	ε''	ε'	ε''	ε'	ε''	ε'	ε''	ε'	ε''
30	7.9	6.1	7.5	5.9	6.9	5.3	5.1	4.6	6.4	4.9	6.6	5.1	7.0	5.5	8.5	10.4	3.5	0.3
40	9.7	8.6	9.6	9.2	8.5	7.9	5.1	6.4	7.4	7.2	7.7	7.6	8.7	8.2	10.4	13.7	4.1	0.4
50	11.6	11.6	11.6	12.6	10.3	11.0	5.2	8.9	8.8	10.1	9.2	10.6	10.6	11.3	12.4	17.0	4.9	0.6
60	13.4	14.9	13.6	16.2	12.2	14.5	6.7	12.1	10.6	13.4	11.0	14.1	12.6	14.8	14.2	20.2	6.0	0.9
70	15.3	18.7	15.6	20.0	14.2	18.4	9.1	16.1	12.8	17.3	13.1	18.0	14.7	18.7	16.1	23.4	7.8	1.5
80	17.2	23.0	17.5	24.0	16.5	22.7	12.4	20.7	15.4	21.7	15.5	22.4	16.9	23.0	17.9	26.5	10.7	2.8
90	19.1	27.7	19.4	28.1	18.9	27.4	16.6	26.1	18.3	26.7	18.3	27.2	19.1	27.6	19.7	29.6	16.6	7.3

TABLE 3(b)

Complex permittivities of Hevea rubber latex at 15°C with the values estimated using the calculation from the mixed models ($\gamma_w / \gamma_r = 1.07$) at 18 GHz

Moisture Content, % (Wet basis)	Fitted Experimental data		Calculation by mixed equations with ε_w = 35.45-j37.55 and ε_r =2.4 -j0.17															
			Bruggeman										Kraszewski		Weiner's			
			a/b = 0.01		*a/b* 0.1		*a/b* = 1		*a/b* = 10		*a/b* = 100				Upper bound		Lower bound	
	ε'	ε''	ε'	ε''	ε'	ε''	ε'	ε''	ε'	ε''	ε'	ε''	ε'	ε''	ε'	ε''	ε'	ε''
30	11.1	6.0	11.4	6.2	8.7	5.5	5.5	3.6	7.9	5.1	8.6	5.3	9.0	5.8	12.8	11.9	3.4	0.3
40	13.1	10.0	14.7	9.8.	11.4	8.4	6.6	4.5	10.1	7.6	10.9	8.1	11.9	8.9	16.2	15.7	4.0	0.4
50	15.5	14.1	18.1	13.7	14.5	11.8	8.7	6.7	12.9	10.9	13.7	11.6	15.1	12.5	19.5	19.5	4.8	0.5
60	18.4	18.4	21.4	17.9	17.9	15.9	11.8	10.3	16.2	14.8	17.0	15.6	18.6	16.5	22.8	23.2	5.9	0.7
70	21.8	12.9	24.7	22.4	21.7	20.4	15.9	15.3	20.1	19.5	20.8	20.2	22.4	21.1	26.0	26.9	7.7	1.1
80	25.7	27.6	27.9	27.3	25.9	25.6	21.1	21.6	24.5	24.9	25.2	25.4	26.5	26.1	29.2	30.5	10.8	2.1
90	30.0	32.4	31.1	32.5	30.4	31.3	27.2	29.2	29.5	31.0	30.0	31.1	30.8	31.6	32.3	34.0	17.9	5.5

TABLE 3(c)

Complex permittivities of Hevea rubber latex at 25°C with the values estimated using the calculation from the mixed models ($\gamma_w / \gamma_r = 1.07$) at 18 GHz

Moisture Content, % (Wet basis)	Fitted Experimental data		Calculation by mixed equations with ε_w = 44-j36.16 and ε_r=2.66-j0.16															
			Bruggeman										Kraszewski		Weiner's			
			a/b = 0.01		a/b =0.1		a/b = 1		a/b = 10		a/b = 100				Upper bound		Lower bound	
	ε'	ε''	ε'	ε''	ε'	ε''	ε'	ε''	ε'	ε''	ε'	ε''	ε'	ε''	ε'	ε''	ε'	ε''
30	9.9	5.9	14.1	6.1	10.2	5.0	4.9	3.5	9.0	4.7	9.9	5.2	10.6	5.6	15.8	11.5	3.8	0.3
40	13.7	9.7	17.7	9.4	13.7	7.8	6.6	4.8	12.4	6.8	13.0	7.9	14.2	8.5	20.0	15.1	4.4	0.4
50	18.0	13.6	21.5	13.0	17.7	11.1	9.7	7.3	16.3	9.7	16.6	11.2	18.2	11.9	24.2	18.8	5.3	0.5
60	22.6	17.5	25.5	17.0	22.1	15.0	13.9	10.8	20.7	13.5	20.9	15.1	22.7	15.9	28.4	22.3	6.5	0.7
70	27.6	21.4	29.8	21.3	26.9	19.4	19.4	15.5	25.7	18.0	25.8	19.5	27.6	20.3	32.5	25.9	8.4	1.0
80	33.0	25.3	34.3	26.0	32.2	24.5	26.2	21.4	35.2	23.3	31.3	24.5	32.8	25.1	36.5	29.3	11.9	1.9
90	38.8	29.2	39.1	31.0	38.0	30.1	34.1	28.4	37.3	29.5	37.5	30.0	38.4	30.4	40.5	32.8	19.8	5.0

TABLE 3(d)

Complex permittivities of Hevea rubber latex at 35°C with the values estimated using the calculation from the mixed models (γ_w / γ_r = 1.07) at 18 GHz

Moisture Content, % (Wet basis)	Fitted Experimental data		Calculation by mixed equations with ε_w= 50.33-j33.43 and ε_r=2.58-j0.2															
			Bruggeman										Kraszewski		Weiner's			
			a/b = 0.01		a/b =0.1		a/b = 1		a/b = 10		a/b = 100				Upper bound		Lower bound	
	ε'	ε''	ε'	ε''	ε'	ε''	ε'	ε''	ε'	ε''	ε'	ε''	ε'	ε''	ε'	ε''	ε'	ε''
30	10.2	5.2	14.9	5.6	10.8	4.6	5.4	2.5	9.8	4.1	10.8	4.7	11.3	5.2	17.6	10.6	3.7	0.3
40	15.0	8.5	18.8	8.9	14.9	7.0	7.9	2.6	13.4	6.0	14.2	7.2	15.3	7.8	22.5	14.0	4.3	0.4
50	20.1	11.9	23.2	12.4	19.2	10.0	11.7	4.2	17.7	8.8	18.4	10.2	20.0	11.0	27.3	17.4	5.1	0.5
60	25.5	15.3	27.9	16.1	24.2	13.6	16.7	7.2	22.8	12.2	23.4	13.8	25.1	14.6	32.0	20.7	6.3	0.7
70	31.3	18.8	32.9	20.1	30.3	17.7	23.0	11.7	28.5	16.5	29.0	17.9	30.7	18.7	36.7	23.9	8.2	1.0
80	37.3	22.4	38.3	24.3	36.1	22.4	30.5	17.6	35.0	21.4	35.4	22.5	36.8	23.2	41.3	27.1	11.6	1.8
90	43.6	26.0	44.1	28.8	42.8	27.6	39.2	25.0	42.1	27.2	42.4	27.6	43.3	28.1	45.8	30.3	19.5	4.4

TABLE 3(e)

Complex permittivities of Hevea rubber latex at 50°C with the values estimated using the calculation from the mixed models ($\gamma_w / \gamma_r = 1.06$) at 18 GHz

Moisture Content, % (Wet basis)	Fitted Experimental data		Calculation by mixed equations with ε_w = 54.37-j27.07 and ε_r =2.62-j0.16															
			Bruggeman										Kraszewski				Weiner's	
			a/b = 0.01		*a/b* =0.1		*a/b* = 1		*a/b* = 10		*a/b* = 100				Upper bound		Lower bound	
	ε'	ε''	ε'	ε''	ε'	ε''	ε'	ε''	ε'	ε''	ε'	ε''	ε'	ε''	ε'	ε''	ε'	ε''
30	6.7	1.8	14.5	5.8	11.3	3.3	5.0	3.1	10.2	3.1	11.1	4.0	11.8	4.1	18.8	8.6	3.7	0.3
40	13.0	5.4	19.2	7.8	15.6	5.1	7.5	3.0	14.0	4.6	14.8	6.1	16.1	6.3	24.0	11.3	4.3	0.3
50	19.5	9.0	24.2	10.2	20.6	7.4	11.5	4.1	18.7	6.8	19.3	8.6	24.0	21.1	29.2	14.0	5.2	0.4
60	26.0	12.4	29.5	13.0	26.1	10.2	17.0	6.3	24.1	9.6	24.7	11.5	26.7	11.8	34.4	16.7	6.4	0.6
70	32.6	15.7	35.1	16.1	32.2	13.6	23.9	9.7	30.4	13.0	30.9	14.7	32.8	15.1	39.5	19.3	8.3	0.8
80	39.2	18.9	41.0	19.7	39.0	17.6	32.4	14.2	37.5	17.1	37.9	18.3	39.5	18.7	44.5	21.9	11.7	1.2
90	45.9	22.0	47.3	23.6	46.3	22.1	42.3	20.0	45.3	21.9	45.7	22.3	46.7	22.7	49.5	24.5	19.6	3.5

Generally, the mixture models from Kraszewski and Bruggeman are suitable for predicting the dielectric properties of hevea latex for frequencies 2.6 to 18 GHz, moisture content of 30 to 98% and temperatures of 2 to 50°C.

CONCLUSION

Dielectric properties of natural rubber *Hevea brasiliensis* latex were measured at microwave frequencies from 0.2 to 20 GHz. The dielectric constant was found to increase with increasing moisture. The losses are governed by conductive losses for frequencies of up to 2.6 GHz and by dipolar losses for frequencies greater than 2.6 GHz. The conductive losses are due to the conducting phases which arise from the non-rubber constituents in hevea latex, while the dipolar losses are mainly governed by the orientation of the water molecules or dipoles. The biphase mixture model from Weiner, Kraszewski and Bruggeman (a/b = 0.1) are therefore suitable for predicting the dielectric properties of hevea latex. All the measured values lie within the Weiner's boundaries and are close to the upper limit of the Weiner's model. This suggests that the water molecules are loosely bound and they can be easily polarised.

ACKNOWLEDGEMENTS

This work was supported by Universiti Putra Malaysia (UPM) through a short term research grant (50205-93-14). The authors wish to thank the technical staff, En. Roslim Mohd. at the Applied Electromagnetic Laboratory, Department of Physics for his invaluable help. The authors would also like to thank the Rubber Research Institute of Malaysia and the University Research Park of UPM for supplying the latex.

REFERENCES

Boned, C. and Peyrelasse, J. (1983). Some comments on the complex permittivity of ellipsoids dispersed in continuum media. *Journal of Physics D: Appllied Physics, 16*, 1777-1784.

Bruggeman, D.A.G. (1935). Dielektrizitatskonstanten und Leitfahigkeiten Der Mischkorper aus Isotropen Substanzen. *Ann. Phys. Lpz, 24*(5), 636.

Chaloupka, H., Ostwald, O. and Schiek, B. (1980). Structure independent microwave moisture measurements. *Journal of Microwave Power, 15*(4), 221.

Chen, S.F. (1979). *Composition of Hevea Latex*. *Training Manual on Analytical Chemistry*. Kuala Lumpur: Rubber Research Institute of Malaysia.

Chin, H.C. (1979). *Methods for measuring the dry rubber content of field latex*. *Training Manual on Analytical Chemistry*. Kuala Lumpur: Rubber Research Institute of Malaysia.

Gorton, A.D.T. and Pendle, T.D. (1985). The use of electrical conductimetry in the examination of natural rubber lattices. *Natural Rubber Technology, 16*(3), 45-51.

Hassan, J., Khalid, K. and W.Yusoff, W.M.D. (1997). Microwave dielectric properties of hevea rubber latex in the temperature range of -30°C to 50°C. *Pertanika Journal of Science & Tech*nology, *5*(2), 179-190.

Hassan, J., Khalid, K. and W. Yusoff, W.M.D. (2003). Microwave measurement on the degree of binding of water in hevea rubber latex. *Journal of Rubber Research, 6*(2), 94-106.

Khalid, K. and W. Yusoff, W.M.D. (1992). Dielectric properties of natural rubber latex at frequencies from 200 MHz to 2500 MHz. *Journal of Naturtal Rubber Research, 7*(4), 281-289.

Khalid, K., Hassan, J. and W. Yusoff, W.M.D. (1994). Dielectric properties of hevea rubber latex at various moisture content. *Journal of Natural Rubber Research, 9*(3), 172-189.

Krazewski, A. (1974). Determination of the strength of water suspension using microwave technique. *Journal of Microwave Power, 9*, 295.

Kraszewski, A., Kulinski, S. and Matuszewski, M. (1976). Dielectric properties and a model of biphase water suspension at 9.4 GHz. *Journal of Appllied Physics, 47*, 1275-1277.

Kraszewski, A., Stuchly, M.A. and Stuchly, S.S. (1982). ANA calibration method for measurements of dielectric properties. *IEEE Trans., IM-32*, 385-387.

Suresh, N., Callaghan, J.C. and Creelman, A.E. (1967). Microwave measurement of the degree of water absorbed in soils. *Journal of Microwave Power, 2*(4), 129-137.

ISSN: 0128-7680
Pertanika J. Sci. & Technol. **18 (1)**: 139– 154 (2010)

Grid Base Classifier in Comparison to Nonparametric Methods in Multiclass Classification

M. R. Mohebpour*, Adznan B. J. and M. I. Saripan
Department of Computer and Communication System Engineering,
Faculty of Engineering, Universiti Putra Malaysia,
43400 UPM, Serdang, Selangor, Malaysia
**E-mail:m_mohebpour@yahoo.com*

ABSTRACT

In this paper, a new method known as Grid Base Classifier was proposed. This method carries the advantages of the two previous methods in order to improve the classification tasks. The problem with the current lazy algorithms is that they learn quickly, but classify very slowly. On the other hand, the eager algorithms classify quickly, but they learn very slowly. The two algorithms were compared, and the proposed algorithm was found to be able to both learn and classify quickly. The method was developed based on the grid structure which was done to create a powerful method for classification. In the current research, the new algorithm was tested and applied to the multiclass classification of two or more categories, which are important for handling problems related to practical classification. The new method was also compared with the Levenberg-Marquardt back-propagation neural network in the learning stage and the Condensed nearest neighbour in the generalization stage to examine the performance of the model. The results from the artificial and real-world data sets (from UCI Repository) showed that the new method could improve both the efficiency and accuracy of pattern classification.

Keywords: Grid, decision boundaries, pattern recognition, supervised, nonparametric, multiclass

INTRODUCTION

There are growing needs for developing both powerful and robust methods to model a pool of data. In many applications, useful models can be defined in terms of their generalization capabilities. Various applications in engineering, statistics, computer sciences, and health sciences are concerned with estimating good predictive models from available data. In such problems, the goal is to estimate a model from unknown data patterns, and use this knowledge to predict future trends.

In statistical pattern recognition, the goal is to classify samples accurately based on a set of descriptive predictor variables (features). The design of pattern recognition systems involves two major tasks, as shown in *Fig. 1*. The description task transforms data collected from the environment into features, i.e. any value which can be derived from and is representative of the data that are used in the classification task to arrive at identification (Ho and Basu, 2002 ; Duda *et al.,* 2001). The end result of the description task is a set of features, commonly known as a *feature vector,* which constitutes a representation of the data. The classification task uses a classifier to map a feature vector to a group. Hence, after the observed data from the patterns to be recognized have been expressed in the form of pattern points or measurement vectors in the pattern space, the researchers want the machine to decide to which pattern group these data belong to.

Received: 9 September 2008
Accepted: 7 August 2009
*Corresponding Author

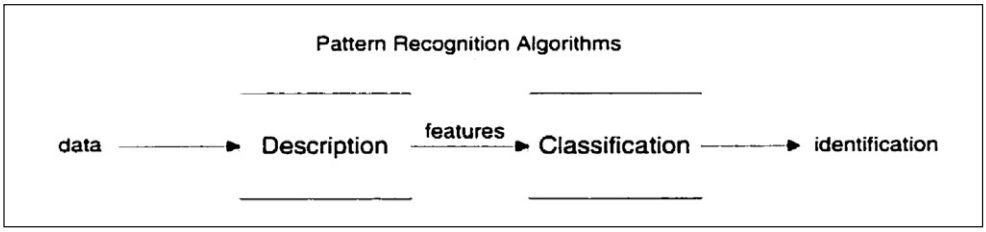

Fig. 1: Two separate tasks commonly used within pattern recognition systems

The two major approaches to building statistical pattern recognition systems are *parametric* and *non-parametric* methods (Duda *et al.,* 2001; Fukunaga, 1990). In the parametric methods, the forms of class-conditional distributions are assumed to be known and the unknown parameters of the distribution are estimated by maximum likelihood, maximum a posteriori, or Bayesian techniques based on a training set. Meanwhile, in the non-parametric methods, no global method is assumed for the class-conditional distributions; the class-conditional densities are therefore estimated in the regions of feature space determined by the training set (such as Parzen Windows and Nearest Neighbour). In other non-parametric methods, the forms of decision boundary are assumed to be known and their parameters are found as a solution to an optimization problem (such as Neural Network). The optimization criterion is, in general, composed of an error term (error on the training set) and regularization term (a smoothness constraint on the decision boundary). Then, the error rate on the training set serves as a good predictor of the error rate on the test set.

There are a large number of classifiers which have been presented in the literature; these include Nearest Neighbour, Parzen Window, Neural Networks, Decision Tree, etc. which are further categorized into two groups, namely *Eager* and *Lazy* methods. The eager classification uses training data to create a single-rule set during the training phase, and this particular rule set is used to classify all test instances. On the other hand, the lazy classification does not create a rule set during the training phase and the rule set generation is delayed until a test instance is given. Nevertheless, the choice between the eager and lazy algorithms is not always simple. Using a single-rule set to perform all the predictions, one may not take advantage of specific characteristics of a test instance. On the other hand, building a specific rule set for each test instance may require excessive computational efforts (Ho, 2004; Veloso and Meira, 2005).

Multiclass classifiers are important for handling classification problems with more than two categories. There are a lot of applications like handwritten recognition, object classification, speech recognition, bioinformatics, information retrieval, and text categorization which require multiclass classifier. Despite the well-known two-class classification problems, the multiclass classification problems are relatively less investigated. Many of the multiclass classifiers were designed by developing the existing binary class classifiers utilizing ‘one versus one’, or ‘one versus rest’ (Guobin and Murphey, 2007). The aim of this paper is to improve the efficiency and accuracy of training and generalization phases in the multiclass classification. To accomplish this goal, the study presents a method which, as compared to some previous methods, gives us a very efficient approach to modelling a multi-class pattern classification problem, decision modules, learning complexity, and system generalization.

Problem Definition

As a branch of artificial intelligence, pattern recognition has extensively been studied in computer science. The design of a complete pattern recognition system consists of multiple stages, which include: 1) data acquisition and pre-processing; 2) feature extraction and selection; 3) learning from examples; 4) testing and evaluation. These pre-processing step and feature extraction and selection are generally dependent very much on the specific application. In contrast, the statistical issues addressed by the classification step (learning and testing) are generally independent of the application.

This paper focuses on the last two stages, namely learning from examples and testing the classifier for evaluation (classification step). It is assumed that all tasks involving pre-processing (such as noise removal), as well as feature extraction and selection (such as dimension reduction) are applied to the dataset if they are required. Therefore, the system proposed in the present study would be given a dataset of labelled objects, whereby each object which is represented by a set of attributes belongs to one of a finite number of classes. The task is to find a rule which can be used to categorize an object into its right class, when only its attribute values are given. In relation to the fact that the classification steps are generally independent of the application, the virtual data made by random function in the MATLAB are generally used to cover various datasets with different complexities. Computer programs were also designed for the proposed classifier using the MATLAB programming tools to be applied on those virtual datasets and compared with other methods. The real datasets, such as the common problem XOR and dataset from UCI repository (Murphy and Aha, 1992), were also provided to test and evaluate the proposed classifier.

Among the current methods, some are efficient in the learning stage, but they are rather disorganized and time-consuming in the generalization stage as compared to the others which are rather time-consuming in the learning step but are effective in classification.

This study also proposed a new non-parametric classification method based on the grid structure, with the aim to improve the efficiency and accuracy of the training and generalization phases in the multiclass classification.

MATERIALS AND METHODS

In this section, a new pattern classification method called the Grid Base Classifier (GBC) based on the grid structure is proposed. Just like the eager method, the proposed model also uses training data to create a decision boundary during the training phase, but this procedure occurs in a very short time as compared to the current eager methods. In addition, predictions are performed using a decision boundary without excessive computational efforts, unlike the lazy method. Therefore, it is capable in both steps and radically improves the performance of the recognizer. Moreover, the GBC can be applied to the design of any kind of statistical recognizer and can be used in any pattern recognition application.

Grid-Based Classifier

The design of a pattern recognition system should consider two important aspects of the pattern recognition operation, namely “learning” and “generalization”. In general, the system proposed in this study should be able to learn and generalize well. There is an important trade-off between learning and generalization that arises quite generally.

In the same vein, the better the time complexity of an algorithm, the faster the algorithm will practically carry out the work. Apart from time complexity, its space complexity is also important. This is essentially the number of memory cells required by an algorithm. In addition, a good algorithm also keeps this number as small as possible.

In general, the lazy methods take a short time to learn because they do not use any training data to create a rule as a decision boundary (low time complexity). Nevertheless, they take a long time to classify new pattern because they may require excessive computational efforts (high time complexity), and it is normally necessary to keep all the training data in memory (high space complexity).

On the other hand, the eager methods require a long time to learn in order to obtain a decision boundary because of their time-consuming algorithms (high time complexity). However, after the learning stage, the training data can be omitted (low space complexity), and they can classify new pattern by simply using the decision boundary very quickly (low time complexity).

Therefore, the proposed method follows the advantages of both methods as described above. Using the simple algorithm illustrated below, this method can find a decision boundary without any misclassification in a short time for the learning phase (low time complexity). Thus, keeping the training data is no longer required (low space complexity), and the classification can be done much quickly, i.e. by simply comparing it to the decision boundary (low time complexity).

The following section describes how the proposed method can learn and classify the multiclass (e.g. 4-class) problem.

Learning

The basic classification rules partition $\mathbb{R}$ into some cells $A_1, A_2, ...$ and classifies in them in each cell according to the majority vote among the labels of the falling in the cell containing. Formally,

$$\phi_n(z) = \begin{cases} 1 & \text{if } \sum_{i=1}^{n} I\{Z_i \in A(z)\} I\{Y_i = 1\} > \sum_{i=1}^{n} I\{Z_i \in A(z)\} I\{Y_i = 0\} \\ 0 & \text{otherwise} \end{cases} \quad (1)$$

Where $A(z)$ denotes the cell containing z.

Furthermore, using the *grid based* idea, as described in the following section, partitioning $\mathbb{R}$ is done into cells containing one label. Thus, after the pre-processing stage of features extraction and selection, the training data are plotted using the Cartesian plane. After a grid is inserted into the space vector and divided into cells, each cell is then checked if it contains only one kind of data. Otherwise, the grid size must be decreased into smaller cells, and it will therefore be rechecked. Both the sizes of the grid are continuously decreased until a situation where only one kind of pattern remaining in each cell (see *Fig. 2*) is obtained.

When the size of the grid has been determined, the decision boundary is sought based on the cells, as shown in *Fig. 3*. After the decision boundary has been found, the training data are no longer required. Hence, they can be eliminated and the decision boundary can then be used as a decision function which separates the M pattern classes.

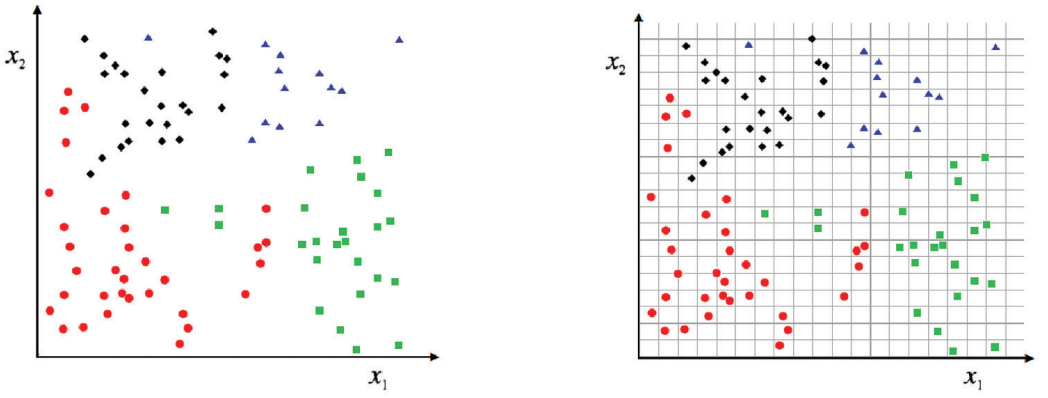

Fig. 2: (L) Multiclass features space and training data; (R) Desirable grid which guarantees that each cell contains only one kind of pattern

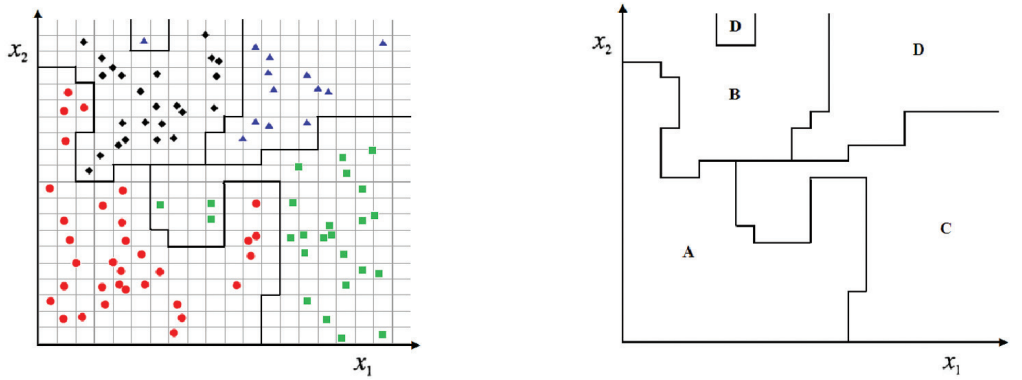

Fig. 3: (L) Finding the decision boundary based on boundary cells; (R) Eliminate the training data and keep the boundary cells

The above description is the main idea used to find the decision boundary in the method proposed in this study. There are various ways which can be used to find the grid size for this particular idea. Here, an optimal and practical way to create the appropriate grid used in the above algorithm is also proposed. Steps taken in obtaining the size of the grid are shown below:

To find α which is considered as the non-zero minimum of distances between the different patterns among the available classes and presents λ as the grid size, the following equation is used:

$$\alpha = \min \left\{ \left\| m_i - n_j \right\| ; m \neq n, m \in X, n \in Y, i, j = 1..K \right\} \quad (2)$$

where X, Y ∈ {Patterns Group]

Now, two different patterns with a minimum distance are determined; for instance, for *M* and *N,* λ is defined for the desirable grid size.

$$\lambda = \max\{\ |M_{x_1} - N_{x_2}|, |M_{x_2} - N_{x_2}|\ \}/2 \quad (3)$$

Finding the grid size using this method guarantees that different patterns are separately located in the different cells. A grid is basically of a double array, with all the points falling in one cell are stored in the same place. All the points will be stored in the same entry if a cell contains more than one point. The next step is to scan the grid cells in order to find the decision boundaries and store them for the generalization phase. At this stage, the training data can be eliminated and the memory can be released.

Generalization

Another important issue related to the conventional pattern recognition design methods which must be addressed is generalization - the performance of the designed recognizer on the data outside the training set, i.e. correctly classify the test patterns it has never seen before, so that the new pattern (novel) belongs to which class can be recognized using the decision boundary which can be found in the previous stage. As the decision boundaries are stored in a hash table, testing the novel can be done using any kind of hash function very quickly. In comparison to the generalization step in the lazy algorithms (which involves checking the relation by all training data or some part of the data that are sensitive) to find a good estimation for the novel, this method seems to be very effective in computational and time complexity.

RESULTS AND DISCUSSION

The strength of a given classification technique is measured by the number of different distinguishable categories (Sarlashkar, Bodruzzaman and Malkani, 1998). It is also measured by computational complexity, execution time of algorithms, and the number of patterns which can be classified correctly despite any distortion (Lu, 1996; McGuire *et al.,* 2001). The experiments have been carried out to evaluate the performance of the proposed method. In this section, the new method was tested on thirty artificial datasets with different numbers of classes and complexities. Then the new method are described and compared with the neural network. The two methods were also tested on ten datasets out of the thirty so as to examine the performance of each classification method when they are trained on different training sets. To demonstrate the competitiveness of the proposed model, the GBC model was tested on the real-world data set which is publicly available from University of California at Irvine (UCI) data repository (Murphy and Aha, 1992).

Experimental Results for the Artificial Datasets

In the experiment for the multiclass problems, two-dimensional data samples were employed including the multiclass samples. Classes A, B, C, and D were generated by random functions. The procedure for the classification was repeated 10 times for all 30 data sets. Some of the results are shown in *Fig. 4*.

When testing a hypothesis on the artificial data is involved, there is a need to test the proposed method on at least 30 data sets. Thus, the above data sets with different numbers of data points were generated randomly using the random function in MATLAB (*randint()*) for this purpose and these data points were divided into 2, 3, and 4 groups, with different levels of complexity to test the proposed method in various conditions. The number of data points, the number of classes, and the distribution of data points change to cover all possible complicated conditions as we move from the first figure to the last one. The results show that no matter how complicated the distribution of the input training samples is, and no matter how many classes and how many samples there are in each class, the proposed model gives a promising performance.

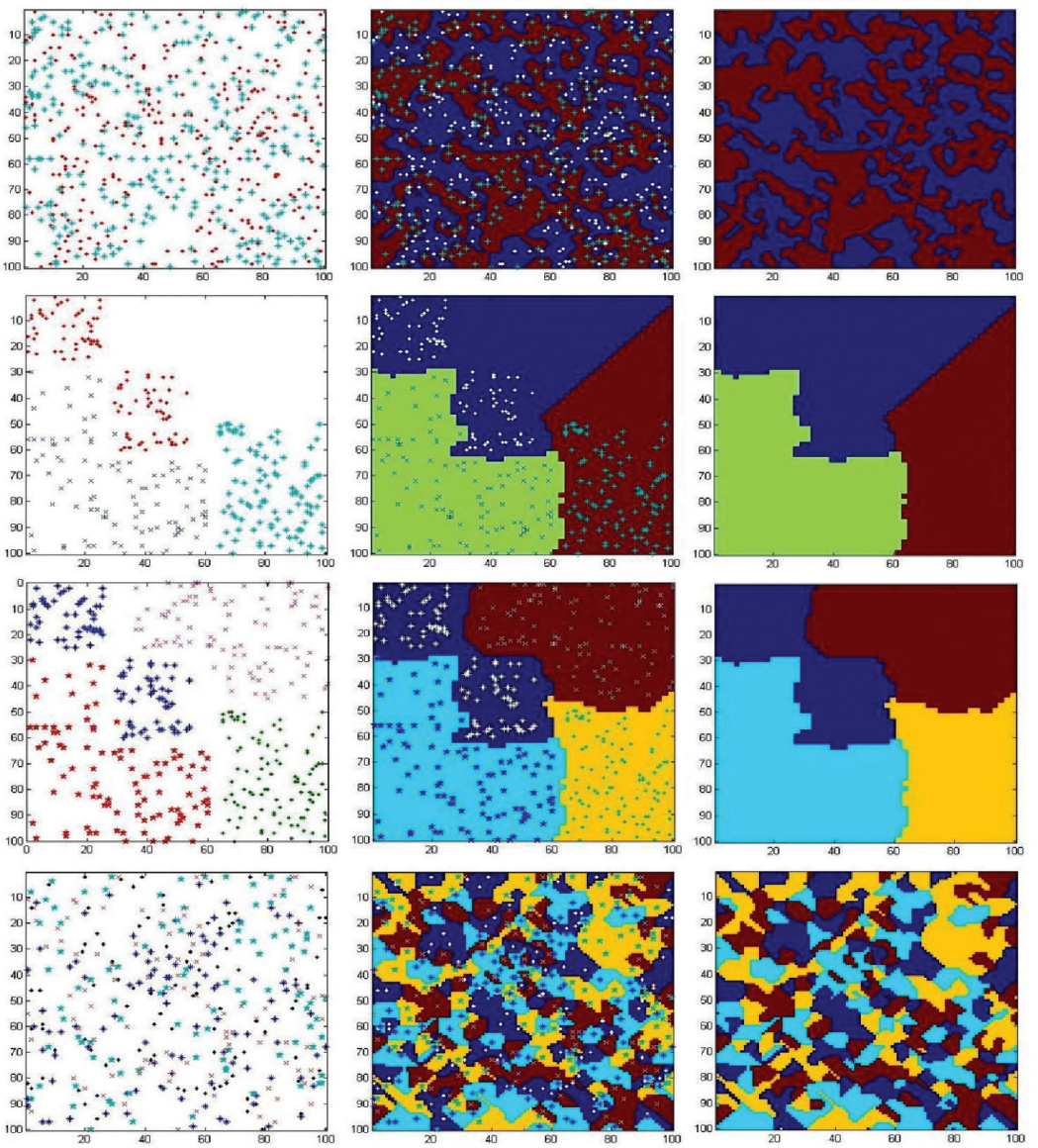

Fig. 4: Data sets (Left) applying the training procedure (Middle) training result (Right)

TABLE 1
Accuracy (%) and training time (s) for finding decision boundary with 2, 3, and 4 classes of artificial data

Artificial data set	No. of classes	Accuracy (%)	Training time (s)
1	2	100	0.28
2	2	100	0.28
3	2	100	0.28
4	2	100	0.28
5	2	100	0.28
6	2	100	0.28
7	2	100	0.28
8	2	100	0.28
9	3	100	0.30
10	3	100	0.30
11	4	100	0.31
12	4	100	0.31
13	4	100	0.31
14	4	100	0.31
15	4	100	0.31
16	4	100	0.31
17	4	100	0.31
18	4	100	0.31
19	4	100	0.31
20	4	100	0.31
21	4	100	0.31
22	4	100	0.31
23	4	100	0.31
24	4	100	0.31
25	4	100	0.31
26	4	100	0.31
27	4	100	0.31
28	4	100	0.31
29	4	100	0.31
30	4	100	0.31

As can be seen in all cases, the GBC method found the decision boundary without any misclassification in a very short time, and therefore, the performance is as impressive as it is expected to be. The accurate results obtained on the test data for the learning step was 100% (or without any misclassification), and the best result for the training time are reported in Table 1. The classification time is almost constant and it is very small for all the cases because a simple hash function is applied on a hash table.

As can be seen from the results, the proposed method has a high performance in the training stage, whereby it can detect any single datum correctly (without any misclassification) and it is also very efficient in terms of training and classification speed. Thus, the training time slightly increases in the case where the data set has more classes, although the amount of data samples is already fixed.

A Comparison between the Lazy and Eager Methods

A comparison was carried out with the neural network (for learning time and accuracy) and the nearest neighbour classifier (for generalization time) on 10 of the above data sets to examine the performance of the new method, and the results are also reported. The evaluation of the generalization accuracy for the real-world example is given in the subsequent section.

Backpropagation neural network in the learning phase

One of the powerful networks for the multiclass classifier is the *backpropagation network*. The backpropagation can train the multilayer feed-forward networks with differentiable transfer functions so as to perform function approximation, pattern association, and pattern classification (Ruck *et al.,* 1990) (note that other types of network can be trained as well, although the multilayer network is most commonly used). The term 'backpropagation' refers to the process by which derivatives of network error, with respect to the weights and biases of the netword, can be computed. This process can be used with a number of different optimization strategies. Input vectors and the corresponding target vectors are used to train a network so that it can be used to approximate a function, associate input vectors with specific output vectors, or classify input vectors in an appropriate way as defined by the user. Networks with biases, a sigmoid layer, and a linear output layer are capable of approximating any function with a finite number of discontinuities. Among the training functions, the Levenberg-Marquardt algorithm is the fastest training algorithm for the networks of moderate size; hence, the most extensively used is the Levenberg-Marquardt backpropagation algorithm, partly because it is much faster than any other algorithms. Therefore, the following code is used to create such a network:

net = newff (minmax(p), [5,1], {'tansig','purelin'}, 'trainlm');

The network was applied on the datasets. Using trial and false method during training, some network parameters (such as the number of hidden layers and performance goal) could be determined to achieve a proper performance. The performance goal parameter (indicating how many errors would be acceptable) determines when the training should be stopped. The training is ended when the performance function drops below the goal. If this parameter is set too high, the algorithm may become unstable. On the contrary, the algorithm will take a longer time to converge if this parameter is too small. Therefore, it is not practical to determine the optimal setting for the performance goal prior to any training, and for this reason, this parameter is set with the trial and false method to achieve an optimal performance. The performance also degrades as the performance goal parameter increases. After adjusting the parameter, the network was applied 10 times for each data set and the best results are presented in Table 2.

TABLE 2
Training time (s) and performance goal of the grid-based classifier and neural network

Data Set	Grid Base Classifier (GBC)		Neural Network (NN)	
	Training time (s)	Performance goal	Training time (s)	Performance goal
3	0.28	0	0.52	0.05
6	0.28	0	0.85	0.25
7	0.28	0	0.90	0.25
9	0.30	0	0.91	0.05
11	0.31	0	1.00	0.10
12	0.31	0	0.98	0.10
15	0.31	0	1.06	0.20
16	0.31	0	1.12	0.70
22	0.31	0	1.56	0.90
27	0.31	0	2.45	1.20

The results show when the new method was used, the training time seemed to slightly increase due to the increasing number of classes, but it was found to remain the same because of the rising level of complexity of input data. On the other hand, when the inputs were trained by the neural network method, the training time seemed to grow considerably because of the complicated input data and the rise in the number of classes, even when the effects of increasing the mean square error were ignored.

Condensed nearest neighbour in the generalization phase

The best-known of the lazy methods is the *condensed nearest neighbour,* which is a greedy algorithm that aims to minimize training error and complexity measured by the size of the stored subset (Hart, 1968; Devijier and Kittler, 1980). Both the time and space complexities of the non-parametric methods are proportional to the size of the training set, and condensing methods have been proposed to decrease the number of stored instances without degrading the performance.

To examine the performance of the proposed model in the generalization phase, it was compared with the condensed nearest neighbour as a candidate of the lazy methods. The fact that the evaluation of the test accuracy seems to be meaningless in the absence of the real-world dataset, checking the real-world problems is discussed in the next section. In this study, only the testing time evaluation of the above artificial datasets was taken into consideration. Table 3 shows the comparison in the speed of both the algorithms. For this purpose, the test vector containing 100 unknown samples was applied to the classifiers.

TABLE 3
Testing time (s) for the grid-based classifier and condensed nearest neighbour

Data set	Grid Base Classifier (GBC)	Condensed Nearest Neighbour
	Testing time (s)	Testing time (s)
3	0.002	1.42
6	0.002	1.57
7	0.002	1.8
9	0.002	1.61
11	0.002	1.69
12	0.002	1.67
15	0.002	1.71
16	0.002	1.75
22	0.002	2.3
27	0.002	2.92

As indicated earlier, there will be a grid after the learning stage, which each cell assigned to one of the classes within this grid. This grid or just a part of it is then kept (the boundary cells) in the hash table. Thus, a function is required in order to categorize the new sample into its right class when only its attribute values are given. In a quick procedure, this function takes these values as an argument and determines this sample to place it in a cell from the grid. Here, the proposed function is very simple and the values are simply divided by the grid size to determine the specific cell, so that the class label of the sample comes from the class label of this particular cell. Hence, the classification complexity for the proposed method is *O (1)* in which there is a single computation for the test pattern which is the same as the procedure of the eager methods. In contrast, the time complexity for the condensed nearest neighbour is *O(nN),* which includes computation of distances from the test pattern to all the condensed training patterns, in which each distance computation is *O(n)*. This is the reasonable cause of the considerable difference between the results presented in Table 3.

Experimental Results for the Real-world Datasets

In the following section, some real data sets are used to examine the classification performance of the new method.

The XOR problem

To find the non-linearly separable problems, going into complicated situations is not required. The well-known *Exclusive OR (XOR)* Boolean function is a typical example of such a problem. The Boolean functions (AND, OR, XOR) can be interpreted as the classification tasks. Indeed, based on the values of the input binary data $[x_1, x_2, ..., x_n]^T$, the output is either 0 or 1, and x is classified into one of the two classes, $A(1)$ or $B(0)$.

Fig. 5 (left) shows the position of the classes in space. It is apparent from this figure that no single straight line exists separates the two classes. Therefore, the major concern is to tackle the XOR problem in order to evaluate the new method. *Fig. 5* (right) shows how the GBC method finds decision boundary based on this problem.

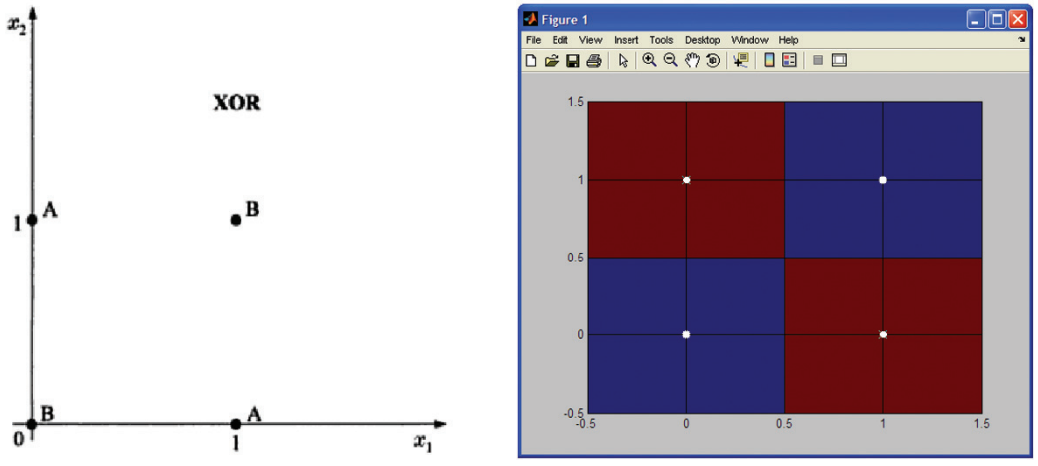

Fig. 5: (L) Classes A and B for the XOR problem; (R) Decision boundary by GBC for the XOR problem

The Haberman dataset

In this section, the experimental results of the proposed method on the *Haberman's Survival* data set from the UCI Machine Learning Repository are presented and discussed. The dataset contains cases from a study conducted at the University of Chicago's Billings Hospital on the survival of patients who had undergone surgery for breast cancer.

The experiments carried out in this study were conducted using the ten-fold cross-validation technique, which is a common technique used to evaluate the performance of a pattern classification algorithm [2]. The researchers conducted the ten-fold cross-validation in the following ways: each data set was randomly partitioned into ten groups, with each group having approximately the same number of points. Then, the GBC (and NN) model was run ten times, and one different group of data was held out to be used as the test set each time, whereas the other nine groups were used as the training set. The reported results are the average values for the ten runs.

The learning procedure used to find the decision boundary for the Haberman dataset is shown in *Fig. 6.*

The numerical results for the GBC, in comparison with BNN (backpropagation neural network), are given in the following tables. In Table 4, the results for learning time and accuracy are listed, while the time and accuracy for the testing phase are given in Table 5.

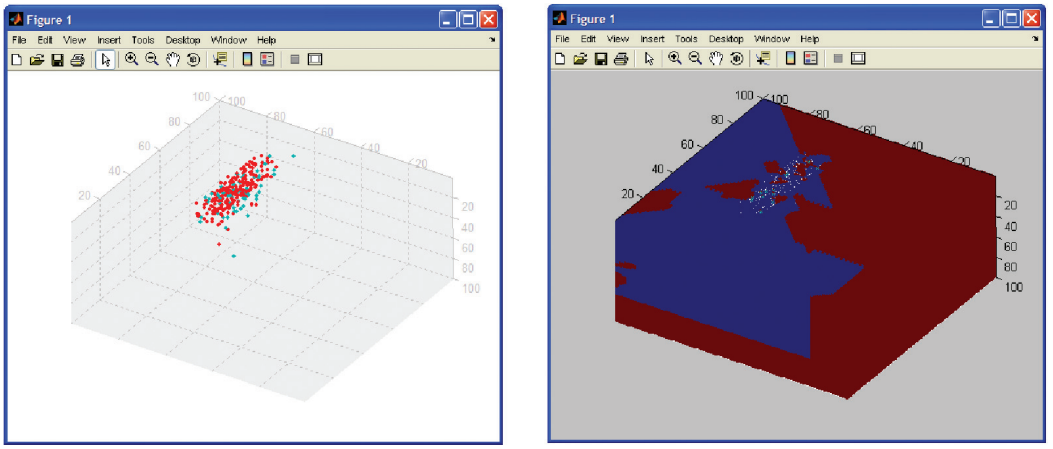

Fig. 6: The Haberman dataset is plotted in 3-dimensional space and decision boundary made by the GBC

TABLE 4
Training time (s) and Training accuracy (%) of the Grid-Based Classifier and Neural Network

	Grid Base Classifier (GBC)		Neural Network (NN)	
	Training time (s)	Accuracy (%)	Training time (s)	Accuracy (%)
1	0.51	98	1.31	96.5
2	0.51	98	1.40	96.3
3	0.51	98.4	1.15	97
4	0.51	98.7	1.52	96
5	0.51	98	1.51	98
6	0.51	98	1.45	98.5
7	0.51	98.4	1.06	96.7
8	0.51	98.4	1.12	97
9	0.51	98	1.56	98.5
10	0.51	98.4	1.45	97.5
Average	0.51	98.2	1.35	97.25

As can be seen from Table 4, the performance of these two models is comparable. From this test, it can therefore be concluded that the GBC model completes the training stage much faster than the neural network, and this was expected for the proposed model. In addition, the accuracy of the training part was also found to be better for the proposed model than the neural network, but it is not as perfect (100%) as the results derived from the artificial datasets, as there is 1.8% error which was caused by some overlapping data points. In this experiment, the data set is composed of 306 data points. Among these data points, which are categorized into two different classes, there are 6 repeated data points within the both classes (overlapped). When these elements are assigned

to one of the classes, user will face an error on the other class and this is the cause of this insolvable error.

As can be seen in Table 5, the results for both methods are almost similar in terms of the overall generalization time and accuracy comparison. From this comparison, as expected, the results are in good agreement and the proposed method carries the advantages of the eager methods in the generalization phase.

TABLE 5
Testing time (ms) and Testing error (%) of the Grid-Based Classifier and Neural Network using the ten-fold cross-validation technique

	Grid Base Classifier (GBC)		Neural Network (NN)	
	Testing time (ms)	Test error (%)	Testing time (ms)	Test error (%)
1	0.6	10	0.8	31
2	0.6	30	0.7	25
3	0.6	35	0.7	29.3
4	0.6	39.9	0.6	32
5	0.6	23.6	0.7	25
6	0.6	36.2	0.8	30.7
7	0.6	30	0.7	35
8	0.6	31.7	0.7	30
9	0.6	24	0.7	30.5
10	0.6	15.3	0.8	26
Average	0.6	27.6	0.7	29.4

However, the results for the testing accuracy are not so impressive because of the overlapping data and the noisy nature of this data set. On the contrary, it is highly comparable with the results previously reported for the other methods. Table 6 reveals the performance of the statistical method known as the *Support Vector Machine (SVM)* and some ensemble methods (multi classifier methods) such as *Bacing*, *Bagging*, *Adaboost* and *Arcing* on the Haberman data set (Zhang and Street, 2008). The error estimates listed are over ten-fold cross-validation runs.

TABLE 6
The best generalization performance reported for the Haberman dataset

	SVM	Bagging	Adaboost	Arcing	Bacing
Haberman	28.10	27.77	25.81	25.89	25.50

In comparison with these results, the proposed method has been shown to give a better performance as compared to the other statistical methods such as the neural network and support vector machine; this is what the researchers were looking for the experiments conducted in this

study. In addition, the proposed model also shows highly acceptable results in terms of testing accuracy as compared to the ensemble methods.

CONCLUSION

In the learning phase, the model was given a set of training samples, in which each sample was represented by a set of attributes. It is better to perform compression in that by fitting a rule to the data, and the explanation obtained is that it is simpler than the data, as it requires less memory for storing and less computation for processing. Therefore, the task is to find a decision boundary which can be used to categorize a sample into its right class when only its attribute values are given. The results indicate that the GBC model can find the decision boundary in a very short time as compared to the other statistical methods, and that the accuracy of this phase was 100%, except in the case of the overlapping data which have caused insignificant error. Based on the results, it is therefore concluded that the outcomes of this stage are independent (or are not determined by) of the size of the data sets, the number of classes and the distribution of data.

In the generalization phase, there is always a certain non-zero probability that the decision for a new sample is wrong when a decision boundary is made from a finite number of the training samples. Therefore, it is desirable to determine the percentage of the error when making a decision for the new instances. The results obtained for the real-world data set show that the proposed model has achieved a better performance in time and accuracy as compared to the other statistical models.

REFERENCES

Devijver, P. A. and Kittler, J. (1980). On the edited nearest neighbor rule. *Proceeding of the fifth International Conference on Pattern Recognition* (pp. 72-88).

Duda, R.O., Hart, P.E. and Stork, D.G. (2001). *Pattern Classification* (2nd ed.). San Diego: Wiley-Interscience.

Fukunaga, K. (1990). *Introduction to Statistical Pattern Recognition*. Academic Press, Inc.

Guobin, O. and Murphey, Y.L. (2007). Multi-class pattern classification using neural networks. *Pattern Recognition, 40*, 4-18.

Hart, P. E. (1968). The condensed nearest neighbor rule. *IEEE Transaction on Information Theory*, *14*(5), 515-516.

Ho, T.K. (2004). Promises and challenges in automatic pattern recognition. *ASP Conference Series*, *314*, 239.

Ho, T.K. and Basu, M. (2002). Complexity measures of supervised classification Problems. *IEEE Transaction on Pattern Analysis and Machine Intelligence, 24*(3), 289-300.

Lu, Y. (1996). Knowledge integration in a multiple classifier system. *Applied Intelligence*, *6*(2),75-86.

McGuire, P. and Eleuterio, G. M. T. D. (2001). Eigenpaxels and a neural network approach to image classification. *IEEE Transaction on Neural Network*, *12*(3), 625-635.

Murphy, P. M. and Aha, D. W. (1992). *UCI repository of machine learning databases*. Retrieved from http://www.ics.usi.edu/~mlearn/MLRepository.html.

Ruck, D. W., Rogers, S. K., Kabirisky, M., Oxley, M. E. and Sutter, B. W. (1990). The multilayer perceptron as an approximation to a bayes optimal discriminant function. *IEEE Transaction on Neural Network, 1*(4), 296-298.

Sarlashkar, M. N., Bodruzzaman, M. and Malkani, M. J. (1998). Feature extraction using wavelet transform for neural network based image classification. *Proceeding of the Thirtieth Southeastern Symposium on System Theory* (pp. 412-416).

Veloso, J. and Meira, W. (2005). Eager, lazy and hybrid algorithms for multi-criteria associative classification. In *Proceeding of the Data Mining Algorithms Workshop,* Uberlandia, MG.

Zhang, Y. and Street, W. N. (2008). Bagging with adaptive costs. *IEEE Transaction on Knowledge and Data Engineering*, *20*(5).

ISSN: 0128-7680
Pertanika J. Sci. & Technol. **18 (1)**: 155 – 166 (2010)

Assessment of Using Tunneling and Trenchless Technology for Constricting Twin Box Culvert

Thamer Ahmad Mohammad[1*], Mohd. Razali Abdul Kadir[1], Megat Johari Megat Mohd. Noor[1] and Ahmad Husaini Sulaiman[2]
[1]Department of Civil Engineering, Faculty of Engineering, Universiti Putra Malaysia, 43400 UPM, Serdang, Selangor, Malaysia
[2]Department of Irrigation and Drainage, 50626 Kuala Lumpur, Malaysia
[*]E-mail: thamer@eng.upm.edu.my

ABSTRACT

Part of the Seremban flood mitigation project in the state of Negeri Sembilan, Malaysia is to mitigate the flood at Jalan Rasah. The mitigation is planned to be implemented in packages. Package I and Package II of River Anak Air Rasah are parts of the project work. In these packages, wider and deeper concrete sections for the river are constructed. The existing undersized culverts were replaced by bigger reinforced concrete box culverts. The size of the box culverts was based on 100-years average reoccurrence interval (ARI). One of these culverts intersected with a rail line connecting Singapore and Malaysia. Trenchless jacking technique was used to lay the box culvert. The total length of the box culvert jacked under the railway line is 33 m, whereas the total width of the twin box culvert is 7.8 m with a total height of 3 m. This was the first time that the trenchless jacking techniques were used for the urban flood mitigation purpose in Malaysia, and it is mainly used to minimise traffic disruption. This study reports the success of using jacking technique in the development of the flood mitigation program of DID in Negeri Sembilan. Among other things, it explains significant performance of the technique under local conditions and experiences gained towards the advancement of tunnelling and trenchless technology.

Keywords: Jacking technique, twin box culvert, construction, flood mitigation

ABBREVIATION

ARI : Average Reoccurrence Interval
BS : British Standards
DID : Department of Irrigation an Drainage
LRT : Light Transit Rail
NATM : New Austrian Tunnelling Method

INTRODUCTION

Tunnelling and trenchless technique is not new in the construction sector. It has been used for decades and many projects around the world have successfully been constructed using this technique. Recently, new technologies which employ trenchless technique are used and this has increased the experiences in this field. Several reasons behind the use of the tunnelling technique in construction are shortage of land availability, intersection with existing strategic traffic routes and water ways, as well as the existence of historical buildings at the project site.

Received: 13 October 2008
Accepted: 26 November 2009
[*]Corresponding Author

The tunnelling and trenchless technique is used in construction worldwide and recently, this technique was used to construct lines 2 and 3 of the Athens Metro in Greece (Leto and Welburm, 1999). In Egypt, it was used to construct the El-Azhar road tunnel in Cairo (Welburn and De Nettancourt, 2002). In United Kingdom, the method was used in the construction of Euro Tunnel and also the large wastewater sewers like the Southern Water's Coastal Clean-up Programme (Peacock and Setterfield, 1999).

Meanwhile, a new tunnelling technique, known as New Austrian Tunnelling Method (NATM) was used in the construction of London Bridge Station on Jubilee Line and this technique was used recently in Germany, Austria and some other developed countries. Several tunnels, with diameters ranging between 5.35 m to 13.67 m and length from 45 m to 50 m, were constructed in the Jubilee Line Project (Field *et al*., 2000).

Denmark and Sweden are linked with a road and a rail line which were opened in July, 2000. The length of the trenchless immersed tunnel is 3510 m, comprising of 20 elements and each element is longitudinally divided into eight segments. The overall section of the immersed tunnel is 41.7 m wide and 8.5 m high. The cross section was designed in such a way that it would achieve the required uplift with 10.6 factor of safety. The design was done according to Euro Code 2. Table 1 shows the loading conditions considered in the design of the immersed tunnel. The jacking technique was used to move 55000 tonnes of tunnel elements. The construction period was exactly 5 years (Busby and Marshall, 2000).

TABLE 1

Loads considered in the design of immersed tunnel

Permanent loads	Imposed loads	Accidental loads
Structural concrete	Road traffic load	Ice
Ballast concrete	Train load	Explosion
Pavement construction	Water level variations	Road vehicle collision
Track form	Temperature	Train collision
M&E equipments	----------	Sunken ship
Hydraulic pressure	----------	Falling anchor
Earth pressure	----------	Earthquake
Differential settlement	----------	Flooding

Source: Mainwaring *et al.*, 2000

An immersed tunnel, with a total length of 375 m, was constructed across Medway River in United Kingdom to link roads between the two sides of the river. The cross-section of the Medway tunnel comprised a twin cell reinforced concrete structure and each cell is required to accommodate two lanes of traffic and emergency walkways. *Fig. 1* shows the dimensions of the immersed tunnel cross-section. The cross-section was designed based on the British Standards (BS5400, BS 8110, and BS 8007). The loadings considered were the deadweight of the structure, hydrostatic pressure, fill material, traffic loadings, temperature differences and accidental loadings which include seismic loadings, vehicle collision, as well as ship and anchor impact on the tunnel roof. A technique called cut and cover was used in the immersion of the tunnel and a lifting barge was used in the implementation, as shown in *Fig. 2*. The construction period was 3 years for the project life of 120 years (Mainwaring *et al*., 2000). The present study summarises the technique and problems faced

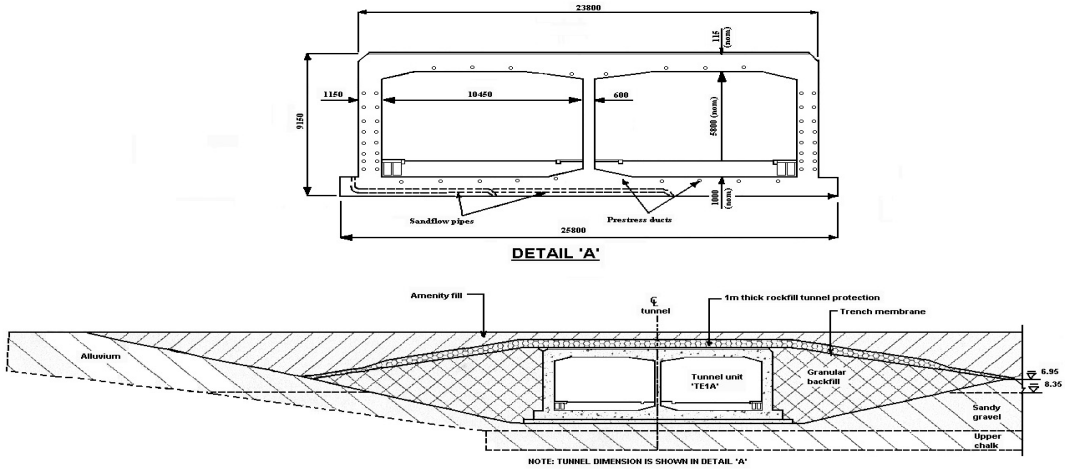

Fig. 1: Cross section of medway tunnel in trench (Mainwaring et al., 2000)

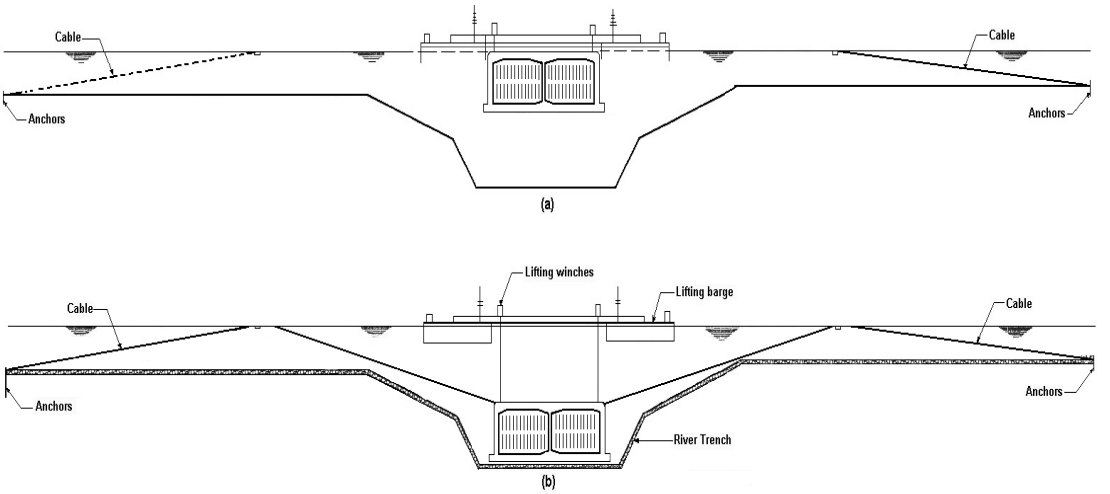

Fig. 2: Cross method used for immersion of medway tunnel elements in trench (Mainwaring et al., 2000)

in the construction of jacking of the twin cells reinforced concrete box culvert across an existing railway line at the intersection of River Anak Air Rasah, Seremban, Negeri Sembilan, Malaysia and the main railway line. Two local contractors conducted the jacking work, with Sebatik Sdn. Bhd. as the main contractor and Drill-Con Sdn. Bhd. as the sub-contractor. This work was done for the Department of Irrigation and Drainage, Negeri Sembilan Darul Khusus. The jacking of the twin cells box culvert was part of the contract which included construction and completion of Precast/Cast in situ rectangular reinforce concrete drain with drop structure, a twin box culvert under the existing railway line and other related work on River Anak Air Rasah, Seremban from Chainage 1939.0 m to Chainage 2260.0 m. The trenchless and tunnelling technique used in the construction of the twin box culvert at the crossing site between River Anak Air Rasah and railway

line was the first work in the flood mitigation projects. In Malaysia, other governmental authorities like the Public Works Department, Railway Authorities, and private developers (such as Putra LRT Sdn. Bhd.) have been employing the tunnelling techniques quite often in their projects.

THE CASE STUDY

Under the Seremban flood mitigation project, an improvement work for River Anak Air Rasah was completed and this improvement included channelling and changing the watercourse of this natural monsoon drain. The improvement work were planned to be conducted in three phases. In Phases I and II, a total length of 1500 m from the River Anak Air Rasah watercourse has completely been improved, while Phase III is not started yet. The actual cost for the construction involved in Phase I and Phase II was RM 4.6 millions. In Phase I, the watercourse of River Anak Air Rasah, between chainage 2029 m and chainage 2079 m, was intersected with a railway line *(Fig. 3)*. At this crossing, a 50 m length twin box culvert (3.65 m x 2.2 m) was constructed. Plan and elevation of the culvert are shown in *Fig. 4*. About 33 m of the total length of the twin box culvert was jacked underneath the railway line using the tunnelling and trenchless technique to avoid disturbances on the railway traffic. Meanwhile, around 17 m of the twin box culvert was located away from the railway line, so it was constructed using the normal method of construction. The jacked portion of the twin box culvert represented 66% of its total constructed length. The tunnelling and jacking work was done using the local expertise.

METHODOLOGY

The jacked reinforced concrete twin box culvert was designed using the British standards, BS 5400: Part 2, BS 5400: Part 4 and BS 8110. The internal dimensions of the single cell of the twin box culvert are 2.2 m x 3.65 m. Meanwhile, the structural analysis of the twin box culvert was idealized as two-dimensional frame and was analysed by direct stiffness method using computer software. The soil overburden, concrete self weight, imposed vertical loads such as the weight of ballast, track, sleepers and rail axle loads, as well as the horizontal earth water pressures, and the jacking loads were considered for a number of load combinations to establish the most critical design. The concrete mix was designed and manufactured in a plant and then taken to the site by a transit mixer and a strict quality control was assured on the grade of the concrete. Grade 40 was used in order to allow for the high concrete stress during the jacking operation. *Fig. 5* shows the details of the reinforcement used in the cross-section of the jacked twin box culvert.

It is important to give an idea about the method used in construction and jacking of the twin box culvert, at the site of the intersection between River Anak Air Rasah and the main railway line in Seremban town. The construction technique comprises of jacking pits, thrust bed, front and rear shields, receiving pit, precast reinforced concrete twin box culvert and jacking mechanism. A brief description of the stages is given below:

Jacking Pit

A jacking pit which houses the thrust bed for the casting and jacking of the precast concrete box segments was constructed. The dimensions of the pit, as measured on plan, were 21.0 m x 15.5 m, with the excavation depth of about 6 m. The pit was formed by installing 9 to 12 m deep sheet-piles and braced by steel strut and wailer system *(Plate 1)*.

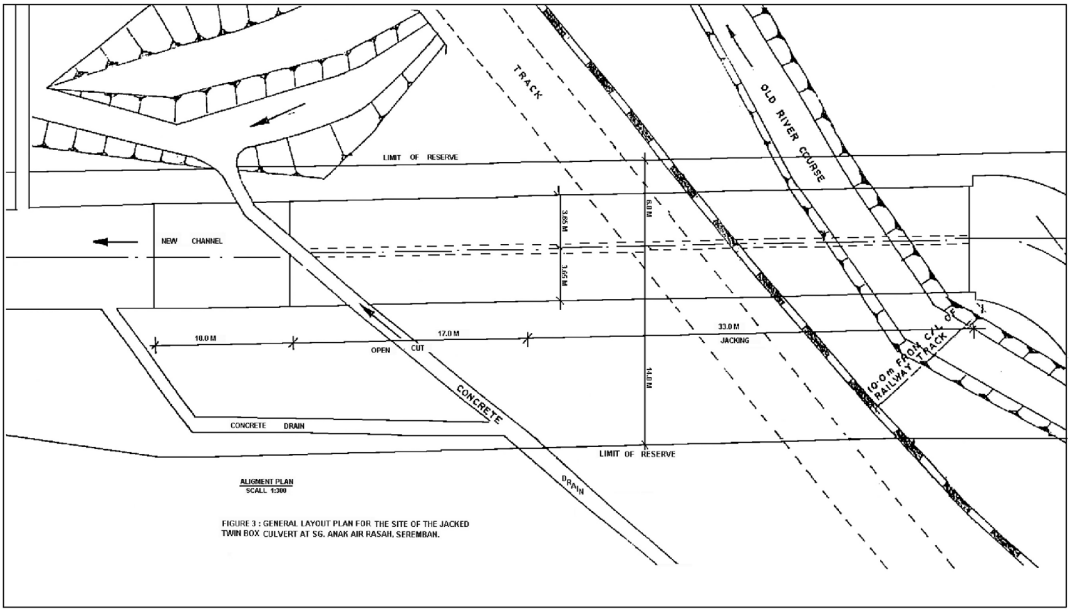

Fig. 3: General layout plan for the site of the jacked twin box culvert

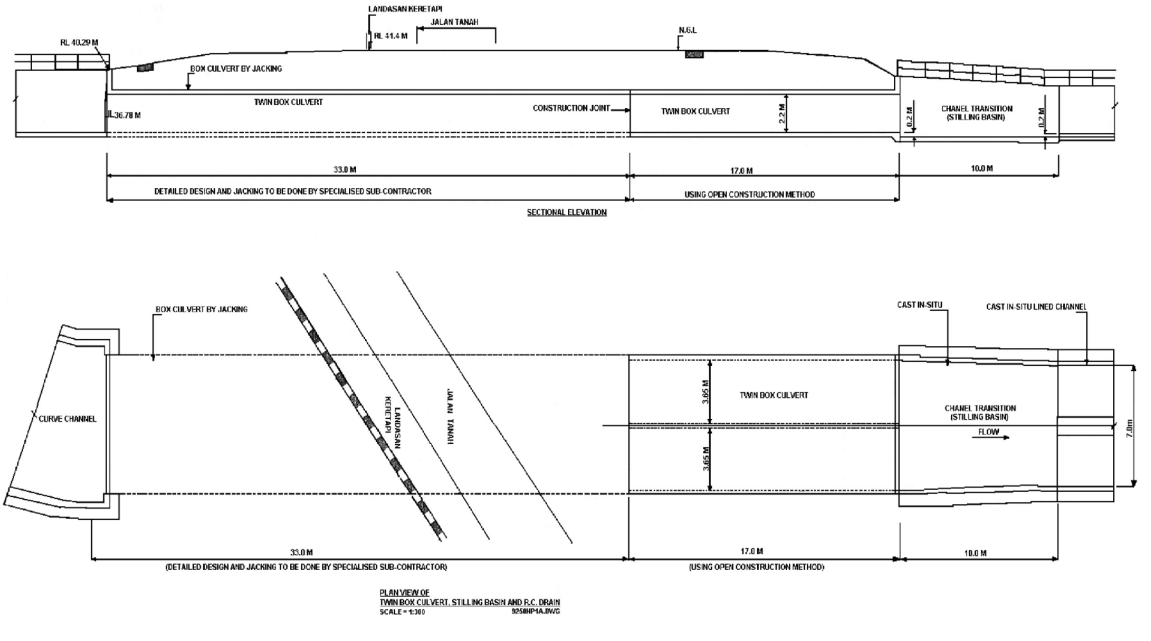

Fig. 4: Longitudinal section of the jacked twin box culvert

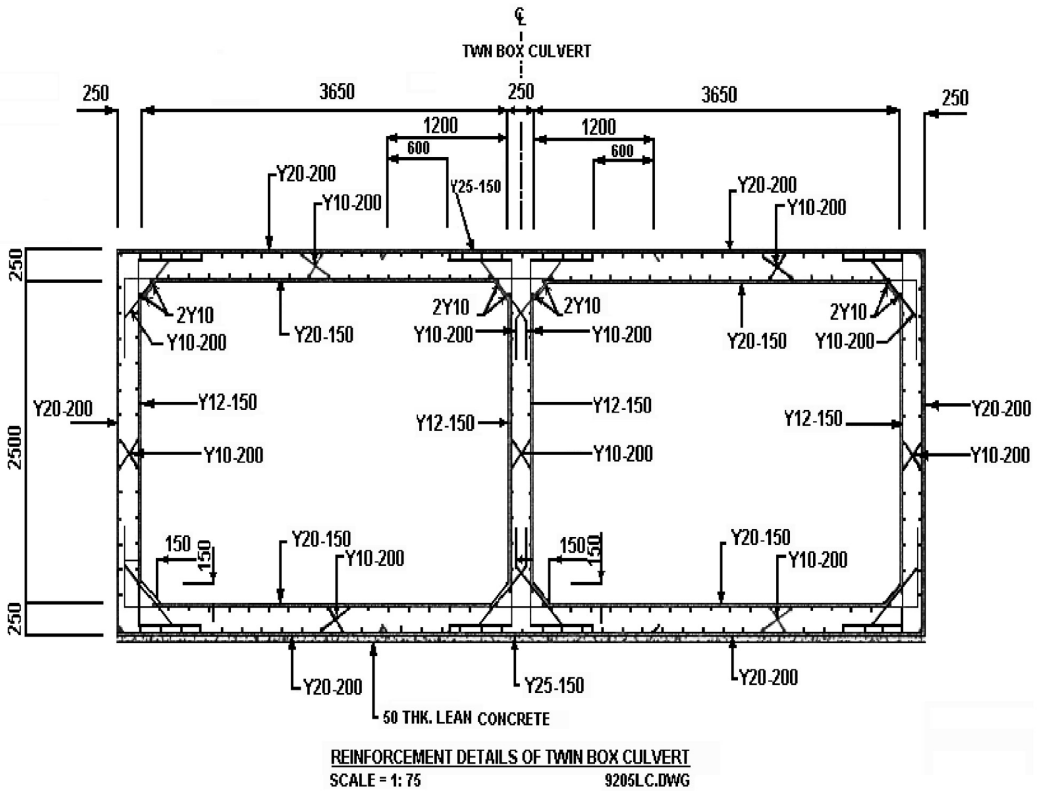

Fig. 5: Cross-section of the jacked twin box culvert

Plate 1: Construction of the jacking pit
Source: DID, Negeri Sembilan

Thrust Bed

The basic feature of the thrust bed is to provide all necessary reactions needed for the jacking operation; 35 jacking pockets were provided at the thrust bed at appropriate locations to house jacking pins designed for resisting the pushing or jacking forces exerted by hydraulic jacks, as the box segment was being jacked.

Front and Rear Shields

The front shield which acts as a cutting edge was fabricated from mild steel plates and anchored to the front end of the first box unit (header unit). The rear shield which was fabricated from mild steel plates was fixed on the rear ends of the first and remaining box units.

Receiving Pit

A receiving pit, with a net dimension of 10 m by 2.5 m, was constructed at the arrival end of the jacked box culvert to facilitate cutting and removal of the front shield and the connection of the jacked box to cast-in-situ box culvert. The pit was formed by steel sheet piles with steel bracing.

Precasting of the Reinforced Concrete Box Culvert

Three units of precast reinforced concrete box segments or units were planned and cast at the jacking pit. The first box unit was 11 m in length, while the second and third units were 11.5 m in length. The first or header unit was cast at the bed aligned with the jacking route, whereas the second unit was cast beside and parallel to the first unit waiting to be shifted and joined to the first unit when the latter was pushed sufficiently into the ground. The third unit was cast after the second unit had been joined to the first unit.

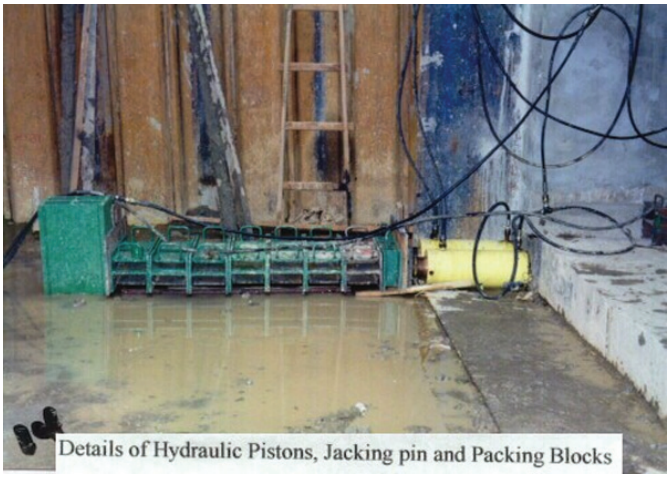

Plate 2: Jacking the box culvert
Source: DID, Negeri Sembilan

Jacking Operation

The technique of box jacking is basically the construction of thrusting bed with jacking pockets, where precast reinforced concrete boxes were cast in units or segments and these box units were jacked by applying pressure through hydraulic jacks, and placed between the jacking pins and the boxes *(Plate 2)*.

Plate 3: Maintenance of railway line
Source: DID, Negeri Sembilan

During the jacking, the jacking pins were inserted into the pockets nearest to the tail end of the box unit, and this was followed by placing of the hydraulic jacks between the jacking pins and the tail end. The first segment was first pushed by hydraulic jacks, whereas the front shield was penetrated into the soil and followed by excavation of the soil at the front shield. The excavated soil was removed using a mini skid before the next stage of pushing. The removed soil was unloaded on buckets at the rear end of the jacking pit which were subsequently lifted by the excavator to the ground surface for disposal. The operation of jacking was continued by adding suitable steel packing boxes and plates between the jacking pins and hydraulic jacking until the pockets in the next row of the thrust bed were exposed. While the pushing of the first segment was in progress, the second box unit was cast at the pit. It was side shifted and positioned in line with the first box after the first box had been jacked into the ground. The box was pushed and joined to the first box through the rear shield to form an intermediate jacking station. Hydraulic jacking pistons were placed at the immediate jacking stations to enable the pushing of individual units one by one so as to take reaction against the rear units and reduce the total jacking force needed at a time. The same process was repeated for the third unit. In total, 32 numbers of 150 tons hydraulic jacks were used. The jacking forces used for pushing each unit ranged from 250 tonnes to 1100 tonnes. The average jacking rate during the jacking period was 300 mm/day.

The alignment and levels of the jacking boxes were monitored using optical theodolite and level, before and after every jacking operation. In case of misalignment, correction was done using the steering jacks which were located at the immediate jacking stations. A maintenance team from the Malaysian Railway Authority made daily inspections to the railway line and the line was corrected and maintained when any deformation was detected *(Plate 3)*.

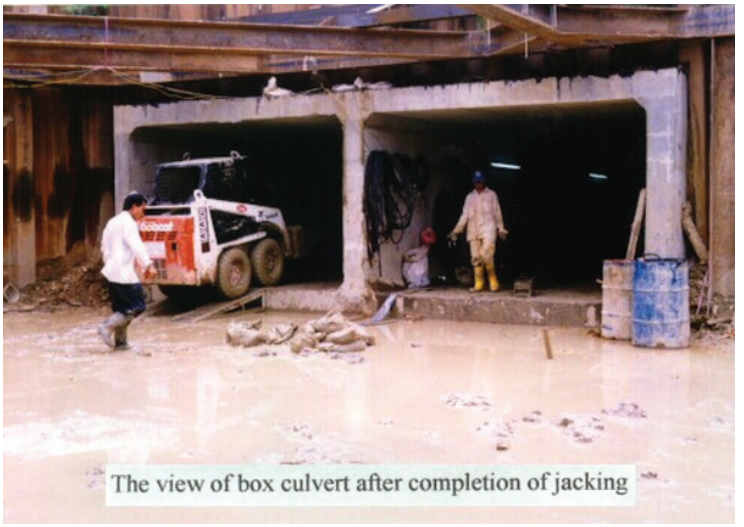

Plate 4: Completion of the Jacking process
Source: DID, Negeri Sembilan

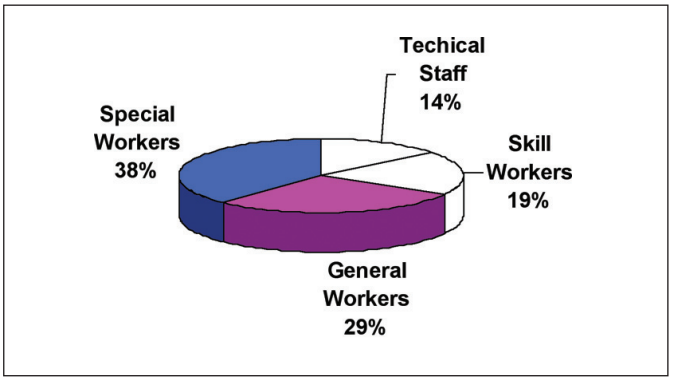

Fig. 6: Manpower used in the jacking technique

RESULTS AND DISCUSSION

The following problems were encountered during the jacking operations:

Existence of Timber Logs and Other Hard Materials

In the case of jacking, timber logs of varying sizes and other foreign material such as steel rails and boulders rendered difficulties in maintaining the alignment of the jacking path which resulted in high jacking force. These obstructions had to be cut and removed in small pieces, and doing so caused some stability problems at the heading face and slowed down the jacking program as well. Therefore, many sand bags had to be placed at the heading face to stabilise the soil during the removal of the obstructions.

Pitching of Box Segments

The subsoil at the jacking path is very poor and it comprises of mainly very soft silty clay/organic clay and very loose silty sand. As a result, the header unit was observed to be pitching and it was unable to adjust the bed level back to the design requirement by steering jacks. Meanwhile, the jacked boxes also experienced settling gradually, and a high pressure grout pump was therefore mobilised to inject bentonite–cement grout and cement grout into the ground below the base of the jacked boxes, at the front part of the header unit to stabilize the subsoil. These solved the problems of pitching and settlement.

Dragging of Soil

The problem of soil dragging adjacent to the jacked box culvert, which was due to the effect of jacking operations, resulted in the development of cracks at the soil above the box culvert, and these could be clearly seen at the ground surface. The dragging problem had also induced some deformations on the railway line. The rail line is monitored daily by the track maintenance team and is corrected as and when required. Meanwhile, the deformed ground surface is regularly backfilled and levelled.

The manpower and equipment used in the completion of the jacking and construction of the twin box culvert are shown in *Fig. 6* and Table 2, respectively. The period of jacking 33 m of the twin box culvert took 110 days to be completed, whereas the construction of the 50 m twin box culvert took around 270 days. *Plate 4* shows the twin box culvert after it was completion.

The trenchless and tunnelling technique was applied successfully in the construction of a twin cell box culvert at the intersection of River Anak Air Rasah, Seremban and the railway line. The work was part of the Flood Mitigation Project for Seremban town. Tunnels are normally used as a solution when any planned traffic routes intersected with rivers, seas, and existing structures. In the present study, the trenchless and tunnelling technique was used in the flood mitigation project, in which River Anak Air Rasah is flowing under the railway line through the jacked twin cell box culvert. This technology is used for the first time ever by the Department of Irrigation and Drainage, Malaysia for flood mitigation work. Standards and loading conditions used in the structural design of the jacked twin cell box culvert form chainage 2029 m to chainage 2079 m of River Anak Air Rasah were compared with other work which was constructed in other parts of the world. As a result, it was found to be in agreement with the design of the Medway immersed tunnel in UK. Several problems were encountered during construction. Suitable solutions were used to solve the problems in the site of jacked twin cell box culvert and to avoid any delay caused in the construction. It is important to note that he railway traffic was not affected during the construction period.

TABLE 2
Equipment used in the jacking and construction of the twin box culvert
(Drill Con Sdn. Bhd., 1997)

Equipment	Quantity (Unit)
150 tons double-acting hydraulic jacking pistons	32
Hydraulic power pack (30 HP)	1
Hydraulic power pack (10 HP)	1
Excavator	1
Mini-excavator	1
Bobcat skid loader	1
High pressure double acting piston grout pump	1
Vibro hammer	1
Submersible pump	3
Welding set	2
Generator set	1
Mobile crane	1
2 ton lorry	1
6 wheeled truck	1
Theodolite	1
Optical level	1

CONCLUSIONS

A 33 m long new box culvert was constructed underneath the railway line using the tunnelling and trenchless technology. The construction period was around 110 days, while the average jacking rate was 300 mm/day. The main problems encountered during the jacking operations include the difficulties in maintaining the alignment of the jacking path, pitching and settlement of the box segments, as well as flooding and dragging of soil which created cracks at the surface of the ground.

Monitoring of the site by the Department of Irrigation and Drainage (DID), Negeri Sembilan after construction and up to the present time indicates that the structure has been performing well without any problem. The contractor managed to complete the work in time and within its budget and as defined in the scope of work. The DID Negeri Sembilan was the first to apply the tunnelling and trenchless technology in flood mitigation projects in Malaysia.

REFERENCES

Busby, J. and Marshall, C. (2000). Design and construction of the Oresund Tunnel. *Journal of the Institution of Engineers*, *138*(4), 157-167.

Drill Con Sdn. Bhd. (1997). Jacking of twin box culvert under the existing railway track at Sungai Anak Air Rasah, Seremban. A study submitted to the Department of Irrigation and Drainage, Negeri Sembilan.

Field, C., Gamble, M. and Karakashian, M. (2000). Design and construction of London Bridge Station on Jubilee Line Extension. *Proceedings of the Institution of Engineers, Civil Engineering, 138*(1), 26-39.

Leto and Welburn, B. (1999). Lines 2 and 3 of the Athens Metro. *Proceedings of the Institution of Engineers, Civil Engineering, 132*(2/3), 68-76.

Madkour, A., Hudson, M.A. and Bellarsoa, A. (1999). Construction of Cairo Metro Line 2. *Proceedings of the Institution of Engineers, Civil Engineering, 132*(2/3), 103-117.

Mainwaring, G.D., Week, C.R. and Brandson, C. (2000). The detailed design of the Medway Tunnel Project. *Journal of the Institution of Civil Engineers*, *141*(1), 9-24.

Peacock, S. and Setterfield, G. (1999). South water's costal clean-up programme. *Proceedings of the Institution of Engineers, Civil Engineering, 132*(2/3), 12-19.

Welburn, B. and De Nettancourt, X. (2002). El-Azhar Road Tunnel Cairo's New Frontier. *Proceedings of the Institution of Engineers, Civil Engineering, 150*(3), 114-123.

ISSN: 0128-7680
Pertanika J. Sci. & Technol. **18 (1)**: 167 – 179 (2010)

Distribution of PAHs and n-alkanes in Klang River Surface Sediments, Malaysia

Alireza Riyahi Bakhtiari[1], Mohamad Pauzi Zakaria[1*], Mohammad Ismail Yaziz[1], Mohamad Nordin Hj Lajis[2], Xinhui Bi[3], Mohamad Reza Mohamad Shafiee[1] and Mahyar Sakari[1]

[1]Environmental Forensics Laboratory, Faculty of Environmental Studies, Universiti Putra Malaysia, 43400 UPM, Serdang, Selangor, Malaysia
[2]Laboratory of Natural Products, Institute of Bioscience, Universiti Putra Malaysia, 43400 UPM, Serdang, Selangor, Malaysia
[3]State Key Laboratory of Organic Geochemistry, Guangdong Key Laboratory of Environment and Resources, Guangzhou Institute of Geochemistry, Chinese Academy of Sciences, Guangzhou, 510640, P.R. China
[*]E-mail: mpauzi@env.upm.edu.my

ABSTRACT

Surface sediment samples were collected from five locations at the downstream of Klang River in January 2007 to examine the spatial distribution, composition, and sources of 19 parent polycyclic aromatic hydrocarbons (PAHs) and aliphatic hydrocarbon (n-alkanes) using gas chromatography-mass spectrometry. The total concentrations of the 19 PAHs in the sediments were found to range from 1304 to 2187 ng g^{-1} sediment. Meanwhile, total concentrations of n-alkanes ranged from 17008 to 27116 μg g^{-1} sediment. The concentration of n-alkanes in the sediment was significantly correlated ($r = 0.991$, $p = 0.001$) with the content of sediment organic carbon. In this study, all the sediments exhibited phenanthrene/anthracene (PHE/ANT >15) fluoranthene/(fluorantene+pyrene) (FLT/FLT+PYR < 0.4), methylphenanthrenes/phenanthrene (MP/P >1), combustion PAHs/total PAHs (CombPAH/∑19PAH <0.3), terrigenous/aquatic ratio for hydrocarbons greater than 23. The also data showed that petrogenic and natural inputs were predominant at all the locations investigated. Multiple sources of n-alkanes and PAHs in the river sediments were also explained by low carbon preference index (CPI) values, different ratios of diploptene/$\sum C_{23}$-C_{25} n-alkanes, poor correlation between diploptene and $\sum C_{23}$-C_{25}, average chain length (ACL) of 29.54 ± 0.09, correlation between CPI and ACL ($r = 0.847$, $p = 0.035$), and high ratio of naphthalene/total PAHs.

Keywords: ACL, CPI, diploptene, Klang river, n-alkanes, PAHs

INTRODUCTION

Polycyclic aromatic hydrocarbons (PAHs) are ubiquitous in sediments and soils, yet they are virtually absent in living organisms (Laflamme and Hites, 1978; Hites *et al.,* 1980). PAHs are derived from natural or anthropogenic sources. Natural sources include: (a) forest and prairie fires (Blumer and Youngblood, 1975), (b) natural petroleum seeps, and (c) post-depositional transformations of biogenic pre-cursors over relatively short period of time (Wakeham *et al.,* 1980). Meanwhile, anthropogenic sources include: (a) combustion of fossil-fuel (Hites *et al*., 1977) and long-range atmospheric transport of PAHs adsorbed into soot or airborne particulate matter (Lunde

Received: 21 October 2008
Accepted: 10 April 2009
[*]Corresponding Author

and Bjorseth, 1977; Laflamme and Hites, 1978), (b) urban runoff containing PAHs derived from abrasion of street asphalt and automobile tyres and vehicular emissions (Wakeham *et al.,* 1980), and (c) spillage of petroleum and its refined products which contain complex assemblages of PAHs (Boehm *et al.,* 1991).

Polycyclic aromatic hydrocarbons (PAHs) form an important class of environmental contamination because some PAHs exhibit carcinogenic or mutagenic potentials (Boonyatumanond *et al.,* 2006). There are several reports of increased incidences of cancer in marine animals from the vicinity of oil spills (Al-Yakoob *et al.,* 1994; Colombo *et al*., 2005). Concerns over PAHs in the environment also arise also from the fact that many of them are persistent (IARC, 1983).

Much of the past work on the organic geochemistry of PAHs has concentrated on understanding their origins and some criteria have been developed to distinguish between different sources of PAHs, namely natural and anthropogenic. Phenanthrene/anthracene and Fluoranthene/pyrene ratios have been commonly used as a means of determining the dominant origins of PAHs (Gschwend and Hites, 1981; Sicre *et al.,* 1987; Colombo *et al.,* 1989; Budzinski *et al.,* 1997; Yang, 2000). The differences in both the reactivity and solubility of these two pairs of isomers have caused their respective ratios to unexpectedly remain constant and, therefore, provide a tracer of PAHs from origin through environmental transport to deposition in marine sediments (Yang, 2000).

The objectives of this study were to determine the distribution of PAHs and n-alkanes in the river surface sediment samples and investigate their sources in Klang River.

MATERIALS AND METHODS

Sampling Locations

Surface sediments were collected from five locations in Klang River which is located in the west coast of Peninsular Malaysia in January 2007 *(Fig. 1)*. The sediment samples were collected using the Ekman Dredge sampler. The sediment cake was placed on a stainless steel pan and the top 0-3 cm layer was taken using a pre-cleaned stainless steel scoop. After that, the samples were placed in ice and transported to the laboratory and stored at -35°C until further analysis.

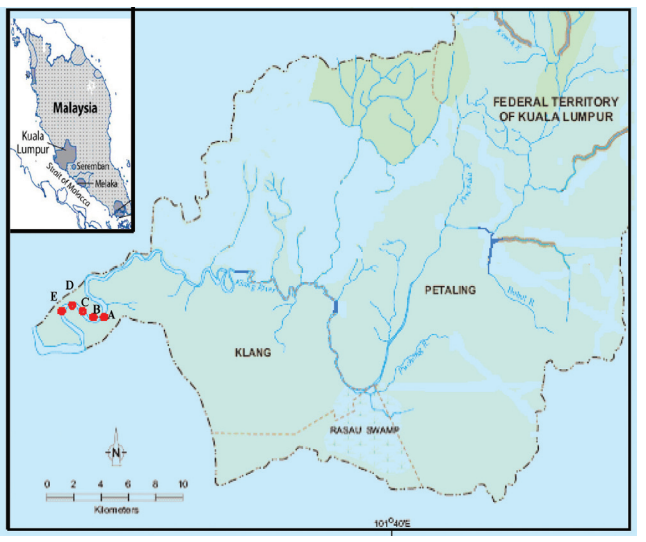

Fig. 1: Map of the sampling sites in the Klang River, Malaysia

Laboratory Analysis

Analytical procedure for PAHs and n-alkanes

Based on the dry weight of the samples, 5 g of each sediment was homogenized using a mortar and pestle in sodium sulphate to remove remaining water. The samples were then purified and fractionated according to the method described earlier (Zakaria *et al.,* 2002). Briefly, the soxhlet extractor was used for the extraction of lipid from the samples using 270 ml of distilled dichloromethane for 10 hours. About 100 µl of the PAH surrogate internal injection standard mixture, where 10 ppm of each component containing naphthalene-d_8, anthracene-d_{10}, chrysene-d_{12}, and perylene-d_{12}, was added for quality control of the PAH analyses. The eluate was purified and fractionated using two-step silica gel column chromatography. The first step silica gel chromatography was accomplished through 5% H_2O deactivated silica gel column (1 cm i.d. × 9 cm, ~6 g, 100–200 mesh; F.C.923, Davison Chemical). Hydrocarbons ranged from n-alkanes to PAHs were eluted with 20 ml of dichloromethane/hexane (1:3 v/v). The second step column chromatography was a fully activated silica gel (0.47 cm i.d.×18 cm, ~3 g, 60–200 mesh; Sil-A-200; Sigma). Alkanes were eluted with 4 ml of hexane and subsequently PAHs were eluted with dichloromethane/hexane (1:3, v/v). Normal and isoprenoid alkanes were determined using capillary gas chromatograph which was equipped with flame ionization detector. The PAHs analyses were carried out using quadrupole mass spectrometer integrated with gas chromatograph.

Each PAH fraction was evaporated to approximately 1 ml, transferred to a 1.5 ml amber ampoule and evaporated to dryness under a gentle stream of nitrogen and re-dissolved in 100 µl of isooctane containing *p*-terphenyl-d_{14} as an internal injection standard (IISTD) for the PAHs analysis. The PAHs analyses were done using Agilent technologies 5973A quadrupole mass spectrometer integrated with an Agilent 6890 gas chromatograph.

Each n-alkane fraction was evaporated to approximately 1 ml, transferred to a 1.5 ml amber ampoule and evaporated to dryness under a gentle stream of nitrogen and re-dissolved in 100 µl of isooctane. It was sealed by teflon and after sonication, while volatile organic carbons (VOCs) were formed in the head space. Meanwhile, the n-alkane analyses were carried out using the Agilent technologies 5973A quadrupole mass spectrometer, which was integrated with an Agilent 6890 gas chromatograph.

Analytical procedure for the total organic carbon (Toc)

The analytical procedure used in this study was described by Nelson and Sommers (1996). Briefly, the sediment samples were dried overnight at 60°C in an oven and then homogenized using mortar and pestle. Sample preparation was carried out to eliminate inorganic carbon. For this purpose, 1-1.5 g of the sample was mixed with 1-2 ml of HCl 1 M to eliminate all carbonates and then dried for about 10 hours at 100-105°C to get rid of Hydrochloric Acid. The TOC% was then determined using LECO CR-412 Carbon Analyzer with the furnace temperature of 1350°C and the oxygen boost time of 60s.

RESULTS AND DISCUSSION

Total Concentration of PAH

All PAH concentrations and TOC values are presented in Table 1. ∑PAH concentrations were normalized with TOC to eliminate the grain size effect. The range of ∑PAH/TOC was from 46 to 108 ng mg^{-1}.

TABLE 1
PAHs concentration (ng g^{-1}) and related parameters in the surface sediments from the Klang River

Compounds	Stations			
	A	B	C	D
Nap	1201.81	1654.04	2167.76	1861.72
DBT	0.81	1.09	N.D	N.D
Phe	11.14	15.09	2.05	10.77
Ant	0.23	0.21	0.04	0.17
3MPhe	2.38	4.70	0.78	3.16
2MPhe	2.93	5.16	0.53	2.62
2MAnt	N.D	0.76	N.D	N.D
9MPhe	2.48	4.21	0.84	3.11
1MPhe	3.82	4.44	0.59	2.55
Fluo	4.87	10.22	3.31	10.13
Pyr	15.74	36.56	5.16	23.35
1MPyr	16.33	7.89	N.D	3.94
Chry	3.81	1.6	N.D	3.52
BaAnt	3.57	2.23	N.D	3.32
BkFluo	8.98	0.49	N.D	N.D
BeAcep	N.D	13.51	N.D	N.D
BePyr	22.89	12.77	5.58	19.63
BaPyr	2.36	N.D	N.D	2.02
Per	N.D	N.D	N.D	N.D
DBahAnt	N.D	N.D	N.D	N.D
∑19PAHs	1304	1775	2187	1950
LMW/HMW	16.7	22.65	202.45	33.94
MP/P	1.45	1.23	1.34	1.1
PHE/ANT	49.33	73.38	53.96	62.93
FLT/(FLT+PYR)	0.24	0.22	0.39	0.3
CombPAH/∑19PAHs	0.06	0.04	0.005	0.03
Nap/∑19PAHs	0.92	0.93	0.99	0.95
TOC	28.16	12.35	23.6	17.92
∑19PAHs/TOC	46.31	143.72	92.67	108.82

∑19PAHs = Sum of (Naphtalene, Dibenzothiophene, Phenanthrene, Anthracene, 3-Methylphenanthrene, 2-Methylphenantrene, 2-Methylanthracene, 9-Methylphenanthrene, 1-Methylphenantrene Fluoranthene, Pyrene, 1-Methylpyrene, Chrysene, Benzo[a]Anthracene, Benzo[k]Fluoranthene, Benzo[e]Acephenanthrene, Benzo[e]Pyrene, Benzo[a]Pyrene, Dibenzo[a-h]Anthracene).
LMW/HMW = (Nap+ DBT+ Phe+ Ant+ 3Mphe+ 2Mphe+ 2MAnt+ 9MPhe+ 1MPhe+ Flu)/(Pyr+ 1MPyr+ Chr+ BaAnt+ BkFluo+ BeAcep+ BePyr+ BaPyr+ Per+DBahAnt).
MP/P = (3MPhe+2MPhe+9MPhe+1MPhe)/Phe.
PHE/ANT = Phenanthrene/Anthracene.
FLT/(FLT+PYR) = Fluoranthene/(Fluoranthene+Pyrene).
CombPAH = (Pyr+ 1MPyr+ Chr+ BaAnt+ BkFluo+ BeAcep+ BePyr+ BaPyr+ Per+DBahAnt).
Nap/∑19PAHs = Naphtalene/ ∑19PAHs.
TOC = Total organic carbon in unit of mg g^{-1}.
∑19PAHs/TOC in unit of ng mg^{-1}.
N.D = non detected

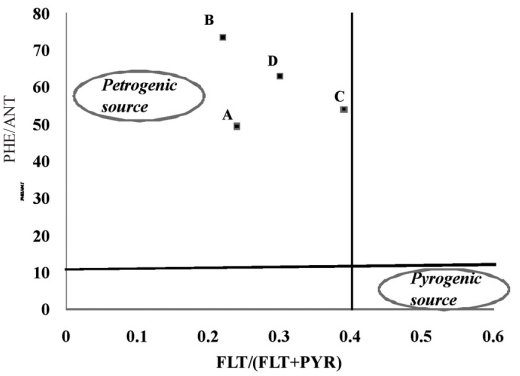

Fig. 2: Values of PHE/ANT and FLT/ (FLT/PYR) ratios for the sediments from Klang River

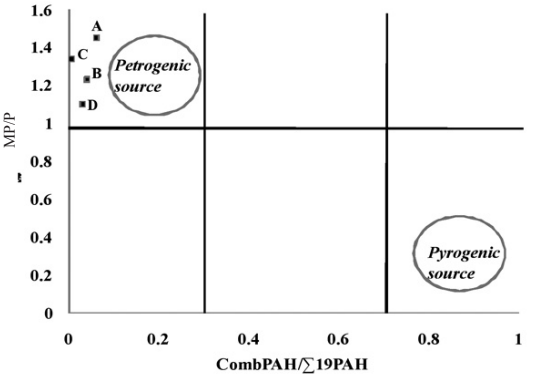

Fig. 3: Values of MP/P and CombPAH/∑19PAH ratios measured in the sediments from the Klang River

The total concentration of the 19 PAHs found in the sediments (expressed as ∑PAH) was found to range from 1300 to 2200 ng g^{-1}. In this study, the sediment PAH concentrations at all the stations investigated were dominated by naphthalene. Meanwhile, the naphthalene concentrations ranged from 1200 to 2167 ng g^{-1}. This is most likely due to the fact that naphthalene occurs at elevated concentrations in woody material (Wilcke *et al.,* 2000). It is believed that naphthalene originated from natural sources in the Klang River sediments. Lower molecular weight versus higher molecular weight ratio has been applied in several studies to distinguish between petrogenic and pyrogenic PAH sources (Bence *et al.,* 1996; Wang *et al.,* 1999; Mai *et al.,* 2002). The results of this study suggest petrogenic inputs to surface sediments in the Klang River.

Source Identification of PAH

As compared to pyrogenic sources, petrogenic sources are characterized by high ratios of phenanthrene/antracene (PHE/ANT >15) and methylephenanthrenes/phenanthrene (MP/P >1), in association with lower ratios of fluoranthene/pyrene (FLT/FLT+PYR<0.4) and combustion PAH/ total PAH (CombPAH/∑19PAH <0.3) (Budzinsky *et al.,* 1997; Benner *et al.,* 1989: 1990; Yunker *et al.,* 2002; Hwang *et al.,* 2003).

Fig. 2 shows that the values of PHE/ANT ranged from 53 to 74, whereas FLT/FLT+PYR ranged from 0.22 to 0.39 in the sediment samples of the Klang River. In addition, the values of MP/P ratio were found to range from 1.1 to 1.45, while the CombPAH/∑19PAH ratio ranged from 0.005 to 0.06, as shown in *Fig. 3*. The results suggest petrogenic inputs of PAHs in the sediments derived from the study area. Among the influencing factors are rapid tourism development, direct effluent discharges into the river, drainage from port areas, and contaminants from ships (Unlu and Alpar, 2006).

n-alkane Concentrations

The hydrocarbon concentrations and related parameters are shown in Table 2. To eliminate the grain size effect, n-alkane concentrations were normalized with TOC. There was found significant positive correlation ($r = 0.991$, $p = 0.001$) between n-alkane concentration and TOC at the 99% confidence level *(Fig. 4)*, indicating changes in n-alkane concentration can be depended on TOC contents.

TABLE 2
Hydrocarbon concentrations (µg g^{-1}) and related parameters in the surface sediments of the Klang River

Compounds	Stations				
	A	B	C	D	E
nC_{10}	31.1	N.D	N.D	N.D	N.D
nC_{12}	5.0	N.D	N.D	N.D	N.D
nC_{14}	26.4	27.4	N.D	N.D	31.1
nC_{15}	36.6	32.0	N.D	46.1	8.6
nC_{16}	57.2	51.3	8.3	51.5	78.1
nC_{17}	81.4	67.5	10.7	62.0	81.2
Pristane	129.9	130.2	20.8	98.9	93.3
nC_{18}	68.5	43.9	12.8	45.9	89.0
Phytane	N.D	N.D	N.D	N.D	N.D
nC_{19}	54.2	42.9	11.0	40.8	63.7
nC_{20}	60.4	35.9	22.7	38.4	74.4
nC_{21}	118.7	68.7	53.0	78.6	186.2
nC_{22}	260.7	128.3	164.4	164.4	451.8
nC_{23}	569.8	234.3	442.4	370.5	900.7
nC_{24}	2101.4	406.6	863.8	683.1	1459.7
nC_{25}	1717.9	636.1	1533.5	1129.5	2154.5
nC_{26}	2320.9	836.5	2118.7	1537.9	2632.0
nC_{27}	2998.8	1036.6	2611.1	1961.3	3118.1
nC_{28}	2894.0	1015.3	2549.9	1867.5	2927.4
nC_{29}	3171.1	1248.0	2680.5	2157.2	3127.7
nC_{30}	2629.6	906.5	2391.7	1647.9	2648.9
nC_{31}	2848.5	979.9	2262.2	2001.5	2727.4
nC_{32}	1887.8	700.8	1486.7	1250.9	1896.9
Diploptene	194.5	151.4	131.6	157.7	158.7
nC_{33}	1500.8	668.0	1102.9	1043.3	1403.4
nC_{34}	759.4	289.9	610.1	498.6	735.4
nC_{35}	434.7	200.2	297.5	331.9	300.1
nC_{36}	156.5	N.D	N.D	N.D	N.D
TOC	28.16	12.35	23.6	17.92	30.49
CPI	1.09	1.21	1.09	1.21	1.11
∑HC/TOC	951.4	781.9	899.7	949.1	889.4
SHC/TOC	6.11	11.53	0.92	8.31	5.70
LHC/TOC	320.26	264.33	320.08	341.52	294.30
TAR_{HC}	52.38	22.93	348.40	41.09	51.73
$Di/\sum C_{25\text{-}33}$	0.016	0.033	0.013	0.019	0.013
Di/TOC	6.9	12.26	5.58	8.80	5.20
ACL	29.54	29.65	29.43	29.59	9.47

SHC/TOC= µg of (nC_{15}+nC_{17}+nC_{19})/ mg of TOC. LHC/TOC = µg of (nC_{27}+nC_{29}+nC_{31})/ mg of TOC.
∑HC/TOC in unit of (µg mg^{-1}). nC_{31}/Terr = $nC_{31}/(nC_{27}+nC_{29}+nC_{31})$.
TAR_{HC} = terrigenous/aquatic ratio = $(nC_{27}+nC_{29}+nC_{31})/(nC_{15}+nC_{17}+nC_{19})$.
CPI = carbon preference index = ½ ×[(nC_{25}+ nC_{27}+nC_{29}+nC_{31}+nC_{33} ÷ nC_{24}+ nC_{26}+nC_{28}+nC_{30}+nC_{32}) + (nC_{25}+ nC_{27}+nC_{29}+nC_{31}+nC_{33} ÷ nC_{26}+nC_{28}+nC_{30}+nC_{32}+nC_{34})]. TOC= Total organic carbon (mg g^{-1}).
$Di/\sum C_{25\text{-}33}$ = diploptene/(nC_{25}+ nC_{27}+nC_{29}+nC_{31}+nC_{33}).
Di/TOC = diploptene/TOC, in unit of (µg mg^{-1}). N. D = non detected
ACL = average chain length

$$\mathbf{ACL}= \frac{27(nC_{27}) + 29(nC_{29}) + 319nC_{31}) + 33(nC_{33})}{nC_{27} + nC_{29} + nC_{31} + nC_{33}}$$

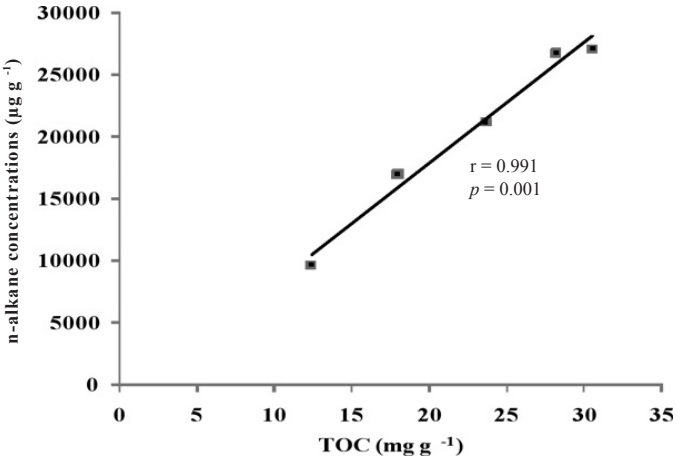

Fig. 4: Correlation between polycyclic aromatic hydrocarbons and total organic carbon in the sediments

n-alkanes were found to range between C_{10} and C_{36}. Total n-alkane concentrations were abundant ranging from 9600 to 27200 µg g $^{-1}$ in sediments of different stations. The long-chain n-alkanes (LHC, $>C_{23}$) were found in higher concentrations when compared to the short-chain n-alkanes (SHC, < C23) and the distribution patterns showed large contributions from even (C_{26}, C_{28}, C_{30}) and odd carbons (C_{27}, C_{29}, C_{31}). For LHC n-alkanes, the C_{27} and C_{29} are diagnostic of waxes from trees and shrubs and n-C_{31} is diagnostic of grass waxes (Jeng, 2007). Our results indicate that the sediments received contribution of the n-alkanes from grass, tree and shrub waxes in the banks of Klang River. This can possibly be attributed to the fact that vegetation types form the main influence on the chain length of terrigenous leaf lipids (Cranwell, 1973). It has been suggested that plants produce longer-chain compounds in warmer climates (Poynter *et al.,* 1989; Simoneit *et al.,* 1991).

Carbon Preference Index (CPI) of n-alkanes

In organic geochemistry, CPI is used to indicate the degree of diagenesis of straight-chain geolipids and it is also a numerical representation of how much of the original chain length specificity has been preserved in geological lipids (Meyers and Ishiwatari, 1995). In addition, it is also useful in determining the degree of biogenic versus petrogenic input (Mazurek and Simoneit, 1984). Hydrocarbons compose of a mixture of compounds originating from land plant material which shows a predominance of odd-numbered carbon chains with CPI~5–10 (Rieley *et al.,* 1991; Hedges and Prahl, 1993), whereas petrogenic inputs have a CPI approximating 1.0 (Farrington and Tripp, 1977; Eganhouse and Kaplan, 1982; Nishimura and Baker, 1986; Saliot *et al.,* 1988; Pendoley, 1992). Meanwhile, the CPI values close to one are also thought to indicate greater inputs from marine micro-organisms and/or recycled organic matter (Kennicutt *et al.,* 1987). The CPI values of the n-alkanes were found to vary from 1.09 to 1.21 in sediments at different locations (Table 2). This finding indicates that the sediments are contaminated by petrogenic hydrocarbons. However, it is important to highlight that exceptions exist in some cases. For example, Zhou *et al.* (2005) obtained low CPI values of n-alkanes during a warm-wet period in the sediment core samples in the Dingnan region in southern China. In addition, the CPI ratios ranging from 1-1.5 had been obtained in the sediment core samples taken from Chini Lake in Malaysia in the tropical environment (Riyahi Bakhtiari *et al.* full article in preparation for publication). They concluded

that the CPI ratio ranging from 1-1.5 indicate greater inputs from higher plants in the study areas. A possible explanation for this might be the fact that plants produce longer-chain compounds in warmer climates (Poynter *et al.,* 1989; Simoneit *et al.,* 1991). Another possible explanation for this is that higher plants produce the same alkonoic acids < C_{20} as microbiota with additional homologs from C_{20} to C_{34} (Simoneit and Mazurek, 1982). These higher plant n-fatty acids are biosynthesized by elongation of low molecular weight homologues which result in predominantly even carbon number n-alkanoic acids (Kolattukudy *et al.,* 1976). The n-alkanes with an even number of carbon atoms can only result from the coupling of fatty acids containing an even and an odd number of carbon atoms. Therefore, due to the fact that the odd carbon number fatty acids are relatively rare, only the odd carbon number n-alkanes are virtually predominant in plants (Bird and Lynch, 1974). The plant wax n-alkanes show a C_{max} in the range of C_{25} to C_{33}, which are dependent on the plant species as well as the season and locality (e.g. Eglinton and Hamilton, 1967; Simoneit and Mazurek, 1982; Mazurek *et al.,* 1991; Rogge *et al.,* 1993d; Stephanou and Stratigakis, 1993; Abas and Simoneit, 1998). As compared to the CPI range of Chini Lake sediments (1-1.5), the sediment from the Klang River has a relatively smaller range from 1.09 to 1.21. One possible cause can be the multiple sources of n-alkanes in the study area. Moreover, the n-alkanes in the Klang river may include high CPI n-alkanes from the plant waxes, but low CPI n-alkanes from microbial or petrogenic sources. These findings seem to be consistent with the data previously reported by some researchers (Pearson and Eglinton, 2000; Reddy *et al.,* 2000).

Average Chain lLh (ACL)

The higher plant n-alkane average chain length (ACL) describes the average number of carbon atoms per molecule based on the abundance of the odd-carbon-numbered higher plant n-alkanes (Poynter and Eglinton, 1990). It has been found that the modal carbon number of a higher plant n-alkane distribution is broadly related to the latitude (Poynter *et al*., 1989; Poynter and Eglinton, 1990), with higher modal carbon numbers occurring at lower latitudes. Furthermore, the distribution of ACL has been linked to the geographical distribution of fluvial and eolian inputs and source regions (Poynter and Eglinton, 1990). In other words, for coastal marine sediments, ACL in a given area can be considered a constant if all these factors are the same. The ACL values were found to range from 28.3 to 29.9 in the surface sediments of NW Africa at ~0–40° N (Huang *et al.,* 2000). It has been reported that the ACL values increased from 29.9 to 30.8 for the north to south latitudinal transect (5–30° S latitude) of the Holocene sediment in the SE Atlantic (Rommerskirchen *et al.,* 2003). This means a change of ~0.04 ACL unit for crossing 1° latitude (Jeng, 2006). The ACL values of Chini Lake sediment core samples (Latitude 03° 26′ N) yield an average of 29.68 ± 0.15, indicate an increment of 0.038 ACL units for crossing 1° latitude compared to that in surface sediments of NW Africa ranging from ~0–40° N (Riyahi Bakhtiari *et al.* full article in preparation for publication). This suggests a predominant input of biogenic (recent) hydrocarbons. In this study, the ACL values of the Klang River sediment samples (Latitude 02° 56′ N) yield an average of 29.54 ± 0.09 indicate an increment of 0.034 ACL units for crossing 1° latitude when compared to the surface sediments of NW Africa ranging from ~0–40° N. The sediment samples of Chini Lake showed a higher increment. This could probably be attributed to the river sediment being contaminated by petrogenic hydrocarbons because petrogenic hydrocarbons are expected to have low ACL values in the C_{25}–C_{33} range (Jeng, 2006).

Both ACL and CPI were calculated using the n-alkanes data derived from higher plants. Therefore, they are expected to be correlated (Jeng 2006). The correlation between the ACL and CPI values of the sediment samples were tested and the data are presented in *Fig. 5*. The results show a significant positive correlation at 95% confidence level in the sediment samples (r = 0.847,

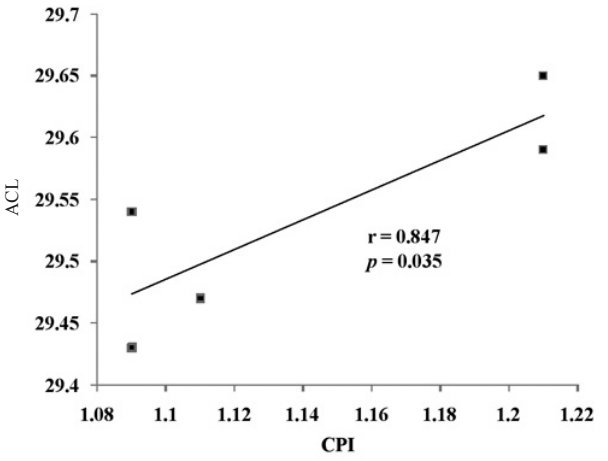

Fig. 5: Correlation between ACL and CPI n-alkanes in Klang River sediments

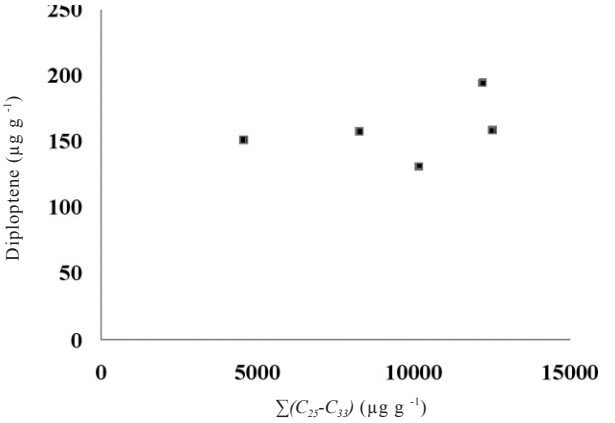

Fig. 6: Plots of diploptene versus ∑(C_{25}-C_{33}) n-alkanes for Klang River sediments

p = 0.035). Therefore, it could be inferred that the CPI ranging from 1-1.5 could be attributed to the mixed petrogenic and natural sources of n-alkanes in the Klang River sediments.

Diploptene (hop-22(29)-ene)

The concentrations of diploptene in the sediment samples (ranging from 131.6 to 194.5 µg g $^{-1}$) are shown in Table 2. Meanwhile, the values of Di/∑ (C_{25}-C_{33}) ratio were found to range from 0.013 – 0.033.

Diploptene is derived from terrestrial higher plants and it is also formed by bacteria (Rohmer *et al.,* 1984). If higher plants are the sole source of diploptene, a strong correlation between diploptene and terrestrial higher plants n-alkanes can be expected. The correlation between diploptene and ∑ (C_{25}-C_{33}) was examined in the sediments *(Fig. 5)*. However, there was no significant correlation

(r = 0.391, p = 0.515) found between diploptene and $\sum C_{23}$-C_{25} n-alkanes (odd carbon only) for the sediments *(Fig. 6)*. This was most likely because the sediments received multi inputs of hydrocarbons and hence contained different ratios of diploptene to $\sum C_{23}$-C_{25} n-alkanes. These findings are in agreement with those of the previous research (Jeng, 2007).

CONCLUSIONS

The results of this study suggest petrogenic and natural sources inputs of hydrocarbons in the study area. These were shown by the high Nap/$\sum$19PAHs and LMW/HMW ratios, as well as the ratios of PHE/ANT >15, MP/P >1, FLT/FLT+PYR < 0.4 and CombPAH/$\sum$19PAH <0.3 for PAHs. Therefore, it is concluded that the downstream sediments in the Klang River contain n-alkane from both petrogenic and natural sources. These could be expressed by predominance of LHC, >C_{23} as compared to SHC, < C23, the CPI values of the n-alkanes (i.e. from 1.09 to 1.21), the ACL values of 29.54 ± 0.09, the positive correlation between ACL and CPI values (r = 0.847, p = 0.035), different ratios of diploptene /$\sum C_{23}$-C_{25} n-alkanes in the stations, as well as no correlation (r = 0.391, p= 0.515) between diploptene and $\sum C_{23}$-C_{25} n-alkanes.

ACKNOWLEDGEMENT

This study was supported by the Ministry of Science, Technology and Innovation, Malaysia (MOSTI), who provided partial funding for this project (Science Fund Project (No. 04-01-04-SF0092).

REFERENCES

Abas, M.R.B. and Simoneit, B.R.T. (1998). Wax lipids from leaf surfaces of some common plants of Malaysia. *Pertanika Journal of Science and Technology, 6,* 171-182.

Al-Yakoob, S.N., Saeed, T. and Al-Hashash, H. (1994). Polycyclic aromatic hydrocarbons in fish: Exposure assessment for Kuwaiti consumers after the Gulf oil spill of 1991. *Environment International, 20,* 221–227.

Bence, A.E., Kvenvolden, K.A. and Kennicutt, M.C. (1996). Organic geochemistry applied to environmental assessments of Prince William Sound, Alaska, after the Exxon Valdez oil spill – a review. *Organic Geochemistry, 24* (1), 7–42.

Benner, B.A., Bryner, N.P., Wise, S.A., Mulholland, G.H., Lao, R.C. and Fingas, M.F. (1990). Polycyclic aromatic hydrocarbons emissions from combustion of crude oil on water. *Environmental Science and Technology, 24,* 1418-1427.

Benner, B.A., Gordon, G.E. and Wise, S.A. (1989). Mobile sources of atmospheric polycyclic aromatic hydrocarbons: A roadway tunnel study. *Environmental Science and Technology, 23,* 1269-1278.

Bird, C.W. and Lynch, J.M. (1974). Formation of hydrocarbons by microorganisms. *Chemical Society Reviews, 3,* 309-328.

Blumer, M. and Youngblood, W.W. (1975). Polycyclic aromatic hydrocarbons in soils and recent sediments. *Science, 188,* 53–55.

Boehm, P.D., Costa, H.J. and Bleczinski, C.F. (1991). Assessment of the changes in composition and concentration of San Joaquin Valley crude oil in estuarine and subtidal habitats: Final Year 1 Report, submitted to the State of California, Department of Justice (Report No. 81-2125). Cambridge: Arthur D. Little.

Boonyatumanond, R., Wattayakorn, G., Togo, A. and Takada, H. (2006). Distribution and origins of polycyclic aromatic hydrocarbons (PAHs) in riverine, estuarine, and marine sediments in Thailand. *Marine Pollution Bulletin, 52,* 942-956.

Budzinski, H., Garrigues, P., Bernard, G., Bellocq, J., Hinrichs, K. and Rullkotter, J. (1997). Identification of polycyclic aromatic hydrocarbons in sediments from the Amazon fan: Occurrence and diagenetic evolution. In R.D. Flood, D.J.W. Piper, A. Klaus and L.C. Peterson (Eds.), *Proceedings of the Ocean Drilling Program, Scientific Results* (pp. 555–564).

Cranwell, P.A. (1973). Chain-length distribution of n-alkanes from lake sediments in relation to post-glacial environmental change. *Freshwater Biology, 3,* 259–265.

Colombo, J.C., Pelletier, E., Brochu, C., Khalil, M. and Catoggio, J.A. (1989). Determination of hydrocarbon sources using n-alkanes and polyaromatic hydrocarbon distribution indexes. Case study: Rio de la Plata, Argentina. *Environmental Science and Technology, 23,* 888-894.

Colombo, J.C., Barreda, C., Bilos, N.C., Migoya, M.C. and Skorupka, C. (2005). Oil spill in the Rio de la Plata estuary, Argentina: 2-hydrocarbon disappearance rates in sediments and soils. *Environmental Pollution, 134*, 267–276.

Eganhouse, R.P. and Kaplan, I.R. (1982). Extractable organic matter in municipal wastewaters. 2. Hydrocarbons: Molecular characterization. *Environmental Science and Technology, 16*, 541–551.

Eglinton, G. and Hamilton, R.J. (1967). Leaf epicuticular waxes. *Science, 156,* 1322-1335.

Farrington, J.W. and Tripp, B.W. (1977). Hydrocarbons in western North Atlantic surface sediments. *Geochimica et Cosmochimica Acta, 41,* 1627–1641.

Gschwend, P.M. and Hites, R.A. (1981). Fluxes of the polycyclic aromatic hydrocarbons to marine and lacustrine sediments in the northeastern United States. *Geochimica et Csmochimica Acta, 45,* 2359-2367.

Hedges, J. I. and Prahl, F. G. (1993). Early diagenesis: Consequences for applications of molecular biomarkers. In M. H. Engel and S.A. Macko (Eds.), *Organic geochemistry: Principles and applications* (pp. 237–253). New York: Plenum Press.

Hites, R.A., Laflamme, R.E. and Farrington, J.W. (1977). Sedimentary polycyclic aromatic hydrocarbons—the historical record. *Science, 198,* 829–831.

Hites, R.A., Laflamme, R.E., Windsor, Jr.JG. and Farrington, J.W. (1980). Werner GD. Polycyclic aromatic hydrocarbons in an anoxic sediment core from the Pettaquamscutt River (Rhode Island, USA). *Geochimica Cosmochimica Acta, 44,* 873–878.

Huang, Y., Dupont, L., Sarnthein, M., Hayes, J.M. and Eglinton, G. (2000). Mapping of C4 plant input form NorthWest Africa into North East Atlantic sediments. *Geochimica et Cosmochimica, 64,* 3505–3513.

Hwang, H.M., Wade, T.L. and Sericano, J.L. (2003). Concentrations and source characterization of polycyclic aromatic hydrocarbons in pine needles from Korea, Mexico, and United States. *Atmospheric Environment, 37,* 2259–2267.

International Agency for Research in Cancer (IARC). (1983). Monographs on the evaluation of the carcinogenic risk of chemical to humans polycyclic aromatic compounds, Part I chemical, environmental and environmental data, Lyon, 32p.

Jeng, W.L. (2006). Higher plant n-alkane average chain length as an indicator of petrogenic hydrocarbon contamination in marine sediments. *Marine Chemistry, 102,* 242–251.

Jeng, W.L. (2007). Aliphatic hydrocarbon concentrations in short sediment cores from the southern Okinawa Trough: Implications for lipid deposition in a complex environment. *Continental Shelf Research, 27,* 2066-2078.

Kennicutt II, M.C., Barker, C., Brooks, J.M., DeFreitas, D.A. and Zhu, G.H. (1987). Selected organic matter source indicators in the Orinoco, Nile and Changjiang deltas. *Organic Geochemistry, 11,* 41–51.

Kolattukudy, P. E. (1976). Introduction to natural waxes. In P.E. Kolattukudy (Eds.), *Chemistry and Biochemistry of Natural Waxes* (pp. 1-15). Amsterdam: Elsevier.

Laflamme, R.E. and Hites, R.A. (1978). The global distribution of polycyclic aromatic hydrocarbons in recent sediments. *Geochimica Cosmochimica Acta, 42,* 289–303.

Lunde, G. and Bjorseth, A. (1977). Polycyclic aromatic hydrocarbons in long-range transported aerosols. *Nature, 268,* 518–519.

Mai, B., Fu, J., Sheng, G., Kang, Y., Lin, Z., Zhang, G., Min, Y. and Zeng, E.Y. (2002). Chlorinated and polycyclic aromatic hydrocarbons in riverine and estuarine sediments from Pearl River Delta, China. *Environmental Pollution, 117,* 457–474.

Mazurrek, M.A., Cass, G.R. and Simoneit, B.R.T. (1991). Biological input to visibility-reducing aerosol particles in the remote arid Southwestern United States. *Environmental Science and Technology, 25,* 684-694.

Mazurek, M. A. and Simoneit, B. R. T. (1984). Characterization of biogenic and petroleum-drived organic matter in aerosols over remote, rural, and urban area. In L.H.Keith (Eds.), *Identification and analysis of organic pollutants in air* (pp. 353-370). Woburn, MA: Ann Arbor Science.

Meyers, P. A. and Ishiwatari, R. (1995). Organic matter accumulation records in lake sediments. In A. Lerman, D.M. Imboden and J.R. Gat (Eds.), *Physics and chemistry of lakes* (pp. 279-328). Berlin: Springer.

Nelson, D.W. and Sommers, L.E. (1996). Total carbon, organic carbon, and organic matter. In D.L. Sparks *et al*. (Eds.), *Methods of soil analysis, Part 3, Chemical methods* (pp. 961-1010). SSSA, Madison, WI.

Nishimura, M. and Baker, E.W. (1986). Possible origin of n-alkanes with a remarkable even-to-odd predominance in recent marine sediments. *Geochimica et Cosmochimica Acta, 50,* 299–305.

Pearson, A. and Eglinton, T. (2000). The origin of n-alkanes in Santa Monica Basin surface sediment: A model based on compound specific $\delta^{14}C$ and $\delta^{13}C$ data. *Organic Geochemistry, 31,* 1103–1116.

Pendoley, K. (1992). Hydrocarbons in Rowley Shelf (Western Australia) oysters and sediments. *Marine Pollution Bulletin, 24,* 210–215.

Poynter, J. G. and Eglinton, G. (1990). Molecular composition of three sediments from hole 717C: The Bengal fan. In J.R. Cochran, D.A.V. Stow *et al.* (Eds.), *Proceedings of the Ocean Drilling Program Scientific Results. vol. 116* (pp. 155–161).

Poynter, J.G., Farrimond, P., Robinson, N. and Eglinton, G. (1989). Aeolian-derived higher plant lipids in the marine sedimentary record: Links with paleoclimate. In M. Leinen and M. Sarnthein (Eds.), *Paleoclimatology and paleometeorology: Modern and past patterns of global atmospheric transport. Dordrecht (Kluwer Academic)* (pp. 435–462). Hingham: Mass.

Reddy, C., Eglinton, T., Palic, R., Benitez-Nelson, B., Stojanovic, G., Palic, I., Djordjevic, S. and Eglinton, G. (2000). Even carbon number predominance of plant wax n-alkanes: A correction. *Organic Geochemistry, 31,* 331–336.

Rieley, G., Collier, R.J., Jones, D.M. and Eglinton, G. (1991). The biogeochemistry of Ellesmere Lake, U.K. - I. Source correlation of leaf wax inputs to the sedimentary lipid record. *Organic Geochemistry, 17,* 901-912.

Rogge, W.F., Hildermann, L.M., Mazurek, M.A., Cass, G.R. and Simoneit, B.R.T. (1993d). Sources of fine organic aerosol. 4. Particulate abrasion products from leaf surfaces of urban plants. *Environmental Science and Technology, 27,* 2700-2711.

Rohmer, M., Bouvier-Nave, P. and Ourisson, G. (1984). Distribution of hopanoid triterpenes in prokaryotes. *Journal of General Microbiology, 130,* 1137-1150.

Rommerskirchen, F., Eglinton, G., Dupont, L., Güntner, U., Wenzel, C. and Rullkötter, J. (2003) A north to south transect of Holocene southeast Atlantic continental margin sediments: Relationship between aerosol transport and compound-specific δ13C land plant biomarker and pollen records. *Geochemistry, Geophysics, Geosystems, 4,* 1101. doi:10.1029/2003GC000541.

Saliot, A., Tronczynski, J., Scribe, P. and Letolle, R. (1988). The application of isotopic and biogeochemical markers to the study of the biochemistry of organic matter in a macrotidal estuary, the Loire, France. *Estuarine, Coastal and Shelf Science, 27,* 645–669.

Sicre, M.A., Marty, J.C., Saliot, A., Aparicio, X., Grimalt, J. and Albaiges, J. (1987). Aliphatic and aromatic hydrocarbons in different sized aerosols over the Mediterranean Sea: Occurrence and origin. *Atmospheric Environment, 21,* 2247-2259.

Simoneit, B.R.T. and Mazurek, M.K. (1982). Organic matter of the troposphere. II: Natural background of biogenic lipid matter in aerosols over the rural western United States. *Atmospheric Environment, 16*(9), 2139–2159.

Simoneit, B.R.T., Sheng, G., Chen, X., Fu, J., Zhang, J. and Xu, Y. (1991). Molecular marker study of extractable organic matter in aerosols from urban areas of China. *Atmospheric Environment, 25A,* 2111–2129.

Stephanou, E.G. and Startigakis, N. (1993). Oxocarboxylic and ά,ώ-dicarboxylic acids: Photooxidation products of biogenic unsaturated fatty acids present in urban aerosols. *Environmental Science and Technology, 27,*1403-1407.

Unlu, S. and Alpar, B. (2006). Distribution and sources of hydrocarbons in surface sediments of Gemlik Bay (Marmara Sea, Turkey). *Chemosphere, 64,* 764–777.

Wakeham, S.G., Schaener, C. and Giger, W. (1980). Polycyclic aromatic hydrocarbons in recent lake sediment Ð II. Compounds derived from biogenic precursors during early diagenesis. *Geochimica et Cosmochimica Acta, 44,* 415-429.

Wang, Z., Fingas, M. and Page, D.S. (1999). Oil spill identification. *Chromatography A, 843,* 369–411.

Wilcke, W., Amelung, W., Martius, C., Garcia, M.V.B. and Zech, W. (2000). Biological sources of polycyclic aromatic hydrocarbons (PAHs) in the Amazonian rain forest. *Journal of Plant Nutrition and Soil Science, 163,* 27–30.

Yang, G.P. (2000). Polycyclic aromatic hydrocarbon in the sediments of the South China Sea. *Environmental Pollution, 45,* 567-575.

Yunker, M.B., Macdonald, R.W., Vingarzan, R., Mitchell, R.H., Goyette, D. and Sylvestre, S. (2002). PAHs in the Fraser river basin: A critical appraisal of PAH ratios as indicators of PAH source and composition. *Organic Geochemistry, 33,* 489–515.

Zakaria, M.P., Takada, H., Tsutsumi, S., Ohno, K., Yamada, J., Kouno, E. and Kumata, H. (2002). Distribution of polycyclic aromatic hydrocarbons (PAHs) in rivers and estuaries in Malaysia: A widespread input of petrogenic PAHs. *Environmental Science and Technology, 36,* 1907–1918.

Zhou, W., Xie, S., Meyers, P.A. and Zheng, Y. (2005). Reconstruction of late glacial and Holocene climate evolution in southern China from geolipids and pollen in the Dingnan peat sequence. *Organic Geochemistry, 36,* 1272-1284.

ISSN: 0128-7680
Pertanika J. Sci. & Technol. **18 (1)**: 181 – 208 (2010)

An Exploratory Study on Influence of Internet in B2B Marketplace for IT Organisations in India

S. L. Gupta*, B. K. Jha and Hitesh Gupta
Department of Management, Birla Institute of Technology, Mesra, Ranchi (Deemed University), Noida Extension Centre, India
**E-mail: slgupta_1965@yahoo.co.in*

ABSTRACT

The Indian B2B marketplace in Information Technology sector is going through a transformation. Both existing and new players are experimenting with new purchasing solutions through the Internet as they lack a seamless flow of information among customers, suppliers, and their employees. The way business organisations purchase products is one of the most important concern for marketing managers of today. In fact, people involved in the purchase process form buying centre in purchase process; some say it as a complex and dynamic process that requires plenty of information and in reality, the Internet is a vast source of information which can influence purchase to a great extent. Recent developments in the Internet have forced business organisations to adapt their purchase process. In addition, the Internet also offers a blend of opportunities to companies due to its speed, variety, control, communication access, and strong distribution. Therefore, this research paper investigates the influence of the Internet on the B2B marketplace for IT organisations in India.

Keywords: B2B, industrial marketing, B2B purchase, B2B procurement, e-procurement, IT sector, Indian B2B, e-sourcing, online purchasing

INTRODUCTION

The increasing globalization and use of the Internet, accompanied with multiple resources, pose challenges to the modern management theories and success of entities in the market, accompanied with the multitudes of emerging technologies which compete for integration within the current market (Arns, Fischer, Kemper and Tepper, 2002). These are coupled by the increasing competition within the market on several criteria such as the five major operational performance objectives and several others. Not only this, the introduction of technology into organizations has posed a big challenge as managers strive to sustain a flatter hierarchy, in addition to the retention of the current employees and maintaining a low cost budget simultaneously (Kotler and Armstrong, 2006).

Individuals may see consumer market as much bigger than the business (B2B) market place. In reality, however, B2B is much bigger than the B2C markets. All commercial markets, trade industries, government organisations, or institutions are involved either directly or indirectly in the B2B transactions. Some firms such as Satyam, TATA, IBM, Wipro, Logitech, Epson, HP, Canon, LG, etc. focus entirely on business markets, while some sell both to consumers and business markets. The B2B markets deal with organisational purchases of good and services to support or facilitate production of other goods and services, either to facilitate daily company operations or for resale.

Received: 12 November 2008
Accepted: 30 November 2009
*Corresponding Author

Moreover, Gupta, Jha and Gupta (2009), and Gupta (2008) stated that in today's fast changing world, everyone is flooded with data but the need of an hour is to convert these data to information which in fact will get transformed to knowledge and finally to wisdom for the organizations and all their stakeholders.

According to Reeder *et al*. (1991), all marketing strategies must begin with a thorough understanding of Organisation Buying Behaviour as this entails a different knowledge about buying situation, process, and criteria to apply when making purchasing decisions. Similarly, a good understanding of Organisational Buying Behaviour is fundamental for the supplier of an industrial firm in order to perceive how to satisfy customer demand in an optimal way (Batista and Forsberg, 1997).

Furthermore, Haas (1995) stated that organisational buying is not simply the action that someone takes. It is actually the outcomes of the interactions between purchasing professionals. Meanwhile, those who are involved in the process may in one way or another influence what is being purchased and supplied. The evolution of technology has changed the traditional way of business purchases. In today's world, new tools have opened a new era and new opportunities in every part of market. The arrival of the Internet as a multifaceted tool continues to change the performance of the organisations (Smith, Berry and Pulford, 1998).

Rational Nature of Business Market

Akin to consumer markets, organisations purchase to fill the needs. However, their primary need, i.e. meeting the demands of their own customers, is similar for all organisations. For instance, a manufacturer buys raw material, machinery, etc. to create company's products, whereas a wholesaler or reseller buys products to resell. The categories of business, markets can simply be defined as *Commercial market, Trade industries, Government organisations and Institutions.*

Furthermore, the Internet era has become a useful tool for businesses in today's era. The Internet provides products and their information to potential buyers and gives marketers the opportunities to make virtual catalogues, forms, product information, etc. available to everyone. Samli, Wills and Herbig (1997) stated that the WWW is expected to offer a much broader range of benefits to both suppliers and customers in the future, particularly due to the improved international communication generated by the Internet.

Unlike the traditional media, the Internet is characterised by interaction and it facilitates two-way communications as well. This means that people can, without any face-to-face contacts, still meet each other and manage their regular work such as communication, businesses and even negotiations.

According to Haas (1995), the way organisations purchase products is one of the most important questions to business marketing managers of today. The buying of goods and services by organisations is complex and difficult task to analyse. Over the years, many models have been developed in the attempt to explain organisational buying behaviour. Without the understanding of this, the marketing strategies and tactical programmes cannot be optimally developed. Haas (1995) further describes that it is the business marketing managers are the ones who are involved in this complex process with the following tasks:

- Describe the process by which customer organisations buy goods and services.
- Discover who in the customer organisations participate in this process and at what stage of the process each becomes involved.
- Find out what each of those people is seeking from the purchase, i.e. what are their buying motives?
- Discover what factors influence the interaction of the participants in the process.

Moreover, one cannot simply focus his/her effort towards purchasing departments of businesses, as he or she has to take care of the external factors along with whole decision makers' web. According to the Department of Information Technology, Electronics and Information Technology is the fastest growing segment of Indian industry, both in terms of production and exports. Today, the electronics industry is completely delicensed with the exception of aerospace and defence electronics, and along with the liberalization in foreign investments and export-import policies of the entire economy. This sector is attracting considerable interest, not only as a vast market but also as a potential production base by international companies. In recent times, 'software development and IT enabled services' have emerged as a niche opportunity for India in the global context. According to the Department of Information Technology (Annual Report, 2007-08), the Indian Information Technology sector showed a remarkable resilience in 2007. Continuing on its established track record, the overall Indian IT-BPO revenue aggregate was expected to grow by over 33 % and reach US$ 64 billion by the end of the current fiscal year 2007-08 as compared to US$ 48.1 billion in the fiscal years of 2006-07. The performance of the industry was marked by sustained double-digit revenue growth, steady expansion into newer service-lines and increased geographic penetration, and an unprecedented rise in investments by Multinational Corporations (MNCs), in spite of lingering concerns over gaps in talent and infrastructure impacting India's cost competitiveness.

Software and services

Global trade in services has entered a new era, with the growing and widespread acceptance of the IT-based global delivery model. International bandwidth and powerful workflow management IT software and services sector today is more easily penetrating into the fabrics of the society than ever before. It is now possible to disaggregate any business process, execute the sub-processes in multiple centres around the world and reassemble it, in near real time, at another location. India has already registered its mark on the globe in Information Technology – Business Process Outsourcing sector.

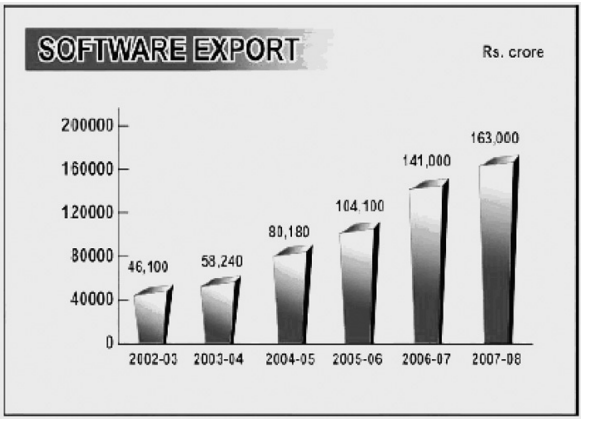

Fig. 1: Software exports from India
Source: Department of Information Technology, 2008

Fig. 1 presents Indian software and services exports including Information Technology Enabled Services, whereby its Business Process Outsourcing was estimated at US$ 40.3 billion

(Rs. 163,000 crore) in 2007-08 as compared to merely US$ 31.4 billion (Rs. 141,000 crore) in the fiscal year 2006-07, i.e. an increase of around 28.3% in dollars and 15.6% in rupees. Though the growth rate is numerically lower than that in the past few years, it is worth highlighting that this comes on the back of strong headwinds including an impending slowdown and a severe financial sector crisis in the US and a sharp appreciation in the value of the Indian Rupee (INR). Furthermore, an absolute value of incremental growth (US$ 8.9 billion) in exports is expected to be achieved by the industry this year is the highest ever achieved in a single year, in its history. This segment will also continue to show robust growth in the future.

While USA and UK remained the largest export markets (accounting for about 61 % and 18 %, respectively in FY 2006-07), the industry is steadily increasing its exposure to other geographies. In particular, exports to Continental Europe have witnessed notable gains, growing at a compounded annual growth rate of more than 55% over FY 2004-2007. Over 600 multinational companies are known to be sourcing product development and engineering services from their centres in India. The growing nature of responsibilities and ownership assumed by these India–based resources are helping India evolve into a strategic hub for R and D. Nevertheless, the Indian Information Technology–Business Process Outsourcing sector is not just about exports.

The overall Indian IT success story has also highlighted India's attractiveness as an investment destination. Another key impact of the global sourcing model popularized by the growth of Information Technology/Information Technology Enabled Services has been the reversal of the brain drain – as the people of Indian origin, as well as young expatriates, now feel motivated to work in India itself.

RESEARCH METHODOLOGY

The research methodology is exploratory in nature, since the research done here describes the influence of the Internet in the B2B Marketplace for IT Organisations in India. The data were obtained through an extensive study of secondary literature obtained from conference proceedings, libraries, the Internet, newspaper, journals, and magazines. Sampling method used is a judgmental sampling which in itself is a type of non-probability sampling. Moreover, the samples included reviews of around 530 available relevant literatures, out of which 77 have been included in the research paper. The scope of this exploratory research paper includes an in-depth study of the Indian IT Industry, B2B (Organisational) Buying Behaviour, and e-Procurement.

LITERATURE REVIEW

Introduction to Organisation Buying Behaviour

With the world growing smaller as a single market and the continuous competition within supply chains on the basis of time and quality, a certain strategy should be acquired in such a way that it helps the organization acquire a sustainable competitive edge (Hartman, 2007). According to Gupta (2008), the way businesses purchase products is one of the most important concern for business marketing managers of today. The buying of goods and services by organisations should not be considered as a simple action that is easy to analyse (Haas, 1995; Hutt and Speh, 1995; Webster and Wind, 1972). Organisational buyer tends to be influenced by a huge array of myriad forces coming from both inside and outside the organisations and their thorough analysis may help to build responsible marketing strategies. Over the years, great effort has been devoted for researchers to develop models as an attempt to explain the so-called Organisational Buying Behaviour (Banting, Beracs and Gross, 1991).

In 1967, Robinson, Faris and Wind published "Organisational Buying and Creative Marketing" which featured a model for the Organisational Buying Process and the Buy grid framework. Moriarty (1980) referred to it as one of the most useful analytical tools for both academics and practitioners interested in Organisational Buying Behaviour, while others simply referred to it as classic (Haas, 1992).

MODELS OF BUYING PROCESS

According to Haas (1995), the conceptual model of the Organisational Buying Process is described as an eight-stage model starting with *"using department requires a product or service"* and ending with *"follow-up is conducted with using department to determine if ordered product and services meet departmental expectation"* (ibid). However, this eight-stage model is widely known as Buygrid Framework. This particular framework compares the three buyclasses/ buying situations, with eight progressive stages in buying, or buyphases. The buyphases are an expression of the progression of thoughts and activities that a buyer goes through in the sequence of activities leading to a purchase (Robinson, Faris and Wind, 1967).

Meanwhile, the phases of the buying process are strongly interrelated. In practice, it may be difficult to identify when one phase ends and the next one begin. The three classes of buying are new-task, modified rebuy, and straight rebuy. Kotler (1984) provides a description of each buyclass and the operational implication of each classification, which ranges from the routine purchasing situation to the exceptional purchase.

According to Hutt and Speh (1995), an important factor in the industrial exchange process is to understand how the buying process is conducted. To achieve an optimal result in the interaction between companies, the selling company must understand the process being carried out by the organisational buyer. Hutt and Speh (1995) stress that Organisational Buying Behaviour can be best understood from the perspective of the decision process. In other words, organisational buying is seen as a process rather than an isolate act or event.

Morris (1992) defines the insight of looking at industrial buying process as "simple and yet, far-reaching." He further continues by describing this process as a logical sequence of purchasing-related decisions which have to be made in each stage. These stages take place over time, and more frequently over months or years (see Table ahead).

Organisational buying activities focus on the level of experience and information which are required for certain purchase of products or services. Making a routine purchase, the buyers need little information because of their past experience. When a purchasing situation is entirely new, information required may be extensive, and this is due to the firm's lack of experience with the products, services, or suppliers (Reeder, Brierty and Reeder, 1991).

During a buying process, a sequence of activities occurs. Tracing these activities has made it easy to uncover the critical decision phases and evolving information requirements of any buying situations. The buying process is usually described as a series of mental stages which include problem recognition, information search, information evaluating, purchasing decision-making, and post-purchase behaviour (Kotler, 1991). Reeder, Brierty and Reeder (1991) indicate that these are physically observable stages which turn to mental stages in the industrial purchasing decision process because of the involvement of several people in each phase. *Fig. 2* illustrates these stages which are further separated into eight significant phases, as follows:

1. *Anticipation or recognition of a problem need:* This stage begins with recognition of a problem/need or any potential opportunity which may originate when any equipment breaks down, existing materials are unsatisfactory, or products become outdated. However, it may also occur outside the buying organisation when the marketer recognises opportunities for

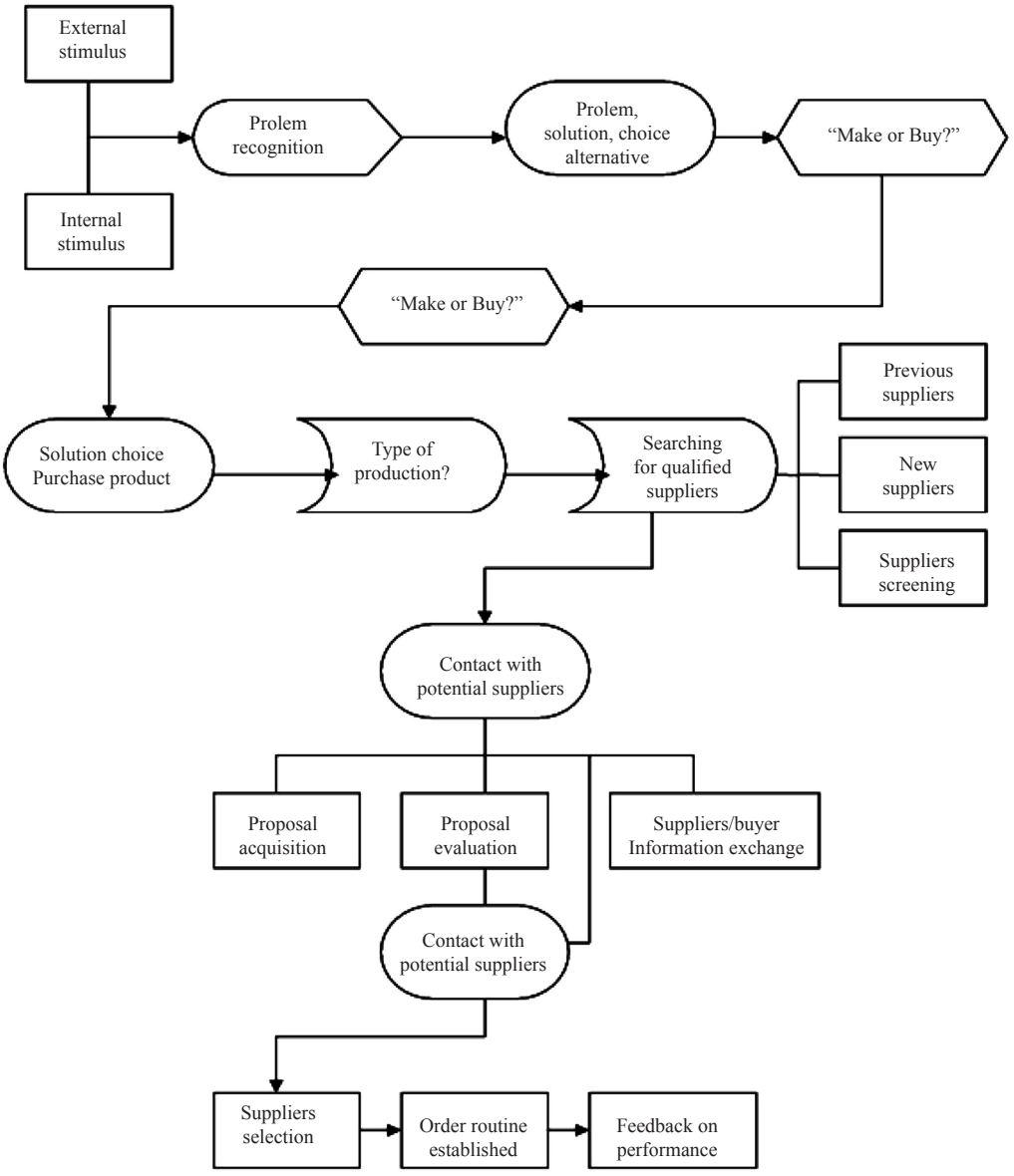

Fig. 2: The Purchasing Decision process in a new task situation
Source: Industrial Marketing, Analysis, Planning, and Control; Reeder, Brierty and Reeder (1991) Englewood Cliffs. N.J.: Prentice Hall, cop

potential performance improvement. However, those who recognise the problem or need will have a distinct advantage in influencing the final decision in term of selecting supplier.

2. *Determination of the characteristics and quality of needed item:* It refers to how the problem recognized in phase one has to be solved. Here, the buying organisation members have to specify the problems and solution alternative displays. The firm will seek answers to questions such as: "What performance specifications need to be met?" "What types of goods and services should be considered?" and "What quantities will be needed?"

3. *Description of the characteristics and quantity of the needed item:* It is often a critical phase for any marketer. It is often during this phase that the influencers prepare to affect specifications enter the purchasing process.

It is important to note that others will also be involved in the process while the buying influencers begin to look outside the firm suppliers and product information for assistance in developing specifications. At this phase, the suppliers have an opportunity to develop a relationship with the *influencers* that will give them opportunity towards their competitive.

4. *Search for and qualification of potential sources:* It describes the search process for alternative sources of suppliers. This leads to the qualification of suppliers which varies according to the type of buying organisation, the specific buying situation, and the buying influencers involved. An important issue at this phase is that decision-makers have determined *which suppliers* to be considered as *potential vendors*.
5. *Acquisition and analysis of proposal:* It is the phase where the bureaucracy process takes place. It is at this time where a request for specific proposal will be made and it takes several months to get exchanging of proposals and counterproposals done. In such purchase situations, the need for information is extensive, and a great deal of time is given to analysing proposals and comparing the products, services, and costs. It is also of importance to mention that phases four and five may occur simultaneously in case of straight rebuy. However, in more complex situations, phases four and five are separated and distinct.
6. *Evaluation and selection of suppliers*: When various proposals of competing vendors are analysed, the buying process will be terminated after that, i.e. if the firm decides to produce the needs by its own. Otherwise, negotiations may continue with selected suppliers on terms, prices, deliveries, or other aspects until the suppliers become vendor or vendors.
7. *Selection of an order routine:* It refers to the establishment of the order routines where the purchase orders will be sent to the selected vendors and the status report to the using department. However, the purchase process is not complete until the ordered items are delivered and accepted for use. The user department does not view its problems solved until the specified products or services have been received and they are deemed available for use. Thus, this particular phase is critical for the suppliers.
8. *Performance feedback and evaluation*: This is the final phase of the buying process and it consists of formal and informal reviews, as well as feedback regarding the performance of the delivered item, and the vendor's performance. The user department will evaluate whether the purchased item has solved the initial problem and/or needs. If it does not, suppliers who were screened earlier might be given further consideration. Feedback given can cause various members of the decision-making units to re-examine their positions.

DESCRIPTION OF BUYING CENTRE

It has been widely acknowledged that organisational purchasing involves different participants (Wind and Thomas, 1980). This is one of the major features which make it a complex problem (Webster and Wind, 1972). "One approach towards understanding purchasing in business is to fetch the decision process as involving a number of roles, rather than simply a set of individuals or departments" (Morris, 1992).

The Buying Centre

Webster and Wind (1972) stated that the composition of this buying centre varies according to the buying situations and it is also dependent in great part on the nature of the buying task and

the structure of the organisation that makes purchase. Bonoma and Johnston (1981) claimed that within the buying process and industrial services, no two purchases in any given company are alike and no two companies in a similar buying situation follow the same pattern. However, the buying centre exists as a communication network which does not necessarily resemble the formal organisation. They further explained that five different dimensions which could be identified when the group of individuals which form the making-decision unit gets involved in a particular purchase. These *five* dimensions are as follows:

- Vertical involvement
- Lateral involvement
- Extensivity
- Connectedness
- Centrality of the purchasing manager

Fig. 3 presents a conceptual picture of an organisation's buying centre for a specific hypothetical purchase. According to Morris (1992), all these dimensions have important implications for marketers. He further states that the more vertical the levels involved, the more influence those at high levels have in the buying decision. Greater Lateral involvement shows less formality and involves more conflict. Extensivity is defined as 'a concern' as the complexity and duration increases with it becoming more difficult for the marketer to reach those persons involved in the decision process. Meanwhile, connectedness is also of importance as it depends on that the marketing message has to be communicated separately to some of the members of the Buying Centre. It is also suggested that connectedness may help to identify the 'central players' in the purchase. Finally, centrality is regarded as relevant in the process.

According to Webster and Wind (1972), members in the buying centre may assume different roles throughout the purchasing process. The identification of the roles they play in this decision unit will help to better understand the nature of interpersonal influences in the buying centre. In the same year, they settled the existence of five different roles performed by different participants in the buying centre. These are Users, Influencers, Buyers, Deciders, and Gatekeepers.

In their review of the state-of-the-art of the Organisational Buying Behaviour, Wind and Thomas (1980) stated that the general findings obtained up to the moment on the composition of the Buying Centre showed that it might vary by organisation and, even in a given organisation, by buying situation and other specific characteristics.

According to Mattson (1998), identification of these roles can be difficult when it comes to purchasing services. However, it is very important that all the individuals involved in the buying process be identified and that the kind of influence exerted by each one be understood.

According to Webster and Wind (1972), it is quite likely that several individuals will occupy the same role within the buying centre, and that one individual may occupy two or more roles. The authors further assert that all members in the buying centre could be seen as influencers, but not all these influencers would occupy other roles. The roles in the buying centre which have been identified by Webster and Wind (1972) are: Users, Influencers, Buyers, Deciders, and Gatekeepers. In order to visualise the influence of these defined roles in the buying process, the author have also present their definitions in the form of a table (see Table 1).

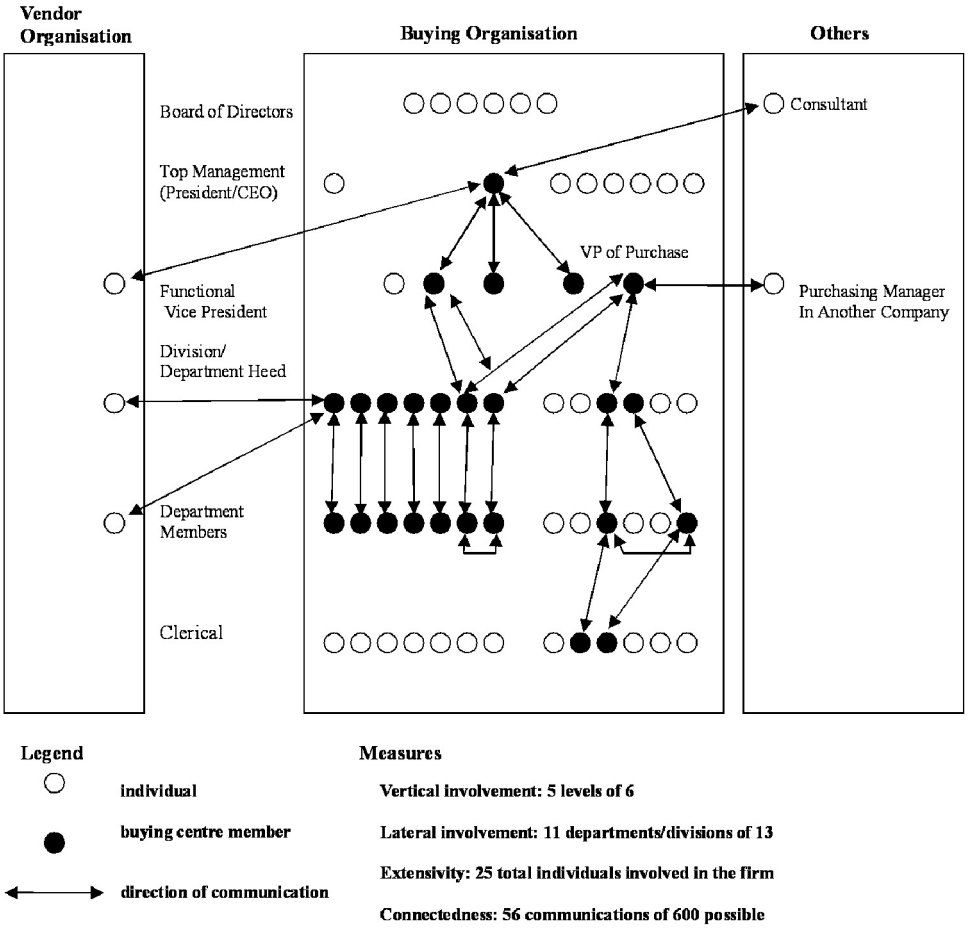

Fig. 3: A communication picture of a Buying Centre
Source: The Buying Centre Structure and Interaction Patterns; Bonoma and Johnston, 1981

TABLE 1
Roles and decision stages in the Buying Centre

	User	Influencer	Buyer	Decider	Gatekeeper
Identification of Need	χ	χ			
Establishing Specifications and Scheduling the Purchase	χ	χ	χ	χ	
Identifying Buying Alternatives	χ	χ	χ		χ
Evaluating Alternative Buying Actions	χ	χ	χ		
Selecting the Suppliers	χ	χ	χ	χ	

Source: Organisational Buying Behaviour; Webster and Wind (1972), Englewood Cliffs. N.J.: Prentice-Hall

FACTORS THAT INFLUENCE THE ORGANISATIONAL BUYING BEHAVIOUR

The organisation buying behaviour is influenced by a wide array of forces both inside and outside that particular organisation. Knowledge about these factors provides the marketers a good understanding of their buyers' behaviour, which is necessarily to plan and build up a strategic market plan (Hutt and Speh, 1995). Therefore, the main point of this section is to review some literatures devoted to study of the factors influencing the organisational buying process and the buying centre. Webster and Wind (1972) classified various influences on Organisational Buying Behaviour. Meanwhile, Hutt and Speh (1995) describe these influences as the forces which are further divided into several sub-influences. However, this paper focuses on only the influences which are directly linked to the buying decision.

There are six types of environmental forces which influence the Organisational Buying Behaviour, namely economical, political, legal, cultural, physical, and technological.

1. Economical influences: The general condition of the economy is reflected in economic growth, employment, price stability, income and the availability of resources, money and credit.
2. Political influences: The political factor refers to the government attitudes towards business and social service activities.
3. Legal influences: The legal part includes the forces at the state and the local levels specifying the boundaries of the buyer-seller relationship.
4. Cultural influences: The habits, norms, customs, and traditions passed on from generation to another influence the structure and functions of the organisation in various aspects.
5. Physical influences: The geographical location and climate of an organisation are the factors which are included in the physical influences.
6. Technological influences: The changes in the technology can restructure the buying plan of an industry and organisation. "The technological environment defines the availability of goods and services to the buying organisation and, in turn the quality of goods and services that the organisation can provide to its consumers" (Hutt and Speh, 1995). This influences the composition of the decision-making unit in the buying organisation. Increasing the technological changes declines the importance of the engineering personal which tends to increase in the organisation.

An understanding of the organisational hierarchy and the relationship between the purchasing department and other departments provides information on interaction, relation, and behaviour in the buying organisation. The four factors which create the organisational forces are:

1. Organisational climate: The organisational climate refers to the health or sickness of an organisation. Different organisational climates can be observed in two competitive organisations of comparable size.
2. Organisational positioning of purchasing: This factor refers to the type of organisational structure. Here, the main task is to position the purchasing department or just to identify where the purchasing decisions are made. The appearance of the purchasing department provides the necessary information to identify if the purchasing is centralised or decentralised.
3. Centralisation versus decentralisation: These two types of organisational structures differ practically. Centralisation leads to specialisation, whereas knowledge about the suppliers increases and personnel involved in the buying process develop their skills. Centralisation

refers to long-term relationship while decentralisation is made for the short-term relationship with the supplier.

4. Contributing factors of Centralisation of Procurement*:* There are several factors which strongly point out the reasons for a centralised purchasing unit. These factors include commonality of requirements, cost-saving potential, structure of supply industry, and involvement of engineering in purchasing. All the contributing factors provide the buyer with a more efficient way of purchasing. However, the nature of the supplier can also determine whether purchasing is centralised.

   Even though the Purchasing Manager is making buying decision independently, there are people who may influence him or her during the buying process. People involved in this complex process will have their opinions which will affect the process on the whole. These people form the Buying Centre, i.e. those or all organisational members who are involved in the purchasing decision. Influences which have been recognised in the Group Forces area are among the influences on the buying centre.

   Since individuals in an organisation are the ones making decisions and not the organisation, and that each member of the buying centre has a unique personality, it is therefore important to review and understand the influences which they have on individuals. These influences are bounded to situations and elements which emerge during the buying process. These situations and elements are differing evaluation criteria, understanding the reward and measurement system, responsive marketing strategy, information processing, selective processes, memory, external memory, risk-reduction strategies, anticipating perceived-risk level, and individual versus group decision making.

Product-specific factors*:*

1. Perceived risk. The higher the level of perceived risk, the greater the likelihood that the decision made will be.
2. Type of purchase. New-task buying situations are more likely to involve group decision making (for example, a first-time purchase of a computer)
3. Time pressure. With minimal time constraints, group decision-making becomes more feasible.

Company-specific factors:

1. Size. Large companies tend to use group decision making.
2. Degree of centralisation. The more decentralised an organisation, the more likely decisions made by a group will be.

In every decision taken, there are always factors which have effects and influences on the process. Thus, understanding the influences on the buying decision is of importance for the Marketing manager because having a sound understanding about how and why the buyer selects a specific product will make it easier for the marketer to introduce and sell the product (Kauffman, 1996). Webster and Wind (1972) described and discussed four influencing factors for the purchasing situations. The four factors are divided into two sub-groups, namely task-related and non-task related (see Table 2).

TABLE 2
Influence factors in buying decision

	Task related	Non-task related
Individual	To make cheap buy	Personal valuation and needs
Social		Informal discussions
Organisational	Policy regarding the suppliers	Evaluation methods about the own purchasing personal
Environmental	Expected price change	Political climate

Source: General model for understanding Organisation Buying Behaviour; Webster and Wind, 1972

Individual influences: The individuals are the targets for the marketer within the purchasing organisation. These are the ones who actually make the buying decision. The psychological facts direct the process depending on their positions and the buying situation. The buying motive is a combination of the individual and the purchasing organisation's goals. Understanding who are involved in the buying process and their roles inside the organisation is a vital thing to take into consideration, into the market strategy in business marketing.

Social influences: Understanding the interaction between those who are involved in the buying process is also crucial in order to get a clearer picture of the buying behaviour. First, the roles have to be identified, and secondly, the variables influencing the interaction among the individuals inside the purchasing organisation as well as the interaction between the individuals as a group and the external individuals.

Organisational influences: The organisation factors of importance in purchasing decisions include Goals and Objectives, Structure, Policies and Procedures, and lastly Resources. Goals and Objectives will determine to a long extent, the attributes stressed in the buying decision process, and in a more indirect way, may also influence the composition of the Buying Centre (BC). The Structural factor often refers to the level of centralisation or decentralisation and it may also be related to the Policies and Procedures implemented for making purchase decisions. Finally, constraint Resources (such as company size, net assets, technical and managerial capabilities, amongst others) may also have impacts on the buying decisions.

Environmental influences: Environmental factors include everything outside the organisation. This is further divided into six different groups of interaction, namely Physical, Technological, Economic, Political, Legal, and Cultural, which are generated by many types of organisations (labour unions, government, suppliers, customers, trade associations, professional groups, other business and social institutions). According to the model, the flow of information into the Purchasing Firm, the availability of goods and services, general business conditions, and values and norms are the results of these variables.

Susan Lynn (1987) presented a result of a study which had analysed the structure of a buying centre for purchasing of professional services. This study was based on a mail questionnaire to survey Chief Executive Officers (CEO), Chief Financial Officers (CFO), and Controllers in 556 businesses firms regarding the structure of the buying centre for professional services in their

firms. The study revealed that decisions were more often jointly made in large companies and independently made in smaller companies. When influence was measured either as the average number of decision steps at which different participants were involved or as the average influence of different participants across all decision steps, the results yielded the followings in order:

Most Influential Buying Centre Members

CEO, CFO and Chairman of the Board of Directors.

Less Influential Buying Centre Members

Other Board Members, individuals involved in the financial functions of their organisations (Treasurer, Internal Auditors, and Controllers) and outsiders (e.g. corporate attorney, banker, and underwriter). The findings also indicated that the influence of different buying centre members varies in business firms with different characteristics. In smaller firms, the CEO and the Corporate Underwriter are more influential, whereas in the larger firms, the Audit Committee and the CFO are more influential with different types of power, as illustrated in Table 3 below.

TABLE 3
The bases of power

Type of manpower	Champion	or	Veto
Reward: Ability to provide monetary, social, political or psychological rewards to others for compliance	●		
Coercive: Ability to provide monetary or other punishments for non compliance	●		
Attraction: Ability to elicit compliance from others because they like you	●		●
Expert: Ability to elicit compliance because of technical expertise, either actual or reputed			●
Status: Compliance-gaining ability derived from a legitimate position of power in a company			●

Source: Major Sales: Who really does the buying; Bonoma (1982). *Harvard Business Review*

PROCUREMENT

The review of literature further identifies many advantages and opportunities from the field of procurement or e-procurement. In the commercial arena, an organisation will procure goods on electronic way only if it sees enough benefits which can be gained from the e-procurement. Moreover, an organisation must take very careful steps to prepare business processes for successful implementation of its e-procurement (Podlogar, 2006).

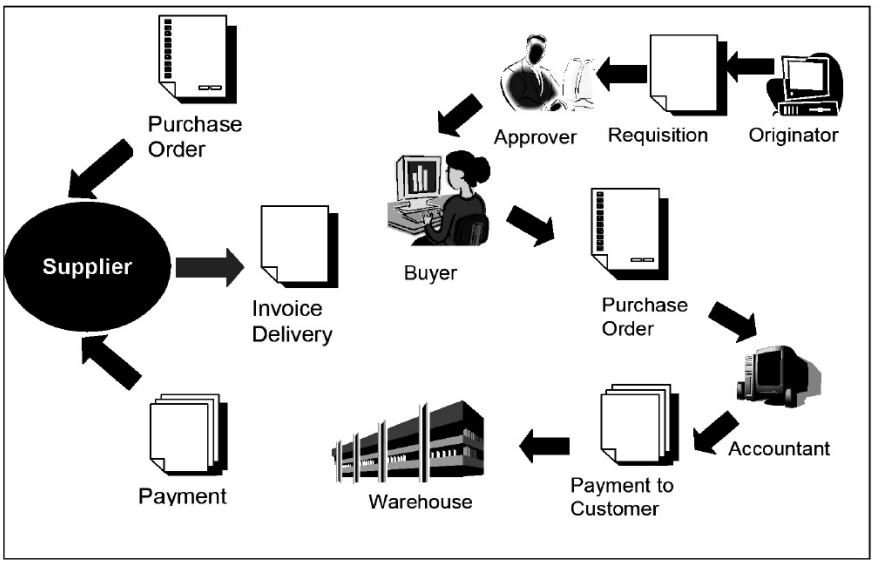

Fig. 4: Key procurement activities within an organisation
Source: Adapted from Chaffey, 2004

The purchasing function should obtain the proper equipment, material, supplies and services of the right quality, in the right quality, at the right price, and from the right sources. In this description, the purchasing function is regarded primarily as an operational activity (Weele, 2002). Meanwhile, procurement refers to all the activities involved with obtaining items from a supplier, and this includes purchasing, and also inbound logistics such as transportation, goods return, and warehousing before the item is used. The key procurement activities and associated information flows within an organisation are shown in *Fig. 4*.

Procurement Process and Activities

The primary job process of procurement is indicated by NECCC (2002) as follows:

- Search for products and services needed by the organisation
- Handle myriad details relating to their requisition
- Approval
- Payment
- Taking responsibility for the delivery of the host of items about which they may or may not know very much

The procurement process is labour-intensive, dominated by paper, and is often centralized and subject to countless costly inefficiency due to re-keying, changing prices, product sets and personnel. According to Dobler and Burt (1996), the purchasing function consists of some essential activities associated with the acquisition of the materials, services, and equipment used in the operation of an organisation. The procurement process encompasses a wider range of supply activities than those included in the purchasing function. In addition, it typically includes a broadened view of the traditional buying role, with more buyer participation in related materials activities (salvage of surplus and scrap) (Ibid). Specific activities usually included in the process are:

- Participation in the development of material and service requirements and their specifications
- Conduct of materials studied and management of value analysis activities
- Conduct of more extensive material market studies
- Conduct of all purchasing function activities
- Management of supplier quality
- Purchase of inbound transportation and management of investment recovery activities

E-PROCUREMENT

Traditionally, procurement involved a number of communication mediums to facilitate the procurement process between the various parties. These included the use of mail, phone, and fax, EDT and more recently, email and the Internet. Meanwhile, e-procurement means that electronic communications are used to support all the transactions which facilitate the procurement process (NECCC, 2002).

Benefits of e-Procurement

An e-procurement solution provides access to, and easy purchasing from, catalogues of many different suppliers while eliminating paperwork, automating the approval process and enforcing the purchase polices which apply to each buyers' suppliers (ITRG, 2002). Cost saving is a typical main motivator for companies to implement e-procurement. As cost per transaction using e-procurement is reduced by 65%, as compared to the "traditional" procurement transaction.

According to ITRG (2002), many companies have found immense benefits from their e-procurement projects, including the following:

- Process efficiencies amounting to annual savings
- Ability to link into existing systems, such as ERP
- Reductions in lead times within the procure-to-pay cycle, in some cases by 50%
- Self-invoicing on behalf of clients can add to the bottom line
- Month-end reconciliation can end the problem of wrong items being ordered or wrong prices being offered as business processes have been streamlined and all are working off the same catalogue.

The buyer is engaged in more strategic product management, leading to:

- Better contracts being negotiated
- Maverick spending is reduced
- Reduction at stock levels can lead to savings of millions of dollars

Companies which have experienced these benefits have reduced cycle times and thus are able to manage relationships with their global suppliers much better. E-procurement technology has also enabled a company to reduce the number of interfaces it maintains with the supplier. The business case for e-procurement is compelling. With the number of cost-effective e-procurement

solutions available today, purchasing organisations cannot afford to miss the opportunity to increase profits for their organisations. To make the proposition even more attractive, service providers offer hosted e-procurement solutions which can be inexpensively deployed with little time or effort, while eliminating the burden of on-going maintenance or support. E-procurement benefits stem from automating procurement activities and streamlining purchasing workflow, both internally and with their vendors (ITRG, 2002).

According to Davila *et al*. (2003) and Presutti (2002), the benefits of e-procurement include:

- Cost saving
- Process efficiency
- Better information flow between buyers and supplier
- Reduced Maverick spending
- Streamlined process and better inventory level

Cost saving is the primary rationale for investment across all technology platforms, through the manner in which these delivered savings vary. Adoption of e-procurement technologies reported saving of 42% in purchasing transaction costs (Davila *et al*., 2002).

More importantly, companies using e-procurement reported saving of 42% in purchasing transaction costs associated with less paperwork which could be translated into fewer mistakes and a more efficient purchasing process. In terms of labour intensive, paper-based purchasing process, transaction costs could range from $70 to $300 per purchase order, for example, GE (General Electronic) saw those costs dropped to 30%. Other firms have experienced even greater reductions (Presutti, 2002). Different authors have elaborated on the benefits which are accrued from adopting e-procurement technologies. These benefits are expected to accelerate the rate of adoption of these technologies once the uncertainties which remain around e-procurement are reduced to levels that encourage significant resources commitments leading towards higher process efficiency (Davila *et al*., 2002).

The more complicated the old paper-based procurement processes, the more authorization stages and exceptions, and therefore the higher the savings will be. To take advantage of these potentials, the procurement process needs to be redesigned. In successful practices, this revamp focuses on:

- Reduction or elimination of authorization stages
- Regulation of exceptions to a limited degree at the beginning
- Elimination of paper
- Integration of suppliers in the entire process chain and consideration of the complete process, from searching for articles through to invoicing (Ibid)

Given the intense publicity surrounding the impact of e-procurement, Croom (2001) states four main benefits of e-procurement, as follows:

- Financial performance, but not as much as widely ‘hyped’ benefits promoted in the press,
- Improved information flow,
- Improved internal and external communications, and
- Improvements in planning and control

Then, the researcher continued to state that a major concern is the apparent lack of clear strategic awareness of the implications and benefits of e-procurement (Croom, 2001).

E-PROCUREMENT IMPLEMENTATION SUCCESS FACTORS

In today's economic climate, cost containment and organisational efficiency are critical to a company's success. E-procurement, i.e. the automation of a firm's procurement process, is becoming increasingly recognized for its ability to improve business operations and reduce expenses. Like any other technology-based systems, however, it may have little effects if not carefully implemented and managed.

Based on his observations, Chiravolo (2004) listed the following key success factors:

1. Obtain top management support to encourage acceptance throughout the organisation, and establish baseline metrics.
2. Undertake a "strategic sourcing" effort prior to system implementation.
3. Do not simply mirror your manual purchasing process.
4. Begin your roll-out with areas of spending that offer the largest and fastest return-on-investment.
5. Never stop measuring results and refining processes.
6. Communicate, communicate, and communicate.

Once limited to the acquisition of goods, e-procurement has been proven to be effective with regard to services, including those related to human capital. Its powerful management capabilities enable companies to strike a purposeful, proactive, and cost-effective balance of fixed (core) and variable (contingent) workers. A well-planned and executed workforce management strategy — one that combines technology and continuous collaboration with talent providers — can directly impact bottom line results and contribute to the achievement of business objectives.

The benchmarking study conducted by Puschmann and Alt (2005) showed that companies which successfully implemented e-procurement rely on proven concepts regarding introduction, organisational change, content and catalogue management, procurement processes and system architecture, in order to achieve operational efficiency. These successful practices demonstrate that e-procurement is merely a non-technical issue. The effort undertaken to implement e-procurement as a strategy is mostly spent on organisational aspects and the redesign of procurement processes rather than on technical questions. All successful practices implemented a globally oriented commodity coordination board to agree upon the products purchased via the e-procurement solution. The strong decentralization of the procurement function in large companies is a barrier to achieving synergies from pooling volumes at a corporate level. In particular, e-procurement has enabled companies to gain greater transparency over their procurement portfolio with the availability of more detailed data (Ibid).

An e-procurement solution plays a fundamental role in the transition of procurement to e-procurement by streamlining the buying process and providing the information needed to make more intelligent purchasing decisions. According to the Cisco Systems (2002), an effectively implemented e-procurement solution can:

- Reduce paperwork and redundant effort, improve productivity, and lower the cost involved in purchasing process
- Enable companies to locate suppliers with the best prices and quality and help streamline negotiations and contracting
- Take full advantage of an enterprise's buying power by enabling it to qualify for volume discounts and ensure that purchases are made through preferred suppliers
- Streamline and automate purchasing through critical suppliers to enable more timely and accurate order fulfilment

Table 4 illustrates the impact e-procurement has on enterprise compliance and spend management initiatives. Performance improvements recorded map very closely to Aberdeen Group's (2004) previous benchmarks, indicating that e-procurement is consistently delivering on its initial value proposition.

TABLE 4
E-procurement impact (Average Performance)

Performance area	Before e-procurement	After e-procurement
% of spending that is off-contact ("maverick)	38%	14.2%
Price savings on maverick purchase brought	-	7.3%
Requisition —to-order cycle	20.4 days	3.8 days
Requisition —to-order cost	$56	$23
% of spend used under management of the	56%	69%

Source: Adapted from Aberdeen Group, December 2004

The Importance of e-Procurement Systems in the B2B Market

According to Gupta and Gupta (2009), business-to-business markets involve more rational nature of buyers rather than impulse buying in case of business to customers. Thus, organizations should also focus on these aspects by following proper procurement tactics, synergies and strategies, as framed by organizational top management keeping in mind the strategic position of the organization.

Recent improvements in the Internet technology connectivity provide an opportunity to make procurement for goods and services more transparent and efficient. When used for public procurement, information technology can be utilized as a mean to achieve the main principles of perfect competition, namely, access to information, no barriers to entry (transparency), and a large number of participants in market exchange (Crayannis and Popescu, 2005). On the other hand, globalization is an irreversible process, and it relates to the increased freedom and capacity of individuals and firms to conduct economic activities with residents of other countries. The driving forces of globalization are related to the reduction in barriers for conducting business with foreigners, and fast reduction and convergence of transaction costs via advances in "transport of information" (Braga, 2002). Braga (2002) further emphasizes that the new wave of globalization, driven by technological advance in transport and communications technologies, has led to a better investment climate in developing countries since 1980.

The use of information and communication technologies (ICT) in developing countries may not be fully benefiting them due to the poor access to information to complement economic policies, in order to boost efficiency and enhance market integration (Treaty establishing the European Community, 1957; Gibson and Ward, 2000; Everard, 2000; Dutton, 1999; Commission Directive, 2001; Cafiero, 1996; Bimber, 1999; Barber, 1998; European Commission, 2000; Arunachalam, 1999; Albarran and Goff, 2000).

Taking advantage of the emerging information technologies requires policies similar to those needed for opening the market and free trade. For example, creating a modern public procurement is a part of the process of an efficient, and a competitive market economy which is necessary for these countries' full integration into the global community. In this respect, information and communication technologies can help to achieve a competitive environment (open bidding), provide opportunities for the private sector (free access to public information), government transparency,

and eliminate a country elite's hold on the key sectors of the national economy (Crayannis and Popescu, 2005).

Procurement is an integral part of B2B processes and an essential part of any organisation's ability to function effectively. Nevertheless, it has only recently emerged as an important topic within the fast growing B2B e-commerce market. An e-procurement B2B system is an open system which enables the organisation to reach and transact with suppliers and customers in the virtual markets (Bakos, 1992). With the introduction of cheaper web-based B2B e-commerce technologies, online procurement has become commercially feasible today (Data monitor, 2000). In particular, the online procurement market is of great significance since it offers opportunities to a different range of companies from those which have implemented electronic data transfer (EDT). Moreover, e-procurement is a user-friendly, and Internet-based purchasing system which offers electronic purchase order processing and enhances administrative functions to buyers and suppliers, resulting in operational efficiencies and potential cost savings (Erridge *et al*., 2001).

The key and broadly accepted principle underlying a modern public procurement system is open competition—unrestricted, universal access to the procurement market. In addition, the procurement process which includes the selection of bidders, tendering procedures, and the award of contracts, should be open to public examination and review, thus making it a transparent process. For instance, to promote transparency, the procurement process should be made open to public scrutiny. This places a heavy burden on the procurement entity within the line ministry or the local authority to award contracts which use taxpayers' money in the most efficient way possible. The transparency of the process is further reinforced when contract awards, and the overall procurement process itself, is subjected to the scrutiny of national parliaments, external audit bodies, and the media (Crayannis and Popescu, 2005).

E-PROCUREMENT PROCESS

The benefits of e-procurement technology will not be apparent if only an automation of existing methods of working is available. To gain the benefits of reduced costs, better sourcing and so on, it is essential that a re-engineering of the procurement process be undertaken. As a result of implementing the Internet-enabled procurement technologies, organisations have found that their supplier relationships are redefined, and that the number of suppliers is generally reduced. Hence, supplier consolidation must be planned for prior to the implementation of the e-procurement technology. In addition, companies should gather input from stakeholders throughout the organisation, since they are likely to be affected by the re-engineering of the procurement process (Rajkumar, 2001).

An organisation must take very careful steps to prepare business processes for successful implementation of e-procurement (Poldgar, 2006). According to Podloger, simplicity is one of the most important e-procurement factors, in a way that organisations have to organize themselves to ensure success. By knowing such factors, organisations will be better prepared for e-procurement and thus operate successfully to be able to compete in the global market.

Michael Shaw believes that the B2B e-Commerce systems provide economic value and it can also be argued that they provide value to process re-engineering. However, it is important to note that e-procurement is not an example of re-engineering old manual processes but a re-engineering of process itself (Sheng, 2002). Actually, Business Process Re-engineering is the redesigning of work activities in order to meet a specific set of requirements.

Kalakota and Robinson (2001) believe that for many companies, development of a truly effective integrated procurement strategy is still in the future. Relatively, a few firms have a clear vision of what they must achieve when re-engineering and integrating their procurement processes.

In the following section, some facts related to process re-engineering which are strongly connected process simplification, from prior published research results, are explained:

Awareness of Technology Opportunities

Literature indicates that many organisations' e-procurement processes with their suppliers are organized in numerous arrangements. First, these processes have to be re-engineered, uniformed, incorporated to collaborative processes, and which will then enable successful e-procurement and, in turn, give access to all data at the time when all business partners need them (ActivMedia Research, 2000; Athabasca University, 2002; Chan and Swatman, 1999; European Commission, 2000; Lindemann and Schmid, 1998; Ody, 2001a; Ody, 2001b; Podlogar *et al*., 2001; Pucihar, 1999; RIS, 2001; Segev *et al*., 1998; Sterle, 2001). With an emphasis on technology and process complexity and compatibility, growing technology opportunities are the most important issues in organizing e-procurement (Chan and Swatman, 1999). Organisations that are healthier in terms of information technology also have a better organized e-procurement (Segev *et al*., 1998).

Ability to Achieve Process Effectiveness

It is important to achieve better control and process tracking of the whole procurement process (European Commission, 2000). Organisations spend billions of dollars for additional costs annually to improve e-procurement effectiveness (Ody, 2001a; Ody, 2001b). Implementing process re-engineering requires removing processes which contribute no added value. It is also important to choose the software and hardware which will/can offer effective support to enhance business processes (Lesnicar, 2002; Sterle, 2001).

Readiness for e-Procurement Collaboration

Organisations want to have e-procurement because they can improve process effectiveness by closely collaborating with all their supply chain business partners. Collaboration is improved, especially through e-commerce and process reengineering, in addition to reviewing an organisation's internal processes, including processes review of activities outside its borders. Implementing collaborative e-processes requires endeavours increase their inputs to improve organisation and business development, and to perform e-procurement (European Commission, 2000). Process re-engineering is necessary for achieving process simplification. Some process simplifying factors which are resulted from the literature review are explained in the subsequent section.

Satisfaction and Positive e-Procurement Experiences Sharing

If e-procurement system provides a pleasant service, buyers will take the view that the experience is positive and simple to use. Benefits and simple e-procurement contribute to a positive perception of e-procurement, which will gradually lead to actual use (Chen, 2000). In practice, successful organisations are the ones which succeed in process simplification with the help of suppliers. It is also important to share savings which are resulted from improvement, with suppliers (win-win situation). This kind of business leads to closer and longer connections with business partners (Komp and Leonard, 1999).

Environment Changing Response

Process simplification leads to a great deal of e-procurement opportunities, particularly because organisations have to react quickly towards a changing environment (such as demand variability), as well as goods and process changes (European Commission, 2000).

- e-Procurement Process Type
  For buyers, it is most important to simplify the following processes: goods availability (goods need to be at hand when a buyer needs them), order cycle, data retrieval, order adaptability, goods receiving, order mistakes dismissing, damaged goods returning, reserved parts availability and technical support (Komp and Leonard, 1999).

- e-Procurement Participants and Its Accessibility
  e-procurement processes allow participants to easily change rules and eliminate some business partners through the whole supply chain, by for example undertaking direct e-procurement from the supplier without other partners, thereby simplifying the whole e-procurement. Generally speaking, however, it is difficult to determine if the total number of participants in the whole supply chain will decrease (Mesenbourg, 2002).

In 2004, a case study concerning the analysis of the Greek governmental purchasing process was carried out by Panayiotou *et al*. (2004), as shown in *Fig. 5*. A set of performance indicators was defined including the mean cycle times, transaction volumes (quantities, values, number of requests, and tenders) and organisational unit capacities. The results of the analysis guided to the re-engineering suggestions at three levels of changes and to the design of the new process with the use of process charts. The functional specification definition was based on the new system design and the overall findings of the analysis. Public sector organisations usually face different challenges than those of the private firms.

In more specific, they have to meet multiple, often conflicting goals, and they are also subject to constraints of financial, legal, contractual, personnel, and institutional nature (Cilek *et al*., 2001).

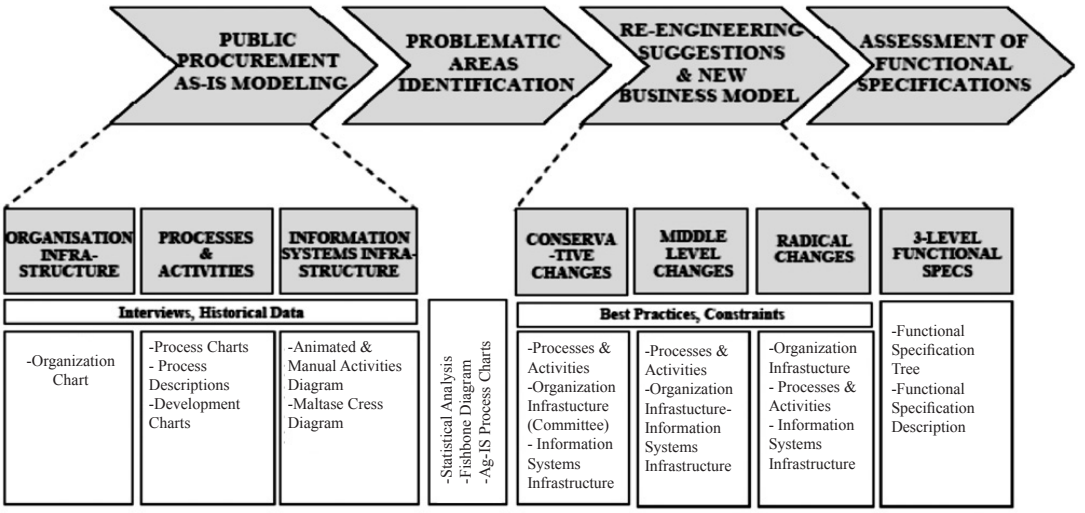

Fig. 5: Methodology for the assessment of functional specifications
Source: Adapted from Panayiotou *et al*., 2004

These constraints are normally much more binding than they are in the private sector. For example, there is probably no possibility to reduce the number of staff according to a new situation due to legislative constraints (Kock and McQueen, 1996; Luck and Peabody, 2000). The radical

process-focused change in the public organisations can only be achieved with deep changes in their bureaucratic practices. This, in turn, is normally not achieved without either change in the law or privatization (Jensen, 1991; Mechling, 1994).

In short, the three introduced areas involved in the research (i.e. Business Buying Behaviour, IT organisations, and the Internet) can clearly be separated from each other and at the same time, the relation between them can be seen *(Fig. 6)*. As discussed in the earlier section, Business Buying Behaviour is a complex and dynamic process which requires plenty of information. However, the Internet has provided both the seller and the buying company the opportunities and access to information and this eases the way to find whatever is required. At the same time, this communication tool is threatening to change and influence the way businesses are conducted. Therefore, marketers have to identify the reasons to, and have an understanding of, how the influence of the Internet can affect different processes.

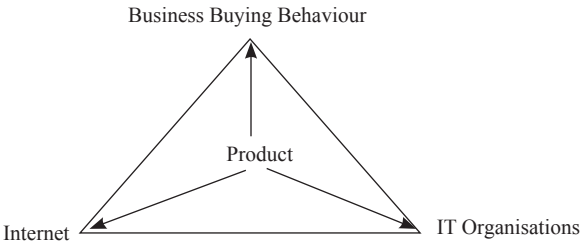

Fig. 6 : IT-B2B-Internet Interaction Model
Source: Gupta, Jha and Gupta, Department of Management, Birla Institute of Technology, 2008

CONCLUSION

In recent years, the growth of the IT Industry in the B2B markets is all set to give a breakthrough in the Indian economy. With relatively competitive budgets and high profit margins, the situation calls for smart and strategic Internet optimization which can help a business to create and enhance its organisational buying.

In this study, three areas were included and investigated: the organisational buying behaviour, the IT organisations and the Internet, based on which the influence of the Internet on the B2B Buying Process with reference to IT organisations in India. According to the study, the buying of goods and services by organisations involves a complex set of interactions, which altogether form the organisational buying behaviour. This involves buyphases and buyclasses. The buyphases, being Anticipation/Recognition of the Need/Problem/Opportunity, include a general solution, Identification of the Characteristics and Quantity of the Product/Service, Description of those Characteristics and Quantity in detail, Search for and qualification of Potential Sources/ Vendors, Request for Proposal/Quotation, Acquisition of Proposals, their analysis and Evaluation, Negotiation and selection of vendor/s, Finalisation of the specific order routine, order status feedback and evaluation of performance, whereas buyclass constitutes of New Task, Modified rebuy and Straight buy.

There are six roles performed by the members of a buying centre. These roles are User, Analyst, Influencer, Purchaser, Engineer and Decision Maker. Now, members of the organisational buying centre also take care of certain factors such as:

- Experience of vendor/supplier
- Relationship and past experience with vendor/supplier
- Geographical location of the vendor/supplier
- One-to-one (face-to-face) contact during buying process
- Internet communication
- Legal issues in purchasing through the Internet
- Cost of product/service

Meanwhile, the influence of the Internet on the overall Purchasing/Buying activity can be seen in terms of:

- Information Gathering – Collecting Product/Service information and specification, Collecting information of current vendor, Searching and Collecting information of new vendor, Collecting competitive and other information for purchase and Cost/price comparison.
- Inter organisational information exchange – Email, Web conferencing with Vendors, Electronic Data Interchange (EDI), Discussion Groups and Just in time inventory planning.
- Negotiation, Bidding and Payment – Online Negotiation, Bidding and Payment.
- Online Ordering – Online ordering, status checking and product/service support.

The perceived influence and benefits of the Internet during buying/purchasing cycle include:
Ease of use - Availability of updated information, easy movement across and around websites, prompt online ordering, and prompt query handling.

Ease of price and product/service comparison - Get the lowest price for product/service purchase, easy comparison of the products/services from several vendors, easy price comparison from several vendors and the ability to obtain competitive and educational information regarding product/ service.

Ease of information access and exchange - Increase in the speed of information gathering from vendor and increase in the speed of information dissemination within the same organisation (between and within departments/ colleagues).

Reduction in paper, time and monetary costs - Reduction in order processing time, reduced paper flow/use and reduced ordering costs.

Moreover, the groups of factors presented in Table 5 explore simplicity of business data processing with regards to processes which are necessary for the execution of the entire procurement process. These processes may capture: (1) possible supplier's requisition request, (2) replacement of supplier, (3) bidding, (4) access to suppliers' goods or catalogues, (5) access to suppliers' inventory data, (6) suppliers' access to your inventory, (7) ordering from supplier, (8) payment to supplier, (9) order tracking, (10) search for transporters, (11) discussion with sales representative, (12) transport ordering, (13) receiving of delivery data announcement, (14) administration of contacts, (15) delivery receiving, (16) reclamation solving, (17) inventory management, (18) maintenance of purchasing needs, and (19) warehousing. This process is usually undertaken in a classical way, where both participants (buyer and supplier) meet and sign a contract.

TABLE 5
Major factors in procurement process based on the literature review

Literature Review	Dobler & Burt (1996)	Gartnet Group RAS Services, 2000	Croom 2001	NECCC 2002	Chaffey, 2004	Podlogar, 2006
possible supplier's requisition request	✓		✓	✓	✓	✓
replacement of supplier	✓					✓
bidding						✓
access to suppliers' goods or catalogs		✓		✓		✓
access to suppliers' inventory data						✓
supplier 's access to your inventory						✓
ordering from supplier	✓			✓	✓	✓
payment to supplier		✓		✓	✓	✓
order tracking					✓	✓
search for transporters						✓
discussion with sales representative	✓					
transport ordering		✓		✓		✓
receiving of delivery data announcement						✓
administration of contracts	✓		✓			
delivery receiving						✓
reclamation solving						✓
inventory management			✓			✓
management of purchasing records	✓	✓				
warehousing			✓		✓	

Finally, the paper suggests that there is a great scope for better and easy decision making by organisational buying centre operating in the B2B markets. In spite of a great number of studies, the conceptualization is still in the immature phase.

REFERENCES

Aberdeen Group. (2004). *E-procurement: Finally ready for Prime Time*. Market View Point. Volume 14. Retrieved from http://www.expensewatch.com/IPLS/pdfs/prime_time.pdf.

ActivMedia Research. (2000). Business-to-Business online 2000. Report. Retrieved from http://www.bitpipe.com.

Albarran, A.B. and Goff, D. (2000). *Understanding the Web: Social, Political, and Economic Dimensions of the Internet*. Ames: Iowa State University Press.

Arns, M., Fischer, M., Kemper, P. and Tepper, C. (2002). Supply chain modelling and its analytical evaluation. *The Journal of the Operational Research Society, 53*(8), 885-894.

Arunachalam, S. (1999). Information and knowledge in the age of electronic communication: A developing country perspective. *Journal of Information Science, 25*(6), 465-576.

Athabasca University. (2002). Supply chain management issues study. Media Release, Centre for Innovative Management, May. Retrieved from http://www.athabascaau.ca/scm.

Bakos, Y.J. and Brynjolfsson, E. (1992). Why information technology hasn't increased the optimal number of suppliers. *Sloan School of Management,* 3472-3492.

Banting, P., Beracs, J. and Gross, A. (1991, May). The industrial buying process in capitalist and socialist countries. *Industrial Marketing Management, 20*(2), 105-114.

Barber, B.R. (1998). Three scenarios for the future of technology and strong democracy. *Political Science Quarterly*, *113*(4), 573-590.

Batista, C. and Forsberg, L.O. (1997). *Industrial buying behaviour in swedish and polish mining industries. A comparative study*. Licentiate thesis, Lulea University of Technology. IES, 971 87 Lulea.

Bimber, B. (1999). The Internet and citizen communication with government: Does the medium matter? *Political Communication*, *16*, 409-428.

Bonoma, T. V. (1982, May-June). Major sales: Who really does the buying Identifying the decision makers and their purchasing motives often requires a psychologist's eve. *Harvard Business Review*, 111-119.

Bonoma, T. V. and Johnston, W. J. (1981, Summer). The buying centre structure and interaction patterns. *Journal of Marketing, 45*, 143-156.

Braga, C.A. (2002). Globalization and Technology: You Can't Put the Genie Back in the Bottle Again, March 2002.

Cafiero, W. (1996). Electronic commerce on Internet—for real! *First Electronic Commerce World 1996, Conference*, Columbus, OH.

Chaffey, D. (2004). *e-Business and e-Commerce Management* (2nd ed.). Practice Hall.

Chan, C. and Swatman, P.M. (1999). Business-to-business e-commerce implementation: The case of BPH Steel. Ecommerce Research Forum. MIT, working paper.

Chen. L. (2000). *Consumer acceptance of virtual stores: A theoretical model and critical success factors for virtual stores*. Doctoral dissertation. The University of Memphis, Memphis.

Chiravolo, Tony. (2004). Director of Information Technology. *Advantage Human Resourcing*®, a leading provider of professional and support-level Talent.

Cisco Systems. (2002). *Technical Implementation Guide: e-Procurement.* Cisco System. Inc.

Cilek. P., Wolfgang, J., Koch, S., Mild, A. and Taudes, A. (2001). The evaluation of IT- investments in public sector organisations, *Proceedings of the Eighth European Conference on IT Evaluation. ECITE 2001* (pp. 43-48). Oxford, UK.

Commission directive on the mandatory use of standard forms for the publication of contract notices. 2001/78/EC. Adopted on 13-09-2001.

Crayannis, E.G. and Popescu, D. (2005). Profiling a methodology for economic growth and convergence: Learning from the eu e-procurement experience for central and eastern European countries. The online journal at www: sciencedirect.com.

Croom, S.R. (2001). *Supply chain management in the e-business era. An investigation into supply chain strategies, practices and progress in e-business adoption*. Warwick Business School, University of Warwick, Coventry, UK.

Davila, A., Gupta, M. and Palmer, R. J. (2003). Moving procurement systems to the internet: The adoption and use of e-procurement technology models. *European Management Journal*, *21*(1), 11-23.

Department of Information Technology, Annual Report 2007-08, Ministry of Communications and Information Technology, Government of India.

Dobler, D.W. and Burt, D.N. (1996). *Purchasing and Supply Management* (6th ed.). New York: McGraw-Hill.

Dutton, W.H. (1999). The web of technology and people: Challenges for economic and social research. *Prometheus*, *17*(10), 5-20.

Erridge, A., Fee, R. and Mcllroy, J. (2001). *Best Practice Procurement: Public and Private Sector Perspectives*. Gover Pub Co., Burlington, VT.

European Commission. (2000). *EcaTT final report*. Electronic commerce and telework trends: Benchmarking progress on new ways of working and new forms of business across Europe. EMPIRICA, Project EcaTT98, EP29299, July.

Everard, J. (2000). *Virtual States: The Internet and the Boundaries of the Nation-State*. London: Routledge.

Gibson, R. and Ward, S. (2000). Social capital, Internet connectedness and political participation: A four country study. Paper presented at the *International Political Science Association World Congress Quebec*, August.

Gupta, H. (2008) "Business to Business – A Focussed Approach towards Win Strategy." EzineArticles. Retrieved on February 26, 2008 from http://ezinearticles.com/?Business-To-Business---A-Focussed-Approach-Towards-Win-Strategy&id=910542.

Gupta, S.L., Jha, B.K. and Gupta, H. (2009). From sourcing to strategic e-sourcing. *Proceedings of International Conference on Technology and Business Management (ICTBM) 2009* (pp. 1316-1330). Dubai: AlGhurair University.

Gupta, S.L. and Gupta, H. (2009). B2B procurement practice in indian sub continent: Opportunities & trends. *Proceedings of International Conference on Technology and Business Management (ICTBM) 2009* (pp. 345-354). Dubai: AlGhurair University.

Haas, R.W. (1992). *Business Marketing Management: An Organisational Approach* (6th ed.). Boston: PWS-KENT Pub. Co, cop.

Haas, R.W. (1995). *Business Marketing. A Managerial Approach. (*6th ed.). Ohio: South-Western College Pub, cop.

Hartman, H.C. (2007). Tune up your supply chain models. *Hydrocarbon Processing*, 91-98.

Hutt, M. D. and Speh, T. W. (1995) *Business Marketing Management: A Strategic View of Industrial and Organisational Markets.* (5th ed.). Fort Worth: Dryden Press, The Dryden press series in marketing.

ITRG (info-tech research group). (2002). *A success guide for e-Procurement*. London, Canada.

Jensen, M.C. (1991). Eclipse of the public corporation. In: M.A. Montgomery, M.E. Porter (Eds.), *Strategy: seeking and securing competitive advantage* (pp. 423-448). Harvard Business School Press, Boston,

Kalakota, R. and Robinson, M. (2001). E-business 2.0. roadmap for success. *Addison-Wesley Management*, *8*(2), 111-122.

Kauffman, R.G. (1996). Influences on organisational buying choice process: Future research directions. *Journal of Business & Industrial Marketing, 11*(3/4), 94-107.

Kock, Jr., N.F. and McQueen, R.J. (1996). Is re-engineering possible in the public sector? A Brazilian case study. *Business Change and Re-engineering*, *3*(3), *3-12.*

Komp, Leonard, L. N. (1999). *Validating the electronic commerce success model through the supply chain management model.* Doctoral dissertation, University of Arkansas, Arkansas.

Kotler, P. (1991). *Marketing Management: Analysis, Planning, Implementation, and Control* (7th ed.). Englewood Cliffs. N.J.: Prentice-Hall, cop.

Kotler, P. and Armstrong, G. (2006). *Principles of Marketing* (8th ed.). New Jersey: Prentice Hall.

Kotler, P. and Bloom, P. N. (1984). *Marketing Professional Services.* Englewood Cliffs. N.J.: Prentice-Hall, cop.

Lesnicar, T. (2002). *e-Commerce influence on supply chains*. Master thesis, University of Ljublijana,

Lindemann, M.A. and Schmid, B.F. (1998). Framework for specifying, building, and operating electronic markets. *International Journal of Electronic Commerce*, *3*(2), 7-21.

Luck, J. and Peabody, J.W. (2000). Improving the public sector: Can reengineering identify how to boost efficiency at a VA medical center? *Health Care Management Review, 25*(2), 34-44.

Mattson, M. R. (1998). How to determine the composition and influence of a buying centre. *Industrial Marketing Manager,* 17.

Mechling, J. (1994). Reengineering government: Is there a "there"? *Public Productivity and Management Review*, *18*(2),189-197.

Mesenbourg, T. L. (2002). Measuring electronic business. Retrieved on February from http://www.census.gov.

Moriarty, Rowland T. (1980). Conceptual Models of Organisational Buying Behaviour. Harvard Business School, Working Paper, pp.80-36.

Morris, M.H. (1992). *Industrial and Organisational Marketing* (2nd ed.). New York: Macmillan Pub. Co.

NECCC e-Procurement Work Group. (2002). e-Procurement: Failure to implement. not an option. Retrieved from http://www.ec3 .org/downloads/2002/e-procurment.pdf.

Ody, P. (2001a). Supply chain collaboration. *Financial Times*, Twice monthly review of Information and Comunications Technology, Wednesday, December 5, pp.x.

Ody, P. (2001b). Winning idea masks hidden problems. *Financial Times*, Twice monthly review of Information and Communications Technology, Wednesday, December 5, pp.x-xi.

Panayiotou, N.A., Gayialis, S.P. and Tatsiopoulos, I.P. (2004). An e-procurement system for governmental purchasing. *International Journal of Production Economics.*

Podlogar, M., Hribar, U. and Gricar, J. (2001). IT use for e-commerce: Chief information officers statements. *Journal of Management, Informatics and Human Resources*, *34*(3), 173-180.

Podlogar, M. (2006). Simplifying procurement process by using e-commerce. *International Journal of Internet and Enterprise Management* (IJIEM), *4*(2).

Pucihar, A. (1999). *Opportunities and threats of e-commerce in organisations in Slovenia*. Master thesis, University of Maribor.

Puschmann, Thomas and Rainer Alt. (2005). Successful use of e-procurement in supply chains. *Supply Chain Management-An International Journal*, *10*(2), 122-133.

Rajkumar, T.M. (2001). *e-procurement: Business and technical issues*, Miami University, Oxford, Ohio. Information System Management.

Reeder, R.R., Brierty, E.G. and Reeder, B.H, (1991). *Industrial Marketing-Analysis, Planning and Control.* (2nd ed.). Englewood Cliffs, N.J.: Prentice Hall.

RIS. (2001). *Slovene research on the Internet*. Report, University of Ljubljana, Slovenia. Retrieved on May, http://www.ris.si.

Robinson, P.J., Faris, C.W. and Wind, Y. (1967). *Industrial Buying and Creative Marketing*. Boston: Allyn and Bacon.

Robinson, P.J., Faris, C.W. and Wind, Y. (1967, November). Understanding the industrial buyer. *Marketing Science Institute, 3.*

Samli, A.C., Willis, J.R.Jr. and Herbig, P. (1997). The information superhighway goes international: Implications for industrial sales transactions. *Industrial Marketing Management.*

Segev, A., Gebauer, J. and Beam, C. (1998). *Procurement in the Internet age, current practices and emerging trends* (Results from a field study). CMIT Working Paper WP-98-1033.

Sheng, M.L. (2002). The impact of internet-based technologies on the procurement strategy. *Proceedings of the 2nd International Conference on Electronic Commerce*, Taipei, December.

Smith, P., Berry, C. and Pulford, A. (1998). *Strategic Marketing Communications: New Ways to Build and Integrate Communications.* London: Kogan Page Limited.

Sterle, V. (2001). Electronic commerce in procurement process of Ministry of defense (Case of Department of defense United States of America). *Journal of Management, Informatics and Human Resources*, *34*(3),143-149.

Treaty establishing the European Community, signed in Rome on 25 March 1957. Retrieved from http//europa.eu.int/abc/obj/treaties/en/entocos.htm.

Webster, F. E. Jr. and Wind, Y. (1972, April). A general model for understanding organisational buying behaviour. *Journal of Marketing, 36*, 12-19.

Wind, Y. and Thomas, R. J. (1980). Conceptual and methodological issues in organisational buying behaviour. *European Journal of Marketing,* 239-269.

ISSN: 0128-7680
Pertanika J. Sci. & Technol. **18 (1)**: 209–221 (2010)

Bootstrapping the Confidence Intervals of R^2_{MAD} for Samples from Contaminated Standard Logistic Distribution

Fauziah Maarof[1], Lim Fong Peng[1*] and Noor Akma Ibrahim[2]
[1]Department of Mathematics, Faculty of Science,
[2]Institute for Mathematical Research, Universiti Putra Malaysia,
43400 UPM, Serdang, Selangor, Malaysia
[*]E-mail: fongpeng2805@yahoo.com

ABSTRACT

This paper investigates the confidence intervals of R^2_{MAD}, the coefficient of determination based on median absolute deviation in the presence of outliers. Bootstrap *bias-corrected accelerated* (BC_a) confidence intervals, known to have higher degree of correctness, are constructed for the mean and standard deviation of R^2_{MAD} for samples generated from contaminated standard logistic distribution. The results indicate that by increasing the sample size and percentage of contaminants in the samples, and perturbing the location and scale of the distribution affect the lengths of the confidence intervals. The results obtained can also be used to verify the bound of R^2_{MAD}.

Keywords: Bootstrap, R^2_{MAD}, confidence interval, contaminated standard logistic distribution

INTRODUCTION

In statistics, the median absolute deviation (MAD) is a resistant measure of the variability of a univariate sample. It can be used to estimate the scale parameter of a distribution, for which variance and standard deviation do not exist, such as the Cauchy distribution. Even when working with distributions for which the variance exists, the MAD has advantages over the standard deviation. For instance, the MAD is more resilient to outliers in a data set. For standard deviation, the distances from the mean are squared. Then, on the average, large deviations are weighted more heavily. In the MAD, the magnitude of the distances of a small number of outliers is irrelevant. Recently, problem related with robust statistic is often discussed and investigated by many researchers. Among other, Crouxa *et al.* (2002) discussed the breakdown behaviour of the maximum likelihood (ML) estimator in the logistic regression model, while Bondell (2008) constructed a new family of procedures to estimate the parameters in the general semi-parametric biased sampling model and then compared it to the existing robust logistic regression procedures via a simulation study and real data example. For the R^2_{MAD}, a review of the statistical literature indicates that the coefficient of determination based on the median absolute deviation is seldom discussed, especially in relation to its application. Many researchers are more interested in investigating the sampling properties, as well as the confidence intervals of the coefficient of determination (R^2) and the adjusted coefficient of determination ($\overline{R}^2$). According to Ohtani (2000), the sampling properties of the R^2 and $\overline{R}^2$ have been examined by Koerts and Abrahamse (1970), Rencher and Pun (1980), Cramer (1987), Carrodus and Giles (1992), Meepagala (1992), Ohtani and Hasegawa (1993), Ohtani (1994), and Srivastava and Ullah (1995), whereas their confidence intervals were examined by Helland (1987) who proposed a simple approximate confidence interval. Ohtani (2000) considered estimating the standard errors of R^2 and $\overline{R}^2$, and constructing their confidence intervals using bootstrap method.

Received: 26 December 2008
Accepted: 26 June 2009
[*]Corresponding Author

In general, bootstrapping is a statistical method used to estimate the sampling distribution of an estimator by sampling with replacement from the original sample, most often with the purpose of deriving robust estimates of standard errors and confidence intervals of a population parameter. It has become an important tool in statistical inference since the pioneering article by Efron (1979). In 2004, Hossain and Khan discussed the non-parametric bootstrapping procedure for the multiple logistic regression model associated with Davidson and Hinkley's (1997) "boot" library in R statistical software. They estimated the sampling distribution of a statistic empirically without making any assumptions about the form of the population, and without deriving the sampling distribution explicitly using the non-parametric bootstrapping. As stated in Press and Zellner (1978), R^2 is rarely accompanied by a measure of precision. It is difficult to calculate since the distribution of R^2 is rather complex and dependent on unknown parameters. Then, Ohtani (2000) stated that the bootstrap method proposed by Efron (1979) is often useful and easier to execute than the Bayesian method when the calculation of precision and the construction of a confidence interval are difficult. Thus, the bootstrap method is considered in this study as a tool for the construction of the confidence intervals of R^2_{MAD}.

In this paper, the confidence intervals of the mean and standard deviation of the sampling distribution of R^2_{MAD}, based on the samples from the contaminated standard logistic distributions, are constructed using the bootstrap method.

In the next section, a short background of the standard logistic distribution and the R^2_{MAD} is given, and this is followed by a simulation study (Section 2), the bootstrap procedure (Section 3) as well as discussions of the results (Section 4) and the conclusion (Section 5).

R^2_{MAD} FROM CONTAMINATED STANDARD LOGISTIC DISTRIBUTION

The Standard Logistic Distribution

The logistic distribution has been used for various growth models and for a certain type of regression which is appropriately known as logistic regression.

In the probability theory and statistics, the logistic distribution is a continuous probability distribution with no shape parameter. Hence, the probability density function (pdf) of the logistic distribution has only one shape (i.e. the bell shape) which resembles the normal distribution but with heavier tails.

In general, let x be a random variable, which is generated from logistic distribution, then the probability density function (pdf) of the logistic distribution is given by:

$$f(x) = \frac{e^{w}}{\sigma(1 + e^{w})^2}; -\infty < x < \infty, -\infty < \mu < \infty, \sigma < 0$$

where, $w = \frac{x - \mu}{\sigma}$, μ = location parameter and σ = scale parameter,
and its cumulative distribution function (cdf) is:

$$F(x) = \frac{e^{w}}{1 + e^{w}}.$$

Therefore, for the standard logistic distribution $(\mu = 0, \sigma = 1)$, the pdf is

$$f(x) = \frac{e^{x}}{(1 + e^{x})^{2}}$$

and its cdf is:

$$F(x) = \frac{e^{x}}{1 + e^{x}},$$

for $-\infty < x < \infty$.

The Median Absolute Deviation Correlation Coefficient, r_{MAD}

This section presents a correlation analogue of the MAD, r_{MAD}. Let (X, H) be a bivariate distribution with parameters, $\mu_x, \mu_h, \sigma_h, \rho$.

Define

$$x_i' = x_i - med(x) \quad h_i' = h_i - med(h)$$

and $MAD_x = med|\, x_i - med(x_i)\,|$ and $MAD_h = med|\, h_i - med(h_i)\,|$;

$i = 1, 2, \ldots, n$, where *med(.)* is the median function.

According to Gideon (2007), the definition of r_{MAD} is as follows:

$$r_{MAD}(x,h) = \frac{1}{2}\left[med\left(\left|\frac{x_i'}{MAD_x} + \frac{h_i'}{MAD_h}\right|\right) - med\left(\left|\frac{x_i'}{MAD_x} - \frac{h_i'}{MAD_h}\right|\right)\right] \quad (1)$$

Then, $R^2_{MAD} = (r_{MAD})^2$. Gideon verified that it is evidently not true that $|r_{MAD}| \leq 1$. Thus, r_{MAD} may sometimes go beyond + 1 or – 1.

Generation of R^2_{MAD} for the Standard Logistic Distribution

Let $X_{(i)}$ be the i^{th} order statistics and T_i is a set of constants ($i = 1, \ldots, n$). A regression test is a graphical method which is related to probability plots, in which the order statistics $X_{(i)}$ (on the vertical axis) are plotted against T_i (on the horizontal axis). After that, a straight line is fitted to the points, and R^2 will indicate the association between $X_{(i)}$ and T_i.

Suppose $F_0(x) \equiv F(w)$ with $w = (x - \mu)/\sigma$, where μ is the location parameter and σ is the scale parameter. When a sample of values W_i are taken from *F(w),* with $\mu = 0$ and $\sigma = 1$, the sample X_i is then constructed from $F_0(x)$ by calculating:

$$X_{(i)} = \mu + \sigma W_{(i)}, \quad i = 1, \ldots, n.$$

Now, let

$$m_i = E(W_{(i)}).$$

Then

$$E(X_{(i)}) = \mu + \sigma m_i \quad (2)$$

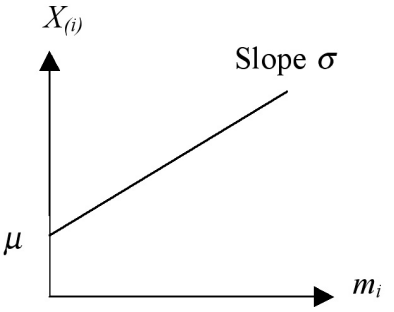

Fig. 1

and a plot of $X_{(i)}$ against m_i is approximately a straight line with an intercept μ on the vertical axis and slope σ, as shown in *Fig. 1*.

Nevertheless, for logistic distribution, m_i is difficult to calculate. Therefore, the expression (2) can be replaced by:

$$X_{(i)} = \mu + \sigma T_i + \varepsilon_i \tag{3}$$

where ε_i is the error term. When $T = m_i$, ε_i will have mean zero.

However, an approximate value of m_i is used for the samples from the standard logistic distribution,

$$H_i = \log\{i/(n+1)\}, \tag{4}$$

which is given by D'Agostino and Stephens (1986).

Then, each pair (X_i, H_i) is substituted into formula (1) for the standard logistic distribution in the previous section.

The study proceeded with the simulation of data to obtain the sampling distribution of R^2_{MAD} from the contaminated standard logistic distribution. The sampling distribution of R^2_{MAD} is simulated for the logistic contaminants (logistic (2, 0.2), logistic (0, 0.2) and logistic (2, 1)) and normal contaminants (normal (3, 0.2)). The contaminants percentages used are 5%, 15%, and 25% with n equals to 20, 40, and 100. For n = 20 with 5% logistic (2, 0.2) contaminants, the contaminated sample contained 95% of the sample from the standard logistic distribution and 5% sample from the logistic (2, 0.2) distribution. The same procedure was used for the other contaminations.

In this study, the contamination in the generation of samples is important as it can be used to observe the effect of the sample size, percentage of contamination and distribution of contaminant on the confidence intervals for the mean and standard deviation of R^2_{MAD}. The logistic (2, 0.2), logistic (0, 0.2), and logistic (2, 1) contaminants were therefore chosen to determine the behaviour of the confidence intervals for the mean and standard deviation of R^2_{MAD}, when the values of location and scale of logistic distribution increased, whereas any values could be chosen as the location and scale of the normal contaminants, provided they were not far from the parameter values of logistic contaminants.

For the cases without outliers, the following steps are used in calculating R^2_{MAD} for the standard logistic distribution.

Step 1. Using S-plus, a random sample of order statistics $\{X_{(1)}, X_{(2)}, ..., X_{(n)}\}$ is generated from the standard logistic distribution with $\mu = 0$ and $\sigma = 1$ for the sample of size n.

Step 2. Calculate the approximate value of m_i, i.e., H_i, using formula (4).

Step 3. Regress X_i 's on H_i 's and calculate r_{MAD} using (1). This is followed by the calculation of R^2_{MAD}.

Step 4. Steps 1 – 3 are repeated 1000 times to generate (1000) R^2_{MAD} for the standard logistic distribution.

Step 5. Steps 1 – 4 are repeated for the different sample sizes (n = 20, 40, 100).

However, for cases with outliers, the samples of order statistics generated for use in the calculation of R^2_{MAD} are obtained from the contaminated standard logistic distribution for logistic (2, 0.2), logistic (0, 0.2), logistic (2, 1), and normal (3, 0.2). Similar procedures in the simulation for the cases without outlier (Steps 2 – 5) are repeated. Then, (1000) R^2_{MAD} for the standard logistic distribution with 5%, 15% and 25% contaminants are obtained for n = 20, 40, 100, respectively.

BOOTSTRAP CONFIDENCE INTERVALS FOR THE MEAN AND STANDARD DEVIATION OF R^2_{MAD}

Bootstrap Procedure

In this study, the *bias-corrected accelerated* (BC_a) confidence intervals were computed by simulation with the sample sizes of 20, 40, and 100, since it possessed a higher degree of correctness as compared to other types of bootstrap confidence intervals. According to Efron (1987), the BC_a bootstrap confidence interval is known to lead to second-order accuracy in correctness, while the *percentile* (*P*), the *bias-corrected* (*BC*), and the asymptotic normal confidence intervals have the first-order accuracy only.

The implementation of the bootstrap procedure can be summarized as follows: Let $\hat{\theta}^{*(\alpha)}$ indicates the 100•α th percentile of B bootstrap replications $\hat{\theta}^{*(1)}, \hat{\theta}^{*(2)}, ..., \hat{\theta}^{*(B)}$. The percentile interval $(\hat{\theta}_{lo}, \hat{\theta}_{up})$ of the intended coverage 1 - 2α is directly obtained from these percentiles:

$$(\hat{\theta}_{lo}, \hat{\theta}_{up}) = (\hat{\theta}^{*(\alpha)}, \hat{\theta}^{*(1-\alpha)})$$

In this study, the step above was repeated 1000 times (B = 1000), and then the averages and standard errors of the mean and standard deviation of the R^2_{MAD} were obtained. Furthermore, 95% confidence intervals for the mean and standard deviation of the R^2_{MAD} could be calculated.

The R^2_{MAD}, which was used in the bootstrap procedure above, was generated using the method presented in the previous section. The bootstrap estimates of the mean and standard deviation of R^2_{MAD} and their confidence intervals for the various cases considered in this investigation were obtained using the S-plus software.

RESULTS AND DISCUSSION

This section presents a discussion on the results of the bootstrap estimates for the mean and standard deviation of the sampling distribution of R^2_{MAD} simulated for various sample sizes, percentage of contamination, as well as distribution of the contaminants, location and scale of the distribution, from which the samples were drawn. Tables 1, 2, 3, 4, and 5 show 95% confidence intervals of R^2_{MAD} for the cases with and without outliers. Tables 6 and 7 show the range of confidence intervals for the mean and standard deviation of R^2_{MAD}, respectively.

As expected for the cases without outliers, Table 1 shows that the range of the confidence intervals for the mean and standard deviation of R^2_{MAD} has become smaller when the sample size increases. For the cases with outliers, on the other hand, Tables 2, 3, 4 and 5 show that there are some similar results just like for the cases without outlier. The range of the confidence intervals for the mean and standard deviation of R^2_{MAD} become smaller when the sample size increases. The same pattern prevails for each type of the contaminants (see Tables 6 and 7). Meanwhile, for each sample size, the results showed that increasing the percentage of contaminants would widen the confidence intervals for the mean and standard deviation of R^2_{MAD} for each type of contaminants, except for the confidence intervals for the standard deviation of R^2_{MAD} with logistic (2, 1) contaminants (see Tables 6 and 7).

In the cases with normal contaminants, the results show that the confidence intervals for the mean of R^2_{MAD} are wider as compared to the cases with logistic contaminants. The trend can be seen more clearly when it is compared to logistic (2, 1) contaminants, as indicated in Tables 6. For the standard deviation, however, the range of the confidence intervals for the normal contaminants does not show any specific trend as compared to the cases with logistic contaminants, as given in Table 7.

For the cases with logistic contaminants, on the other hand, the range of the confidence intervals for the mean and standard deviation of R^2_{MAD} increases with an increase in the location of the logistic distribution as shown in Tables 6 and 7. Meanwhile, increasing the scale of the logistic distribution was found to widen the confidence intervals for the mean and standard deviation of R^2_{MAD} for the samples with 5% contaminations. For the samples with 15% and 25% contamination, however, the range of the confidence intervals for the mean and standard deviation of R^2_{MAD} was found to decrease with the increase in the scale of the logistic distribution, as indicated in Tables 6 and 7. In all the constructed BCa 's, R^2_{MAD} is bounded between -1 and 1.

TABLE 1

95% Confidence intervals of R^2_{MAD} for cases without outliers

N		Observed	BCa (95%)
20	mean	0.8099	(0.8044, 0.8157)
	sd	0.09474	(0.08967, 0.09993)
40	mean	0.8468	(0.8416, 0.8514)
	sd	0.07802	(0.07352, 0.08291)
100	mean	0.8966	(0.8934, 0.8998)
	sd	0.04993	(0.04669, 0.05359)

TABLE 2
95% Confidence intervals of R^2_{MAD} for cases with logistic (2, 0.2) contaminants

n		Contaminant	Observed	BCa (95%)
20	mean	5%	0.7999	(0.7935, 0.806)
		15%	0.7973	(0.79, 0.8034)
		25%	0.7798	(0.7718, 0.7871)
	sd	5%	0.1001	(0.09538, 0.1064)
		15%	0.1042	(0.09896, 0.1105)
		25%	0.1253	(0.1184, 0.1324)
40	mean	5%	0.8486	(0.8437, 0.8532)
		15%	0.8375	(0.8323, 0.8428)
		25%	0.8043	(0.797, 0.8107)
	sd	5%	0.08016	(0.07583, 0.08518)
		15%	0.08438	(0.07979, 0.0894)
		25%	0.1094	(0.104, 0.1164)
100	mean	5%	0.8976	(0.8946, 0.9006)
		15%	0.8809	(0.8773, 0.8844)
		25%	0.8426	(0.8376, 0.8476)
	sd	5%	0.0494	(0.04668, 0.05245)
		15%	0.0581	(0.0548, 0.06213)
		25%	0.07979	(0.07524, 0.0846)

TABLE 3
95% Confidence intervals of R^2_{MAD} for cases with logistic (0, 0.2) contaminants

n		Contaminant	Observed	BCa (95%)
20	mean	5%	0.8005	(0.7945, 0.8063)
		15%	0.7921	(0.7845, 0.7973)
		25%	0.7809	(0.7738, 0.7874)
	sd	5%	0.09811	(0.09291, 0.1032)
		15%	0.1053	(0.09955, 0.1107)
		25%	0.1069	(0.1014, 0.1127)
40	mean	5%	0.8501	(0.8453, 0.8546)
		15%	0.8346	(0.829, 0.8393)
		25%	0.8234	(0.8182, 0.829)

Table 3 continued

	sd	5%	0.073	(0.06845, 0.078)
		15%	0.08091	(0.07599, 0.085)
		25%	0.0864	(0.08186, 0.09121)
100	mean	5%	0.8972	(0.8942, 0.9005)
		15%	0.8806	(0.8773, 0.8836)
		25%	0.8593	(0.8557, 0.863)
	sd	5%	0.04961	(0.04706, 0.05267)
		15%	0.05056	(0.04789, 0.0536)
		25%	0.05913	(0.05602, 0.06256)

TABLE 4
95% Confidence intervals of R^2_{MAD} for cases with logistic (2, 1) contaminants

n		Contaminant	Observed	BCa (95%)
20	mean	5%	0.7983	(0.7914, 0.8042)
		15%	0.8033	(0.7972, 0.8093)
		25%	0.8017	(0.796, 0.8079)
	sd	5%	0.1014	(0.09669, 0.108)
		15%	0.09906	(0.0934, 0.1048)
		25%	0.1001	(0.09489, 0.1051)
40	mean	5%	0.8464	(0.8414, 0.8513)
		15%	0.8446	(0.839, 0.849)
		25%	0.8468	(0.8412, 0.8514)
	sd	5%	0.07908	(0.07467, 0.08404)
		15%	0.07882	(0.07462, 0.08395)
		25%	0.07769	(0.07359, 0.082)
100	mean	5%	0.8975	(0.8944, 0.9005)
		15%	0.8963	(0.893, 0.8991)
		25%	0.8926	(0.8893, 0.8958)
	sd	5%	0.05049	(0.0473, 0.05402)
		15%	0.05162	(0.04829, 0.05629)
		25%	0.05237	(0.04934, 0.05593)

TABLE 5
95% Confidence intervals of R^2_{MAD} for cases with normal (3, 0.2) contaminants

n		Contaminant	Observed	BCa (95%)
20	mean	5%	0.7982	(0.7915, 0.8045)
		15%	0.8055	(0.7989, 0.8117)
		25%	0.7941	(0.7869, 0.8026)
	sd	5%	0.1011	(0.09564, 0.1071)
		15%	0.107	(0.1008, 0.1137)
		25%	0.1216	(0.1147, 0.1289)
40	mean	5%	0.8473	(0.8426, 0.8523)
		15%	0.8391	(0.8338, 0.8444)
		25%	0.8219	(0.8156, 0.8274)
	sd	5%	0.07848	(0.074, 0.08299)
		15%	0.08671	(0.08248, 0.09124)
		25%	0.099	(0.09409, 0.1051)
100	mean	5%	0.8955	(0.8925, 0.8985)
		15%	0.8805	(0.8765, 0.8843)
		25%	0.8471	(0.8425, 0.851)
	sd	5%	0.05051	(0.0479, 0.05347)
		15%	0.06278	(0.05962, 0.06738)
		25%	0.07173	(0.06882, 0.07524)

TABLE 6
The range of the confidence intervals for the mean of R^2_{MAD}

Contaminant	Contamination	*n*	Range
Logistic (2, 0.2)	5%	20	0.0125
		40	0.0095
		100	0.006
	15%	20	0.0134
		40	0.0105
		100	0.0071
	25%	20	0.0153
		40	0.0137
		100	0.01

Table 6 continued

Logistic (0, 0.2)	5%	20	0.0118
		40	0.0093
		100	0.0063
	15%	20	0.0128
		40	0.0103
		100	0.0063
	25%	20	0.0136
		40	0.0108
		100	0.0073
Logistic (2, 1)	5%	20	0.0128
		40	0.0099
		100	0.0061
	15%	20	0.0121
		40	0.01
		100	0.0061
	25%	20	0.0119
		40	0.0102
		100	0.0065
Normal (3, 0.2)	5%	20	0.013
		40	0.0097
		100	0.006
	15%	20	0.0128
		40	0.0106
		100	0.0078
	25%	20	0.0157
		40	0.0118
		100	0.0085

TABLE 7
The range of the confidence intervals for the standard deviation of R^2_{MAD}

Contaminant	Contamination	*n*	Range
Logistic (2, 0.2)	5%	20	0.01102
		40	0.00935
		100	0.00577
	15%	20	0.01154
		40	0.00961
		100	0.00733
	25%	20	0.014
		40	0.0124
		100	0.00936
Logistic (0, 0.2)	5%	20	0.01029
		40	0.00955
		100	0.00561
	15%	20	0.01115
		40	0.00901
		100	0.00571
	25%	20	0.0113
		40	0.00935
		100	0.00654
Logistic (2, 1)	5%	20	0.01131
		40	0.00937
		100	0.00672
	15%	20	0.0114
		40	0.00933
		100	0.008
	25%	20	0.01021
		40	0.00841
		100	0.00659
Normal (3, 0.2)	5%	20	0.01146
		40	0.00899
		100	0.00557
	15%	20	0.0129
		40	0.00876
		100	0.00776
	25%	20	0.0142
		40	0.01101
		100	0.00642

CONCLUSIONS

As expected, the range of the confidence intervals for the mean and standard deviation of R^2_{MAD} becomes smaller when the sample size increases for both the cases with and without outliers, based on the results presented in the previous section. The same trend can be seen for each distribution of the contaminants. Meanwhile, increasing the percentage of contaminants widens the confidence intervals for each sample size, except for the confidence intervals for the standard deviation of R^2_{MAD} with logistic (2, 1) contaminants. Increasing the location and scale of the distribution of logistic contaminants has also been found to affect the range of confidence intervals for the mean and standard deviation of R^2_{MAD}. The results obtained are used to verify the bound of R^2_{MAD}, i.e. whether or not $|r_{MAD}|$ is always less than 1.

ACKNOWLEDGEMENT

The authors are grateful to Prof. Rahmatullah Imon for useful comments. A special thank you is due to the Graduate Research Fellowship, supported by Universiti Putra Malaysia, Malaysia.

REFERENCES

Ahmed Hossain and Abdullah Khan H. T. (2004). Nonparametric bootstrapping for multiple logistic regression model using r. *BRAC University Journal*, *I* (2), 109 – 113.

Carrodus, M.L. and Giles, D.E.A. (1992). The exact distribution of R^2 when regression disturbances are autocorrelated. *Economics Letters, 38*, 375-380.

Crouxa, C., Flandre, C. and Haesbroeck, G (2002). The breakdown behavior of the maximum likelihood estimator in the logistic regression model. *Statistics & Probability Letters, 60*, 377–386.

Cramer, J.S. (1987). Mean and variance of R^2 in small and moderate samples. *Journal of Econometrics, 35*, 253-266.

D'Agostino, R. B. and Stephens, M. A. (1986). *Goodness-of-fit Techniques*. Marcel Dekker, Inc.

Davidson, A. C. and Hinkley, D. V. (1997). *Bootstrap Methods and Their Application*. Cambridge: Cambridge University Press.

Efron, B. (1979). Bootstrap methods: Another look to the jackknife. *The Annals of Statistics, 7*, 1-26.

Efron, B. (1987). Better bootstrap confidence intervals. *Journal of the American Statistical Association, 82,* 171 – 200.

Gideon, R A. (2007). The correlation coefficients. *Journal of Modern Applied Statistical Methods*, *6*(2), 517 – 529.

Hall, P. (1988). Theoretical comparisons of bootstrap confidence intervals (with discussion). *The Annals of Statistics, 16*, 927-985.

Helland, I.S. (1987). On the interpretation and use of r^2 in regression analysis. *Biometrics, 43*, 61-69.

Howard, D.B. (2008). A characteristic function approach to the biased sampling model, with application to robust logistic regression. *Journal of Statistical Planning and Inference*, *138*, 742 – 755.

Koerts, J. and Abrahamse, A.P.J. (1970). The correlation coefficient in the general linear model. *European Economics Review, 1,* 401-427.

Meepagala, G. (1992). The small sample properties of r^2 in a misspecified regression model with stochastic regressors. *Economics Letters, 40*, 1-6.

Ohtani, K. and Hasegawa, H. (1993). On small sample properties of r^2 in a linear regression model with multivariate t errors and proxy variables. *Econometric Theory, 9*, 504-515.

Ohtani, K. (1994). The density function of r^2 and $\overline{R}^2$, and their risk performance under asymmetric loss in misspecified linear regression models. *Economic Modelling, 11,* 463-471.

Ohtani, K. (2000). Bootstrapping R^2 and adjusted R^2 in regression analysis. *Economic Modelling*, *17*, 473-483.

Press, S.J. and Zellner, A. (1978). Posterior distribution for the multiple correlation coefficient with fixed regressors. *Journal of Econometrics, 8*, 307-321.

Rencher, A.C. and Pun, F.C. (1980). Inflation of R^2 in best subset regression. *Technometrics, 22*, 49-53.

Srivastava, A.K. and Ullah, A. (1995). The coefficient of determination and its adjusted version in linear regression models. *Econometric Review, 14*, 229-240.

Pertanika

Our goal is to bring high quality research to the widest possible audience

Journal of Science & Technology

INSTRUCTIONS TO AUTHORS

(Manuscript Preparation & Submission Guidelines)

Revised January 2010

We aim for excellence, sustained by a responsible and professional approach to journal publishing.
We value and support our authors in the research community.

Please read the guidelines and follow these instructions carefully; doing so will ensure that the publication of your manuscript is as rapid and efficient as possible. The Editorial Board reserves the right to return manuscripts that are not prepared in accordance with these guidelines.

About the Journal

Pertanika is an international peer-reviewed journal devoted to the publication of original papers, and it serves as a forum for practical approaches to improving quality in issues pertaining to tropical agriculture and its related fields. *Pertanika* began publication in 1978 as Journal of Tropical Agricultural Science. In 1992, a decision was made to streamline *Pertanika* into three journals to meet the need for specialised journals in areas of study aligned with the interdisciplinary strengths of the university. The revamped Journal of Science and Technology (JST) is now focusing on research in science and engineering, and its related fields. Other *Pertanika* series include Journal of Tropical Agricultural Science (JTAS); and Journal of Social Sciences and Humanities (JSSH).

JST is published in **English** and it is open to authors around the world regardless of the nationality. It is currently published two times a year i.e. in **January** and **July**.

Goal of *Pertanika*

Our goal is to bring the highest quality research to the widest possible audience.

Quality

We aim for excellence, sustained by a responsible and professional approach to journal publishing. Submissions are guaranteed to receive a decision within 12 weeks. The elapsed time from submission to publication for the articles averages 5-6 months.

Indexing of *Pertanika*

Pertanika is now over 30 years old; this accumulated knowledge has resulted in *Pertanika* JST being indexed in EBSCO.

Future vision

We are continuously improving access to our journal archives, content, and research services. We have the drive to realise exciting new horizons that will benefit not only the academic community, but society itself.

We also have views on the future of our journals. The emergence of the online medium as the predominant vehicle for the 'consumption' and distribution of much academic research will be the ultimate instrument in the dissemination of the research news to our scientists and readers.

Aims and Scope

Pertanika Journal of Science and Technology aims to provide a forum for high quality research related to science and engineering research. Areas relevant to the scope of the journal include: *bioinformatics, bioscience, biotechnology and bio-molecular sciences, chemistry, computer science, ecology, engineering, engineering design, environmental control and management, mathematics and statistics, medicine and health sciences, nanotechnology, physics, safety and emergency management*, and related fields of study.

Editorial Statement

Pertanika is the official journal of Universiti Putra Malaysia. The abbreviation for *Pertanika* Journal of Science & Technology is *Pertanika J. Sci. Technol.*

Guidelines for Authors

Publication policies

Pertanika policy prohibits an author from submitting the same manuscript for concurrent consideration by two or more publications. It prohibits as well publication of any manuscript that has already been published either in whole or substantial part elsewhere. It also does not permit publication of manuscript that has been published in full in Proceedings.

Editorial process

Authors are notified on receipt of a manuscript and upon the editorial decision regarding publication.

Manuscript review: Manuscripts deemed suitable for publication are sent to the Editorial Advisory Board members and/or other reviewers. We encourage authors to suggest the names of possible reviewers. Notification of the editorial decision is usually provided within to eight to ten weeks from the receipt of manuscript. Publication of solicited manuscripts is not guaranteed. In most cases, manuscripts are accepted conditionally, pending an author's revision of the material.

Author approval: Authors are responsible for all statements in articles, including changes made by editors. The liaison author must be available for consultation with an editor of *The Journal* to answer questions during the editorial process and to approve the edited copy. Authors receive edited typescript (not galley proofs) for final approval. Changes **cannot** be made to the copy after the edited version has been approved.

Please direct all inquiries, manuscripts, and related correspondence to:

The Executive Editor
Pertanika Journals
Research Management Centre (RMC)
IDEA Tower II, UPM-MTDC Technology Centre
Universiti Putra Malaysia
43400 UPM, Serdang, Selangor
Malaysia
Phone: + (603) 8947 1622
ndeeps@admin.upm.edu.my

or visit our website at http://www.pertanika2.upm.edu.my/jpertanika/index.htm for further information.

Manuscript preparation

Pertanika accepts submission of mainly four types of manuscripts. Each manuscript is classified as **regular** or **original** articles, **short communications**, **reviews**, and proposals for **special issues**. Articles must be in **English** and they must be competently written and argued in clear and concise grammatical English. Acceptable English usage and syntax are expected. Do not use slang, jargon, or obscure abbreviations or phrasing. Metric measurement is preferred; equivalent English measurement may be included in parentheses. Always provide the complete form of an acronym/abbreviation the first time it is presented in the text. Contributors are strongly recommended to have the manuscript checked by a colleague with ample experience in writing English manuscripts or an English language editor.

Linguistically hopeless manuscripts will be rejected straightaway (e.g., when the language is so poor that one cannot be sure of what the authors really mean). This process, taken by authors before submission, will greatly facilitate reviewing, and thus publication if the content is acceptable.

The instructions for authors must be followed. Manuscripts not adhering to the instructions will be returned for revision without review. Authors should prepare manuscripts according to the guidelines of *Pertanika*.

1. Regular article
Definition: Full-length original empirical investigations, consisting of introduction, materials and methods, results and discussion, conclusions. Original work must provide references and an explanation on research findings that contain new and significant findings.
Size: Should not exceed 5000 words or 8-10 printed pages (excluding the abstract, references, tables and/or figures). One printed page is roughly equivalent to 3 type-written pages.

2. Short communications
Definition: Significant new information to readers of the Journal in a short but complete form. It is suitable for the publication of technical advance, bioinformatics or insightful findings of plant and animal development and function.
Size: Should not exceed 2000 words or 4 printed pages, is intended for rapid publication. They are not intended for publishing preliminary results or to be a reduced version of Regular Papers or Rapid Papers.

3. Review article
Definition: Critical evaluation of materials about current research that had already been published by organizing, integrating, and evaluating previously published materials. Re-analyses as meta-analysis and systemic reviews are encouraged. Review articles should aim to provide systemic overviews, evaluations and interpretations of research in a given field.

Size: Should not exceed 4000 words or 7-8 printed pages.

4. Special issues
Definition: Usually papers from research presented at a conference, seminar, congress or a symposium.

Size: Should not exceed 5000 words or 8-10 printed pages.

5. Others
Definition: Brief reports, case studies, comments, Letters to the Editor, and replies on previously published articles may be considered.

Size: Should not exceed 2000 words or up to 4 printed pages.

With few exceptions, original manuscripts should not exceed the recommended length of 6 printed pages (about 18 typed pages, double-spaced and in 12-point font, tables and figures included). Printing is expensive, and, for the Journal, postage doubles when an issue exceeds 80 pages. You can understand then that there is little room for flexibility.

Long articles reduce the Journal's possibility to accept other high-quality contributions because of its 80-page restriction. We would like to publish as many good studies as possible, not only a few lengthy ones. (And, who reads overly long articles anyway?) Therefore, in our competition, short and concise manuscripts have a definite advantage.

Format
The paper should be formatted in one column format with the figures at the end. A maximum of eight keywords should be indicated below the abstract to describe the contents of the manuscript. Leave a blank line between each paragraph and between each entry in the list of bibliographic references. Tables should preferably be placed in the same electronic file as the text. Authors should consult a recent issue of the Journal for table layout.

There is no need to spend time formatting your article so that the printout is visually attractive (e.g. by making headings bold or creating a page layout with figures), as most formatting instructions will be removed upon processing.

Manuscripts should be typewritten, typed on one side of the ISO A4 paper with at least 4cm margins and double spacing throughout. Every page of the manuscript, including the title page, references, tables, etc. should be numbered. However, no reference should be made to page numbers in the text; if necessary, one may refer to sections. Underline words that should be in italics, and do not underline any other words.

Authors are advised to use Times New Roman 12-point font. Be especially careful when you are inserting special characters, as those inserted in different fonts may be replaced by different characters when converted to PDF files. It is well known that 'μ' will be replaced by other characters when fonts such as 'Symbol' or 'Mincho' are used.

We recommend that authors prepare the text as a **Microsoft Word** file.

1. Manuscripts in general should be organised in the following order:

    - **Page 1: Running title.** (Not to exceed 60 characters, counting letters and spaces). This page should **only** contain your running title of your paper. In addition, the **Subject areas** most relevant to the study must be indicated on this page. Select one or two subject areas (refer to the *Scope Form).*
      A **list** of number of **black and white / colour figures and tables** should also be indicated on this page**.** Figures submitted in color will be printed in colour. See "*5. Figures & Photographs"* for details.

    - **Page 2: Author(s) and Corresponding author information.** This page should contain the **full title** of your paper with name(s) of all the authors, institutions and corresponding author's name, institution and full address (Street address, telephone number (including extension), hand phone number, fax number and e-mail address) for editorial correspondence. The names of the authors **must** be abbreviated following the international naming convention. e.g. Salleh, A.B., Tan, S.G., or Sapuan, S.M.

      Authors' addresses. Multiple authors with different addresses must indicate their respective addresses separately by superscript numbers:

      George Swan[1] and Nayan Kanwal[2]

[1]Department of Biology, Faculty of Science, Duke University, Durham, North Carolina, USA.
[2]Research Management Centre, Universiti Putra Malaysia, Serdang, Malaysia.

- **Page 3**: This page should **repeat** the **full title** of your paper with only the **Abstract** (the abstract should be less than 250 words for a Regular Paper and up to 100 words for a Short Communication). **Keywords** must also be provided on this page (Not more than eight keywords in alphabetical order).
- **Page 4 and subsequent pages**: This page should begin with the **Introduction** of your article and the rest of your paper should follow from page 5 onwards.

Abbreviations. Define alphabetically, other than abbreviations that can be used without definition. Words or phrases that are abbreviated in the introduction and following text should be written out in full the first time that they appear in the text, with each abbreviated form in parenthesis. Include the common name or scientific name, or both, of animal and plant materials.

Footnotes. Current addresses of authors if different from heading.

2. **Text.** Regular Papers should be prepared with the headings **Introduction**, **Materials and Methods**, **Results and Discussion, Conclusions** in this order. Short Communications should be prepared according to "*8. Short Communications."* below.
3. **Tables.** All tables should be prepared in a form consistent with recent issues of *Pertanika* and should be numbered consecutively with Arabic numerals. Explanatory material should be given in the table legends and footnotes. Each table should be prepared on a separate page. (Note that when a manuscript is accepted for publication, tables must be submitted as data - .doc, .rtf, Excel or PowerPoint file- because tables submitted as image data cannot be edited for publication.)
4. **Equations and Formulae.** These must be set up clearly and should be typed triple spaced. Numbers identifying equations should be in square brackets and placed on the right margin of the text.
5. **Figures & Photographs.** Submit an original figure or photograph. Line drawings must be clear, with high black and white contrast. Each figure or photograph should be prepared on a separate sheet and numbered consecutively with Arabic numerals. Appropriate sized numbers, letters and symbols should be used, no smaller than 2 mm in size after reduction to single column width (85 mm), 1.5-column width (120 mm) or full 2-column width (175 mm). Failure to comply with these specifications will require new figures and delay in publication. For electronic figures, create your figures using applications that are capable of preparing high resolution TIFF files acceptable for publication. In general, we require **300 dpi or higher resolution for coloured and half-tone artwork** and **1200 dpi or higher for line drawings**. For review, you may attach low-resolution figures, which are still clear enough for reviewing, to keep the file of the manuscript under 5 MB. Illustrations may be produced at extra cost in colour at the discretion of the Publisher; the author could be charged Malaysian Ringgit 50 for each colour page.
6. **References.** Literature citations in the text should be made by name(s) of author(s) and year. For references with more than two authors, the name of the first author followed by 'et al.' should be used.

   Swan and Kanwal (2007) reported that …
   The results have been interpreted (Kanwal et al. 2009).

   - References should be listed in alphabetical order, by the authors' last names. For the same author, or for the same set of authors, references should be arranged chronologically. If there is more than one publication in the same year for the same author(s), the letters 'a', 'b', etc., should be added to the year.
   - When the authors are more than 11, list 5 authors and then et al.
   - Do not use indentations in typing References. Use one line of space to separate each reference. The name of the journal should be written in full. For example:
     - Jalaludin, S. (1997a). Metabolizable energy of some local feeding stuff. *Tumbuh, 1,* 21-24.
     - Jalaludin, S. (1997b). The use of different vegetable oil in chicken ration. *Malayan Agriculturist, 11,* 29-31.
     - Tan, S.G., Omar, M.Y., Mahani, K.W., Rahani, M., Selvaraj, O.S. (1994). Biochemical genetic studies on wild populations of three species of green leafhoppers *Nephotettix* from Peninsular Malaysia. *Biochemical Genetics*, *32,* 415 - 422.
   - In case of citing an author(s) who has published more than one paper in the same year, the papers should be distinguished by addition of a small letter as shown above, e.g. Jalaludin (1997a); Jalaludin (1997b).
   - Unpublished data and personal communications should not be cited as literature citations, but given in the text in parentheses. 'In press' articles that have been accepted for publication may be cited in References. Include in the citation the journal in which the 'in press' article will appear and the publication date, if a date is available.

7. **Examples of other reference citations**:
   Monographs: Turner, H.N. and Yong, S.S.Y. (2006). *Quantitative Genetics in Sheep Breeding*. Ithaca: Cornell University Press.

   Chapter in Book: Kanwal, N.D.S. (1992). Role of plantation crops in Papua New Guinea economy. In Angela R. McLean (Eds.), *Introduction of livestock in the Enga province PNG* (p. 221-250). United Kingdom: Oxford Press.

   Proceedings: Kanwal, N.D.S. (2001). Assessing the visual impact of degraded land management with landscape design software. In N.D.S. Kanwal and P. Lecoustre (Eds.), *International forum for Urban Landscape Technologies* (p. 117-127). Lullier, Geneva, Switzerland: CIRAD Press.

8. **Short Communications** should include **Introduction, Materials and Methods, Results and Discussion, Conclusions** in this order. Headings should only be inserted for Materials and Methods. The abstract should be up to 100 words, as stated above. Short Communications must be 5 printed pages or less, including all references, figures and tables. References should be less than 30. A 5 page paper is usually approximately 3000 words plus four figures or tables (if each figure or table is less than 1/4 page).

   *Authors should state the total number of words (including the Abstract) in the cover letter. Manuscripts that do not fulfill these criteria will be rejected as Short Communications without review.

STYLE OF THE MANUSCRIPT

Manuscripts should follow the style of the latest version of the Publication Manual of the American Psychological Association (APA). The journal uses British spelling and authors should therefore follow the latest edition of the Oxford Advanced Learner's Dictionary.

SUBMISSION OF MANUSCRIPTS

All articles submitted to the journal **must comply** with these instructions. Failure to do so will result in return of the manuscript and possible delay in publication.

The **four copies** of your original manuscript, four sets of photographic figures, as well as a CD with the **electronic copy in MS Word** (including text and figures) together with a **cover letter**, **declaration form**, **referral form A**, **scope form** need to be enclosed. They are available from the *Pertanika*'s home page at http://www.rmc.upm.edu.my/j*Pertanika*/index.htm or from the Executive Editor's office upon request.

Please do **not** submit manuscripts directly to the editor-in-chief or to the UPM Press. All manuscripts must be **submitted through the executive editor's office** to be properly acknowledged and rapidly processed:

Dr. Nayan KANWAL
Executive Editor
Research Management Centre (RMC)
IDEA Tower II, UPM-MTDC Technology Centre
Universiti Putra Malaysia
43400 UPM, Serdang, Selangor, Malaysia
email: ndeeps@admin.upm.edu.my; tel: + 603-8947 1622

Authors should retain copies of submitted manuscripts and correspondence, as materials can not be returned.

Cover letter

All submissions must be accompanied by a cover letter detailing what you are submitting. Papers are accepted for publication in the journal on the understanding that the article is original and the content has not been published or submitted for publication elsewhere. This must be stated in the cover letter.

The cover letter must also contain an acknowledgement that all authors have contributed significantly, and that all authors are in agreement with the content of the manuscript.

The cover letter of the paper should contain (i) the title; (ii) the full names of the authors; (iii) the addresses of the institutions at which the work was carried out together with (iv) the full postal and email address, plus facsimile and telephone numbers of the author to whom correspondence about the manuscript should be sent. The present address of any author, if different from that where the work was carried out, should be supplied in a footnote.

As articles are double-blind reviewed, material that might identify authorship of the paper should be placed on a cover sheet.

Note When your manuscript is received at *Pertanika*, it is considered to be in its final form. Therefore, you need to check your manuscript carefully before submitting it to the executive editor (see also **English language editing** below).

Electronic copy
Preparation of manuscripts on a CD or DVD is preferable and articles should be prepared using MS Word. File name(s), the title of your article and authors of the article must be indicated on the CD. The CD must always be accompanied by four hard-copies of the article, and the content of the two must be identical. The CD text must be the same as that of the final refereed, revised manuscript. CDs formatted for IBM PC compatibles are preferred, as those formatted for Apple Macintosh are not acceptable. Please do not send ASCII files, as relevant data may be lost. Leave a blank line between each paragraph and between each entry in the list of bibliographic references. Tables should be placed in the same electronic file as the text. Authors should consult a recent issue of the Journal for table layout.

Peer review
In the peer-review process, three referees independently evaluate the scientific quality of the submitted manuscripts. The Journal uses a double-blind peer-review system. Authors are encouraged to indicate in **referral form A** the names of three potential reviewers, but the editors will make the final choice. The editors are not, however, bound by these suggestions.

Manuscripts should be written so that they are intelligible to the professional reader who is not a specialist in the particular field. They should be written in a clear, concise, direct style. Where contributions are judged as acceptable for publication on the basis of content, the Editor or the Publisher reserves the right to modify the typescripts to eliminate ambiguity and repetition and improve communication between author and reader. If extensive alterations are required, the manuscript will be returned to the author for revision.

The editorial review process
What happens to a manuscript once it is submitted to *Pertanika*? Typically, there are seven steps to the editorial review process:

1. The executive editor and the editorial board examine the paper to determine whether it is appropriate for the journal and should be reviewed. If not appropriate, the manuscript is rejected outright and the author is informed.

2. The executive editor sends the article-identifying information having been removed, to three reviewers. Typically, one of these is from the Journal's editorial board. Others are specialists in the subject matter represented by the article. The executive editor asks them to complete the review in three weeks and encloses two forms: (a) referral form B and (b) reviewer's comment form along with reviewer's guidelines. Comments to authors are about the appropriateness and adequacy of the theoretical or conceptual framework, literature review, method, results and discussion, and conclusions. Reviewers often include suggestions for strengthening of the manuscript. Comments to the editor are in the nature of the significance of the work and its potential contribution to the literature.

3. The executive editor, in consultation with the editor-in-chief, examines the reviews and decides whether to reject the manuscript, invite the author(s) to revise and resubmit the manuscript, or seek additional reviews. Final acceptance or rejection rests with the Editorial Board, who reserves the right to refuse any material for publication. In rare instances, the manuscript is accepted with almost no revision. Almost without exception, reviewers' comments (to the author) are forwarded to the author. If a revision is indicated, the editor provides guidelines for attending to the reviewers' suggestions and perhaps additional advice about revising the manuscript.

4. The authors decide whether and how to address the reviewers' comments and criticisms and the editor's concerns. The authors submit a revised version of the paper to the executive editor along with specific information describing how they have answered' the concerns of the reviewers and the editor.

5. The executive editor sends the revised paper out for review. Typically, at least one of the original reviewers will be asked to examine the article.

6. When the reviewers have completed their work, the executive editor in consultation with the editorial board and the editor-in-chief examine their comments and decide whether the paper is ready to be published, needs another round of revisions, or should be rejected.

7. If the decision is to accept, the paper is sent to that Press and the article should appear in print in approximately two to three months. The Publisher ensures that the paper adheres to the correct style (in-text citations, the reference list, and tables are typical areas of concern, clarity, and grammar). The authors are asked to respond to any queries by the Publisher. Following these corrections, page proofs are mailed to the corresponding authors for their final approval. At this point, only essential changes are accepted. Finally, the article appears in the pages of the Journal and is posted on-line.

English language editing
Authors are responsible for the linguistic accuracy of their manuscripts. Authors not fully conversant with the English language should seek advice from subject specialists with a sound knowledge of English. The cost will be borne by the author, and a copy of the certificate issued by the service should be attached to the cover letter.

Author material archive policy
Authors who require the return of any submitted material that is rejected for publication in the journal should indicate on the cover letter. If no indication is given, that author's material should be returned, the Editorial Office will dispose of all hardcopy and electronic material.

Copyright
Authors publishing the Journal will be asked to sign a declaration form. In signing the form, it is assumed that authors have obtained permission to use any copyrighted or previously published material. All authors must read and agree to the conditions outlined in the form, and must sign the form or agree that the corresponding author can sign on their behalf. Articles cannot be published until a signed form has been received.

Lag time
The elapsed time from submission to publication for the articles averages 5-6 months. A decision of acceptance of a manuscript is reached in 2 to 3 months (average 9 weeks).

Back issues
Single issues from current and recent volumes are available at the current single issue price from UPM Press. Earlier issues may also be obtained from UPM Press at a special discounted price. Please contact UPM Press at penerbit@putra.upm.edu.my or you may write for further details at the following address:

UPM Press
Universiti Putra Malaysia
43400 UPM, Serdang
Selangor Darul Ehsan
Malaysia.

Pertanika

Our goal is to bring high quality research to the widest possible audience

Pertanika is an international peer-reviewed leading journal in Malaysia which began publication in 1978. The journal publishes in three different areas — Journal of Tropical Agricultural Science (JTAS); Journal of Science and Technology (JST); and Journal of Social Sciences and Humanities (JSSH).

JTAS is devoted to the publication of original papers that serves as a forum for practical approaches to improving quality in issues pertaining to tropical agricultural research or related fields of study. It is published twice a year in **February** and **August**.

JST caters for science and engineering research or related fields of study. It is published twice a year in **January** and **July**.

JSSH deals in research or theories in social sciences and humanities research with a focus on emerging issues pertaining to the social and behavioural sciences as well as the humanities, particularly in the Asia Pacific region. It is published twice a year in **March** and **September**.

Call for Papers

Pertanika invites you to explore frontiers from all fields of science and technology to social sciences and humanities. You may contribute your scientific work for publishing in UPM's hallmark journals either as a ***regular article, short communication,*** or ***a review article*** in our forthcoming issues. Papers submitted to this journal must contain original results and must not be submitted elsewhere while being evaluated for the Pertanika Journals.

Submissions in **English** should be accompanied by an abstract not exceeding 300 words. Your manuscript should be no more than 6,000 words or 10-12 printed pages, including notes and abstract. Submissions should conform to the Pertanika style, which is available at www.pertanika2.upm.edu.my/jpertanika/index.htm or by mail or email upon request.

Papers should be double-spaced 12 point type (Times New Roman fonts preferred). The first page should include the title of the article but no author information. Page 2 should repeat the title of the article together with the names and contact information of the corresponding author as well as all the other authors. Page 3 should contain the title of the paper and abstract only. Page 4 and subsequent pages to have the text - Acknowledgments - References - Tables - Legends to figures – Figures, etc.

Questions regarding submissions should only be directed to the Executive Editor, *Pertanika* Journals.

Remember, ***Pertanika is the resource to support you in strengthening research and research management capacity.***

Why should you publish in Pertanika Journals?

Benefits to Authors

PROFILE: our journals are circulated in large numbers all over Malaysia, and beyond in Southeast Asia. Recently, we have widened our circulation to other overseas countries as well. We will ensure that your work reaches the widest possible audience in print and online, through our wide publicity campaigns held frequently, and through our constantly developing electronic initiatives via Pertanika Online and e-pertanika.

QUALITY: our journals' reputation for quality is unsurpassed ensuring that the originality, authority and accuracy of your work will be fully recognised. Our double-blind peer refereeing procedures are fair and open, and we aim to help authors develop and improve their work. Pertanika JTAS is now over 30 years old; this accumulated knowledge has resulted in Pertanika being indexed in SCOPUS (Elsevier) and EBSCO.

AUTHOR SERVICES: we provide a rapid response service to all our authors, with dedicated support staff for each journal, and a point of contact throughout the refereeing and production processes. Our aim is to ensure that the production process is as smooth as possible, is borne out by the high number of authors who publish with us again and again.

LAG TIME: Submissions are guaranteed to receive a decision within 14 weeks. The elapsed time from submission to publication for the articles averages 5-6 months. A decision of acceptance of a manuscript is reached in 3 to 4 months (average 14 weeks).

An Award Winning International-Malaysian Journal

FEB. 2008

Mail your submissions to:

The Executive Editor
Pertanika Journals
Reseach Management Centre (RMC)
Publication Division
1st Floor, IDEA Tower II
UPM-MTDC, Technology Centre
Universiti Putra Malaysia
43400 UPM, Serdang, Selangor, Malaysia

Tel: +603-8947 1622
ndeeps@admin.upm.edu.my
www.pertanika2.upm.edu.my/jpertanika/index.htm

Pertanika Journal of Science & Technology
Vol. 18 (1) Jan. 2010

Contents

Research Management Centre (RMC)
1st Floor, IDEA Tower II
UPM-MTDC Technology Centre
Universiti Putra Malaysia
43400 UPM Serdang
Selangor Darul Ehsan
Malaysia

http://www.rmc.upm.edu.my
E-mail : ndeeps@admin.upm.edu.my
Tel : +603 8947 1622 /1620

UPM Press
Universiti Putra Malaysia
43400 UPM Serdang
Selangor Darul Ehsan
Malaysia

http://penerbit.upm.edu.my
E-mail : penerbit@putra.upm.edu.my
Tel : +603 8946 8855/8854
Fax : +603 8941 6172

ISSN 0128-7680
01
9 770128 768083